

**ROLE OF FOLATES IN NORMAL AND  
HYDROCEPHALIC  
FETAL BRAIN DEVELOPMENT**

A thesis submitted to The University of Manchester

for the degree of

**DOCTOR OF PHILOSOPHY**

in the Faculty of Life Sciences

**2016**

**ALICIA REQUENA JIMENEZ**

<b>TABLE OF CONTENTS</b>	<b>Page</b>
<b>GENERAL ABSTRACT</b>	18
<b>CHAPTER 1. GENERAL INTRODUCTION</b>	
1.1 Overview	19
1.2 CNS	22
1.2.1 CNS development	22
1.2.2 Congenital Hydrocephalus	28
1.3 CSF production and flow circulation	32
1.3.1 CSF production	32
1.3.2 CSF flow circulation	38
1.4 CSF composition	39
1.5 CSF absorption: the leptomeninge arachnoid	44
1.5.1 Morphology	44
1.5.2 CSF absorption	47
1.6 The hydrocephalic Texas rat as animal model	49
1.7 Treatment for congenital hydrocephalus	53
1.8 Folates/vitamin B9	54
1.8.1 Folates and the folate metabolic cycle	54
1.8.2 Folate binding enzymes and the folate metabolic cycle	56
1.8.3 Folate transporters and FDH as a folate binding protein	58
1.8.3.1 Known folate transporters	58
1.8.3.2 FDH as a folate binding protein	62
1.8.3.3 Folates and folate deficiencies	64
1.8.3.4 Folate treatment	66

1.9 Summary	68
1.10 Experimental aims and hypothesis	70
1.11. Alternative format	76
1.12 References	78

**CHAPTER 2. FDH AND FOLATES ROLE IN BRAIN DEVELOPMENT AT EARLY PREGNANCY: IMPLICATIONS FOR CONGENITAL HYDROCEPHALUS**

ABSTRACT	93
2.1 Introduction	94
2.2 Materials and methods	99
2.2.1 Cell growth with folates in the presence and absence of FDH	99
2.2.2 DAPI staining of cell cultures exposed to folates exposed to folates in the presence and absence of FDH	100
2.2.3 Cell growth in response to folate (THF) conjugated to IgG	101
2.2.3.1 THF-IgG effect on cell growth and cell quantification using DAPI fluorescence's analysis	101
2.2.3.2 THF-IgG fluorescent tracking	102
2.2.3.3 Bioavailability study of primary cell cultures in the presence of THF-IgG	103
2.2.4 FDH-5mTHF "in house" sandwich ELISA assay development	
2.2.4.1 Production of commercial and non-commercial FDH standard curves to quantify FDH binding to solid phase	103
2.2.4.2 Preparation of fluorescent 5mTHF antibody to be used in an "in house" fluorescent ELISA	105
2.2.4.3 Determination of 5mTHF binding to FDH using an	

“in house” fluorescent ELISA	105
2.2.5 FDH, 5mTHF and FR $\alpha$ immunolocalization in normal and hydrocephalic brain	107
2.2.5.1 Fluorescent dual immunostaining of coronal brain sections	107
2.2.5.2 Image analysis of sections captured by fluorescence microscopy	108
2.2.5.3 Fluorescent dual immunostaining and sequential detection by confocal microscopy	109
2.2.6 Expression of FDH mRNA in normal and hydrocephalic brain	110
2.2.6.1 FDH mRNA location in normal and hydrocephalic brain using reverse transcription “in situ” PCR	110
2.2.6.2 FDH mRNA quantification in cerebral cortex tissue using real time quantitative PCR	118
2.3 Results	120
2.3.1 5mTHF in combination with FDH is detrimental for cell growth	120
2.3.1.1 Decreasing concentration of 5mTHF plus constant FDH	120
2.3.1.2 Decreasing concentration of FDH plus constant 5mTHF	122
2.3.2 Cell growth not inhibited with folic acid in the presence of FDH	125
2.3.3 Commercial and unstable THF does not promote growth with or without FDH	126
2.3.4 DAPI staining of cell cultures treated with folates and FDH	127
2.3.5 THF conjugated to immunoglobulin (IgG) has a positive effect on cell growth	128
2.3.5.1 DAPI staining of cell culture treated with IgG-THF	128
2.3.5.2 IgG-THF fluorescent tracking demonstrates THF is	

taken in by cerebral cortex cells	130
2.3.5.3 Bioavailability studies suggest conjugated THF	
has a positive effect on cell growth	131
2.3.6 Negative FDH effect on cell growth depends on folate	
presence in the media	133
2.3.7 FDH shows affinity for 5mTHF	134
2.3.7.1 Standard curves parallelism between non-commercial	
and commercial FDH is confirmed using a commercial FDH	
ELISA prior to development of an “in house” ELISA for	
detection of 5mTHF binding to FDH	134
2.3.7.2 “In house” ELISA using commercial FDH ELISA	
and fluorescent 5mTHF antibody shows FDH affinity for	
5mTHF	135
2.3.8 FDH protein colocalizes with 5mTHF and FR $\alpha$	138
2.3.9 FDH is significantly overexpressed in CC of the hydrocephalic brain	149
2.3.10 FDH mRNA is expressed in CC and CP	151
2.4 Conclusion-discussion	157
2.5 References	169
<b>CHAPTER 3. FOLATES ARE CRUCIAL FOR FETAL MENINGEAL</b>	
<b>ARACHNOID CELL GROWTH: IMPLICATIONS FOR CONGENITAL</b>	
<b>HYDROCEPHALUS</b>	
ABSTRACT	174
3.1. Introduction	175
3.2 Material and methods	178
3.2.1 Animals	178
3.2.2 Matings	178

3.2.3 Collection of fetal brain and dissection	179
3.2.4 Arachnoid tissue processing and identification	179
3.2.4.1 Arachnoid tissue processing and identification	179
3.2.4.2 Arachnoid cell-type identification	180
3.2.5 Primary arachnoid cell culture treated with folates and FDH	181
3.2.6 DAPI staining of primary arachnoid cell cultures treated with folates and FDH	182
3.2.7 CSF treatment	182
3.2.8 Statistical analysis	183
3.3 Results	184
3.3.1 Immunocytological assessment	184
3.3.2 Morphological and confluency assessment	185
3.3.3 FDH is counterproductive for arachnoidal cell growth in the presence of FDH	186
3.3.4 THF with or without FDH does not potentiate cell arachnoid growth	189
3.3.5 Folic acid exacerbates growth with and without FDH	191
3.3.6 FDH effect on arachnoidal cell growth depends on folate presence in media	193
3.3.7 DAPI staining reveals different effects on growth of arachnoid cells co-culture with folates and FDH	194
3.3.8 CSF effect on arachnoid cell growth	196
3.4 Conclusion-discussion	198
3.5 References	202

## **CHAPTER 4. NORMAL VERSUS HYDROCEPHALIC CSF**

### **INGENUITY PATHWAY ANALYSIS (IPA) OF PROTEIN PROFILES**

## **OBTAINED FROM LCMS**

ABSTRACT	205
4.1 Introduction	206
4.2 Material and methods	210
4.2.1 EXCEL analysis	210
4.2.2 LCMS protein analysis	211
4.2.3 IPA analysis	213
4.3 Results	215
4.3.1 EXCEL analysis	215
4.3.2 IPA results	286
4.3.2.1 Normal and hydrocephalic CSF do not share the same protein profile and metabolic pathways	286
4.3.2.2 Different top canonical pathways were found for normal and hydrocephalic CSF	297
4.3.2.3 Different biological functions were associated with normal and hydrocephalic CSF	299
4.4 Conclusion-discussion	302
4.5 References	311

## **CHAPTER 5. CONCLUDING REMARKS, DISCUSSION AND FUTURE AIMS**

5.1.1 Chapter 2 concluding remarks flow chart	314
5.1.2 Chapter 2 concluding remarks and discussion	315
5.1.3 Chapter 2 future aims	318
5.2.1 Chapter 3 concluding remarks flow chart	320

5.2.2 Chapter 3 concluding remarks and discussion	321
5.2.3 Chapter 3 future aims	322
5.3.1 Chapter 4 concluding remarks flow chart	323
5.3.2 Chapter 4 concluding remarks and discussion	324
5.3.3 Chapter 4 future aims	325

**Word count: 63,288**



## **TABLE OF FIGURES**

### **CHAPTER 1**

<b>Figure 1.1. Development of the CNS</b>	<b>22</b>
<b>Figure 1.2. Layers of the cerebral cortex</b>	<b>24</b>
<b>Figure 1.3. Primary cell culture micrographs of CC progenitor cells</b>	<b>25</b>
<b>Figure 1.4. CC progenitor cells (radial glia)</b>	<b>25</b>
<b>Figure 1.5. Schematic representation of the normal and HC fetal brain</b>	<b>28</b>
<b>Figure 1.6. CSF flow</b>	<b>36</b>
<b>Figure 1.7. Choroid plexus structure and the blood-CSF barrier</b>	<b>37</b>
<b>Figure 1.8. Ion transporters and channels in mammalian choroid plexus</b>	<b>41</b>
<b>Figure 1.9. CSF outflow through arachnoid granulations</b>	<b>44</b>
<b>Figure 1.10. Graphic reconstruction of mammal arachnoid granulation</b>	<b>46</b>
<b>Figure 1.11. The Sprague Dawley pup</b>	<b>49</b>
<b>Figure 1.12. Schematic representation of the ventriculoperitoneal shunt technique</b>	<b>53</b>
<b>Figure 1.13. The folate metabolic cycle</b>	<b>54</b>
<b>Figure 1.14. Folate transport across the choroid plexuses in adults</b>	<b>59</b>
<b>Figure 1.15. Hypothetical model of human cerebral folate (5mTHF) transport by FR<math>\alpha</math></b>	<b>61</b>
<b>Figure 1.16. FDH domains</b>	<b>62</b>
<b>Figure 1.17. Diagram representing 5mTHF transport by FR<math>\alpha</math> versus our hypothesis related to the role of FDH in folate transport of 5mTHF</b>	<b>72</b>
<b>Figure 1.18. CSF flow and drainage into the superior sagittal sinus</b>	<b>73</b>

## CHAPTER 2

<b>Figure 2.1. Commercial sandwich ELISA for quantification of FDH/ALDH1L1</b>	<b>104</b>
<b>Figure 2.2. “In house” ELISA assay to identify FDH-5mTHF complexes</b>	<b>106</b>
<b>Figure 2.3. Effect of decreasing 5mTHF and constant active and inactive FDH concentration on cell proliferation</b>	<b>120</b>
<b>Figure 2.4. Effect on cell proliferation of decreasing 5mTHF alone, decreasing active FDH plus constant 5mTHF+ decreasing inactive FDH plus constant 5mTHF</b>	<b>123</b>
<b>Figure 2.5. Effect on cell proliferation of folic acid alone, folic acid plus inactive ALDHL and folic acid plus active FDH</b>	<b>125</b>
<b>Figure 2.6. Effect on cell proliferation of THF alone, THF plus inactive ALDHL1 and THF plus active FDH</b>	<b>126</b>
<b>Figure 2.7. DAPI nuclei staining snapshots of primary cell cultures in the presence of different types of folates with and without FDH</b>	<b>127</b>
<b>Figure 2.8 DAPI nuclei staining snapshots of primary cell cultures in the presence of IgG-THF, THF and media control</b>	<b>128</b>
<b>Figure 2.9 Inhibitory effect of THF in contrast to IgG-THF positive effect on cell growth of primary cerebral cortex cells</b>	<b>129</b>
<b>Figure 2.10 Uptake of fluorescent THF-labelled IgG by cerebral cortex cells</b>	<b>130</b>
<b>Figure 2.11 Effect on cell proliferation of THF versus no folates at starting point (zero growth; t=0) and after 24 hours (t=24H)</b>	<b>131</b>
<b>Figure 2.12 Effect on cell proliferation of active and inactive FDH</b>	<b>133</b>
<b>Figure 2.13 Commercial and non-commercial (FDH) standard curves</b>	<b>134</b>
<b>Figure 2.14 “In house” Fluorescent ELISA assay for identification of FDH binding to 5mTHF</b>	<b>136</b>

<b>Figure 2.15 Fluorescence photomicrographs of coronal sections show immunolocalization and colocalization of FDH and 5mTHF in LV of normal and abnormal cerebral cortex</b>	<b>138</b>
<b>Figure 2.16 Immunofluorescence staining of coronal sections identified FDH and 5mTHF in choroid plexus of normal and abnormal brain</b>	<b>139</b>
<b>Figure 2.17 Immunohistochemical staining of coronal sections identified FDH and FR<math>\alpha</math> in cerebral cortex of normal and abnormal brain</b>	<b>140</b>
<b>Figure 2.18 Immunohistochemical staining of coronal sections identified FDH and FR<math>\alpha</math> in choroid plexus of normal and abnormal brain</b>	<b>141</b>
<b>Figure 2.19 Confocal images of fluorescent immunohistochemical staining for FDH and FR<math>\alpha</math> in III V</b>	<b>142</b>
<b>Figure 2.20 Cerebral cortex immunohistochemical fluorescence quantification in normal and hydrocephalic rat</b>	<b>144</b>
<b>Figure 2.21. Choroid plexus immunohistochemical fluorescence quantification in normal and hydrocephalic rat</b>	<b>146</b>
<b>Figure 2.22 Representative fluorescence micrographs of FDH and FR<math>\alpha</math> staining of FDH and FR<math>\alpha</math> staining in cerebral cortex neuroepithelia, striatum and vesicle-like structures</b>	<b>148</b>
<b>Figure 2.23 Expression of FDH mRNA in normal and hydrocephalic cerebral cortex</b>	<b>149</b>
<b>Figure 2.24 Representative fluorescence (rhodamine) micrographs of FDH mRNA tissue distribution in neuroepithelia of normal and abnormal cerebral cortex and choroid plexus</b>	<b>153</b>
<b>Figure 2.25. Confocal images of double staining (DAPI + FDH mRNA/cDNA) rhodamine in neuroepithelia cerebral cortex and striatum</b>	<b>155</b>

<b>Figure 2.26. Fluorescence micrograph of liver positive control for FDH mRNA/cDNA rhodamine labelled amplification by “in situ” PCR</b>	<b>156</b>
---	------------

### **CHAPTER 3**

<b>Figure 3.1 Fluorescence immunohistochemical staining of arachnoid tissue at embryonic day 18</b>	<b>184</b>
<b>Figure 3.2 Cultured arachnoid cells micrographs using bright-field microscopy</b>	<b>185</b>
<b>Figure 3.3 Effect of decreasing 5mTHF and constant active and inactive FDH/ALDH1L1 concentration on cell proliferation</b>	<b>186</b>
<b>Figure 3.4 Effect on cell proliferation of THF alone, THF plus inactive FDH/ALDH1L1 and THF plus active FDH</b>	<b>189</b>
<b>Figure. 3.5 Effect on cell proliferation of folic acid alone, folic acid plus inactive FDH and folic acid plus active FDH at decreasing concentration</b>	<b>191</b>
<b>Figure 3.6 Effect on cell proliferation of active and inactive FDH</b>	<b>193</b>
<b>Figure 3.7 DAPI nuclei staining snapshots of primary cell cultures in the presence of different types of folates with and without FDH</b>	<b>194</b>
<b>Figure 3.8 CSF effect on arachnoid cell proliferation</b>	<b>196</b>

### **CHAPTER 4**

<b>Figure 4.1 Percentage of protein only present in normal CSF versus percentage common to abnormal CSF</b>	<b>215</b>
<b>Figure 4.2 Percentage of protein only present in abnormal CSF versus percentage common to normal CSF</b>	<b>216</b>
<b>Figure 4.3 Canonical pathways for proteins only found in normal CSF</b>	<b>287</b>

**Figure 4.4 Canonical pathways for proteins only found in abnormal CSF 291**

## **CHAPTER 5**

**Figure 5.1 Chapter 2 concluding remarks flow chart 314**

**Figure 5.2 Chapter 3 concluding remarks flow chart 320**

**Figure 5.3 Chapter 4 concluding remarks flow chart 323**

## **LIST OF TABLES**

### **CHAPTER 2**

<b>Table 2.1 Thermocycler parameters used for “in situ” PCR i.e.: FDH cDNA amplification</b>	<b>117</b>
--	------------

<b>Table 2.2 Gene sequences and annealing temperature (<math>T_a</math>) for primers targeting FDH/ALDH1L1 and housekeeping genes</b>	<b>119</b>
---	------------

### **CHAPTER 4**

<b>Table 4.1 Proteins in normal CSF no present in abnormal CSF</b>	<b>217</b>
--	------------

<b>Table 4.2 Proteins in abnormal CSF no present in normal CSF</b>	<b>265</b>
--	------------

<b>Table 4.3 Top canonical pathways uniquely identified in normal CSF</b>	<b>297</b>
---	------------

<b>Table 4.4 Top canonical pathways uniquely identified in abnormal CSF</b>	<b>298</b>
---	------------

<b>Table 4.5 IPA summary of biological functions associated with proteins found in normal CSF</b>	<b>299</b>
---	------------

<b>Table 4.6 IPA summary of biological functions associated with proteins found in abnormal CSF</b>	<b>301</b>
---	------------

## **Declaration**

No portion of the work referred to in the thesis has been submitted in support of an application for another degree or qualification of this or any other university or other institute of learning.

## **Copyright statement**

**i.** The author of this thesis (including any appendices and/or schedules to this thesis) owns certain copyright or related rights in it (the “Copyright”) and he has given The University of Manchester certain rights to use such Copyright, including for administrative purposes.

**ii.** Copies of this thesis, either in full or in extracts and whether in hard or electronic copy, may be made only in accordance with the Copyright, Designs and Patents Act 1988 (as amended) and regulations issued under it or, where appropriate, in accordance with licensing agreements which the University has from time to time. This page must form part of any such copies made.

**iii.** The ownership of certain Copyright, patents, designs, trade marks and other intellectual property (the “Intellectual Property”) and any reproductions of copyright works in the thesis, for example graphs and tables (“Reproductions”), which may be described in this thesis, may not be owned by the author and may be owned by third parties. Such Intellectual Property and Reproductions cannot and must not be made available for use without the prior written permission of the owner(s) of the relevant Intellectual Property and/or Reproductions.

**iv.** Further information on the conditions under which disclosure, publication and commercialisation of this thesis, the Copyright and any Intellectual Property and/or Reproductions described in it may take place is available in the University IP Policy (see <http://documents.manchester.ac.uk/DocuInfo.aspx?DocID=487>), in any relevant Thesis restriction declarations deposited in the University Library, The University Library’s

regulations (see <http://www.manchester.ac.uk/library/aboutus/regulations>) and in The University's policy on Presentation of Theses



## **Acknowledgements**

Firstly I would like to thank my supervisors Dr. Jaleel Miyan and Dr. John Gig for giving me the opportunity to do this PhD, and for their knowledge and guidance throughout my project. Special thanks to John Corcoran and Simon Corcoran for the time and commitment given to my work. Also, thanks to Aurora Requena Jimenez, Dr. Jocelyn Glazier and Dr. Eleni Tsitsiou for their valuable input with some experimental design. Additionally, I would like to give special thanks to Larisa Logunova. Her help in the lab has been greatly appreciated.

## GENERAL ABSTRACT

Brain Cerebrospinal fluid (CSF) bulk flow is maintained thanks to a balance between CSF secretion from the choroid plexus and CSF absorption by arachnoid villi, where it drains into nearby blood vessels, thereby reaching the general blood circulation. Congenital hydrocephalus starts during the first trimester of pregnancy with impeded CSF flow, and consequent CSF build-up within the brain ventricles. This event is followed by CSF compositional changes, increased intracranial pressure, and, if untreated, brain damage and fetal death. Previous research has revealed a unique folate delivery system which serves the developing cerebral cortex. Abnormal folate provision due to impairment of this system was directly connected to a decrease in a CSF folate enzyme: 10-Formyl-Tetrahydrofolate dehydrogenase (FDH). In light of these findings, low FDH was linked with folate deficiency and the poor cortical development found in congenital hydrocephalus. In this context, investigations were carried out to ascertain whether folates in the presence and absence of the folate enzyme FDH are beneficial for fetal brain development. The current study also aims to investigate the FDH -folate delivery system in the fetal brain in order to understand its role in CNS development and its relationship to currently known folate transport mechanisms (FR $\alpha$ ). Furthermore, we hypothesize that folates may prevent congenital hydrocephalus through a re-establishment of CSF drainage and flow circulation at the level of the arachnoid membrane/villi. This assumption implies that the leptomeninge arachnoid may also be dysfunctional in the hydrocephalic brain due to a variation in hydrocephalic CSF composition (folates). Finally, an overall metabolic pathway analysis of the constituents uniquely present in abnormal CSF, hence missing in normal CSF, and vice versa, was carried out to establish associations with suggested activated and inactivated biological processes during congenital hydrocephalus.

# **GENERAL INTRODUCTION**

## **1.1 OVERVIEW**

Congenital hydrocephalus is a worldwide neurological condition with an estimated incidence range of 1/5000-1/280 (Greenberg 2001). This medical condition is the outcome of cerebrospinal fluid drainage obstruction that results in CSF accumulation and increased intracranial pressure (Bulat and Klarica, 2010), which in turns leads to neurological deficit, brain damage and death (Brodbelt and Stoodley 2007, Oreskovic and Klarica, 2011). The specific causes and sites of obstruction are currently not fully known (Johnston et al. 2004, Johanson et al. 2008), but two areas of the brain have been suggested to have important roles in the condition: the choroid plexus (site of CSF production), (Catala et al. 1998, Rodriguez et al. 2006, Zhao et al. 2011, Grapp et al. 2013) and the leptomeninge arachnoid (where CSF exits the brain), (Conegero and Chopard 2003, Cornelius et al. 2011).

Past research in this laboratory used the hydrocephalic Texas rat as the animal model to demonstrate that development of the fetal cerebral cortex is impaired in hydrocephalus through compositional changes in CSF (Masayekhi et al. 2002 and Owen-Lynch et al. 2003), and specifically through changes in folate and folate-associated proteins (Nabiuni et al. 2004). Moreover, a lack in CSF of a key folate enzyme: 10-formyl-tetrahydrofolate dehydrogenase (FDH) was associated with reduced cell proliferation and cortical plate thickness (Nabiuni et al. 2004 and Cains et al. 2009). Decreased FDH concentration in CSF meant the folate metabolic cycle was altered, rendering the brain deficient in specific folates. In this scenario, a folate treatment based on a mixture of two specific folates was devised, taking into account the metabolic reaction where FDH is involved. The treatment, administrated through maternal supplementation, decreased the incidence of hydrocephalus

by 60%. Preliminary *in vitro* studies also showed that hydrocephalic fetal rats exhibited an elevated concentration of 5mTHF in CSF compared to Sprague Dawley (SD) control rats (Cain et al. 2009).

The role of FDH in the brain is yet not understood (Champion et al. 1994, Anguera et al. 2006) as it is not the accepted mechanism for delivery of folates to specific areas like the cerebral cortex and meninge arachnoid (Rodriguez et al. 2006, Grzybowski, et al. 2006, Antony and Heintz, 2007, Johanson et al 2008, Wollack et al 2008, Zhao et al. 2011, Grapp et al. 2013). In this context, this investigation aims firstly to elucidate the role of FDH in cell growth in the presence and absence of different types of folates, as well as to identify FDH's specific location, expression and potential interrelationships with known folate receptors (FR $\alpha$ ) (Zhao et al. 2011 and Grapp et al 2013). for folate delivery to the developing brain. Past immunostaining analysis of the fetal brain located FDH on the fetal cerebral cortex of gestational day 20 H-Tx and SD control rats (Cains et al. 2009). In the current study, we used "in situ" PCR, and suggest that FDH is produced in the cerebral cortex, and that it binds to folates from the CSF at the level of the radial glia in the germinal epithelium. Folates bound to FDH are transported in the cerebral cortex by radial glia, as well as in the CSF, to the required areas for further development (Dziegielewska et al. 2000 and Miyan et al. 2001). The FDH-folate transport system may thus present an alternate folate transport mechanism to the classic folate transport by folate receptors and carriers (FR $\alpha$ , PCFT and RFC) in the choroid plexus (Wollack et al. 2008 and Steinfeld et al. 2009).

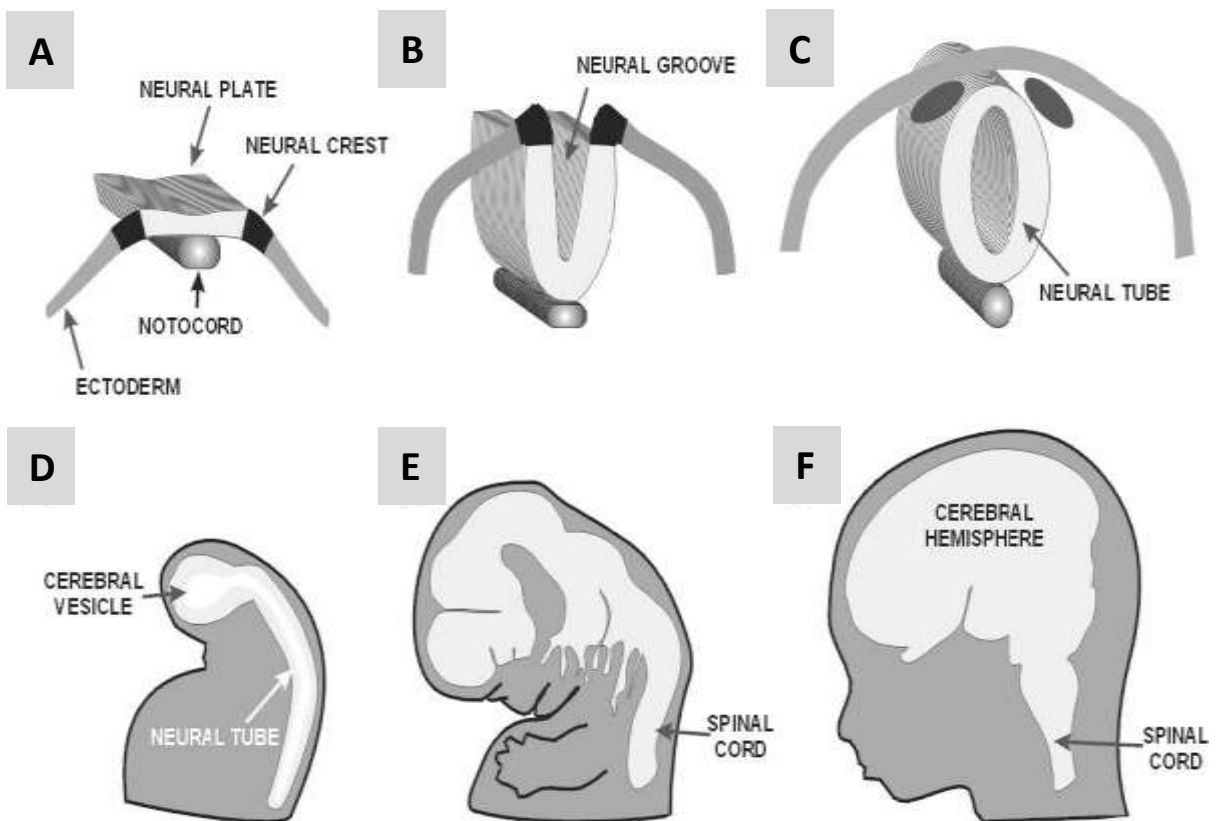
A second aspect of this research is related to the leptomeninge arachnoid. CSF flow in the brain is maintained thanks to a flow balance between CSF production in the choroid plexus and absorption in the arachnoid villi (Brown et al. 2004, Oreskovic and Klarica 2011). Studies by other research groups showed that impeded CSF absorption results in an altered flow and CSF accumulation leading to hydrocephalus (Grzybowski, et al. 2006, Glimcher et al. 2008 and Cornelius et al 2011). In addition, preliminary studies in our lab showed how hydrocephalic CSF has a strong inhibitory effect on cerebral cortex cell proliferation (Cains et al. 2009). We suggest that hydrocephalic CSF may also be inhibitory or even cytotoxic for the arachnoid, the main site for CSF egress resulting in drainage insufficiency. Consequently, the brain improvement observed in the offspring after our folate treatment was possibly due to increased CSF flow through the arachnoid villi, and we postulate that arachnoid functionality may be affected by FDH depletion in the hydrocephalic CSF, leading to reduced CSF outflow. Thus, our previous studies suggest that with folate supplementation, the hydrocephalic brain bypass the impaired FDH step in the folate cycle allowing in this way reestablishment of flow circulation and normalized cerebral cortex development at the same time (Cains et al. 2009). However, the folate mechanisms to explain these two parallel events are still poorly understood (Grapp et al. 2013), and in this context, the current studies focus on elucidating the role of FDH in folate transport in the presence and absence of folates, its interrelationship with folate receptors such as FR $\alpha$  (the main receptor involved in brain folate transport (Steinfeld et al. 2009 and Grapp et al. 2013), and the potential role of FDH and folates in cerebral cortex and arachnoid cell growth and differentiation. Finally, the present study suggests new avenues for further research into specific metabolic pathways potentially activated and inactivated in congenital hydrocephalus. To this end, we used for the first time a bioinformatic tool called Ingenuity Path Analysis (IPA), ([www.ingenuity.force.com](http://www.ingenuity.force.com)) to analyse metabolomics' data obtained from LCMS analysis of CSF in our previous studies.

## 1.2 CNS DEVELOPMENT AND CONGENITAL HYDROCEPHALUS

### 1.2.1 CNS development

The development of a complex structure such as the CNS requires the simultaneous and interdependent action of several developmental processes including morphogenesis, the establishment of positional identities and histogenesis. The individual regulation and coordination between these mechanisms is only partially known.

Cerebral cortex development in vertebrates starts at the expanded anterior end of the neural tube (see Figure 1.1 below). The notocord exerts its effects on the neural plate through secretion of sonic hedgehog (shh) (Echelard et al., 1993; Martí' et al., 1995).



**Figure 1.1. Development of the CNS. Development of the CNS starts with proliferation of ectodermic cells that differentiate to give rise to the neural plate and neural crests (a). Neuroectoderm folds and gives rise to the neural groove (b). Neuroulation is directed by an underlying notochord that secretes paracrine factors (d, e, f). The anterior end of the tube swells to form the cerebral vesicles that determine the shape of the brain including the cerebral hemispheres (f). (Miyan, J.A. et al. 2003)**

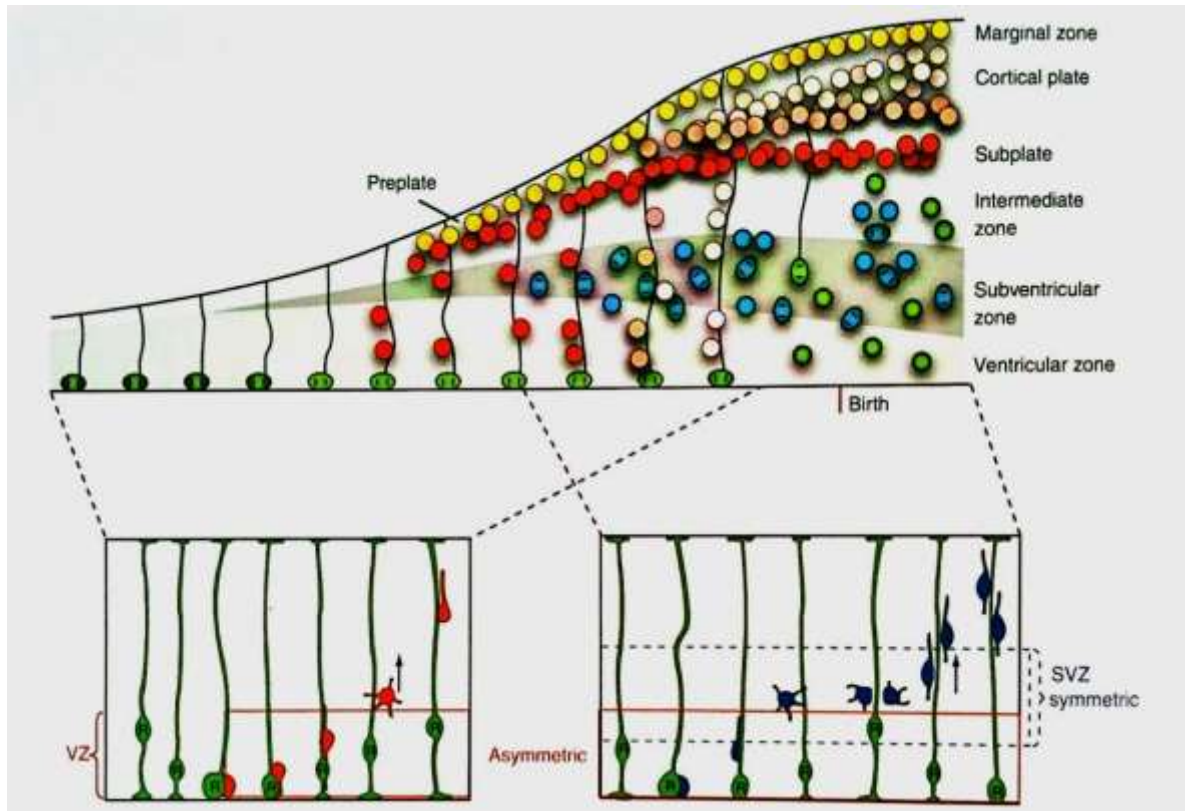
The brain and spinal cord walls are lined with a pseudostratified neuroepithelium containing neural stem cells with autonomous behaviour and rapid proliferation. Proliferation is stimulated and coordinated through the secretion of autocrine and paracrine molecules. (Panchision and McKay, 2002, Vaccarino et al. 1999)

Organizing centres have been identified within the neuroepithelium. These are the floor plate, the mesencephalic-rhombencephalic isthmus, and the anterior part of the telencephalic vesicles as well as adjacent structures such as the notochord (Bueno et al., 1996; Crossley et al., 1996). The organizing centres yield diffusible molecules that are identifiable by cell receptors within the organizing centre or at a certain distance from it. These secreted molecules have an important role in the patterning or regionalisation of the fetal brain (Shamim et al., 1999; Vaccarino et al., 1999a, 1999b; Toresson et al., 2000; Garda et al., 2001; Panchision and McKay, 2002,).

In previous work in our laboratory, FDH in normal and abnormal brains was found to be located in the radial glia of the cerebral cortex and in CSF inside vesicles close to the germinal epithelium of the cerebral cortex, but not in other important areas of the brain where proteins are secreted into CSF i.e. choroid plexuses (Cain, 2009).

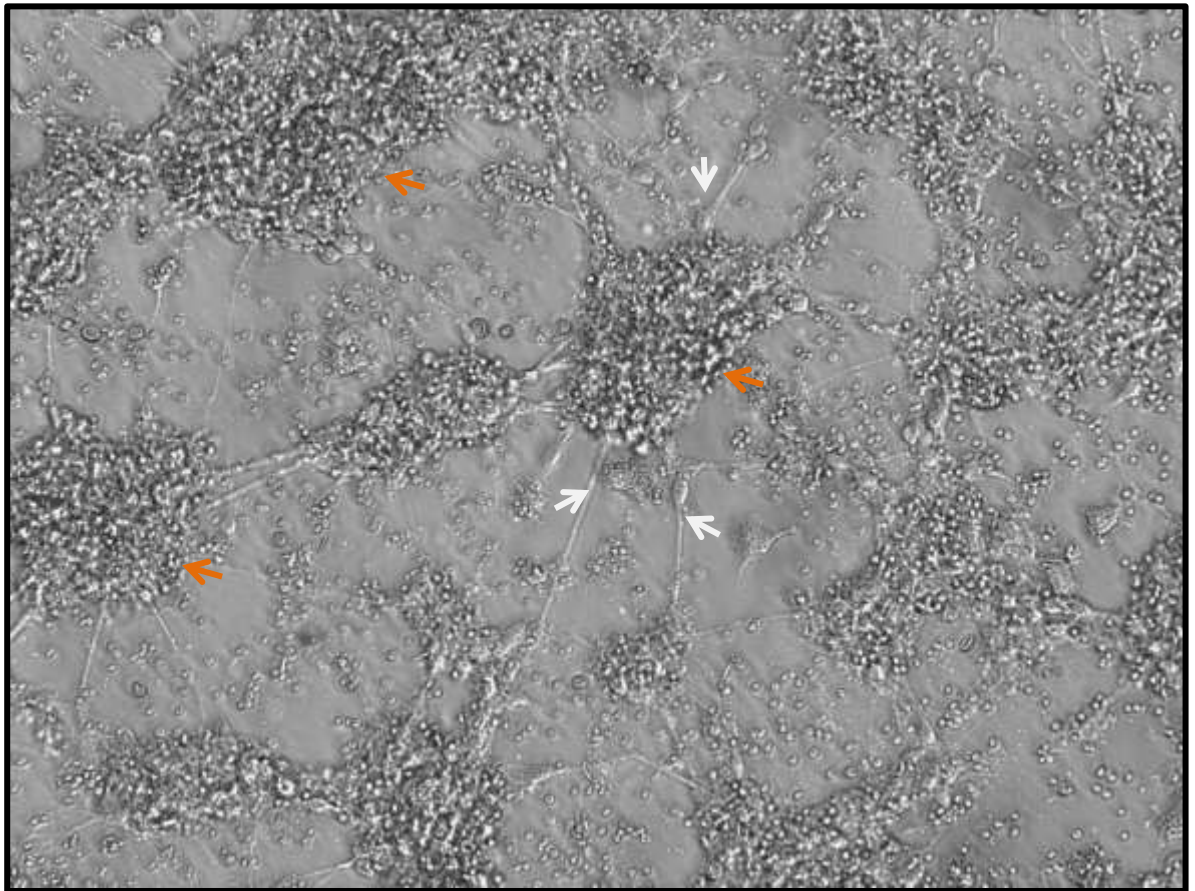
In the cerebral cortex, progenitor cells give rise to radial glia which shows interkinetic nuclear migration (see Figure 1.2, 1.3 and 1.4 below). The nucleus migrates to the inner ventricular surface just before mitosis and divides into two daughter cells, while the nuclei of the daughter cells move away from the inner ventricular surface during S-Phase to later move back to the ventricular surface to complete division (Norden et al. 2009). Progenitor cells are the precursors of all types of neurons and glia, except microglia in the cerebral cortex. Neurons and glia migrate away from the VZ to continue differentiating into mature

neurons, astroglia and oligodendrocytes. It has been suggested that progenitor cells move to the ventricular surface to get access to the nutrients present in CSF, and that CSF acts a growth medium and orchestrator of development (Miyan 2003).

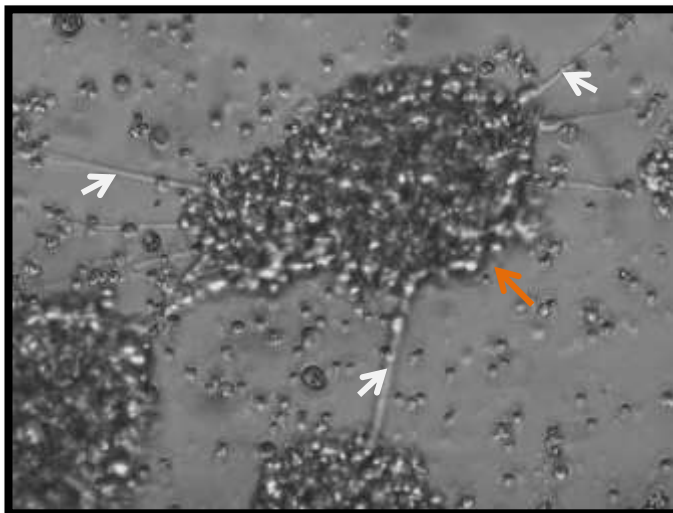


**Figure 1.2. Layers of the cerebral cortex. Six layers have been described in the cerebral cortex of mammals: The ventricular zone (VZ), the subventricular zone (SVZ), the intermediate zone, the subplate, the cortical plate and the marginal zone. The cerebral cortex begins as a simple neuroepithelium made up of apical progenitor cells also called radial glia (green cells). As they proliferate they develop a bipolar shape. Radial glia divides symmetrically or asymmetrically and represents the scaffolding for neurons and astroglia that originate from them by mitotic division (Sanes, DH 2010).**





**Figure 1.3. Primary cell culture micrographs of cerebral cortex progenitor cells (orange arrows) showing cell projections and cell differentiation into radial glia (white arrows) at embryonic day 18. (Interference microscope, x20)**



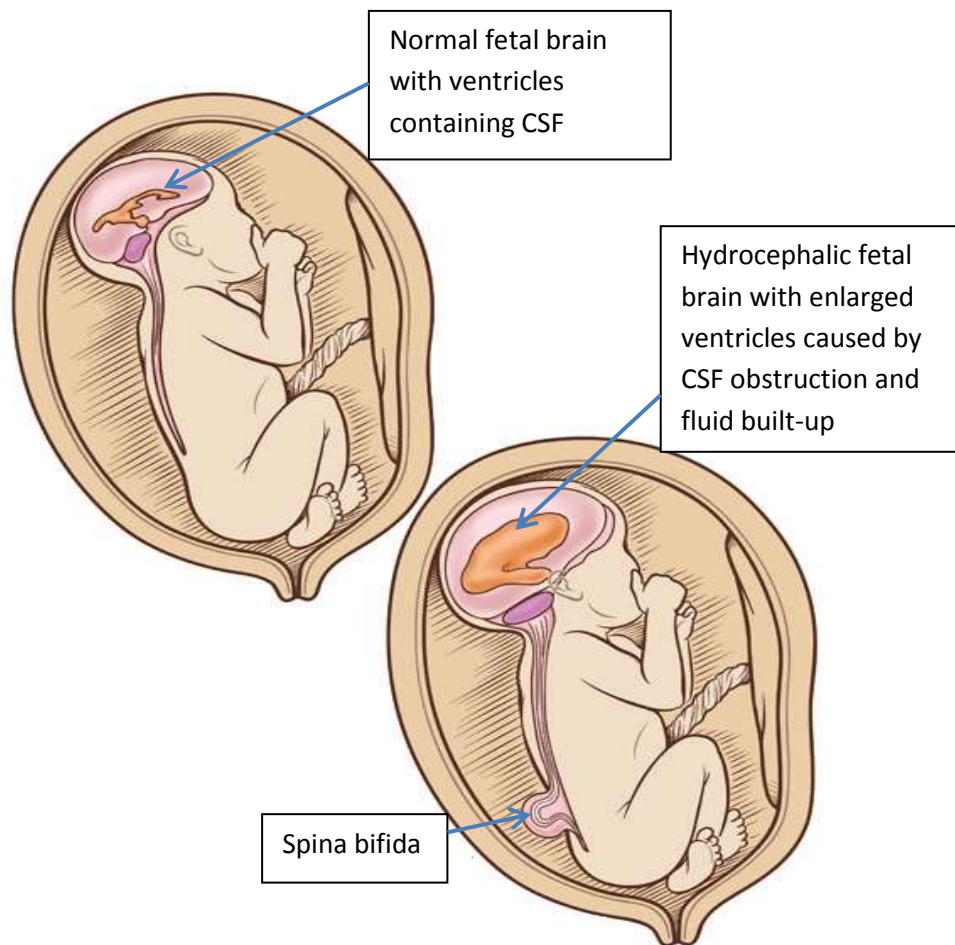
**Figure 1.4. Cerebral cortex progenitor cell (orange arrow) showing radial glia cells (white arrows) (Interference microscope x40).**

Migration is made possible by a group of specific hierarchical signals from the germinal epithelium to the cortical areas. The cells in the marginal zone (Cajal-Retzius) secrete the extracellular glycoprotein reelin that stimulates receptor and intracellular signalling systems across the cerebral cortex, and mediates migration and stratification (Cooper, J.A. 2008).

During development, the cavities of the brain ventricles are filled with protein-rich embryonic CSF. Although the role of this fluid has not been fully characterized, it is considered to directly influence neuroepithelial stem cell growth and proliferation, and differentiation of the cerebral cortex by means of growth factors FGF2 and EGF that are present in embryonic CSF (Panchision and McKay, 2002; Rajan et al. 2003). Furthermore, some studies have found that the protein content in CSF is more complex in embryos than in adults. A greater protein concentration in embryonic CSF suggests that it has a role in the regulation of cerebral cortex neuroepithelial cell behaviour (Dziegielewska et al., 1980b, Dziegielewska et al., 2000, Ojeda and Piedra, 2000; Miyan et al., 2003; Gato et al., 2004). Embryonic CSF also plays a key role in the expansion of the brain at the earliest stages of growth (Desmond and Jacobson, 1977; Desmond, 1985; Alonso et al., 1998), and abnormal embryonic CSF in some congenital malformations has been associated with altered cortical brain development (Mashayekhi et al., 2002; Owen-Lynch et al., 2003). Gato and colleagues (2005) studied the effect of embryonic CSF on mesencephalic neuroepithelium, and revealed its inability to self-stimulate basic cellular behaviour “in vitro”, concluding that normal behaviour is promoted by extraneural signals and diffusible factors present in embryonic CSF. In conclusion, the aforementioned body of work highlights the importance of embryonic CSF in fetal brain development. Notably, this work is also in accordance with our results from CSF LCMS analysis of Texas rats. At embryonic day 18, CSF LCMS analysis showed a 6-fold FDH decrease in CSF compared

to embryonic day 16, when the closure of the neural tube in both normal unaffected and affected Texas rats is still incomplete and CSF flow is still restricted due to an as yet unopened SAS. Therefore, it was proposed that the reduced FDH levels observed in CSF at later embryonic days (day 18) were a response to the high demand for this enzyme and associated folates at earlier stages of development (day 16), when FDH is needed for completion of the neural tube closure as well as for the establishment of CSF flow circulation and drainage (Dr. Miyan personal communication).

### 1.2.2 Congenital hydrocephalus



**Figure 1.5. Schematic representation of the normal and hydrocephalic fetal brain. The image above shows a normal fetus surrounded by placenta and normal size brain ventricles. The image below represents a hydrocephalic brain with enlarged ventricles and spina bifida, a condition also associated with congenital hydrocephalus. Adapted from [www.mottchildren.org](http://www.mottchildren.org)**

Congenital hydrocephalus is considered to be caused by accumulation of CSF in the fetal brain due to obstruction of the common CSF pathways leading to ventricular distension and brain injury (Oreskovic et al. 2010 and Miyan et al. 2003). This condition affects from 1 in 500 to 1 in 5000 children worldwide (Schurr et al. 1953, Greenberg et al. 2001, Sipek et al. 2002 and NIH 2005) and it occurs in isolation or in association with other disorders such as neural tube defects, spina bifida (figure 1.5) and Chiari II syndrome (Liddon 2004).

Due to the broad variety of events leading to this condition, congenital hydrocephalus is one of the most challenging pediatric diseases in terms of medical complications. It is known that fetal-onset hydrocephalus is triggered by an alteration in CSF dynamics provoked by fluid drainage insufficiency or obstruction. This leads to fluid accumulation in the brain ventricles, as well as raised intracranial pressure and ventricle enlargement; the latter is the main phenotypical characteristic observed in fetal brain scans (Del Bigio et al. 2010). However, congenital hydrocephalus should not be seen only as a mechanical phenomenon, but rather a sequence of disorders occurring at a specific time and brain location (Rodriguez et al. 2006). Although the pathophysiology of congenital hydrocephalus is still not fully understood, despite more than 100 years of research, extensive literature has reported numerous brain alterations associated with this disorder. These alterations include brain loss in the form of severe reduction in cerebral cortex thickness, and abnormal development of certain neuron sub-types, resulting in cognitive deficits (Cain et al. 2009, Miyan et al. 2003, and Rodriguez et al. 2006). Brain loss is also a consequence of neuroepithelium denudation, which leads to obliteration of the Sylvius Aqueduct and CSF accumulation as well as alterations of the hypothalamus and neuroendocrine deficiencies (Mashayekhi et al. 2002, Rodriguez et al. 2006 and Johanson et al. 2008). Nevertheless, congenital hydrocephalus is also accompanied by brain gain, in terms of elevated astrocyte proliferation around the Aqueduct of Sylvius and third ventricle, in response to brain loss and an attempt to restore brain areas negatively affected by denudation (Rodriguez et al. 2006).

CSF accumulation in the fetal brain is also linked to intraventricular haemorrhage (IVH) at a time in development (24 to 32 weeks' gestation) when the subependymal germinal matrix in brain ventricles is metabolically highly active. Further, it is in contact with

capillaries not supported by adventitia and unprotected in terms of autoregulation, making the fetus vulnerable to brain hemorrhage (Cherian et al. 2004). 25% of low birth weight babies develop posthemorrhagic hydrocephalus (PHH) (Batton et al. 1994 and Sheth et al. 1998), and neurological deficiencies are more accentuated in PHH than IVH (Murphy et al. 2002 and Sasidharan et al. 1986). The specific causes for PHH and IVH are unknown; however, it is thought that hemorrhage may occur after blockage of CSF by various mechanisms including CSF obstruction by blood products, inflammation in brain sites closed to CSF pathways, gliosis and arachnoidal inflammation. Furthermore, ventricular distension and therefore physical stress leads to white matter injury in PHH and IVH (Volpe et al. 2008 and Du Plessis et al. 1998). It has been suggested that brain injury in babies with IVH and PHH may also be due to cytotoxins from blood products that damage the germinal matrix of the ependyma after hemorrhage (Du Plessis et al. 1998).

There is molecular genetic evidence that in humans, 5 to 15% of cases of congenital hydrocephalus are caused by missense mutations in the X sexual chromosomes. The mutations are distributed specifically within the Xq28 gene encoding for the functional domains of LICAM protein or L1 protein, an immunoglobulin involved in neural cell adhesion in neurons and Schwann cells (Jouet et al. 1993). X-linked recessive inheritance in females means they are carriers of the condition, whereas males with the mutant recessive gene die after birth (Renier et al. 1982). In contrast to humans, where only one gene has been associated with congenital hydrocephalus (Xq28), investigations in animal models found that 9 genes and more than 43 mutants/loci are linked to hereditary hydrocephalus, with the products of these genes being mainly cytokines, growth factors and molecules related to cellular signal pathways activated during early brain development (Zhang et al. 2006). Unfortunately, there is very limited understanding about the genetic

and molecular mechanisms involved in human hydrocephalus and for this reason it is not yet possible to extrapolate to humans the genetic data obtained from animal models.

## **1.3 CSF PRODUCTION AND FLOW CIRCULATION**

### **1.3.1 CSF production.**

CSF is produced in the ventricular system by highly vascularized small organs called choroid plexuses (Figure 1.6 and 1.7). They start developing between the second and third month of pregnancy in humans and originate from the neural tube after its closure, arising from an extension of the ependyma lining the lateral, third and fourth ventricles (Hartwig and Paulus, 2010, Gato et al. 2004, Catala et al., 1998 and Dziegielewska et al. 2001).

The choroid plexus has morphological and functional polarity presenting ciliated, cuboidal choroidal cells, which are joined by tight junctions at the apical side. These cells form the apical membrane which is in contact with CSF, and on the opposite site a basal membrane with lateral interdigitations in immediate contact with fenestrated (leaky) nearby cerebral capillaries (Figure 1.7). The endothelium of capillaries, basal and apical membranes, and CSF form the blood-CNS barrier. The adequate functioning of this barrier is critical for CSF production and regulation of the brain's internal environment through production and movement of solutes that help to maintain homeostasis, CSF hydrodynamics and general brain health (Johanson et al. 2008, Hartwig and Wernes 2010, Oreskovic et al. 2010).

Human CSF is produced at a high rate (0.5 ml/min/g tissue) which varies from 0.3 to 0.6 ml/min. Production is controlled by hormonal and neuroendocrine modulation, and most CSF is contained in ventricles (25% of total space) and subarachnoid space (75% of total space) (Johanson et al. 2008). With age and in neurodegenerative diseases like dementia and Alzheimer, CSF volume increases while CSF outflow decreases leading to accumulation of toxic substances within the brain (Rubenstein 1998, Silverberg et al. 2003)



At early stages of fetal brain development, there are unique barrier mechanisms between blood, CSF and brain. These cause elevated levels of solutes (proteins) in the CSF by allowing high rates of transport of specific proteins from blood to CSF through the tubulocisternal endoplasmic reticulum of choroidal cells (Dziegielewska et al. 2000). Interestingly, these proteins are prevented from entering the brain extracellular space thanks to barriers at the CSF-brain interfaces on the ventricular lumen and the Piamater. These barriers consist of junctions between choroidal cells and disappear at early stages when CSF decreases its protein content in adulthood (Dziegielewska et al. 2000). The presence of unique barriers at early stages is crucial for prevention of free exchange of molecules at a critical time for the fetal brain, when CSF transports important signaling molecules for coordination of brain development (Dziegielewska et al. 2000 and Miyan et al. 2003). In addition, high protein content in CSF at early stages also favours the production of an elevated osmotic pressure in the ventricular system which contributes to ventricle expansion as the brain grows (Dziegielewska et al. 2000 and Dziegielewska et al. 2001). Since the protein content in CSF is much lower than in serum, the blood-CSF barrier permeability in the immature brain decreases with time and eventually becomes highly efficient at impeding movement of potentially damaging molecules from plasma to CSF through active transport mechanisms in the mature brain (Dziegielewska et al. 2000, Zhao et al. 2011).

The choroid plexus is a kidney-type organ and it has similar renal epithelial mechanisms and transfers a large volume of ions and water (Johanson et al. 2008). The secretion of ions, water and proteins for CSF production is an active process that involves pumps, ion channels, cotransporters and antiporters, and aquaporins that control fluid and solute exchange (Redzic and Segal 2004). Movement of solutes by membrane transporters occurs

in the basal membrane (plasma-facing) and apical membrane (CSF-facing) of the choroid plexuses, inducing osmosis as well as the transport of water and molecules inside the choroid plexus (Kimelberg 2004, Speake et al. 2001, Brown et al. 2004, Emerich et al. 2005).

Transport mechanisms in the choroid plexus respond to CSF variation in composition and concentration by modulating the transport of solutes through membrane receptors. Receptors are stimulated by CSF neuropeptides to alter metabolism of secondary messengers and the ion transport occurring in parallel with CSF production (Scavone et al. 1995). Hormones like vasopressin and angiotensin II stimulate their corresponding receptors and induce choroidal cells to down-regulate CSF production (Johanson et al. 1999). Similarly, stimulation of vasopressinergic receptors by hormones results in reduction of Cl<sup>-</sup> efflux from choroid plexus epithelium and decreased CSF formation (Faraci et al. 1990). Atrial natriuretic peptide (ANP), a regulator of AQP-1 channels, is also involved in modulation of CSF production through downregulation or upregulation of receptors' expression in hydrocephalus (Steardo et al 1987). Variations in ANP receptor density and CSF production also follow changes in CSF hydrodynamics (Mori et al. 1990). Transport of proteins and vitamins across the choroid plexus also occurs through endocytosis and transcytosis (Smith et al. 2004, Zhao et al. 2011). Vitamin transport within the choroid plexus, specifically, is mediated by vitamin receptors and carriers, and this is described in detail in figures 1.14 page 58. A hypothetical model for folate transport from the choroid plexus to cerebral cortex and possibly to other areas of the brain by means of exosomes acting as folate shuttles in CSF was recently reported by Grapp et al. in 2013 and this model is described in figure 1.15 on page 61.

In conclusion, the choroid plexus has a secretory function in the release of water, proteins, ions, vitamins, hormones and growth factors into CSF. Interestingly, this function happens in parallel to a second function, which is the clearing of CSF acting as “ectopic renal tubular epithelium”, removing toxic metabolites from the fluid by pumping them into the blood, “filtering” CSF in reverse direction to the known blood filtration system observed in the kidney (Johanson et al. 1995 and Johanson et al. 2008).

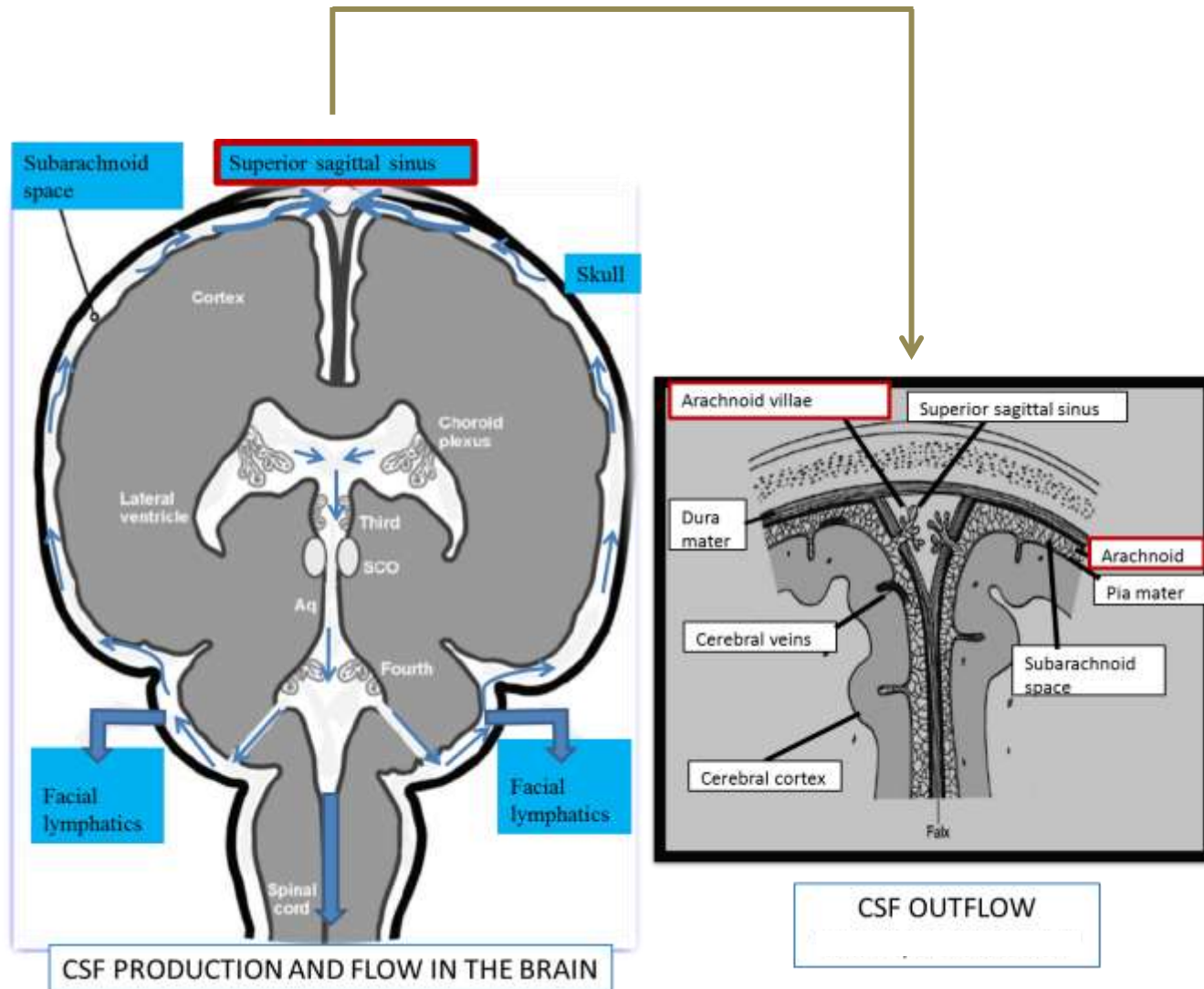
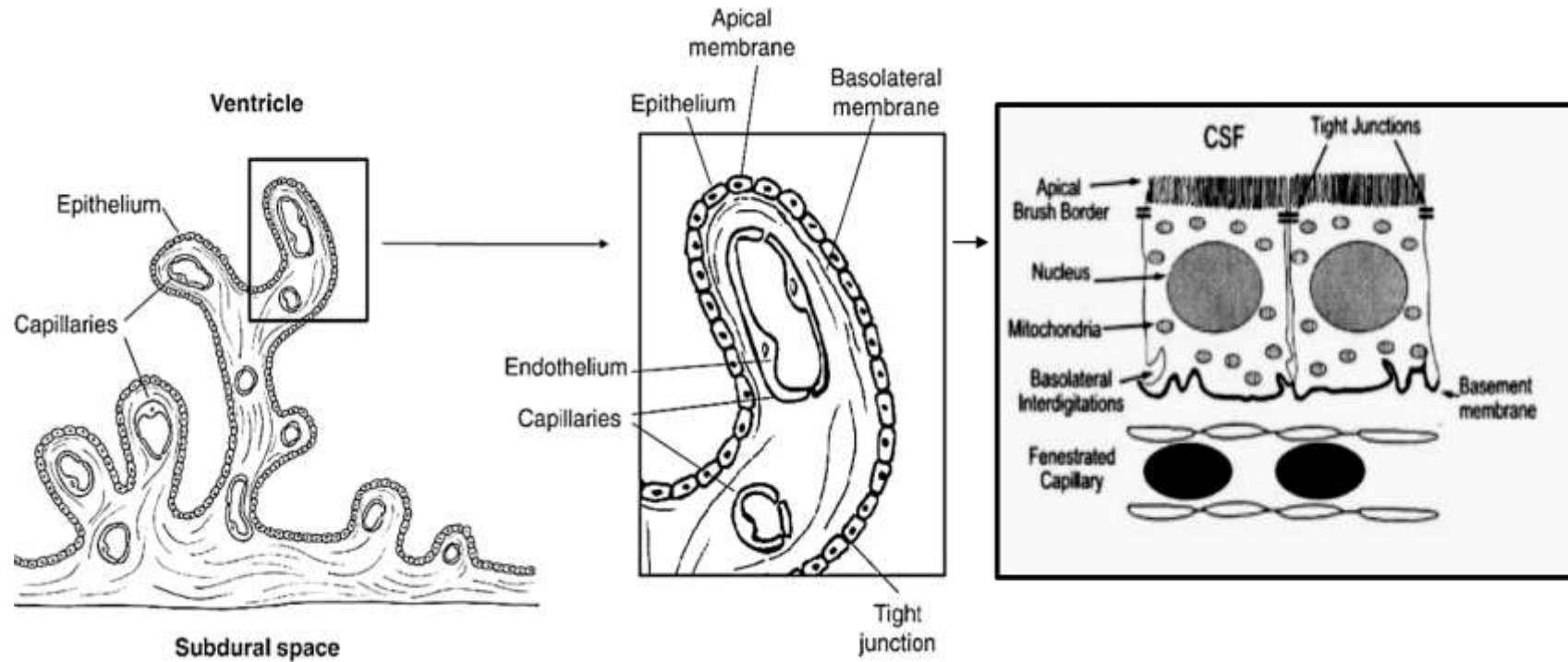


Figure 1.6. CSF FLOW. CSF (blue arrows) is produced in the choroid plexuses of lateral, third and fourth ventricles and progresses towards the spinal cord, facial lymphatics and the subarachnoid space, leaving the brain through the arachnoid villae in contact with the superior sagittal sinus. The grey arrow indicates the CSF outflow area (arachnoid and superior sagittal sinus), (square).



**Figure 1.7. Choroid plexus structure and the blood-CSF barrier. The choroid plexus is formed of ciliated and cubical epithelia cells joined by tight junctions at the apical membrane bathed by CSF. At the opposite site of the apical membrane, the basal membrane is in contact with fenestrated capillary. Capillary, basal membrane and apical membrane along with the CSF form the blood-CSF barrier. Numerous unique fenestrated capillaries go through the choroid plexus and connect creating an intricate network (Speake, T. et al. 2001). The choroid plexus epithelia folds, creating branched structures which contain a large number of villi. (Modified from Oreskovic et al., 2010 and Johanson et al. 2008)**

### **1.3.2 CSF flow circulation**

According to the traditional hypothesis of hydrodynamics, CSF circulation is possible thanks to the cardiac cycle, which creates a pulsatile flow from the main site of production (choroid plexuses) to the sites of absorption (arachnoid villi or granular arachnoid and nasal facial lymphatics) (Wagshul et al. 2011) (see Figure 1.6) It is also thought that CSF pulsations depend on arterial hemodynamics in the choroid plexuses (Egnor et al 2002). CSF flow is unidirectional and fluid is actively and continuously produced against intracranial pressure. Formation of CSF and reabsorption is balanced to keep high CSF pressure within the ventricles (100 mm H<sub>2</sub>O) in humans (Upton et al. 1985). At the same time, CSF pressure within the ventricles is higher than vascular pressure in dural venous sinuses, and disturbances of CSF pressure (low pressure) by toxic substances can inhibit production of fluid by the choroid plexus (Murphy et al. 1989, Johanson et al. 1990 and Maren 1988). CSF flows from the lateral ventricle to the III and from the III to the IV through the aqueduct of Sylvius (Figure 1.6). The flow continues from the IV ventricle, through Foramina into the subarachnoid space, and finally reaches the granular arachnoids where it is “filtered” and passed to the superior cortical sagittal sinuses in the subarachnoid space and the spinal subarachnoid spaces (Egnor et al. 2002). Most of the CSF leaves the brain through the leptomeninge arachnoid, and a small proportion is absorbed in the facial lymphatics (Miyan et al. 2003). CSF is constantly replenished with an average production of 500ml in 24 hours, and it is the continuous CSF secretion into the ventricles what creates a flow that allows CSF nutrients to reach every single area of the brain for cell division and cell differentiation into specialized tissues and organs of the CNS (Johanson et al. 1995 and Johanson et al. 2008). Only a balance between absorption and production of CSF can lead to permanent and normal fluid flow through the brain and subarachnoid spaces, and thus the correct functioning of the brain (Rekate, 2008).

## 1.4 CSF COMPOSITION

Adult CSF is colourless and very similar in composition to plasma but with lower protein content: 25 nM compared to 6500 nM in plasma (Segal 2001). 99% of adult CSF is water, but importantly, the remaining 1% comprises ions ( $\text{Na}^+$ ,  $\text{K}^+$ ,  $\text{Mg}^{2+}$ ,  $\text{Cl}^-$  and  $\text{HCO}_3^-$ ) vitamins (folates), hormones (angiotensin and vasopressin), growth factors and proteins principally globulins, albumin and immunoglobulins which are crucial to provide an optimal microenvironment for brain cell function (Segal 2001, Chodobski and Szmydynger-Chodobska, 2001). On the other hand, CSF in the developing brain, particularly in the fetal stages, is more complex and is highly rich in protein content, acting as a growth medium for neural stem cells, and providing all the components needed for neuroepithelial cell proliferation and cell survival, neurogenesis and CNS development (Dziegielewska et al 2000, Gato et al. 2004, Bueno et al. 1996, Miyan et al. 2003). The elevated protein content in fetal CSF is due to unique barrier mechanisms between blood, CSF and brain that encourage transport of specific proteins from blood to CSF through the tubulocisternal endoplasmic reticulum of choroidal cells (Dziegielewska et al. 2000). High protein content in CSF at early stages favors the production of an elevated osmotic pressure in the ventricular system, which contributes to ventricle expansion as the brain grows (Dziegielewska et al. 2000 and Dziegielewska et al. 2001). Remarkable evidence about the elevated level of proteins in embryonic CSF compared to adult CSF was found by Gato and colleagues in 2004, who demonstrated that at early stages of a chick's brain development there is a progressive accumulation of proteins in CSF.

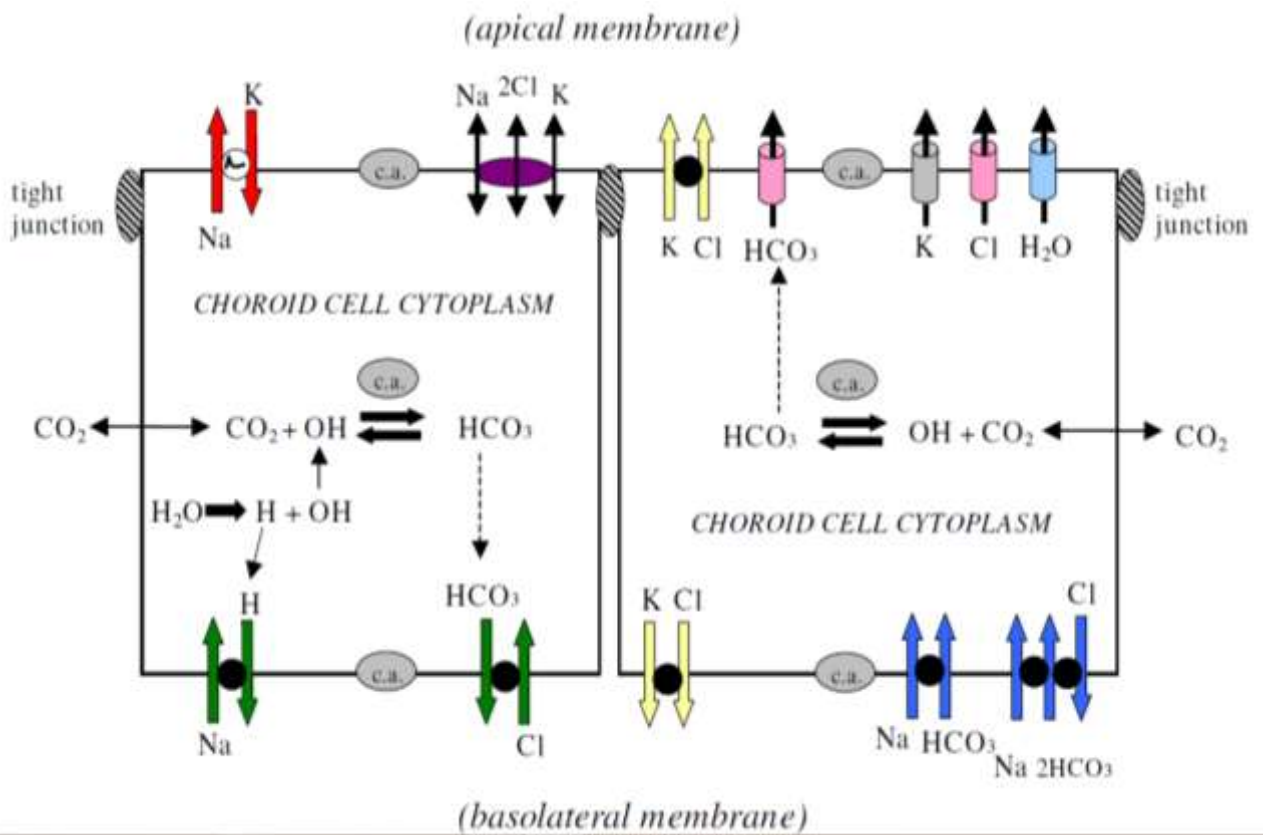
Proteins in fetal CSF need to be prevented from entering the brain's extracellular space. Otherwise, brain functioning can be compromised, and it is thanks to barriers at the CSF-

brain interfaces on the ventricular lumen and the Piamater that free exchange of molecules is avoided at a critical time when CSF transports key signaling molecules for coordination of development in the developing brain (Dziegielewska et al. 2000 and Dziegielewska et al. 2001, Miyan et al. 2003). Also, since the protein content in fetal CSF is much lower than in fetal serum, the blood-CSF barrier permeability decreases with time and eventually becomes highly efficient in impeding movement of potential damaging molecules from plasma to CSF through active transport mechanisms (Dziegielewska et al. 2000, Johanson et al 2008, Gato et al. 2004, Zhao et al. 2011).

The key components in CSF, other than proteins, are ions. These are present in adult and fetal CSF, and are involved in osmosis, a process coupled with the transport of water inside the choroid plexus for CSF production. These ions are sodium ( $\text{Na}^+$ ), chloride ( $\text{Cl}^-$ ), and bicarbonate ( $\text{HCO}_3^-$ ).  $\text{Na}^+$  efflux from choroid plexus to CSF is controlled by  $\text{Na}^+/\text{K}^+$  ATPase pumps that maintain the adequate  $\text{Na}^+$  concentrations inside and outside the choroidal cells, and create an osmotic gradient through the apical membrane to keep  $\text{Na}^+$  intracellularly low. Low intracellular  $\text{Na}^+$  also encourages the transport of  $\text{Na}^+$ , present in blood, through the choroidal basal membrane by means of  $\text{Na}^+/\text{H}^+$  and  $\text{Na}^+/\text{Cl}^-$  co-transport (Figure 1.8). This continuous  $\text{Na}^+$  influx through the basal membrane into the choroidal cells, and the intracellular  $\text{Na}^+$  efflux into CSF through the apical membrane results in a constant transport of  $\text{Na}^+$  from blood to CSF and the creation of a  $\text{Na}^+$  osmotic gradient that allows  $\text{H}_2\text{O}$  to be transported from blood to CSF, (Brown et al. 2004). Additionally, water is secreted from the choroid plexus into CSF by means of trans-membrane channels called Aquaporins (AQP) which are present in the apical membrane (Figure 8). Inhibition of AQP1 has been suggested as a potential treatment for hydrocephalus (water accumulation in the brain), (Gunnarson et al. 2004). Other secondary active transport



involved in maintaining the osmotic gradient for CSF production occurs in the blood facing choroidal membrane to permit  $\text{Cl}^-$  inward transport through exchange with extracellular  $\text{HCO}_3^-$ . Intracellular  $\text{HCO}_3^-$  is also produced by carbonic anhydrase (c.a) from  $\text{CO}_2$  for exchange with  $\text{Cl}^-$ .  $\text{K}/\text{Cl}$  cotransport helps maintain cell volume (Johanson et al. 2008).



**Figure 1.8. Ion transporters and channels in mammalian choroid plexus. CSF production is possible thanks to coordinated transport of ions and water from the basolateral membrane to cytoplasm and from cytoplasm across the apical membrane into ventricles (Adapted from Johanson et al. 2008).**

CSF composition changes as it flows away from the site of production (choroid plexuses) to the site of absorption (arachnoid villae and nasal facial lymphatics). This is due to ion-exchange of CSF with the interstitial fluid that is produced from the capillary bed in the brain, and the ion-exchanged between CSF and the limiting membrane of neurones, piamater and glial cells (Johansson 1995). Additional components are added to the fluid from the choroid plexus, located in the third and fourth ventricles, as well as from the circumventricular organs circling the cerebral aqueduct at the exit of the third ventricle and the pineal gland (Miyan et al. 2003). For instance, the subcommissural organ (SCO) in the roof of the aqueduct of Sylvius (figure 1.6) secretes glycoproteins into CSF, with a function in axonal guidance and activity on neurite outgrowth. These glycoproteins produced early in development are called SCO-spondins and they aggregate in CSF to create Reissner's fibres forming thread-like structures that are part of the central canal of the spinal cord (Gobron et al. 2000 and Vio et al. 2008).

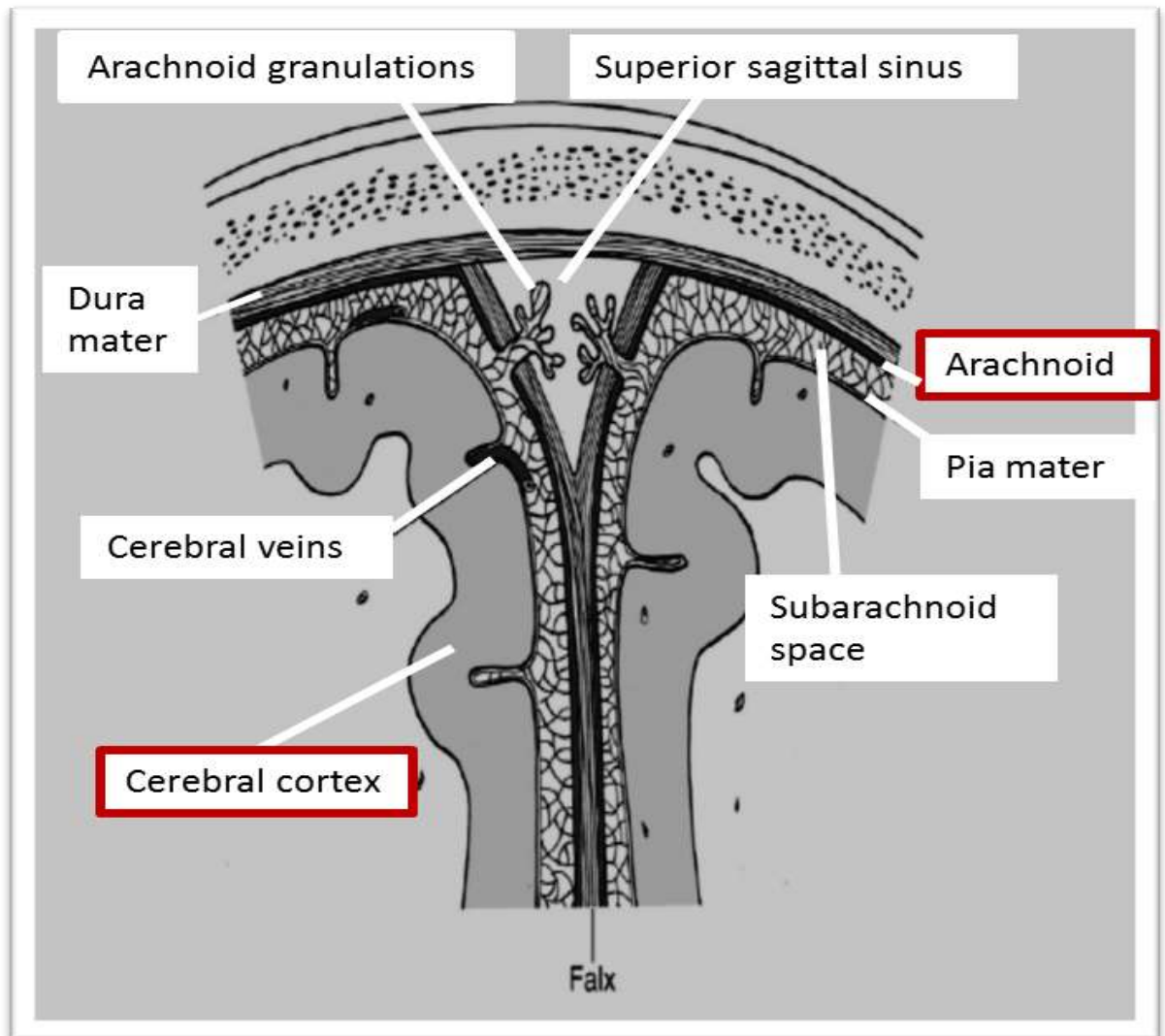
Abnormalities in CSF composition separately and/or in combination with impaired secretion, circulation and absorption have all been linked to different neurological conditions. For instance, high levels of immunoglobulins in CSF are indicative of inflammatory neurological disease (Harrington and Merrill 1988, Chu et al. 1983). Alterations in the levels of nerve growth factor (NGF), transforming growth factor (TGF) and fibroblast growth factor (FGF) are associated with Alzheimer's disease (AD), (Nishio et al. 1998). Furthermore, NGF has been acknowledged as a biomarker for the diagnosis of multiple sclerosis, where this growth factor is highly increased (Suzaki et al. 1997). Other growth factors like stem cell growth factor (SCF) are thought to be linked to deficiencies in hematopoietic brain support caused by growth factor depletion in CSF and plasma, leading to AD (Laske et al. 2008). Our past investigations also demonstrated compositional

changes related to low levels of folate enzyme (FDH) in hydrocephalic CSF, which suggests that CSF variations in protein profile may lead to congenital hydrocephalus (Miyan et al. 2003, Cain et al 2009).

## 1.5 CSF ABSORPTION: THE LEPTOMENINGE ARACHNOID

### 1.5.1 Morphology

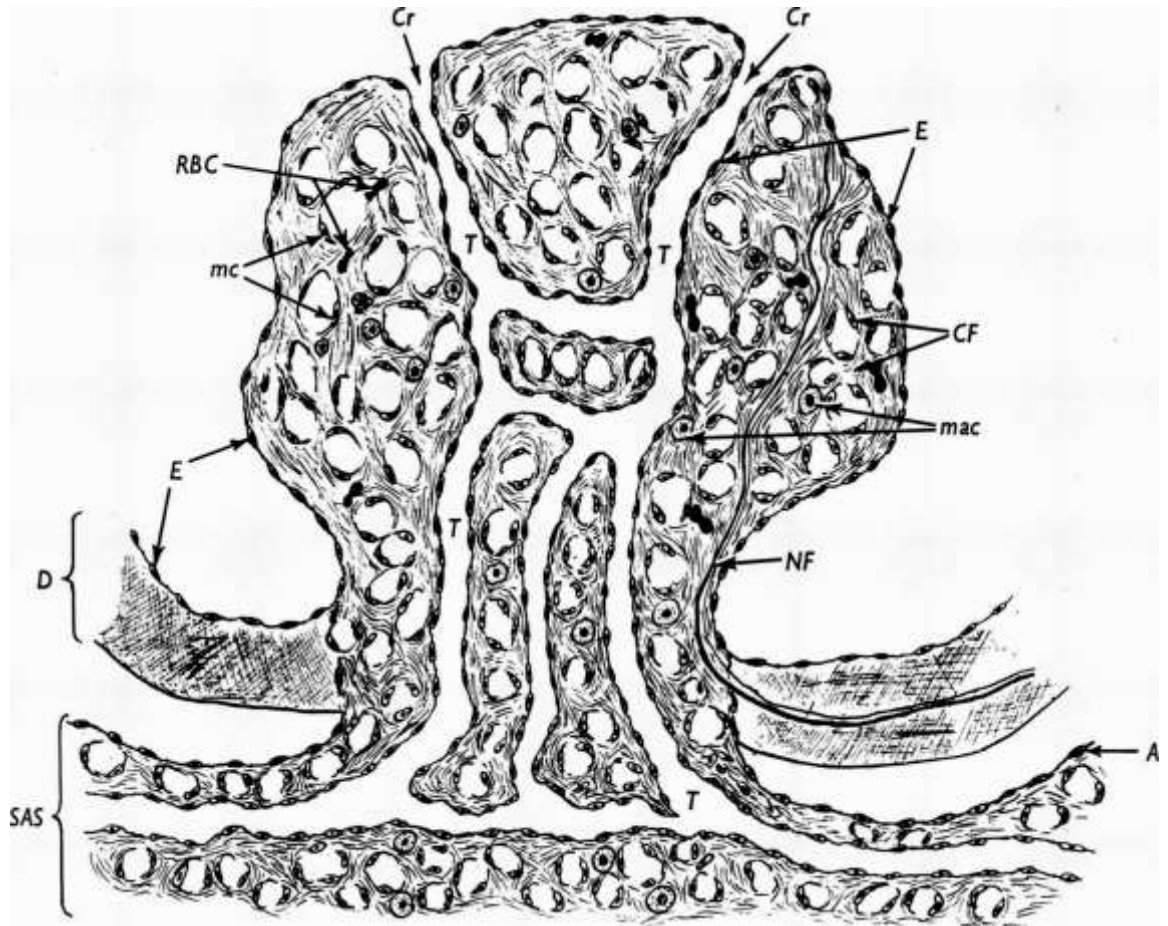
The leptomeninge arachnoid derives from the neuroectoderm, extending from the filum terminale to the external surface of the cerebrum, and is located between the meninges duramater and piamater (Figure 1.9).



**Figure 1.9. CSF outflow through arachnoid granulations. The arachnoid is a web-like layer of the brain in contact with the duramater in its apical side and with piamater in the basal side. The arachnoid tissue protrudes to produce arachnoid granulations that allow an increased surface area for CSF drainage. Arachnoid granulations are in contact with the endothelia of the superior sagittal sinus for CSF egress (adapted from Oreskovic et al., 2010).**

Similarly to the choroid plexuses, arachnoid cells are part of the CSF-blood barrier, and have apical-basal polarity, forming tight junctions to create a barrier to solute and water flow (Janson et al. 2011). In the human fetal brain the arachnoid protrudes, forming the arachnoid microvilli that differentiate into arachnoid granulations at 18 months of age (Clark 1920). Arachnoid granulations are in contact with the dural wall of the sinus for CSF egress in conditions of high CSF pressure (Turner et al. 1961, Upton et al. 1985 and Zakharov et al. 2004). Arachnoid villi and granulations are similar in structure. Thus, the term 'granulation' is used to denote structures visible to the eye while "villi" are structures very similar in morphology but only observed with the aid of a microscope. Arachnoid granulations or arachnoid villi physiological role in the brain is still a subject of controversy and after several attempts to elucidate its involvement in CSF outflow the specific mechanism is not yet understood and awaits fully characterization.

Both, arachnoid villi and arachnoid granulation are composed of protuberances with small channels or tubules that remained closed within the venous sinus at low pressure and open when CSF pressure is high, working similarly to a one-valve mechanism (Welch & Friedman 1960, Upton et al. 1985 and Upton et al. 2010).



**Figure 1.10. Graphic reconstruction of mammal arachnoid granulation. SAS: subarachnoid space, D: dura, A: arachnoid membrane, T: tubule, NF: nerve fibres, E: endothelia, mc: mesothelial cell, mac: macrophage cell, CF: collagen fibres, NF: nerve fibres, Cr: crypt (adapted from Jayatilaka, 1965).**

Externally, arachnoid granulations are cauliflower-like shape structures with 1100  $\mu$  width and 1000  $\mu$  height that appear near the opening of cerebral veins into the superior sagittal sinus. Subarachnoid tissue and arachnoid membrane is compressed and through gaps in the dura reaches the venous sinuses to form part of their walls. Further, surface epithelial cells cover the arachnoid granulation to become part of the walls of blood vessels (endothelia) in the dura. Internally, arachnoid granulation presents crypts and channels or tubules lined with endothelia as well as a core of mesothelial cells that create networks (trabeculae) surrounded by collagen fibres that are at the same time engulfed by endothelia (Jayatilaka 1965, Conegero & Chopard 2003 and Grzybowski et al.2006).

### **1.5.2 CSF absorption**

A large body of research on CSF outflow models describes the arachnoid villae and arachnoid granulations as the main brain structures for CSF egress, with unidirectional flow through each single villus in situations of elevated CSF pressure, and lower surrounding blood pressure (Clark and Le gross in 1920, Bradbury 1979, Levine et al. 1982, Butler et al. 1984, Upton et al. 1985, Glimcher et al. 2008 and Holman et al. 2010). Arachnoid granulations are created as a result of raised CSF pressure, which forces the arachnoid villi to protrude further into the sinus. Such a phenomenon was observed by Butler in 1984 who detected numerous pinocytotic vesicles in the endothelium lining the arachnoid villi. In another similar study, vacuoles, rather than vesicles were observed in the monkey sinus endothelium at elevated CSF pressure, suggesting that a macrovacuolar system may allow passage of particulate matter through arachnoid villi into the venous sinus and then into the general circulation (Tripathi et al. 1974 and Takahashi et al. 1993). Micropinocytotic vesicles, as well as paracellular transport in wider spaces between endothelial cells and large intracellular vacuoles, were also identified in human arachnoid granulation cells grown “in vitro” on filter membranes that were subjected to water flow pressure, mimicking the effect of CSF pressure on arachnoid granulation. These vacuoles fused to create transendothelial channels for transport of molecules from arachnoid granulation into venous sinus (Grzybowski et al. 2006). Other studies by Gupta and colleagues in 2010 revealed that CSF pressure is approximately 3 to 5 mmHg higher in the venous sinuses than in the granular arachnoid, and that this difference in pressure forces CSF flow from the subarachnoid space across the basal membrane of arachnoid granulations to the apical membrane, to finally drain into the venous sinuses. This finding supports previous published research and thoughts by many scientists, among others Tripathi et al. 1974, Upton et al. 1985, Takahashi et al. 1993, Glimcher et al. 2008, Holman

et al. 2010 and Gupta et al. 2010). Thus, arachnoidal CSF drainage is considered the main approach to CSF outflow (Holman et al. 2010); however, how this occurs is not yet fully understood, and until now, the given explanatory mechanisms have remained controversial. In this context, other plausible sites proposed for CSF absorption are the olfactory nerves (Erlich et al. 1986) and optic nerves (Erlich et al. 1989) as well as the cribriform plate, nasal submucosa and cervical lymphatics (Mollanji et al. 2001, Koh et al. 2006, Johnston et al. 2004 and Johnston et al. 2005). An important alternative explanation for CSF outflow mechanisms is the work of Mollanji and colleagues in 2001. They demonstrated that obstruction of the cribriform plate impedes CSF drainage and increases intracranial pressure. Also in agreement with this investigation, Johnston and colleagues microfilm injection studies on non-human primates provided evidence that the main route for CSF drainage at low intracranial pressure is via the extracranial nasal lymphatics. These researches proposed that arachnoid villi and granulations may be an auxiliary system for CSF egress, occurring only in conditions of high intracranial pressure. However, whether the olfactory route is the primary site for CSF absorption in humans remains to be proven, as the specific mechanism for CSF flow in cranial nerves reaching the eyes and nose is still awaiting characterization (Johanson et al. 2008).



## 1.6 THE HYDROCEPHALIC TEXAS RATS ANIMAL MODEL



**Figure 1.11.** The image shows a Sprague Dawley pup (animal above, control normal rat) in contrast to a hydrocephalic pup (animal below, Texas rat). The red arrow points to the dome cranium on the hydrocephalic head, which is absent on control head (blue arrow).

Hydrocephalic Texas rats were first discovered in 1981 in Texas, after observations of sudden death from an unknown cause within a colony. Brother-sister matings from this colony were carried out to establish a breeding colony that gave rise to 23% of newborn pups with hydrocephalus. Hydrocephalic pups had an apparent normal growth until the third week of age but stopped growing after that (Kohn et al. 1981)

Genetic analysis of this colony suggested that Texas rats are the result of an autosomal monogenetic spontaneous mutation (Cai et al. 2000). Jones and colleagues genome-wide linkage studies in 2001 using backcross progeny revealed that there are 4 loci involved in

the development of hydrocephalus in Texas rats, although the specific genetic defect still requires clarification (Jones et al. 2001).

Congenital hydrocephalus onset in Texas rats happens between the 17 and 18 gestational days, and it is apparently due to stenosis of the aqueduct of Sylvius and morphological changes of the subcommissural organ (Jones et al. 1988). Discrepancies in these findings were stated by Oi and colleagues in 1998, as they did find negligible changes in the development of periaqueductal structures at gestational day 17 using LEW/Jms rats; (an animal model for inherited congenital hydrocephalus). Oi and colleagues compared Texas rats with LEW/Jms rats' morphological changes for aqueductal occlusion, and reported differences between animal models. Thus, whereas in Texas rats the aqueduct collapses at day 17, in LEW/Jms there is a reduction in number of ependymal cells at the level of the narrowest site of the aqueduct with an intact aqueduct. Hence, it was concluded that the mechanisms for stenosis of the aqueduct of Sylvius in these two types of congenital hydrocephalus models is completely different. Unfortunately, at present, the aqueduct changes during development in humans cannot be properly characterized. Nevertheless, brain development in rodents during the neonatal period is similar to that in humans in the late fetal period, and this means that the Texas rat model is suitable for studying human congenital hydrocephalus. Proof of this is that human fetal hydrocephalus at stage 23 (56 days) shares comparable cerebral cortex abnormalities with Texas rats between embryonic days 17 and 18 (O'Rahilly and Müller 1987, Raimondi et al. 1976 and Kohn et al. 1981).

Texas rats are classified as affected and unaffected depending on the type of changes occurring in brain parenchyma and the presence or absence of brain dilation at gestational day 18. Thus, unaffected rats' brain parenchyma grows similarly to that of normal rats, whilst affected rats present enlarged ventricles and no development of the brain

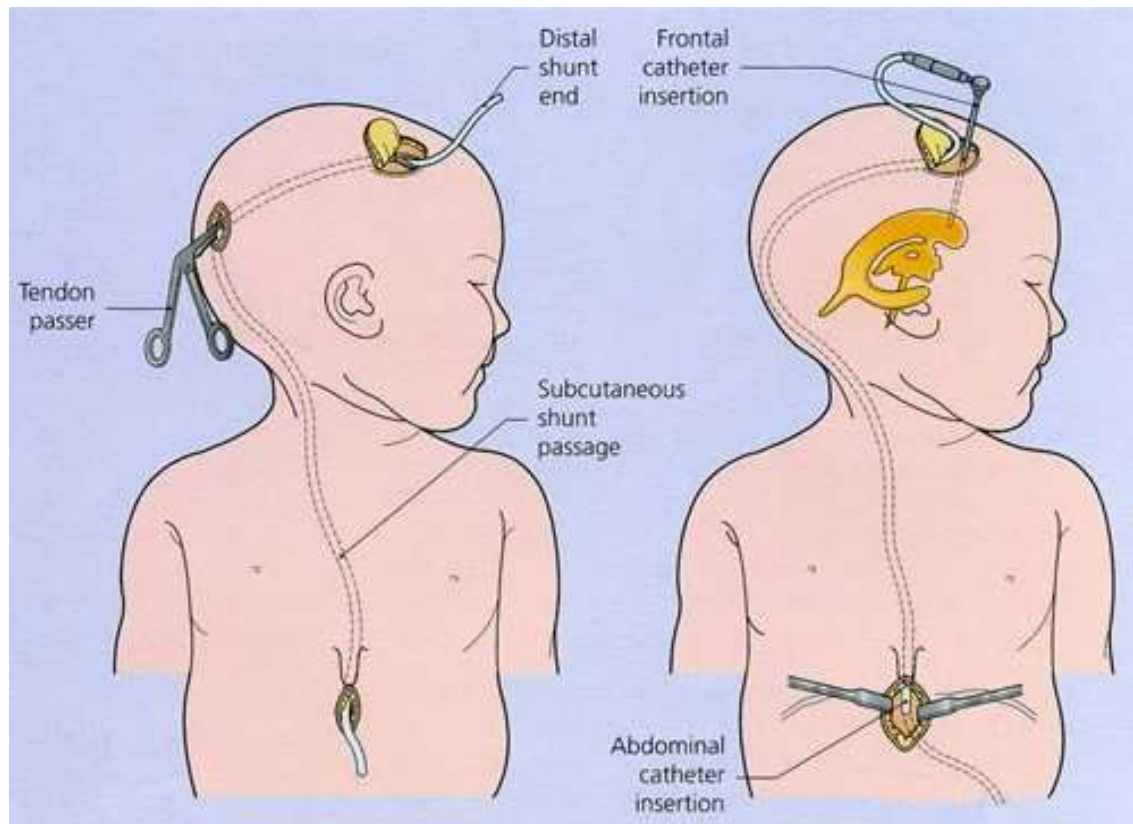
parenchyma at all (Mashayekhi et al. 2002). Ventriculomegaly in affected rats continues from embryonic day 18 towards the postnatal period (Jones et al. 1998). In addition, cerebral cortex morphological analyses of affected Texas rats demonstrate that the germinal neuroepithelia of these rats is narrower than in normal rats during fetal stages (Jones et al. 1998). Interestingly, reduced cortical thickness is not caused by raised intracranial pressure, as was thought in the past, as this event happens earlier in development, at day 10, instead of day 19 when decreased in brain parenchymal thickness is clearly noticeable (Mashayekhi et al. 2002, Owen-lynch et al. 2003).

Therefore, studies with the Texas rats animal model provided evidence that congenital hydrocephalus is not only related to brain damage caused by elevated intracranial pressure due to CSF built-up in the brain ventricles. In this context, Owen-Lynch and colleagues' studies in 2003 demonstrated that decreased cortical mantle in the affected Texas rats is due to an inefficient radial glia, blocked in the S phase of their cell cycle and unable to proliferate and exert their functions as scaffolding for subsequent generation of enough neurons to populate the upper layers of the cerebral cortex. Histological analysis showed that radial glia cells have elevated levels of DNA, and when these cells were exposed to hydrocephalic CSF "in vitro" proliferation was impeded. This contrasted with normal, CSF which was beneficial for cell growth, and demonstrated the importance of CSF for brain development. Since "in vivo" cerebral cortex cells were arrested in the S phase of the cell cycle but remain able to proliferate "in vitro", a lack of nucleotide availability was suggested. These findings also explain the inability of radial glia to complete the S phase of the cell cycle and progress into mitosis. Since folate metabolism is vital for the production of nucleotides, it was proposed that the folate metabolic cycle may be impaired in hydrocephalic Texas rats. Nabuni and colleagues' experimental results in 2004, as well as Cain and colleagues' findings in 2009, confirmed this postulate after LCMS and

Western blotting analysis of CSF showed a lack of the folate enzyme FDH in hydrocephalic CSF. Further “in vitro” experiments using cerebral cortex progenitor cells treated with hydrocephalic CSF, showed an increase in cell proliferation when folates and the nucleoside thymidine were added to the media. As a result of these findings, it was concluded that a defective folate metabolic cycle may lead to congenital hydrocephalus caused ultimately by changes in CSF composition and folate protein profile.

## 1.7 TREATMENT FOR CONGENITAL HYDROCEPHALUS

At present, ventriculoperitoneal shunt or ventriculostomy is the conventional method for treating hydrocephalus. This technique involves making surgical insertions of bypass tubes or catheters in the brain and peritoneal cavity to channel brain CSF outflow into the peritoneal cavity, thus improving drainage of obstructed CSF (figure 1.12). Unfortunately, failure rates are high in the shunting techniques and the complication rate in terms of infections and/or shunt failure for the first year of a newborns' life is about 17%. By 2 years of age, this rises to almost 50% (Kazan et al. 2005). In spite of shunting, neurological deficits still remain in hydrocephalic patients, due to the increased intracranial pressure exerted by CSF before shunting (Oreskovic et al., 2010). These facts highlight the necessity of an alternative non-invasive treatment in the future to replace the current methods.



**Figure 1.12. Schematic representation of the ventriculoperitoneal shunt technique. Surgical incisions are carried out at the frontal and parietal bone as well as at the abdominal level, to incorporate a catheter that connects brain ventricles with abdominal cavity for release of obstructed ventricular CSF into the stomach. Adapted from [www.seattlechildren.org](http://www.seattlechildren.org)**



Folates are THF polyglutamate water-soluble cofactors that belong to the B9 vitamin family and are crucial for brain development. They are involved in a huge range of metabolic reactions, where their role is to accept and donate carbon atoms. All folate metabolic reactions are interrelated and constitute the folate-mediated, one-carbon metabolism cycle (Figure. 1.13). This cycle is active in the cytoplasm and in the mitochondria of mammals (Molloy and Scott 2001), and active folates carry one carbon atoms at three oxidation states, ranging from formate to methanol (Wagner 1995). Cytoplasmic folate-mediated one- carbon metabolism is required for the de novo synthesis of purines (provides the carbon-2 and the carbon-8 of the purine ring) and thymidylate (methylation of dUMP to dMTP), as well as for remethylation of homocysteine to methionine. Methionine can be converted to S-adenosylmethionine, which acts as a methyl donor for various methylation reactions (methylation of DNA, RNA and proteins). Further, the main source of folate-activated one-carbon units is serine (Wagner 1995, Shane 1995, Davis et al. 2004 Anguera et al. 2006 and Solansky et al. 2010). Cytoplasmic serine hydroxymethyltransferase catalyzes the THF-dependent aldol cleavage of serine to methylene-THF and glycine. Alternatively, Serine can be converted to glycine and formate in the mitochondria as folate-mediated one-carbon metabolism also takes place there (Suh et al. 2001, Anguera 2006). The formate produced in the mitochondria is a major source of one-carbon units for cytoplasmic one-carbon metabolism through its conversion to 10-formyl-THF by the trifunctional enzyme C1-THF synthase, also called methylenetetrahydrogenase-1. This encodes 10-formyl-tetrahydrofolate synthetase, methylene-THF dehydrogenase, and methenyl-THF cyclohydrolyase activities.

### **1.8.2 Folate binding enzymes and the folate metabolic cycle.**

There are two important folate binding enzymes associated with impairment of folate-mediated one-carbon metabolism: Methylene-THF reductase and FDH. Methylene-THF reductase disease is the most common inborn error of folate metabolism and consists of a deficiency in the mitochondrial version of this enzyme leading to severe psychomotor retardation, microcephalus and seizure (Garcia-Cazorla et al. 2008 and Megumi et al 2011).

A second important folate binding protein suspected to be involved in deficient folate metabolic cycle is the enzyme 10-formyl-THF dehydrogenase (FDH), also called Aldehyde Dehydrogenase L1 (ALDH1L1). FDH is a soluble protein (Cook and Wagner, 1991) mainly expressed in liver and brain (Girgis et al. 1998 and Hong et al. 1999). Its metabolic role in folate-mediated one-carbon metabolism has not been totally clarified yet (Anguera et al. 2006, Krupenco 2009, and Krupenco, 2010) but cellular in vitro models suggest that FDH may regulate the folate-mediated one-carbon metabolic network in specific cell-types (Min et al. 1988, Anthony and Heintz 2007, Strong and Schirch 1989 and Anguera 2006). Four physiological functions have been attributed to FDH. The first one is its function in removing excess of one-carbon units from folate metabolism by depleting 10-formyl-THF pools (Krebs et al. 1976, Champion et al 1994). Its second function is to facilitate the production of folate-activated one-carbons by channelling THF to enzymes that are located at the primary entry points in the one-carbon metabolic cycle. These enzymes are the cytoplasmic serine hydroxymethyltransferase and the trifunctional enzyme methylene-THF dehydrogenase 1, both of which have an important role in suppressing FDH activity in situations of high THF concentration (Fu et al 1999 and Kim et al 1996). According to Anguera (2006) these functions may be working alternatively, depending on the levels of FDH expression. Anguera also proposed that high levels of



FDH expression greatly reduce the supply of folate activated one-carbon units, meaning that THF becomes the primary cellular folate derivative. In other words, high FDH expression levels mean an increase in the amount of binding site availability for 10-formyl-THF, and this result in depletion of 10-formyl-THF pools through the FDH-catalyzed conversion of 10-formyl-THF to THF. This may cause defective cell growth by depletion of the supply of the one-carbon units in the form of 10-formyltetrahydrofolate. At the same time, low levels of FDH expression increase the 10-formyl-THF/folate ratio. This is consistent with the suggested role of FDH in facilitating the generation of folate activated one-carbon units. Since FDH has a higher affinity for THF than 10-formyl-THF in situations of low FDH expression, its activity depleting 10-formyl-THF pools is expected to be lower comparing to its folate channelling activity through cytoplasmic serine hydroxymethyltransferase and the trifunctional enzyme methylen-THF dehydrogenase 1 (Fu et al 1999 and Kim et al 1996, Anguera et al. 2006).

A third function attributed to FDH is its capability to sequester cellular folate and store it in the form of THF *in vivo* in normal conditions (Fu et al. 1999). The sequestering mechanism is due to the intracellular FDH levels exceeding the THF concentrations. In this scenario, all cytoplasmic THF is expected to be bound to FDH. This matches experimental results from animal models of mice lacking FDH expression, where in spite of a folate sufficient diet; the total folate concentration is reduced (Champion et al. 1994).

Finally, as a forth function, FDH has been suggested to inhibit purine biosynthesis by also depleting 10-formyl-THF pools (Krupenko and Oleinik 2002).

### **1.8.3 Known folate transporters and FDH as a potential folate transporter.**

Folate transporter mutations and loss of folate transport in the brain are both linked to cerebral folate deficiency and brain neurodegeneration in childhood (Steinfeld et al. 2009 and Grapp et al. 2014). Furthermore, the presence of folate receptor autoantibodies in plasma is associated with low folate in CSF, and with neurodegenerative disease (Ramaekers et al. 2005). The known folate transporters and the potential role of the folate bind to enzyme FDH are described below.

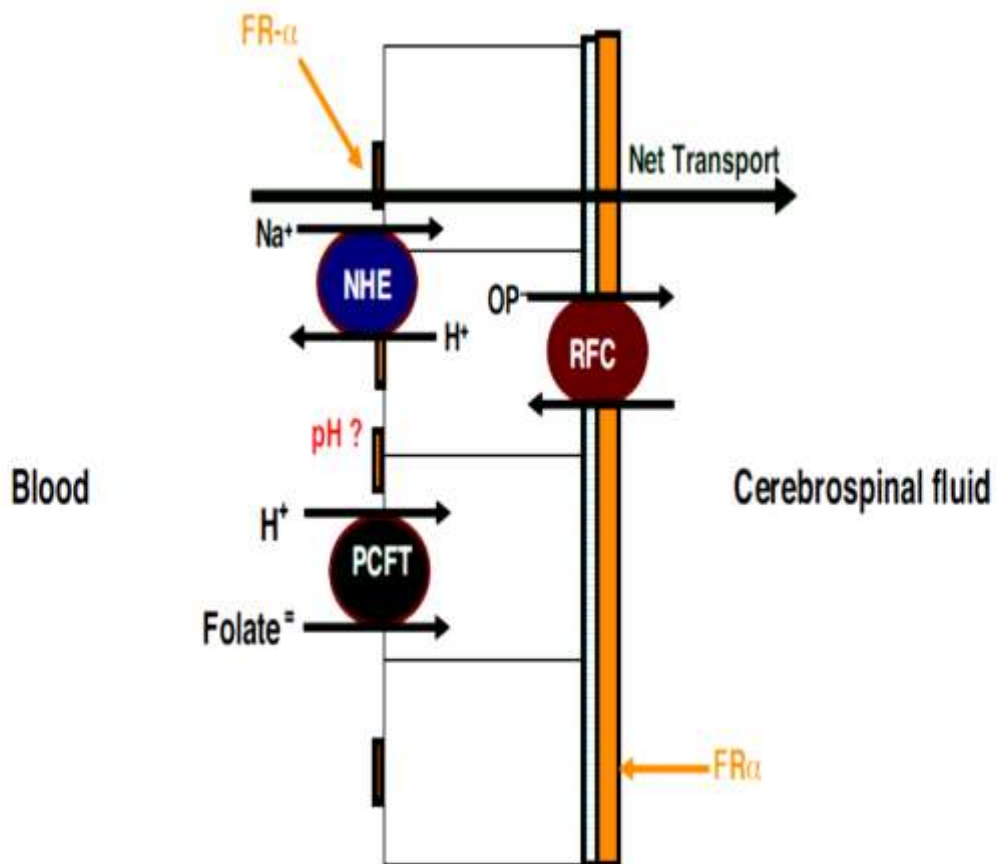
#### 1.8.3.1 Known folate transporters

The main known folate transporters in the brain are PCFT, RFC, and FR $\alpha$ . They have been characterized in the choroid plexuses; however, their potential expression in other areas of brain is also to be considered (Ramaekers et al. 2004 and Requena Jimenez et al. 2015).

It is accepted that folate transporters bind to soluble folates in blood for later secretion into CSF, with folate concentration in CSF doubling the systemic circulation levels due to the active transport occurring in the choroid plexuses. Folate transporters are only active at specific pHs, and rely on basal membrane transport (Na<sup>+</sup>/H<sup>+</sup> exchange), which is coupled to active transport by ATPases to achieve the suitable intracellular acidity that allows its functionality (Segal 2001, Zhao 2011).

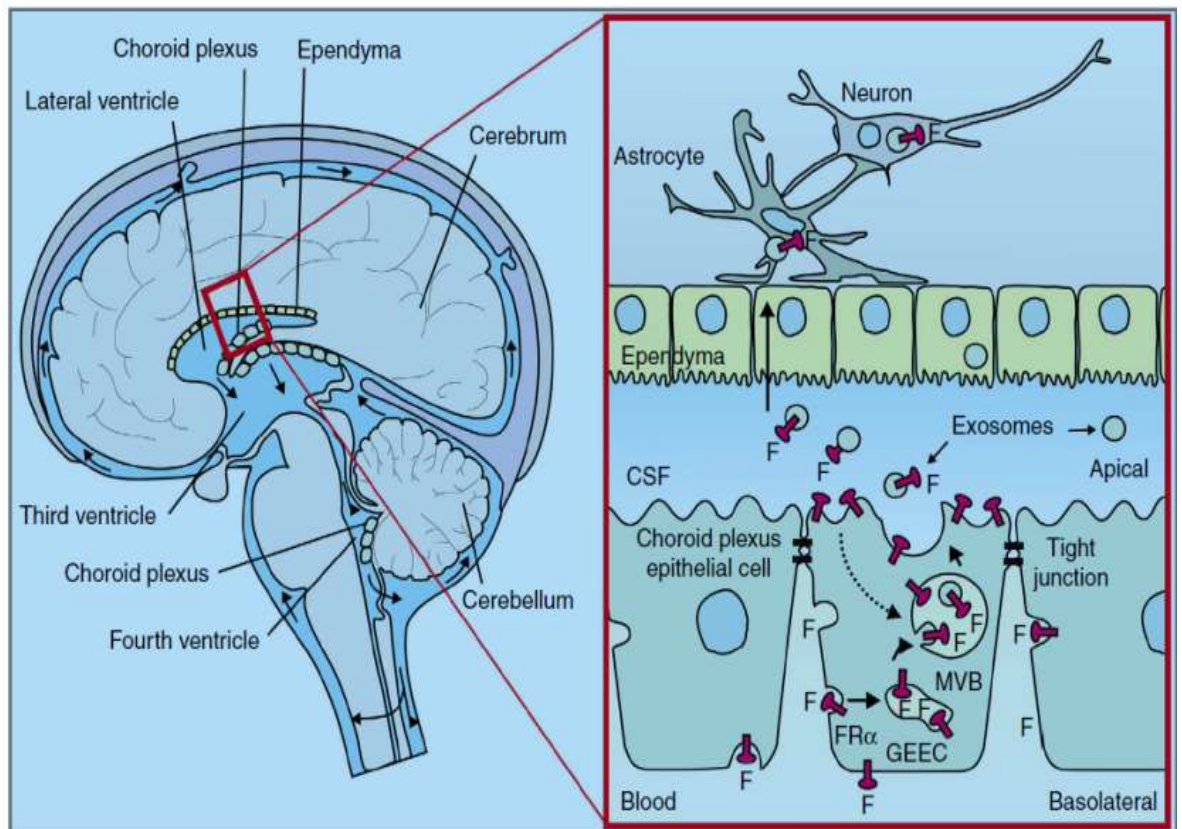
As illustrated in figure 1.14 below, FR $\alpha$  is anchored to the basolateral membrane of the choroid plexus by a glycosylphosphoinositol (GPI) domain, and transports folate via receptor-mediated endocytosis. At the same time, PCFT is also expressed along the basolateral membrane and carries folates from blood into choroid plexus cells in parallel with FR $\alpha$ . It has been also reported that PCFT transports 5mTHF in acidified endosomal compartments into the cytoplasm for later bind to FR $\alpha$  (Solanky et al. 2010).

Whereas FR $\alpha$  transports folates from blood to CSF (Selhub 1984 and Weitman 1992), RFC (SLC19A1) operates bidirectionally and is highly expressed at the apical brush-border of the choroid plexus membrane (Wang et al 2001). Accordingly, it is proposed that folate transporters work in tandem and they are all required for folate transport from blood to CSF (Zhao et al. 2011). A hypothetical model for folate transport including the three transporters is detailed below.



**Figure 1.14. Folate transport across the choroid plexuses in adults. Both the proton-coupled folate transporter (PCFT) and folate receptor (FR $\alpha$ ) are key transporters of folates from blood to cerebrospinal fluid across the choroid plexus cells. FR $\alpha$  is mostly expressed at the apical brush-border membrane along with the reduced folate carrier (RFC) whereas PCFT expression and net proton exchange (NHE) are mainly present in the basal membrane in contact with blood (Modified from Zhao R et al. 2011).**

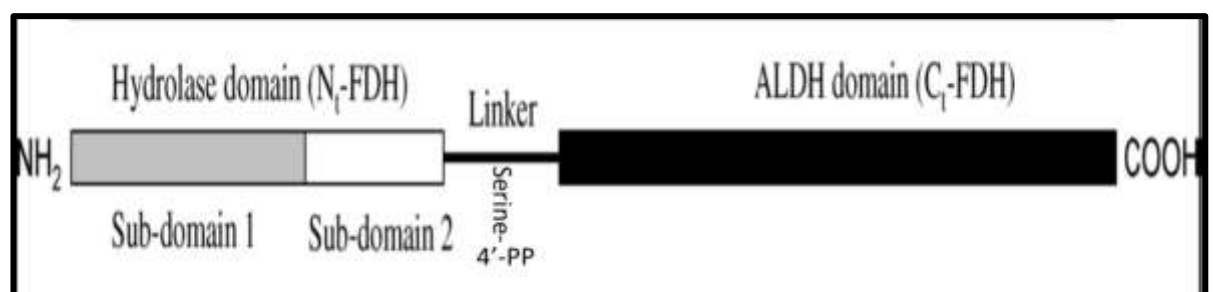
It is suggested that FR $\alpha$  depends on PCFT for folate transport as the former is susceptible to the acidity levels present within vesicles where PCFT transports 5mTHF. Moreover, FR $\alpha$  transport and its high affinity for 5mTHF may depend on folate extracellular concentrations. In this respect, folate transport through FR $\alpha$  seems to happen only at low folate extracellular concentrations, whilst folate transport at elevated folate extracellular levels is carried out by RFC (Zhao et al. 2011). Folate transport has been further described, and it is now believed that FR $\alpha$  is the main folate receptor responsible for folate (5mTHF) transport in the brain. Folate receptor-mediated endocytosis seems to allow transport of FR $\alpha$ -5mTHF complexes through the basolateral membrane of the choroid plexus, and the production of internal vesicles (endosomes) permits shuttling of FR $\alpha$ -5mTHF complexes across the choroid plexus to finally deliver them into CSF within exosomes. Exosomes reach the ependyma bathed with CSF, and provide folate to nearby astrocytes and neurons. See figure 1.15 below.



**Figure 1.15. Hypothetical model of human cerebral folate (5mTHF) transport by  $FR\alpha$ .** The black arrows show CSF flow and the rectangle indicates the magnified area including the choroid plexus and the ependyma lining the lateral ventricle. The basolateral membrane is in contact with blood circulation, where folates are transported. Folates bind to  $FR\alpha$  receptors anchored to this membrane by means of glycosphosphatidylinositol (GPI). Afterwards,  $FR\alpha$ -folate complexes are internalized through endocytosis, forming GPI-anchored protein-enriched early endosomal compartments (GEECs), and this is followed by translocation of  $FR\alpha$ -folate complexes from GEECS to multivesicular bodies (MVBs) or endosomes. Some folate is also transferred to PCFT located within acidic vesicles, to be later transported into the cytoplasm.  $FR\alpha$ -folate complexes leave the choroid plexus within exosomes to reach the ependyma and from here to astrocytes in immediate contact, to be later further transported into nearby neurons (adapted from Grapp et al. 2014).

### 1.8.3.2 FDH as a folate binding protein

Recent findings in our laboratory showed how the folate enzyme FDH may function as a folate transporter (Krupenko, 2009). FDH consists of three domains, the hydrolase domain, the intermediate or linker domain and the aldehyde dehydrogenase domain (See Figure 1.16). The intermediate domain, or linker, allows the enzyme to be enzymatically active by acting as a bridge between the other two domains (Krupenko 2009). Analysis of the linker sequence using the data base of proteins domains ([www.expasy.org/prosite/](http://www.expasy.org/prosite/)) suggests that this domain is a member of a group of carrier proteins with a serine bound to a 4-phosphopantetheine prosthetic (4-PP) swinging arm. This swinging arm allows the transfer of chemical groups between different domains displayed in multicomplex enzymes such as acyl carrier proteins. Therefore, it is suggested that FDH is a formyl carrier protein able to transport formyl groups from the N domain to the C domain through the linker or swinging arm similarly to acyl carrier proteins. Further, FDH may control in this way the production of THF and 10-formyl-THF pools by formyl transfer between domains (Anguera et al. 2006, Donato et al. 2007). Importantly, it is also thought that the addition of the serine-4-PP intermediate domain to FDH is a posttranslational modification occurring once the protein is folded and therefore FDH N domain may be found as a single domain within the cells (Donato et al. 2007) before later enzyme modifications.



**Figure 1.16. FDH domains. The linker domain is serine dependent and linked to a 4'-phosphopantetheine prosthetic group (4'-PP). The linker or intermediate domain joins the hydrolase domain (N domain) and the aldehyde dehydrogenase domain (C domain), making FDH functionally active.**

Thus, we hypothesize that enzymatically active FDH may co-exist with enzymatically inactive FDH acting as a mere folate binding protein handling folate to FR $\alpha$  to further transport it to different areas of the fetal brain.

In our laboratory, Sprague Dawley rat brain immunolocalization and Western blotting techniques detected high levels of FDH in cerebral cortex and embryonic CSF before the neural tube closes (day 17 of rat embryonic development). Interestingly, FDH was not detected at the choroid plexuses, and the FDH levels fell dramatically at embryonic day 18. In contrast, in hydrocephalic rats, FDH at embryonic day 18 was not released into CSF, but was immunolocalized at the same site as in normal rats; the cerebral cortex. In CSF, FDH was identified in vesicles (data not published yet) in normal and abnormal rats, and consistent with these results, other research group revealed the presence of CSF vesicles or nanospheres with an unusual membrane. These nanospheres were found in health and disease, and it was suggested they are responsible for humoral signaling mechanisms in the brain (Harrington et al. 2009 and Bachy et al. 2008).

Following our results, we suggest FDH may present an alternate folate transport mechanism to the usual folate transport by folate receptors, and reduced folate carriers. FDH-folate transport may be specific for certain areas of the brain like the cerebral cortex whereas other regions such as the choroid plexuses use preferentially PCFT, FR $\alpha$  and RFC.

### 1.8.3.3 Folates and folate deficiency

Low folate concentration in CSF is associated with different types of folate deficiency. A first type of folate deficiency is due to hereditary folate malabsorption, which is a condition clinically manifested after birth. Interestingly, this condition involves severe folate transport impairment at the choroid plexuses, and even when the blood folate levels are normal, CSF folate remains very low (Geller J et al. 2002). Folate deficiency can also be the result of mutations of the Folate Receptor 1 gene (FOLR1); FR $\alpha$ , leading to a type of folate deficiency that manifests several years after birth (Steinfeld et al. 2009).

In addition, folate deficiency, specifically 5-methylTHF deficiency, is associated with the presence of autoantibodies in blood against high affinity folate receptors located at the blood brain and blood-cerebrospinal fluid barrier. This type of folate deficiency has important negative repercussions for brain development, as 5-methylTHF is the predominant folate in blood, CSF and food (Ramaekers et al. 2004, and Ramaekers et al. 2005). Decreased 5mTHF levels are also linked to cerebellar ataxia, psychomotor retardation, dyskinesia, severe developmental delay, CNS calcifications, epilepsy and autism spectrum manifestations (Moretti et al. 2008). In our laboratory, recent studies on animal models of hydrocephalic rats revealed a possible relationship between folate imbalance and deficiency of specific folates in CSF (Cain et al. 2009). This finding implies that congenital hydrocephalus is also a type of folate deficiency. Folate deficiency alters dTMP, methionine, and S-adenosylmethionine synthesis, resulting in elevated rates of uracil misincorporation into DNA and DNA hypomethylation. Thus, maintenance of cellular folate concentration is vital for DNA synthesis, stability and expression. At the same time, intracellular folate concentrations depend on folate availability, uptake, polyglutamation, and turnover and export (Suh et al. 2001).



Previous findings in our laboratory from “in vitro” cerebral cortex primary cell cultures also showed that cell proliferation decreases when exposed to embryonic day 20 hydrocephalic CSF. This meant that CSF lacking FDH induced cell cycle arrest. Proliferation assays were used to measure DNA biosynthesis, and it was observed that cells were blocked at the S phase, which explained the inability of progenitor cells/radial glia cells to proliferate and differentiate. Also, stained sections from cerebral cortex showed a poorly developed cerebral cortex, and it was hypothesized that depletion of DNA due to a lack of FDH in CSF may explain the reduced thickness of the cerebral cortex and germinal epithelia observed after embryonic day 18, which coincides with CSF obstruction in the Sylvius aqueduct in the hydrocephalic rat (Mashayekhi et al. (2002). The possibility that components in hydrocephalic CSF may have inhibitory factors for normal cell growth and FDH release was considered.

In conclusion, our data lead to the conclusion that alterations in the expression or function of FDH cause an imbalance in folate metabolism, and abnormal cortical development of the brain (Cains, S. et al. (2009); Moretti P. et al. (2005); Hansen FJ. and Blau N. (2005)).

In relation to folate metabolites, our experiments also showed a decrease in 5-methylTHF in serum samples from adult H-Tx rats when compared with controls (Cains, S. et al. (2009)). However, 5-methylTHF concentration was similar in normal and abnormal foetal CSF, and this result did not lead to any conclusion.

#### 1.8.3.4 Folate treatment

The synthetically produced folic acid (pteroylglutamic acid) is used to fortify food in the USA (Geraldine et al. 2007). Food fortification has proven to be successful in increasing folic acid intakes pre-conceptually, preventing premature delivery, congenital malformations and neural tube defects such as spina bifida (Refsum 2001, Antony 2007, Scholl et al. 1996). Also, common dementia in the elderly is associated with folate and vitamin B12 deficiency. Consumption of fortified food, however, has negative effects for the elderly, as fortified food increases the risk of ‘masking’ megaloblastic anaemia caused by vitamin B12 deficiency. This is explained by the fact that metabolic functions of folate and vitamin B12 intertwine in the methylation cycle, and they affect each other, and the processes they modulate together (Lindenbaum et al. 1994, Joosten et al. 1997 and Geraldine et al 2007). Folic acid fortification masking vitamin B12 deficiency is also important in vegetarian populations which are deficient in vitamin B12 (Yajnik et al. 2006). Other negative effects of folic acid have been seen in epileptic patients, who experience frequent seizures (Reynolds 1968 and Dennis and Taylor 1969). Finally, folic acid has also been described as a risk factor for strokes (Motulsky, 1996). Interestingly, these investigations are in agreement with our results about the negative effects of folic acid supplementation. Thus, folic acid did not prevented hydrocephalus in pregnant Texas rats and even more, it did increased significantly the incidence of hydrocephalus within the progeny (Cain et al. 2009).

Folinic acid/leucovorin is considered a good alternative to folic acid because it is efficiently transformed into 5, 10-methyleneTHF and 5-methyl THF and has a higher bioavailability than folic acid (Spector, 1979 and Brocker, Bonhomme, Lods 1990). Folinic acid (5-formyl THF) has been used to improve psychomotor development in Down’s syndrome children, with success and no side effects despite its intense use during

the treatment (Blehaut 2010). Children with developmental delay and autism presenting low levels of 5-methylTHF have also benefited from treatment with folinic acid in terms of improvement in their motor skills. Nevertheless, their cognitive language and socialization skills remained delayed (Moretti 2005, Steinfeld, R et al. 2009).

In our laboratory, treatment with folinic acid and THF was carried out to study their effect on hydrocephalic rats at embryonic day 20. A mixture of folinic acid and THF at both at 2.25mg/kg successfully reduced the incidence of congenital hydrocephalus by 60%. In contrast and as aforementioned, treatment with folic acid did not decrease the incidence of hydrocephalus. It was proposed that whereas in conditions such as spina bifida, folic acid is needed for prevention before and during the first trimester of pregnancy (Tamura T. et al. 2006), in hydrocephalus, cerebral cortex abnormalities have to be fixed with folates throughout pregnancy, and perhaps a specific folate profile demand may be required by the foetus at different time points during its growth (Cains et al. 2009).

## **1.9 SUMMARY.**

Brain Cerebrospinal fluid (CSF) bulk flow is unidirectional and maintained thanks to a balance between CSF secretion from the choroid plexus and CSF absorption by arachnoid villi, where it drains into nearby blood vessels, thereby reaching the general blood circulation. Congenital hydrocephalus starts during the first trimester of pregnancy with impeded CSF flow, and consequent CSF build-up within the brain ventricles. This event is followed by CSF compositional changes, increased intracranial pressure, and, if untreated, brain damage and fetal death. Previous research has revealed a unique folate delivery system which serves the developing cerebral cortex. Abnormal folate provision due to impairment of this system was directly connected to a decrease in a CSF folate enzyme: 10-Formyl-Tetrahydrofolate dehydrogenase (FDH), which is also called aldehyde dehydrogenase type 1 (ALDH1L1). This enzyme acts as a folate binding protein and it is believed to be part of the brain mechanisms for folate transport and provision. In light of these findings, low FDH was linked with folate deficiency and the poor cortical development found in congenital hydrocephalus. Furthermore, it was proposed that this disorder is due to a folate deficiency caused by low FDH in hydrocephalic CSF, and that it can be alleviated through maternal folate supplementation. Past studies demonstrated that neither folic acid nor folinic acid supplementation on their own fix congenital hydrocephalus. However, folinic acid in combination with THF did successfully prevent and reduce the incidence of the condition in rodents. In this context, further investigation was carried out in this study to ascertain whether folates in the presence and absence of the folate enzyme FDH are beneficial for fetal brain development. The current study also aims to investigate the FDH - folate delivery system in the fetal brain in order to understand its role in CNS development and its relationship to currently known folate transport mechanisms (FR $\alpha$ ). Furthermore, we hypothesize that folates may prevent congenital hydrocephalus through a re-

establishment of CSF drainage and flow circulation at the level of the arachnoid membrane/villi. This assumption implies that the leptomeninge arachnoid may also be dysfunctional in the hydrocephalic brain due to a variation in hydrocephalic CSF composition. Finally, an overall analysis of the constituents uniquely present in normal CSF, hence missing in abnormal CSF, and vice versa, was carried out to establish associations with predicted activated and inactivated biological processes in congenital hydrocephalus, other than impaired folate metabolic cycle.

In general, the present study intends to achieve a better understanding of the roles of FDH and folates, as well as the discovery of other potential key CSF components involved in brain development. It is hoped that this will allow the discovery of key supplements and an adequate treatment for the prevention of a condition that can at present only be treated with invasive surgical procedures entailing life-threatening side-effects for the baby.

## **1.10 EXPERIMENTAL AIMS AND HYPOTHESIS**

### Aim and hypothesis 1: Effect of folates and FDH on cerebral cortex cell proliferation.

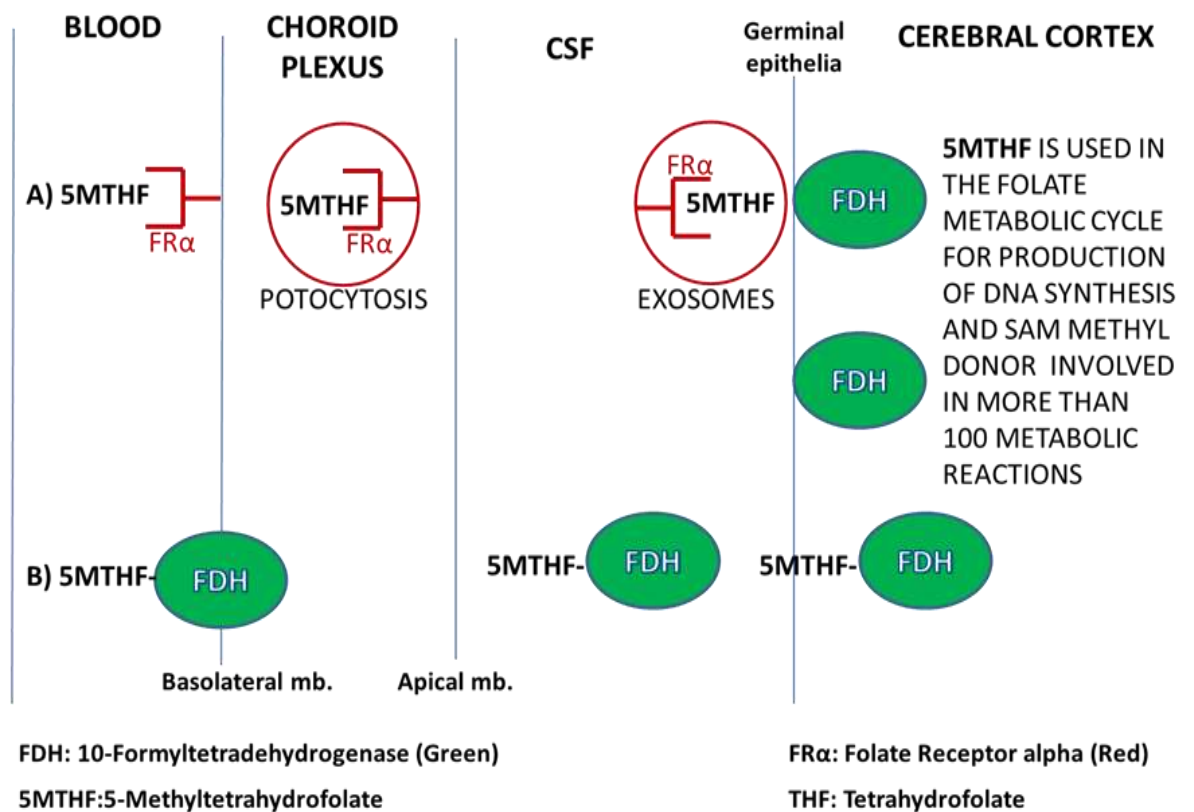
This study aims first to determine if there is a positive effect of folates on cerebral cortex cell division in the presence and absence of FDH, focusing on THF as this folate is proven to be a promising candidate for the treatment of congenital hydrocephalus in Texas rats. THF is an unstable natural folate, and for this reason we intended to stabilize it by linking it to specific fluorescence immunoglobulins using a commercially available kit. Fluorescence dyes may permit tracking of THF inside cells and visual confirmation and quantitative analysis of THF effect on cell growth. In conclusion, we hypothesize that folates, and specifically THF may encourage cerebral cortex cell division. “In vitro” experiments using primary cell cultures exposed to different concentrations of folates and FDH were performed to achieve this aim.

### Aim and hypothesis 2: FDH binds to 5mTHF.

FDH is a folate binding protein that binds to THF and 10-formyltetrahydrofolate. Interestingly, FDH binds to THF, its product of reaction, with 10 times more strength than its substrate 10-formyltetrahydrofolate. However, FDH affinity for 5mTHF has never been studied. Since, “In vitro” experiments in this research showed evidence that the presence of active ALDH1L in media supplemented with 5mTHF in the range  $10^{-4}$  –  $10^{-6}$  M (CSF levels) affects cell growth negatively, it was hypothesized that FDH may bind to 5mTHF extracellularly, impeding its transport inside the cells. To envisage a possible explanation for this finding, an “in house” ELISA technique was developed and optimized to evaluate whether FDH has any affinity for 5mTHF, our second hypothesis in this study.

**Aim and hypothesis 3: mRNA and FDH protein are expressed in the brain and co-localize with other folate transporters (FR $\alpha$ )**

This project also aims to clarify the folate delivery system to the developing cerebral cortex in the context of the known folate transport by FR $\alpha$ . The experimental approach is to determine the location of FDH protein and mRNA expression, and to measure and compare protein expression quantification in the normal and hydrocephalic brain. Within this aim, we also investigated whether FDH co-localized with FR $\alpha$ , the principal folate transporter in the brain. Sprague Dawley rats are used as control and Texas rats as the animal model for the condition. All animals are studied at embryonic day 18 when CSF starts circulating. The rationale behind this experimental approach is supported by the fact that FDH is a folate bind to protein and therefore may also function as a folate transporter that handles folate with FR $\alpha$ , working in tandem to provide the brain with the most abundant folate in food, 5mTHF. See Figure 1.17 below for hypothesis explanation:

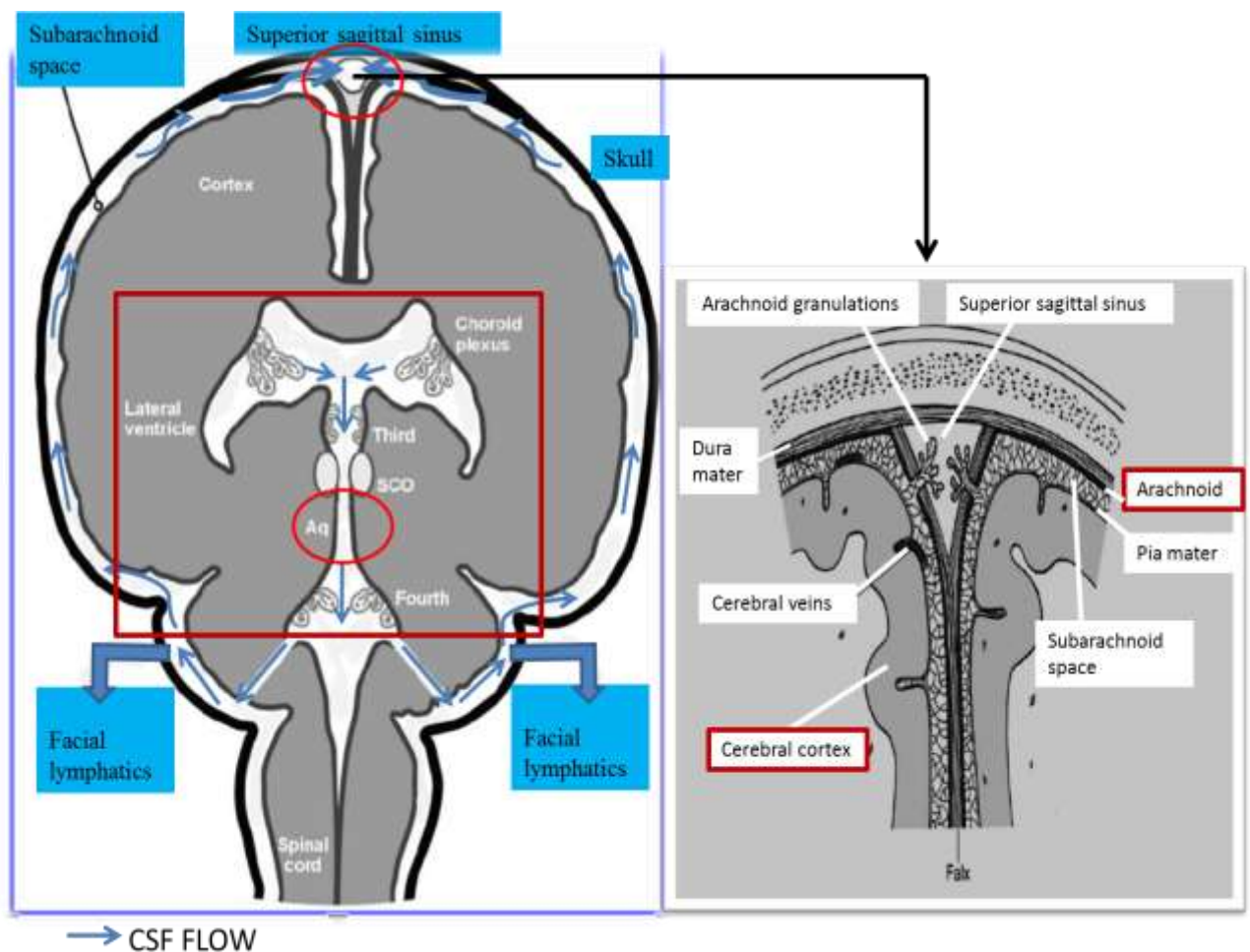


**Figure 1.17. Diagram representing 5mTHF transport by FR $\alpha$  (A) versus our hypothesis related to the role of FDH in folate transport (5mTHF) (B). A) 5mTHF is transported by FR $\alpha$  through the choroidal basolateral membrane by potocytosis (Solanky et al. 2010) 5mTHF-FR $\alpha$  complexes are engulfed by vesicles that leave the choroid plexus to enter the CSF as exosomes (Grapp et al. 2014). Exosomes shuttle 5mTHF-FR $\alpha$  complexes in CSF to later reach the cerebral cortex. 5mTHF is stored or used in the folate metabolic cycle. B) Hypothetical role of FDH in 5mTHF transport from choroid plexus to CSF and within cerebral cortex.**



Aim and hypothesis 4: Folates and FDH have an effect on arachnoidal cell growth.

The role of folates and FDH in arachnoid development is still unknown. Yet, it has been reported that CSF malabsorption due to a dysfunctional arachnoid can lead to congenital hydrocephalus. In this regard, the forth aim of this project is to verify whether folates and folate enzyme FDH have an effect on arachnoid cell growth. A negative effect of folates on cell growth may explain abnormalities in the development of the arachnoid, and inability to divert CSF into the general blood circulation (Figure 1.18)



**Figure 1.18. CSF flow and drainage into the superior sagittal sinus. CSF is produced in the choroid plexuses (red rectangle) and reaches the subarachnoid space to leave the brain through the arachnoid, in contact with the superior sagittal sinus. Detailed arachnoid tissue is shown in the second image (black arrow), which illustrates arachnoid tissue projections (arachnoid granulations) towards the superior sagittal sinus where the CSF is drained. Blockage of CSF (top red circle) may be caused by exacerbated growth of arachnoid tissue rendering the arachnoid dysfunctional. The red circle inside the red rectangle indicates a second area of the brain, where CSF flow can be obstructed; the aqueduct of Sylvius. This area is not considered in our studies.**

**Aim and hypothesis 5: Identification of specific metabolic pathways in normal and hydrocephalic CSF is possible by IPA as well as comparison of metabolic pathway profile between normal and hydrocephalic CSF.**

Past studies related to identification of proteins in normal and abnormal CSF by LCMS revealed a lack of the folate enzyme FDH in hydrocephalic CSF. Thus, we focused our studies on the study of proteins related to the folate metabolic cycle. However, no attention was given to the remaining 485 proteins also missing in hydrocephalic CSF. In the present study, we aim first to group into categories the global proteomic profile obtained from LCMS using EXCEL commands to organize LCMS data-sets into two groups. A first group includes proteins exclusively expressed in abnormal CSF, whereas a second category consists of proteins that are absent in abnormal CSF but present in normal CSF. Excel categories are later analysed by Ingenuity Path Analysis (IPA), which is a bioinformatic tool that allows us to match proteins in CSF with their corresponding genes to predict whether these proteins are related and fall within specific metabolic pathways as well as identifying their potential relationship with specific biofunctions. Our approach here is to consider that genes may be activated or inactivated depending on whether their corresponding proteins are expressed or absent in CSF. The logic behind this approach is that proteins exclusive to abnormal CSF imply activation of certain specific genes in congenital hydrocephalus (genes codifying for these proteins), whilst the missing genes expressed only in normal CSF must be inactivated. IPA analysis, on the other hand, finds relationships between these genes and their involvement in specific metabolic pathways (canonical pathways), whilst linking them to potential biological functions and diseases. In conclusion, we hypothesize that those proteins only present in hydrocephalic CSF imply involvement of the corresponding metabolic pathways where these proteins fall. In other words, activation of these metabolic pathways may be linked exclusively to congenital

hydrocephalus, and this information may prove useful in the future for development of a clinical tool for identification, diagnosis and prevention of congenital hydrocephalus.

## **1.11 ALTERNATIVE FORMAT**

This thesis is presented in the alternative format following the rules and regulations of the University of Manchester. It focuses on the general role of folate in normal and hydrocephalic brain development, and the experimental work was structured in relation to three main aspects of this theme:

First, we aim to understand the role of vitamin B9 (folates) in the cerebral cortex, its location along with the key folate enzyme FDH and folate receptor (FR $\alpha$ ) and the potential similarities and interrelationships between enzyme and receptor. Second, we aim to examine the effect of folates in arachnoid cell proliferation “in vitro”, to determine whether extracellular folate imbalance results in changes in normal cell arachnoid growth, which may lead to arachnoid dysfunction. Finally, an analysis of CSF’s protein composition was undertaken to explore the potential metabolic pathways involved in the development of congenital hydrocephalus with reference to the normal brain. Each aim of this research has a corresponding chapter and each chapter is an intended article for publication as follows:

- 1) Role of FDH and vitamin B9 in brain development at early pregnancy: implications for congenital hydrocephalus.**
- 2) Vitamin B9 (5mTHF) is crucial for fetal meningeal arachnoid cell growth: implications for congenital hydrocephalus.**
- 3) Normal versus hydrocephalic CSF Ingenuity Path Analysis (IPA) of proteins profiles obtained from LCMS.**

The three articles as a whole contribute to characterizing the role of FDH and variants of vitamin B9 during brain development in normal and hydrocephalic conditions, and hence they are all related in this respect. Each article’s introduction and conclusion is written with the aim of establishing links between all papers. For instance, the findings in article 1

support the results of article 2 and 3. In this way, all three articles are linked together as cohesive piece of work. The relevant material and methods are described for every corresponding chapter.

The vast majority of the work in these articles is the result of my own original thinking, experimental design and assay development. My project ideas, experimental work and experimental outcomes were always discussed with my main supervisor, Dr. Jaleel Miyan, who guided me throughout this project.

## 1.12 REFERENCES

- Anguera, M.C. et al. (2006). Regulation of folate-mediated one-carbon Metabolism by 10-Formyl-THF Dehydrogenase. *J. Biol. Chem.* Vol.: 281/27: 18335-18342.
- Antony, T.E. and Heintz, N. (2007). The folate metabolic enzyme FDH is restricted to the midline of the early CNS, suggesting a role in human neural tube defects. *J. Comp. Neurol.* 500: 368-383.
- Antony, A.C. (2007). In utero physiology: role of folic acid in nutrient delivery and fetal development. *Am. J. Clin. Nutr.* 85: 5985-6035.
- Antony, A. C. (1996). Folate receptors. *Annu. Rev. Nutr.* 16, 501–521
- Appling, D. R. (1991). Compartmentalization of folate-mediated one-carbon metabolism in eukaryotes. *J. FASEB.* 5: 2645–2651.
- Bachy, I. et al. (2008). The particles of the embryonic cerebrospinal fluid: How could they influence brain development? *Br. Res. Bull.* 75: 289-94.
- Baker, P. et al (1981). Role of placenta in maternal-fetal vitamin transfer in humans. *Am. Obstet. Gynecol.* 141: 792-6.
- Bally-Cuif, L. and Bonicelli, L. (1997). Transcription factors and head formation in vertebrates. *Bioassays.* 19: 127-135.
- Barlowe, C. K. and Appling, D. R. (1988). In vitro evidence for the involvement of mitochondrial folate metabolism in the supply of cytoplasmic one-carbon units. *Biofactors* 1: 171–176.
- Batton, D.G. et al. (1994). Current gestational age-related incidence of major intraventricular hemorrhage. *J. Pediatr.* 125:623-25.
- Bradbury, M. (1979). *The concept of a Blood-Brain Barrier.* Chichester. Ed: Wiley and Sons.
- Bergsneider, M. (2001). Evolving concepts of cerebrospinal fluid physiology. *Neurosurg. Clin. N. Am.* 12: 631-638.
- Bisseling, J. et al. (2004). Placental folate transport and binding are not impaired in pregnancies complicated by fetal growth restriction. *Plac.* 25: 588-93.
- Blehaut, H. et al. (2010). Effect of Leucovorin (Folinic Acid) on the Developmental Quotient of Children with Down's syndrome (Trisomy 21) and Influence of Thyroid Status. *J. Plos One* 5: 8394.
- Bloch, O., Auguste, K.I., Manley, G.T. and Verkman, A.S. (2006). Accelerated progression of kaolin-induced hydrocephalus in aquaporin-4-deficient mice. *J. Cereb. Blood Flow. Metab.* 26: 1527-37.

- Brocker, P. and P. Lods, J.C. (1990). Folates: de la deficiencia a la carencia. *La Revue de Geriatrie* 15: 365–373.
- Brodbelt, A. and Stoodley, M. (2007). CSF pathways: a review. *Br. J. Neurosurg.* 21: 510-520.
- Brown, P.D. et al. (2004). Molecular mechanisms of cerebrospinal fluid production. *Neurosci.* 129: 957-970.
- Boulton, M., Flessner, M., Armstrong, D., Hay, J. and Johnston, M. (1997). Lymphatic drainage of the CNS: effect of lymphatic diversion/ligation on CSF protein transport to plasma. *Am. J. Physiol. Regul. Integr. Comp. Physiol.* 272: 13-19.
- Boulton, M., Flessner, M., Armstrong, D., Mohamed, R., Hay, J. and Johnston, M. (1999). Contribution of extracranial lymphatics and arachnoid villi to the clearance of a CSF tracer in the rat. *Am. J. Physiol. Regul. Integr. Comp. Physiol.* 276: 818-23.
- Bueno, D. et al. (1996) Spatial and temporal relationships between Shh, Fgf4 and Fgf8 gene expression at diverse signalling centers during mouse development. *Dev. Dyn.* 207: 291-299.
- Bulat, M. and Klarica, M. (2010) Recent insights into a new hydrodynamics of the cerebrospinal fluid. *J. Br. Res.* 65: 99-112.
- Champion, K. M., Cook, R. J., Tollaksen, S. L. and Giometti, C. S. (1994). Identification of a heritable deficiency of the folate-dependent enzyme 10-formyltetrahydrofolate dehydrogenase in mice. *Proc. Natl. Acad. Sci. U.S.A.* 91: 11338–11342.
- Chen, L. Qi, H. Korenberg, J. Garrow, T. A. Choi, Y. J. and Shane, B. (1996). Purification and properties of human cytosolic folylpoly- $\gamma$ -glutamate synthetase and organization, localization, and differential splicing of its gene *J. Biol.Chem.* 271: 36-39.
- Cherian S. et al. (2004). The pathogenesis of neonatal post-hemorrhagic Hydrocephalus. *Br. Pathol.* 14: 305-11.
- Chodosbski, A and Szmydynger-Chodobska, J (2001). Choroid plexus: target for polypeptides and site of their synthesis. *Micro. Res. Tech.* 52: 65-82.
- Chu, A. B. et al. (1983). Oligoclonal IgG bands in cerebrospinal fluid in various neurological diseases. *Ann. Neurol.* 13: 434-39.
- Cai, X. et al. (2000). Hydrocephalus in the H-Tx rat: a monogenic disease? *Exp. Neurol.* 163:131-5.
- Cains, S et al. (2009). Addressing a folate imbalance in fetal cerebrospinal fluid can decrease the incidence of congenital hydrocephalus. *J. Neuropathol.* 68: 404-416.
- Cao, Y., Brown, S.L., Knight, R.A., Fenstermacher, J.D. and Ewing, J.R. (2005). Effect of intravascular-to-extravascular water exchange on the determination of blood-to-tissue transfer constant by magnetic resonance imaging. *Magn. Reson. Med.* 53: 282-93.

- Cook, R. J., Lloyd, R. S., and Wagner, C. (1991). Isolation and characterization of cDNA clones for rat liver 10-formyltetrahydrofolate dehydrogenase. *J. Biol. Chem.* 266: 4965–4973.
- Cooper, J.A. (2008). A mechanism for inside-out lamination in the neocortex. *Trends in Neurosci.* 31: 113-119.
- Catala, M. (1998). Embryonic and foetal development of structures associated with cerebrospinal fluid in man and other species. Part I: The ventricular system, meninges and choroid plexus. *Arch. Anat. Cytol. Pathol.* 46: 153-69.
- Conegero, C.I., Chopard, R.P. (2003). Tridimensional architecture of the collagen element in the arachnoid granulations in humans: a study on scanning electron microscopy. *Arq. Neuropsiquiatr.* 61: 561-5.
- Cornelius, H. et al. (2011). Arachnoid Cells on Culture Plates and Collagen Scaffolds: Phenotype and Transport Properties. *Tiss. Eng.: Part A.* 17: 1759- 66.
- Cosan, T.E., Guner, A.I., Akcar, N. and Uzuner, K. (2002). Progressive ventricular enlargement in the absence of high ventricular pressure in an experimental neonatal rat model. *Child's Nerv. Syst.* 18: 10-14.
- Courtney, S.M. et al. (1996). Object and spatial visual working memory activate separate neural systems in human cortex. *Cereb. Cortex* 6: 39-49.
- Crossley, P.H. and Martin, G.R. (1995). The mouse *Fgf8* gene encodes a family of polypeptides and is expressed in regions that direct outgrowth and patterning in the developing embryo. *Dev. Biol.* 121: 439-451.
- Curley, J.P. and Mashood, R. (2010). Parent- of-origin and trans-generational germline influences on behavioural development: the interacting roles of mothers, fathers, and grandparents. *J. Dev. Psychobiol.* 52: 312-330.
- Davis, S., Stacpoole, P., Williamson, J., Kick, L., Quinlivan, E., Coats, B., Shane, B., Bailey, L., and Gregory III, J. F. (2004). Tracer-derived total and folate-dependent homocysteine remethylation and synthesis rates in humans indicate that serine is the main one-carbon donor. *Am. J. Physiol.* 286: 272–279.
- Del Bigio, M.R., Wilson, M.J. and Enno, T. (2003). Chronic hydrocephalus in rats and humans: white matter loss and behaviour changes. *Ann. Neurol.* 53: 337-46.
- Del Bigio, M.R. and Zhang Y.W. (1998). Cell death, axonal damage, and cell birth in the immature rat brain following induction of hydrocephalus. *Exp. Neurol.* 154: 157-69.
- Denis, J. and Taylor, D.C. (1969). Epilepsy and folate deficiency. *BMJ.* 4: 807-808.
- Dere, E. et al. (2007). The pharmacology, neuroanatomy and neurogenetic of one-trial object recognition in rodents. *Neurosci. and Behav. Rev.* 31: 673-704.



- Desmond, M.E. and Jacobson, A.G. (1977). Embryonic brain enlargement requires cerebrospinal fluid pressure. *Dev. Biol.* 57: 188-198.
- Desmond, M.E. (1985). Reduced number of brain cells in so-called neural overgrowth. *Anat. Rec.* 212: 195–198.
- Desmond, M.E. and Levitan, M.L. (2002). Brain expansion in the chick embryo initiated by experimentally produced occlusion of the spinal cord. *Anat. Rec.* 268: 147–159.
- Donato, H. et al. (2007). 10-Formyltetrahydrofolate Dehydrogenase requires a 4'Phosphopantetheine Prosthetic Group for Catalysis. *J. Biol. Chem.* 282:34159-34166.
- Duboule, D. (1994). Temporal colinearity and the phylotypic progression: a basis for the stability of a vertebrate and the evolution of morphologies through heterochrony. *Dev. Biol.* 1: 135–142
- Du Plessis, A. J. (1998). Posthemorrhagic hydrocephalus and brain injury in the preterm infant: dilemmas in diagnosis and management. *Sem. Pediatr. Neurol.* 5:161-79.
- Dziegielewska, K.M., Knott, GW and Saunders NR. (2000). The nature and composition of the internal environment of the developing brain. *Cell. and Mol. Neurobiol.* 20: 41–56.
- Dziegielewska, K.M. et al. (2001). Development of the choroid plexus. *Micros. Res. Tech.* 52: 5-20.
- Echelard, Y., Epstein, D.J., St-Jacques, B., Shen, L., Mohler, J., McMahon, J.A. and McMahon, A.P. (1993). Sonic hedgehog, a member of a family of putative signalling molecules, is implicated in the regulation of CNS polarity. *Cell.* 75: 1417–1430.
- Egnor, M.Z. et al. 2002. A model of pulsations in communicating hydrocephalus. *Pediatr. Neurosurg.* 36: 281-303.
- Elnakat, H., Ratnam, M. (2004). Distribution, functionality and gene regulation of folate receptor isoforms: implications in targeted therapy. *Adv. Drug Deliv. Rev.* 56: 1067–84.
- Emeric, D.F. et al. (2005) The choroid plexus in the rise, fall and repair of the brain. *Bioessays.* 27: 262-74.
- Ennaceur, A. and Delacour, J. (1988). A new on-trial test for neurobiological studies of memory in rats. *Behav. Brain Res.* 31: 47-59.
- Erlich, J.C. et al. (1989). Ultrastructural morphology of the orbital pathway for cerebrospinal fluid drainage in rabbits. *J. Neurosurg.* 70: 926-31.
- Faraci et al. (1990). Effect of vasopressin on production of cerebrospinal fluid: possible role of vasopressin (V1)-receptors. *Am. J. Physiol.* 258: 94-98.
- Fiori, M.G., Sharer, L.R., Lowndes, H.E. (1985). Communicating hydrocephalus in rodents treated with beta, beta'-iminodipropionitrile (IDPN). *Acta. Neuropathol.* 65: 209-16.

- Fonteh A.N. et al. (2006). Identification of disease markers in human cerebrospinal fluid using lipidomic and proteomic methods. *Dis. Markers*. 22:39-64.
- Fu, T.-F., Maras, B., Barra, D. and Schirch, V. (1999). A Noncatalytic Tetrahydrofolate Tight Binding Site Is on the Small Domain of 10-Formyltetrahydrofolate Dehydrogenase. *Arch. Biochem. Biophys.* 367.
- Ganapathy et al. (2004). SLC19: the folate/thiamine transporter family. *Plfugers Arch.* 447: 641-6.
- Garcia-Cazorla, A. et al. (2008). Mitochondrial diseases associated with cerebral folate deficiency. *Neurol.* 70: 1360-2.
- Garda, A.L., Echevarria, D., Martinez, S. (2001). Neuroepithelial co-expression of Gbx2 and Otx2 precedes Fgf8 expression in the isthmic organizer. *Mech. Dev.* 101: 111–118.
- Gato, A. et al. (2005). Embryonic cerebrospinal fluid regulates neuroepithelial survival, proliferation, and neurogenesis in chick embryos. *The Anat. Rec.* 284: 475-484.
- Gato, A. et al. (2004). Analysis of cerebro-spinal fluid protein composition in early developmental stages in chick embryos. *J. Exp. Zool.* 301/4: 280-9.
- Gaufo, G.O., Thomas, K.R., Capecchi, M.R. (2003). Hox3 genes coordinate mechanisms of genetic suppression and activation in the generation of branchial and somatic motoneurons. *Dev.* 130: 5191–5201.
- Geraldine, G. et al. (2007). Symposium on ‘Micronutrients through the life cycle’ Folate and vitamin B12: friendly or enemy nutrients for the elderly. *Proc. Nutr. Soc.* 66: 548–558.
- Girgis, S., Nasrallah, I.M., Suh, J.R., Oppenheim, E., Zanetti, K.A., Mastri, M.G., Stover, P. J. (1998). Molecular cloning, characterization and alternative splicing of the human cytoplasmic serine hydroxymethyltransferase gene. *Gene* 210: 315–324
- Glimcher, S.A., Holman, D.W., Lubow, M., Grzybowski, D.M. Ex vivo model of cerebrospinal fluid outflow across human arachnoid granulations. *Invest. Ophthalmol. Vis. Sci.* 49: 4721-8.
- Grapp, M. et al. (2013) Choroid Plexus transcytosis and exosome shuttling deliver folate into brain parenchyma. *Nat.* 2123: 589-93.
- Greenberg, M.S. (2001). *Handbook of Neurosurgery*. 5<sup>th</sup> ed. New York: Thieme Medical Publishers.
- Gregg, C. et al. (2010). Sex-specific parent-of-origin allelic expression in the mouse brain. *Science* (Epub ahead of print).
- Geller, J. et al. (2002). Hereditary folate malabsorption: family report and review of the literature. *Medicine (Baltimore)* 81: 51–68.
- Gobron S. et al. Subcommissural organ/Reissner’s fiber complex: Characterization of SCO Spondin, a glycoprotein with potent activity on neurite outgrowth. *Glia* 32:177-191.

- Grzybowski, D.M. et al. (2006). In vitro model of cerebrospinal fluid outflow through human arachnoid granulations. *Invest. Ophthalmol.* 47/ 8-16.
- Gunnarson E. M. et al. (2004). Regulation of brain aquaporins. *Neurosci.* 129: 947-55.
- Gupta et al. 2010. Cerebrospinal fluid dynamics in the human cranial subarachnoid space: an overlooked mediator of cerebral disease. I. Computational model. *J. R. Soc. Interface.* 7:1195-1204.
- Halverson, A.L., Barrett, W.L., Iglesias, A.R. (1999). Decreased cerebrospinal fluid absorption during abdominal insufflation. *Surg. Endosc.* 13: 797-800.
- Hammon, R.S. et al. (2004). On the delay-dependent involvement of the hippocampus in object recognition memory. *J. Neurobiol.* 82: 26-34.
- Hansen, F.J. and Blau, N. (2005). Cerebral folate deficiency: Life-changing supplementation with folinic acid. *Mol. Genet. Metab.* 84: 371-73.
- Harrington, M.G. et al. (2009). The morphology of nanostructures provides evidence for synthesis and signalling functions in human cerebrospinal fluid. *Cereb. Fluid Res.* doi: 10.1186/1743-8454-6-10.
- Harrington M. G. and Merrill C. R. (1988). Cerebrospinal fluid protein analysis in diseases of the nervous system. *J. Chromatograph.* 429:345-58.
- Hartwig, W. and Wernes, P. (2010). Choroid plexus. *Biol. and Pathol.* 119: 75-78.
- Henderson et al. (1995). Maternal-to-fetal transfer of 5-methylTHF by the perfused human placental cotyledon: evidence for a concentrative role by placental folate receptors in fetal folate delivery. *J. Lab. Clin. Med.* 126: 184-203.
- Holman et al. (2010). Cerebrospinal fluid dynamic in the human cranial subarachnoid space: an overlooked mediator of cerebral disease II. In vitro arachnoid outflow model. *J.R. Interface* 7: 1205-1218.
- Hong, M., Lee, Y., Kim, J.W., Lim, J.-S., Chang, S.Y., Lee, K.S., Paik, S.-G., and Choe, I.S. (1999). Isolation and characterization of cDNA clone for human liver 10-formyltetrahydrofolate dehydrogenase. *Biochem. Mol. Biol. Int.* 47: 407-415.
- Hyland, K. et al. (2010). Cerebral folate deficiency. *J. Inherit Metab. Dis.* 33: 563-570.
- Janson, C. et al. (2011). Immortalization and functional characterization of rat arachnoid cells lines. *Neurosci.* 177: 23-34.
- Jayatilaka, A.D.P. Arachnoid granulation in sheep. *J. Anat.* 99: 315-327.
- Johanson, C. et al. (2011). The Distributional Nexus of Choroid Plexus to Cerebrospinal Fluid, Ependyma and Brain: Toxicologic/Pathologic Phenomena, Periventricular Destabilization, and Lesion Spread. *Toxicol. Pathol.* 39: 186-212.

- Johanson, C.E. (2008). Choroid plexus-CSF circulatory dynamics: impact on brain growth, metabolism and repair. In: Totowa, C.P. (Ed.) *Neuroscience en Medicine* 173-200. New Jersey: The Humana Press.
- Johanson, C.E. et al. (2008). Multiplicity of cerebrospinal fluid functions: new challenges in health and disease. *Cerebrospinal Fluid Res.* 5: 1743-84.
- Johanson, C.E. et al. (1999). AVP V1 receptor-mediated decrease in Cl<sup>-</sup> efflux and increase in dark cell number in choroid plexus epithelium. *Am. J. Physiol.* 276: 82-90
- Johanson, C.E., Szmydynger-Chodobska, J., Chodobski, A., Baird, A., McMillan, P., Stopa, E.G. (1999). Altered formation and bulk absorption of cerebrospinal fluid in FGF-2-induced hydrocephalus. *Am. J. Physiol.* 277: 263-71.
- Johanson C.E. and Murphy V.A. (1990) Acetazolamide and insulin alter choroid plexus epithelial cell (Na<sup>+</sup>), pH and volume. *Am. J. Physiol.* 258:1538-46.
- Johnston et al. 2004. Evidence of connections between cerebrospinal fluid and nasal lymphatic vessels in humans, non-human primates and other mammalian species. *Cerebrospinal. Fluid Res.* 1:2.
- Johnston et al. 2005. Subarachnoid injection of Microfil reveals connections between cerebrospinal fluid and nasal lymphatics in the non-human primate. *Neuropathol. Appl. Neurobiol.* 31:632-40.
- Jones, H. C. and Bucknal, R.M. (1988). Inherited prenatal hydrocephalus in the H-Tx rat: a morphological study. *Neuropathol. Appl. Neurobiol.* 14: 263-74.
- Jones, H.C. et al. (1997). Aqueduct stenosis in animal models of hydrocephalus. *Child. Nerv. Syst.* 13: 503-4.
- Jones, H. C. et al. (1998). The relation between CSF pressure and ventricular dilatation in hydrocephalic HTx rats. *Eur. J. Pediatr. Surg.* 8:55-8.
- Jones H.C. et al. (2001). Genome-wide linkage analysis of inherited hydrocephalus in the H-Tx rat. *Mamm. Genome.* 12: 22-6.
- Joosten, E. (1997). Is metabolic evidence for vitamin B12 and folate deficiency more frequent in elderly patients with Alzheimer's disease? *J. Gerontol.* 52: 76-79.
- Jouet M. et al. (1993). A missense mutation confirms the L1 defect in X-linked hydrocephalus (HSAS). *Nat. Genet.* 4:331-336.
- Kaiser, G. (1985). Hydrocephalus following toxoplasmosis. *Dev.* 40: 10-1.
- Kamen, B.A., Smith, A.K. (2004). A review of folate receptor alpha cycling and 5-methylTHF accumulation with an emphasis on cell models in vitro. *Adv. Drug Deliv. Rev.* 56: 1085-97.
- Kauritz, J.D. and Lidenbaum, J. (1977). The bioavailability of folic acid added to wine. *Annals of Internal Med.* 87: 542-5.

Khan, O.H., Enno, T.L., Del Bigio, M.R. (2006). Brain damage in neonatal rats following kaolin induction of hydrocephalus. *Exp. Neurol.* 200: 311-20.

Khon, D.F. et al. (1981). A new model of congenital hydrocephalus in the rat. *Acta Neuropathol.* 54: 211-218.

Kim, D.W., Huang, T., Schirch, D., and Schirch, V. (1996). Properties of Tetrahydropteroylpentaglutamate Bound to 10-Formyltetrahydrofolate Dehydrogenase. *Biochem.* 35: 15772–15783.

Kimelberg, H.K. (2004) Water homeostasis in the brain: basic concepts. *Neurosci.* 129: 851-60.

Klinge, P.M., Samii, A., Mhlendyck, A., Visnyei, K. (2003). Cerebral hypoperfusion and delayed hippocampal response after induction of adult kaolin hydrocephalus. *Stroke* 34: 193-9.

Koh L. et al. 2006. Development of cerebrospinal fluid absorption sites in the pig and rat: connections between the subarachnoid space and lymphatic vessels in the olfactory turbinates. *Anat. Embryol.* 211:335-44.

Krebs, H.A., Hems, R., and Tyler, B. (1976). The regulation of folate and methionine metabolism. *Biochem. J.* 158: 341–353.

Krupenko, N.I. (2010). ALDH1L2 is the Mitochondrial Homolog of 10-FormylTHF Dehydrogenase. *J. Biol. Chem.* 285: 23056-23063.

Krupenko, S.A. (2009). FDH: An aldehyde dehydrogenase fusion enzyme in folate metabolism. Minireview. *Chem-Biol Interact.* 178: 84-93.

Krupenko, S. A., and Oleinik, N. (2002). 10-formyltetrahydrofolate dehydrogenase, one of the major folate enzymes, is down-regulated in tumor tissues and possesses suppressor effects on cancer cells. *Cell Growth Diff.* 13: 227–236.

Lam C. H. et al. 2012. The characterization of arachnoid cell transport II: paracellular transport and blood-cerebrospinal fluid barrier formation. *Neuroscience.* 222:228-38.

Laske C. et al. (2008). Decreased plasma and cerebrospinal fluid levels of stem cell factor in patients with early Alzheimer's disease. *J. of A.D.* 15:451-60.

Levine, J.E., Povlishock, J.T., Becker, D.P. (1982). The morphological correlates of primate cerebrospinal fluid absorption. *Brain Res.* 241: 31-41.

Li, J., McAllister, J.P., Shen, Y., Wagshul, M.E., Miller, J.M., Egnor, M.R., et al. (2008). Communicating hydrocephalus in adult rats with kaolin obstruction of the basal cisterns or the cortical subarachnoid space. *Exp. Neurol.* 211: 351-61.

Lidenbaum, J. et al. (1994). Prevalence of cobalamin deficiency in the Framingham elderly population. *American Journal of clinical nutrition* 60: 2-11.

- Liddon, J.L. (2004). Neuropsychological profile of young adults with spina bifida with or without hydrocephalus. *J. Neurol. Neurosurg. Psychiatry* 75: 1112-1118 doi:10.1136/jnnp.2003.029058.
- Mao, X., Enno, T.L., Del Bigio, M.R. (2006). Aquaporin 4 changes in rat brain with severe hydrocephalus. *Eur. J Neurosci.* 23: 2929-36.
- Maren T.H. (1988) The kinetics of HCO<sub>3</sub>-synthesis related to fluid secretion, pH control, and CO<sub>2</sub> elimination. *Annu. Rev. Physiol.* 50:695-717.
- Marti, E., Takada, R., Bumcrot, D.A., Sasaki, H., McMahon, A.P. (1995). Distribution of sonic hedgehog peptides in the developing chick and mouse embryo. *Dev.* 121: 2537–2547.
- Mashayekhi, F. et al. (2002). Deficient cortical development in the hydrocephalic Texas (H-Tx) rat: a role for CSF. *Brain* 125: 1859-1874.
- Mashayekhi, F. and Salehi, Z. (2006). The importance of cerebrospinal fluid on neural cell proliferation in developing chick cerebral cortex. *European J. Neurol.* 13: 266-272.
- Massicote and Del Bigio (1999). Human arachnoid villi response to subarachnoid hemorrhage: possible relationship to chronic hydrocephalus. *J. Neurosurg.* 91: 80-84.
- Megumi, T. et al. (2011). 5,10-MethylenTHF reductase deficiency with progressive polyneuropathy in an infant. *Brain and Dev.* 33: 521-524.
- Min, H., Shane, B., and Stokstad, E.L.R. (1988). Identification of 10-formyltetrahydrofolate dehydrogenase-hydrolase as major folate bind to protein in liver cytosol. *Biochim. Biophys. Acta* 967: 348–353.
- Miyan, J.A. et al. (2003). Development of the brain: a vital role for cerebrospinal fluid. *Can. J. Physiol. Pharmacol.* 81: 317-328.
- Miyan, J.A. et al. (2001). Brain Stem cells. Chapter 8. Ed: Society for Experimental Biology.
- Moinuddin, S.M., Tada, T. Study of cerebrospinal fluid flow dynamics in TGF-beta 1 induced chronic hydrocephalic mice. *Neurol. Res.* 22: 215-22.
- Mollanji R. et al. (2001). Intracranial pressure accommodation is impaired by blocking pathways leading to extracranial lymphatics. *Am. J. Physiol. Regul. Integr. Comp. Physiol.* 280:1573-1581.
- Molloy, A.M., and Scott, M.J. (2001). Folates and prevention of disease. *PHN.* 4: 601-609.
- Moretti, P. et al. (2005). Cerebral folate deficiency with developmental delay, autism, and response to folinic acid. *Neurol.* 64: 1088-90.

Mori K. et al. (1990). Alteration of atrial natriuretic peptide receptors in the choroid plexus of rats with induced or congenital hydrocephalus. *Childs Nerv. Syst.* 6:190-93.

Murphy B.P. et al. (2002). Posthemorrhagic ventricular dilatation in the premature infant: natural history and predictors of outcome. *Arch. Dis. Child Fetal Neonatal Ed.* 87: 37-41.

Murphy V.A. and Johanson C.E. (1989). Acidosis, acetazolamide, and amiloride: effects on Na<sup>+</sup> transfer across the blood-brain and blood-CSF barriers. *J. Neurochem.* 52:1058-1063.

Naibiuni, M. et al. (2004). Proteomics study of CSF composition in the developing H-Tx rat. *Cerebrospinal Fluid Res.* 1 (Suppl 1): S29.

Nishio et al. (1998). Nerve growth factor levels in cerebrospinal fluid are high in the inflammatory neurological disorder. *Clin. Chim. Acta.* 275:93-98.

Ojeda, J.L., Piedra, S. (2000). Evidence of a new transitory extracellular structure within the developing rhombencephalic cavity: an ultrastructural and immunoelectron-microscopic study in the chick. *Anat Embryol* 202: 257–264.

Oleinik, N.V. and Krupenko, S.A. (2003). Ectopic expression of 10-formyl-tetrahydrogenase in A549 cells induces G1 cell cycle arrest and apoptosis. *Mol. Cancer Res* 1: 577-588.

Oleinik, N.V. et al. (2010). FDH inhibits cell motility via dephosphorylation of cofilin by PP1 and PP2A. *Oncogen.* 29: 6233-6244.

Oleinik, N.V. and Krupenko S.A. (2003). Ectopic expression of 10-formylTHF dehydrogenase in A459 cells induces G1 cell cycle arrest and apoptosis. *Mol Cancer Res.* 11: 577-88.

O’Rahilly and Müller (1987). Developmental stages in human embryos. Carnegie Institution of Washington publication 63: 1-317.

Oreskovic, D. and Klarica, M. (2010). The formation of cerebrospinal fluid: Nearly a hundred years of interpretations and misinterpretations. *Brain research reviews.* 64: 241-262.

Oreskovic, D. and Klarica, M. (2011). Development of hydrocephalus and classical hypothesis of cerebrospinal fluid hydrodynamics: Facts and illusions. *Progr. in Neurobiol.* 94: 238-258.

Oshio, K. et al. (2005). Reduced cerebrospinal fluid production and intracranial pressure in mice lacking choroid plexus water channel Aquaporin-1. *FASEB J.* 19: 76-78.

Owen-Lynch, P.J. et al. (2003). Defective cell cycle control underlies abnormal cortical development in the hydrocephalic Texas rat. *Brain* 126: 623-631.

Panchision, D.M., McKay, R.D.G. (2002). The control of neural stem cells by morphogenic signals. *Curr. Opin. Genet. Dev.* 12: 478–487.

- Papaiconomou, C., Bozanovic-Sosic, R., Zakharov, A., Johnston, M. (2002). Does neonatal cerebrospinal fluid absorption occur via arachnoid projections or extracranial lymphatics? *Am. J. Physiol. Regul. Integr. Comp. Physiol.* 283: R869-76.
- Praetorius, J. et al. (2004). A SCL4A10 gene product maps selectivity to the basolateral membrane of choroid plexus epithelial cells. *Am. J. Physiol.* 286: C601-C610.
- Raimondi, A.J. et al. (1976). Pathogenesis of the aqueductal occlusion in congenital murine hydrocephalus. *J. Neurosurg.* 45:66-77.
- Ramaekers, V.R. et al. (2004). Cerebral folate deficiency. *Dev. Med Child Neurol* 46: 843-51.
- Ramaekers, V.R. et al. (2005). Autoantibodies to folate receptors in the cerebral folate deficiency syndrome. *New England J.* 352: 19.
- Redzic, Z.B. and Segal, MB. (2004) The structure of the choroid plexus and the physiology of the choroid plexus epithelium. *Adv Drug Deliv. Rev.* 56 (12): 1695-716.
- Refsum, H. (2001). Folate, vitamin B12 and homocysteine in relation to birth defects and pregnancy outcome. *Br.J. Nutr.* 85 (Suppl. 2): S109-13.
- Rekate J, (2008). The definition and classification of hydrocephalus: a personal recommendation to stimulate debate. *Cerebrospinal fluid research.* Doi: 10.1186/1743-8454-5-2.
- Reynolds, E.H. (1968). Mental effects of anticonvulsants and folic acid metabolism. *Brain* 91: 197-214.
- Robinson, M.L., Allen, C.E., Davy, B.E., Durfee, W.J., Elder, F.F., Elliott, C.S. et al. (2002). Genetic mapping of an insertional hydrocephalus-inducing mutation allelic to *hy3*. *Mamm Genome* 13: 625-32.
- Rodriguez E.M. et al. (2006). Long-lasting hydrocephalus in HYH mutant mice: gain and loss of a brain surviving hydrocephalus. *Cerebrospinal Fluid Res.* 3 (1): S15.
- Roubertoux, P.L., et al. (2003). Mitochondrial DNA modifies cognition in interaction with the nuclear genome and age in mice. *Nature Genetics.* 35: 65-69.
- Rubestein E. (1998). Relationship of senescence of cerebrospinal fluid circulatory system to dementias of age. *Lancet.* 351:283-85.
- Sanes, D.H. et al. (2010). *Development of the Nervous System.* Ed. Academic Press. Third edition. Chapter 3. Page 58-61.
- Satyajit, M. et al. (1994). Sequestration of GPI-anchored proteins in caveolae triggered by cross-linking. *Sci.* 264: 1948-1951.
- Segal, M.B.(2001). Transport of nutrients across the choroid plexus. *Microsc. Res. Tech.* 52: 38-48.



- Scavone et al. (1995). Atrial natriuretic peptide molecules modulates sodium and potassium-activated adenosine triphosphatase through a mechanism involving cyclic GMP and cyclic GMP-dependent protein kinase. *J. Pharmacol. Exp. Ther.* 272: 1036-1043.
- Scholl et al. (1996). Dietary and serum folate: their influence on the outcome of pregnancy. *Am. J. Clin. Nutr.* 63: 520-5.
- Schurr et al. (1953). Experimental studies on the circulation of the cerebrospinal fluid and methods of producing communicating hydrocephalus in the dog. *J. Neurosurg.* 10:515-25.
- Selhub, J., Franklin, W.A. (1984). The folate-binding protein of rat kidney. Purification, properties, and cellular distribution. *J. Biol. Chem.* 259: 6601–6.
- Serrano et al. (2010). Kearns-Sayre syndrome: cerebral folate deficiency, MRI findings and new cerebrospinal fluid biochemical features. *Mitochondrion* 10: 429-32.
- Sheth R.D. et al. (1998). Trends in incidence and severity of intraventricular hemorrhage. *J. Child. Neurol.* 13:261-64.
- Shamim, H., Mahmood, R., Logan, C., Doherty, P., Lumsden, A., Mason, I. (1999). Sequential roles for Fgf4, En1 and Fgf8 in specification and regionalisation of the midbrain. *Dev.* 126: 945–959.
- Shane, B. (1995). Folate Chemistry and Metabolism. In: Bailey, L. B., ed. *Folate in Health and Disease*. pp. 1–22. New York: Marcel Dekker Inc.
- Sasidharan P. et al. (1986). Developmental outcome of infants with severe intracranial-intraventricular hemorrhage and hydrocephalus with and without ventriculoperitoneal shunt. *Childs Nerv. Syst.* 2: 149-52.
- Shen, X.Q., Miyajima, M., Ogino, I., Arai, H. (2006). Expression of the water-channel protein aquaporin-4 in the H-Tx rat: possible compensatory role in spontaneously arrested hydrocephalus. *J Neurosurg* 105: 459-64.
- Silverberg G.D. et al. (2003). Alzheimer's disease, normal-pressure hydrocephalus, and senescent changes in CSF circulatory physiology: a hypothesis. *Lancet Neurol.* 2:506-11.
- Sipek A. et al. 2002. Congenital hydrocephalus 1961-2000 incidence, prenatal diagnosis and prevalence based on maternal age. *Ceska Gynekol.* 67:360-64.
- Sirotnak, F. M., and Tolner, B. (1999). Carrier-mediated membrane transport of folates in mammalian cells. *Annu. Rev. Nutr.* 19: 91–122
- Smith.D.E. et al. 2004. Peptide and peptide analog transport systems at the blood-CSF barrier. *Ad. Drug Deliv. rev.* 56: 1765-91.
- Solanky et al. (2010). Expression of folate transporters in human placenta and implications for homocystein metabolism. *Plac.* 31: 134-143.
- Speake, T. et al. (2001). Mechanisms of CSF secretion by the Choroid Plexus. *Micros. Res. and Tech.* 52: 49-59.

Spector, R. et al. (2006). Micronutrient and urate transport in choroid plexus and kidney: Implications for drug therapy. *Pharm Res.* 23: 2515-24.

Spector, R. (1979). Cerebrospinal fluid folate and the blood-brain barrier. In: Botez, M.I., Reynolds, E.H. eds. *Folic acid in neurology, psychiatry, and internal medicine.* pp. 187–194. New York: Raven Press.

Steardo L. and Nathanson J.A. (1987) Brain barrier tissues: end organs for atriopeptins. *Sci.* 235: 470-73.

Steinfeld, R et al. (2009). Folate receptor alpha defect causes cerebral folate transport deficiency: A treatable neurodegenerative disorder associated with disturbed myelin metabolism. *Am. J. of Hum. Genet.* 85: 354-363.

Stoddart, J.H., Ladd, D., Bronson, R.T., Harmon, M., Jaworski, J., Pritzker, C. et al. (2000). Transgenic mice with a mutated collagen promoter display normal response during bleomycin-induced fibrosis and possess neurological abnormalities. *J. Cell Biochem.* 77: 135-48.

Strong, W.B., and Schirch, V. (1989). In vitro conversion of formate to serine: effect of tetrahydropteroylpolyglutamates and serine hydroxymethyltransferase on the rate of 10-formyltetrahydrofolate synthetase. *Biochem.* 28: 9430–9439.

Suh, J. R., Herbig, A. K., and Stover, P. J. (2001). New perspectives on folate catabolism. *Annu. Rev. Nutr.* 21: 255–282.

Suzaki et al. (1997). Nerve growth factor levels in cerebrospinal fluid from patients neurologic disorders. *J. Child Neurol.* 12: 205-207.

Tada, T., Kanaji, M., Kobayashi, S. (1994). Induction of communicating hydrocephalus in mice by intrathecal injection of human recombinant transforming growth factor-beta1. *J Neuroimmunol* 50: 153-8.

Takahashi Y. et al. 1993. Scanning electron microscopic observations of the arachnoid granulations in monkeys with cerebrospinal fluid hypotension. *The Kurume medical J.* 40: 201-11.

Tamura, T. et al. (2006). Folate and human reproduction. *Am. J. Clin. Nutr.* 83: 993-1016.

Tapanes-Castillo, A. et al. (2010). Modifier locus on chromosome 5 contributes to L1 cell adhesion molecule X-linked hydrocephalus in mice. *Neurogenet.* 11: 53-71.

Titus, S. A., and Moran, R. G. (2000). Retrovirally Mediated Complementation of the glyB Phenotype. *J. Biol. Chem.* 275: 36811–36817.

Toresson, H., Potter, S.S., Campbell, K. (2000). Genetic control of dorsoventral identity in the telencephalon: opposing roles for Pax6 and Gsh2. *Development* 127: 4361–4371.

Tripathi et al. 1974. Vacuolar transcellular channels as a drainage pathway for cerebrospinal fluid. *J. of Physiol.* 239: 195-206.

Upton, M.L. & Weller, R.O. (1985). The morphology of cerebrospinal fluid drainage pathways in human arachnoid granulations. *J. Neurosurg.* (63): 867-72.

Vaccarino, F.M., Schwartz, M.L., Raballo, R., Nilsen, J., Rhee, J., Zhou, M., Doetschman, T., Coffin, J.D., Wyland, J.J., Hung, Y.T. (1999a). Changes in cerebral cortex size are governed by fibroblast growth factor during embryogenesis. *Nat. Neurosci.* 2: 246–253.

Vaccarino, F.M., Schwartz, M.L., Raballo, R., Rhee, J., Lyn-Coo, K.R. (1999b). Fibroblast growth factor signalling regulates growth and morphogenesis at multiple steps during brain development. *Dev. Biol.* 44: 179–201.

Van der Put, N. et al. (1998). A Second Common Mutation in the MethyleneTHF Reductase Gene: An additional Risk Factor for Neural-Tube Defects? *Am. J. Hum. Genet.* 62: 1044-1051.

Vio K. et al. (2008). The subcommissural organ of the rat secretes Reissner's fiber glycoproteins and CSF-soluble proteins reaching the internal and external CSF compartments. *Cerebrospinal Fluid Res.* 5: 3-36.

Volpe J.J. et al. (2008). *Neurology of the newborn*. Ed. 5. Amsterdam. Elsevier Health Sciences.

Wagner, C. (1995). Biochemical role of folate in cellular metabolism. In: Bailey, L. B. ed. *Folate in Health and Disease*. pp. 23–42. New York: Marcel Dekker Inc

Wagshul et al. (2011). The pulsating brain: A review of experimental and clinical studies of intracranial pulsatility. *Fluis Barriers CNS.* 18: 8-15.

Wang, Y., Zhao, R., Russell, R.G., Goldman, I.D. (2001). Localization of the murine reduced folate carrier as assessed by immunohistochemical analysis. *Biochim. Biophys. Acta* 1513: 49–54

Weitman, SD et al. (1992). Distribution of the folate receptor GP38 in normal and malignant cell lines and tissues. *Cancer Res.* 52: 3396–401

Weitman, SD et al. 1992. Cellular localization of the folate receptor: potential role in drug toxicity and folate homeostasis. *Cancer Res.* 52: 6708–11.

Weller, S. et al. (2001). Genetic and clinical aspects of X-linked hydrocephalus (L1 Disease): Mutations in L1CAM gen. *Hum. muta.* 18: 1-12.

Wilkinson, L.S. et al. (2007). Genomic imprinting effects on brain development and function. *Nature Reviews. Neurosci.* 8: 832-843.

Winters, B.D. (2008). Object recognition memory: Neurobiological mechanisms of encoding, consolidation and retrieval. *Neurosci. and Behav.. Rev.* 32: 1055-1070.

Wollack, J.B. et al. (2008). Characterization of folate uptake by choroid plexus epithelial cells in a rat primary culture model. *J. Neurochem.* 104: 1494-1503.

Yajnik, C.S. et al. (2006). Vitamin B12 deficiency and hyperhomocysteinemia in rural and urban Indians. *J Assoc. Physicians India*. 54: 775-782.

Zakharov A. et al. (2004). Integrating the roles of extracranial lymphatics and intracranial veins in cerebrospinal fluid absorption in sheep. *Microvas. Res*. 67:96-104.

Zhao, R. et al. (2011). Mechanisms of membrane transport of folates into cells across epithelia. *Annu. Rev. Nutr*. 31: 177-201.

Zhang J. et al. (2006) Genetics of human hydrocephalus. *J. Neurol*. 253:1255-1266.

## **CHAPTER 2**

# **FDH AND FOLATES ROLE IN BRAIN DEVELOPMENT AT EARLY PREGNANCY: IMPLICATIONS FOR CONGENITAL HYDROCEPHALUS**

### **ABSTRACT**

Past investigations revealed an association between decreased concentrations in CSF of the soluble folate binding enzyme 10-formyl-THF-dehydrogenase (FDH) and reduced cerebral cortex development in the fetal condition congenital hydrocephalus. We hypothesize that it is FDH deficit in the brain which leads to insufficient folate brain transport, causing abnormalities in cerebral cortex progenitor cell division and prompting the cortical plate to diminish in thickness. Because the cerebral cortex plays a key role in vision, audition, memory, language and perception, developmental cerebral cortex aberrations can only have negative implications for the correct functioning of the brain later in life, leading to cognitive and neurological impairment. Thus, the current study aimed to investigate the role of FDH in folate transport and its contribution to the development of the fetal cerebral cortex.

## 2.1 INTRODUCTION

Congenital hydrocephalus is a medical condition which is described as an accumulation of cerebrospinal fluid (CSF) in the brain ventricles caused by blockage of CSF flow (Miyan et al. 2003, and Bulat and Klarica 2010). CSF is constantly produced in the choroid plexuses (Speake et al. 2001) and leaves the brain mainly via the meninge arachnoid. Arachnoid villi are in contact with the venous sinus where they drain into the general blood circulation system (Bulat and Klarica 2010). CSF flow impediment is thought to be the result of one or a combination of the following problems: brain infection during pregnancy (Kaiser et al. 1985 and Ajzenberg et al. 2002), dysfunctional arachnoid (Boulton et al. 1999 and Grzybowski et al. 2006), genetic factors such as X-linked aqueductal stenosis (Fryns JP, et al. 1991, Jones et al. 1997 and Zhang et al. 2006) and more recently, and the object of this research, folate deficit (Cain et al. 2009). Hydrocephalus leads to ventricular dilation, increased intracranial pressure and brain parenchymal damage (Brocker et al. 1990 and Bergsneider 2001), occasioning CSF accretion inside brain ventricles and fetal death if CSF is not removed (Oreskovic & Klarica 2011). Although the pathology of congenital hydrocephalus is still unknown, a growing body of evidence reveals folate deficiency as a presumptive cause for the malformation of the central nerve system during fetal development, in some cases being hereditary and due to folate malabsorption (Denis et al. 1969, Brocker et al. 1990, Geller et al. 2002, Geraldine et al 2007 and Cain et al. 2009, Hyland et al. 2010).

The vitamin B9 family consists of enzyme cofactors called folates. These are polyglutamated one-carbon molecules vital for the correct functioning of the folate metabolic cycle (Antony 2007). Past experiments in our research group described congenital hydrocephalus as a disorder caused by an impaired folate metabolic cycle. Hence, a treatment based on a mixture of folates (folinic acid and tetrahydrofolate (THF) was used to bypass the defective site of the cycle. The treatment reduced the incidence of

congenital hydrocephalus in the progeny to 60% (Cain et al. 2009) and improved cerebral cortex development. This brain area is narrowed in thickness during the condition due to defective cell cycle control (Mashayekhi et al. 2002 and Owen-Lynch et al. 2003). However, whilst spina bifida and cerebral folate transport deficiency conditions are successfully treated with folic acid and folinic acid respectively, congenital hydrocephalus was not ameliorated by any of these folates, on its own, in our previous studies. Following these results, we propose THF as the folate responsible for the reduced incidence of hydrocephalus with our previous treatment, and consequently the study of THF is an important aspect of the present study.

In relation to FDH, it is known that this multifunctional enzyme converts 10-formyl-THF to THF in a NADPH fashion. This reaction regulates intracellular 10-formyl-THF/THF pools (Champion et al. 1994), thereby controlling *de novo* purine biosynthesis (Krupenco et al. (2002) and Oleinik et al. 2005), and affecting the methylation potential of the cell (Anguera et al. 2006). These functions are only observed when the N and C domain are brought together in one polypeptide by the intermediate domain, a domain which is proposed to have a similar sequence to carrier proteins with a 4-PP swinging arm. It is also reported that the FDH N domain is solely responsible for the protein binding to folates, and that attachment of the N domain to the C domain through the linker is a posttranslational modification (Krupenco et al. 2002 and Krupenco et al. 2005). These characteristics suggested that single-N domains may be found bound to folates in cytoplasm in early embryonic days, and it was proposed that at this stage FDH may function as a mere folate binding protein (Donato et al. 2007).

Past experimental results in our research group pointed to the folate enzyme FDH, as the key folate enzyme responsible for folate deficit and the folate metabolic cycle impairment

observed in congenital hydrocephalus, which leads to variations in CSF composition in terms of folate profile. The resulting folate CSF imbalance was linked to the total absence of FDH in this body fluid (Nabiuni et al. 2006 and Cain et al 2009). Thus, our previous research focused mainly on CSF analysis, comparing normal and abnormal brains, rather than investigating the problem at tissue level. In this context, this research aims to further study FDH function as a folate regulatory enzyme, as well as its role in folate handling along with folate transporters at histological level.

Thus, we first aimed to investigate what specific folate-types are involved in cerebral cortex development in the presence and absence of FDH, focusing on the folate binding properties of the enzyme. Special attention was given to THF as it was the folate candidate chosen in our previous treatment and a vitamin at the core of the folate metabolic cycle. Since FDH binds to THF, its product of reaction, with tenfold more affinity than 10-formyltetrahydrofolate, its enzymatic substrate (Schirch et al. 1994), it is suggested that FDH acts as a THF reservoir for its later use in the folate metabolic cycle (Kin et al 1996, Fu et al. 1999 and Anguera et al. 2006). Moreover, because of THF's vital role in the production of key DNA components, such as nitrogenic bases as well as the amino acid methionine and S-adenosylmethionine (Krebs et al. 1976), it is expected that any variation in either extracellular or intracellular FDH concentration may be detrimental for folate metabolic cycle activity, resulting in compromised brain development. For this reason, it was important to assess FDH and THF effects on cell proliferation. Additionally, THF is a vitamin which is highly susceptible to oxidization, and exposure to air renders it inactive if not protected through stabilization by means of conjugation to structurally complementary molecules in hypoxic conditions (Krebs et al. 1976, Shane 1995, Ramaekers 2004, Davis et al 2004 and Krupenco 2009). Noble gases like Argon, a gas which reduces oxygen concentration to very low levels in hermetic areas (Krebs et al. 1976), was used for THF



conjugation to a specific immunoglobulin G (IgG). THF-IgG experiments were performed to demonstrate whether or not THF has a direct effect on cell growth. At present, it is not known whether the success of the previous treatment on hydrocephalic rats (THF + Folinic acid) was due to THF alone or its mixture with folinic acid. Since folinic acid did not have a positive effect on growth on its own (Cains et al. 2009), we wanted to determine whether stable THF is enough for potentiating cerebral cortex cell growth, thereby confirming its suitability for a future treatment, a second aim of this research.

In spite of the THF's crucial role in metabolism, the most abundant folate in food and body fluids is 5-methyl-THF (5mTHF), a vitamin which is in high demand during the first trimester of pregnancy for development of the central nervous system (Ramaekers et al. 2004, and Ramaekers et al. 2005, Solansky et al 2010 and Reynolds 2014). Yet, 5mTHF cannot be used directly by brain cells and needs to be converted to dihydrofolate and THF in the folate metabolic cycle (Molloy et al 2001 and Kamen et al. 2004). Also, since 5mTHF is found alongside FDH in CSF, and as ALDH1L1 is a folate binding protein, we were also interested in demonstrating whether 5mTHF binds to ALDH1L1, our third objective in this research. An FDH characteristic that should be highlighted in this study is the fact that this soluble protein when free in body fluids is able to bind to folates very early in its biosynthesis (Donato et al 2007 and Krupenco et al 2009). Thus, FDH behaves at early stages of brain development mainly as a folate binding protein rather than a hydrolase and/or aldehyde dehydrogenase. Consequently, a fourth aim of this project is to assess FDH affinity for 5mTHF in order to discover plausible ALDH1L1 functional similarities to soluble folate binding proteins like Folate Receptor Alpha (FR $\alpha$ ), (Selhub et al. 1984). FR $\alpha$  is a vitamin transporter of great importance in the provision of 5mTHF to the cerebral cortex (Zhao et al. 2011) during development, and is responsible for 50% of the folate transport in the brain (Anguera et al. 2006 and Steinfeld et al. 2009). In this regard, CSF

devoid of ALDH1 may explain not only folate imbalance in CSF during hydrocephalus, but also a reduced folate delivery downstream with negative repercussions for brain development as a whole.

Summarizing, we focused first on folate's impact on cerebral cortex proliferation in the presence and absence of FDH. Secondly, we concentrated on the effect of natural versus stabilized THF on cell division to ultimately explain and improve treatment efficiency. Thirdly, we studied for the first time FDH folate binding affinity for 5mTHF, and finally we assessed FDH expression and location in normal and abnormal brains in relation to 5mTHF and FR $\alpha$ .

With these investigations, we intend to contribute to broadening knowledge about folate handling mechanisms by FDH, as well as its interrelationships with folate transporters in normal and hydrocephalic brain, and ultimately to provide a potential treatment based on supplementation to the mother of just stabilized key folate (THF). Stable THF may allow a plausible increase in treatment efficiency when compared to the previously developed treatment (THF and folic acid), overcoming the problem of working with a vitamin which is known to be highly sensitive to oxidation. Even more importantly, stabilized THF treatment will avoid the need for life-threatening and invasive procedures which are the only form of cure at present. The risk of complications associated with these procedures in infants within the first weeks of life highlights the need for a non-surgical treatment like stabilized THF (Greenberg et al 2001, Kazan et al. 2005 and Warf et al. 2009).

## **2.2 MATERIAL AND METHODS**

### **2.2.1 Cell growth with folates in the presence and absence of FDH**

Cortical progenitors were prepared as previously described (Owen-Lynch et al. 2003). Cells were plated in poly-D lysine-coated 96-well plates at a density of  $1 \times 10^5$  cells/ml in standard commercial Neurobasal media contains 4mg/L of folic acid, and therefore, for the purpose of our studies, a tailor-made media without folic acid was purchased and supplemented with 1% B 27, without vitamin A (Invitrogen, Paisley, UK) for the specific growth of embryonic cerebral cortex cells. The cultures were maintained at 37 °C in 5% carbon dioxide for 24 hours to allow us to study the cells' response to media containing 5mTHF, THF and folic acid at concentration range ( $10^{-4}$ - $10^{-9}$  M) found in human plasma (Pietrzik et al. 2010), with and without inactive ALDHL1 (point mutation in intermediate domain) and active FDH (intact intermediate domain) at constant concentration ( $10^{-5}$  M) found in CSF by Western blotting (Cain et al. 2009). Inactive and active FDH was kindly provided by Dr. S Krupenco in the department of biochemistry and molecular biology, Medical University of South Carolina, Charleston, SC. Regarding inactive FDH; it was used to study exclusively its folate binding properties in isolation avoiding its enzymatic function, hence only the N domain was active to bind to folates (Fu et al. 1999). The effect of constant 5mTHF specifically at  $10^{-8}$  M along with decreasing ALDHL1 concentration at range ( $0.3$ - $10 \times 10^{-5}$ ) was also determined as well as the effect of inactive and active FDH at concentration range ( $10^{-4}$ - $10^{-9}$ ). Media without folic acid was used as negative control. Cell proliferation was measured using the fluorescent PrestoBlue cell viability reagent kit following the company's protocol (Invitrogen, Paisley, UK). Briefly, PrestoBlue reagent was 1/10 diluted in deionized water and 10µl of solution added to 100µl media per well. This step was followed by 30 minutes incubation at 37°C. Fluorescence signal due to enzymatic activity, and therefore cell division was measured on a Magellan 200

fluorimeter (TECAN, UK) set up at 535 nm and 615 nm for wavelength excitation and emission respectively. All folate solutions were purged with Argon before adding to the neurobasal media to avoid folates' oxidation, which renders folates unstable and inactive.

### **2.2.2 DAPI staining of cell cultures exposed to folates in the presence and absence of FDH.**

DAPI staining was performed for imaging and visualization of “in vitro” cell growth carried out to assess the effect on cell proliferation of FDH and folates (paragraph 2.2.1). Blue-fluorescent DAPI nucleic acid stain (Invitrogen, Paisley UK) was done following the company instructions, and cortical progenitors cells were prepared as previously described (Owen-Lynch et al. 2003). Briefly, cells were plated in poly-D lysine-coated 96-well plates containing 5 mm glass round coverslips (VWR International, Ltd.) where cells attached and grew at a density of  $1 \times 10^5$  cells/ml in Neurobasal media without folic acid supplemented with 1% B 27 without vitamin A (Invitrogen, Paisley, UK). Cultures with and without folates were maintained at 37 °C in 5% carbon dioxide for 24 hours. DAPI stains preferentially dsDNA giving rise to fluorescence enhancement detected by a fluorescence microscope with a violet filter. Coverslips were removed from wells, and mounted on slides. Photos were taken from cells attached to coverslips using a Leica DMLB fluorescence microscope connected to a coolsnap digital camera (Princeton Scientific Instruments, Monmouth Junction, New Jersey, USA).

## **2.2.3 Cell growth in response to folate (THF) conjugated to IgG.**

### **2.2.3.1 THF-IgG effect on cell growth and cell quantification using DAPI fluorescence analysis**

A study into the effect of THF on cell proliferation, but on this occasion linked to immunoglobulin G (IgG), was carried out to promote THF stability. This experiment was carried out previously to the fluorescence THF tracking experiments explained in paragraph 2.2.3.2., where THF is this time linked to a fluorescent anti-THF IgG for fluorescent tracking. Thus, in this experiment THF was first linked to IgG as follows: THF was attached to anti-THF immunoglobulin G immediately before adding it to the media as described by Leamon et al. in 1991. Briefly, THF metabolite was dissolved in dimethylsulfoxide (DMSO) and incubated with a 5 fold molar excess of 1-ethyl-3-(3-dimethylaminopropyl) carbodiimide (EDC) for 30 minutes at 23°C in the dark to “activate” the metabolite. 1mg/ml of THF antibody was added to a 10-fold molar excess of the “activated THF” and the labelling reaction was allowed to proceed at 23°C for 16h. Unreacted material was separated from the labelled THF using a Sephadex G-25 column equilibrated in PBS at pH 6.7. The extent of THF conjugation to THF antibody was determined spectrophotometrically by measuring the difference in absorbance between conjugated and non-conjugated THF at 297nm in PBS (pH 6.7). Overall, 2 folates were covalently link per IgG. Absorbance was measured on a NanoDrop ND-1000 UV/Vis spectrophotometer (NanoDrop Technologies, Inc).

THF alone and THF-IgG conjugates were added to the media at  $10^{-9}$  M, a suitable concentration for cell growth known from previous experiments. Cultures were DAPI stained as detailed before in paragraph 2.2.2. Fluorescence signal due to binding of DAPI to dsDNA correlated with cell number, and the signal was measured using a fluorimeter set

up according to the fluorescence excitation and emission profile for DAPI-dsDNA complexes: 358 nm excitation and 461 emissions respectively. The relative fluorescence index was plotted versus type of media i.e.: with and without THF after 24 hours growth.

#### 2.2.3.2 THF- IgG fluorescent tracking

To visualize and confirm whether THF enter the cells, the following experimental procedure was undertaken: cells were plated in poly-D lysine-coated 96-well plates at  $10^2$  cells/ml in neurobasal media. Neurobasal media does not contain folic acid, and it was supplemented with 1% B 27 without vitamin A (Invitrogen, Paisley, UK) to maintain cells undifferentiated. The cultures were kept at 37 °C in 5% carbon dioxide for 24 hours to study the cells response to media containing THF bound to fluorescent anti-tetrahydrofolate immunoglobulin G. Fluorescent THF antibody was prepared using 1 mg/ml THF antibody (Millipore) linked to cyanine dye. Linking was performed using the lightning link Cy3 conjugation kit following the company's protocol (Novus Biological, UK). The folate was attached to the fluorescent THF immunoglobulin G immediately before adding it to the media, and unreacted material was removed from the labelled THF as previously described in paragraph 2.2.3.1. Assessment of the extent of THF conjugation to fluorescent THF antibody is also described in this paragraph. THF-IgG complexes were added to the media at 25µg/ml. Snapshots were taken using a Leica inverted fluorescence microscope (Deirdre Bioimaging unit, University of Manchester) set up at a maximum absorbance of 670 nm suitable for Cy3.

#### 2.2.3.3 Bioavailability study of primary cell cultures in the presence of THF-IgG

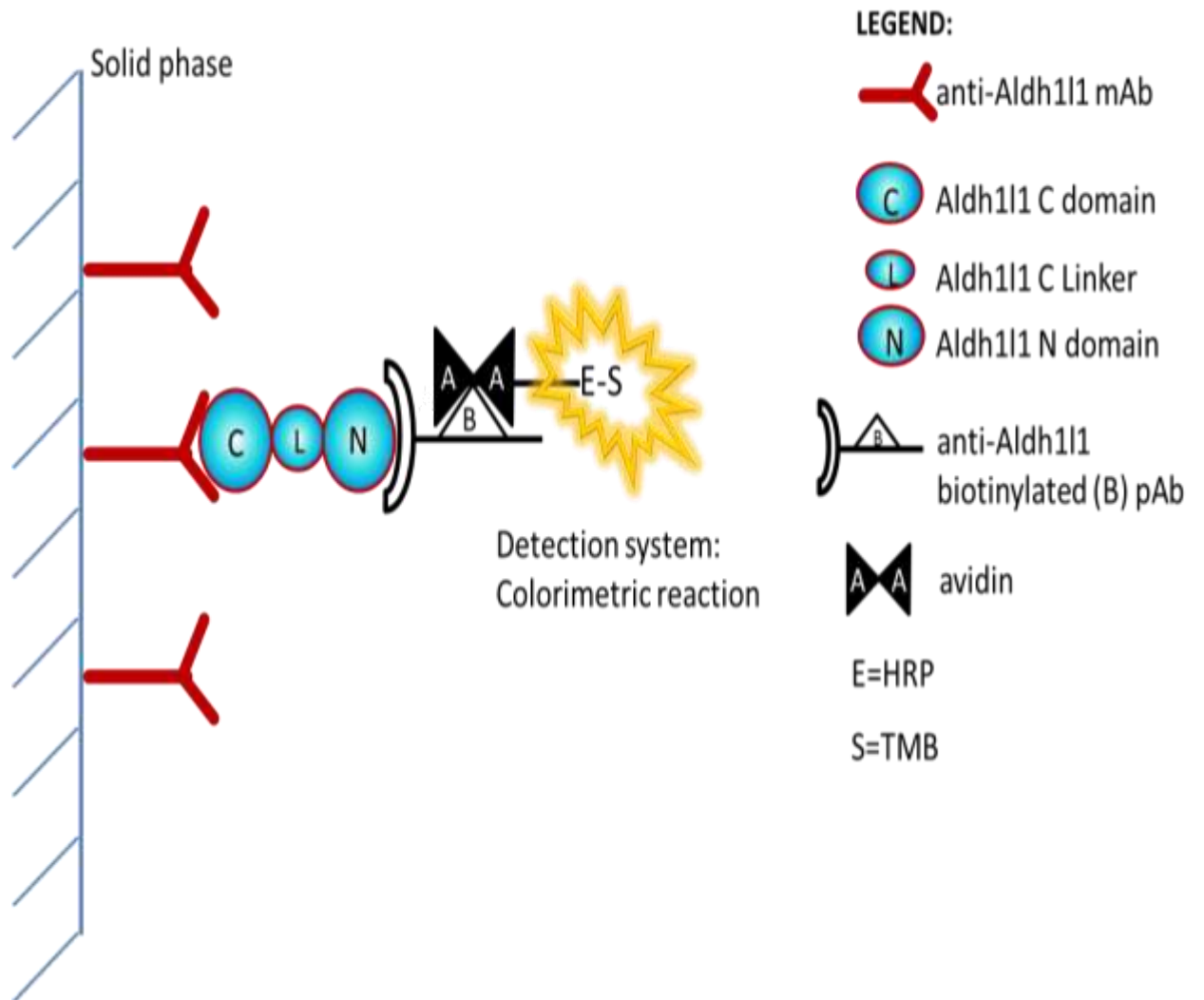
To investigate if conjugated THF had any effect on cell proliferation during the fluorescent tracking experiments, cell bioavailability was measured in parallel using the fluorescent

PrestoBlue cell viability reagent kit (Invitrogen, Paisley, UK) as described before. Fluorescence signal correlates with enzymatic activity and it was measured on a Magellan 200 fluorimeter (TECAN, UK) set up at 535 nm and 615 nm for wavelength excitation and emission respectively. Fluorescence measurements versus type of media containing THF alone and IgG-THF complexes at the start of the experiment (t=0) and after 24 hours growth were recorded and plotted in graphs.

## **2.2.4 FDH-5mTHF “in house” sandwich ELISA assay development**

### 2.2.4.1 Production of commercial and non-commercial FDH standard curves to quantify FDH binding to solid phase.

To determine the potential FDH affinity for 5mTHF, an “in house” ELISA assay was developed (Figure 2.1 below). A first step consisted of producing FDH standard curves utilizing an FDH ELISA commercial kit (Cusabio Biotech CO). The same kit was used to create a second ALDHL1 standard curve using a non-commercial FDH protein. Non-commercial ALDHL1 was added in cell culture, and for this reason its affinity for 5mTHF was also assessed to ensure this protein had a similar behaviour to the standard protein provided in the commercial kit. Non-commercial ALDHL1 was kindly provided by Dr. S Krupenco. Commercial and non-commercial FDH were full length proteins, and their corresponding standard curves were created following the company’s instructions provided in the kit. Figure 2.1 below shows kit’s sandwich enzyme immunoassay diagram used for quantification of rat FDH. FDH top standard was used at  $2 \times 10^7$  pg/ml and two fold serial dilutions were carried out to create the standard curves. The kit limit of detection was 10.93pg/ml. Fluorescent 5mTHF antibody was prepared using the Lightning Link Cy3 conjugation kit following the manufacturer’s protocol (Novus Biologicals, USA).



**Figure 2.1. Commercial sandwich ELISA for quantification of rat FDH/ALDH111.**

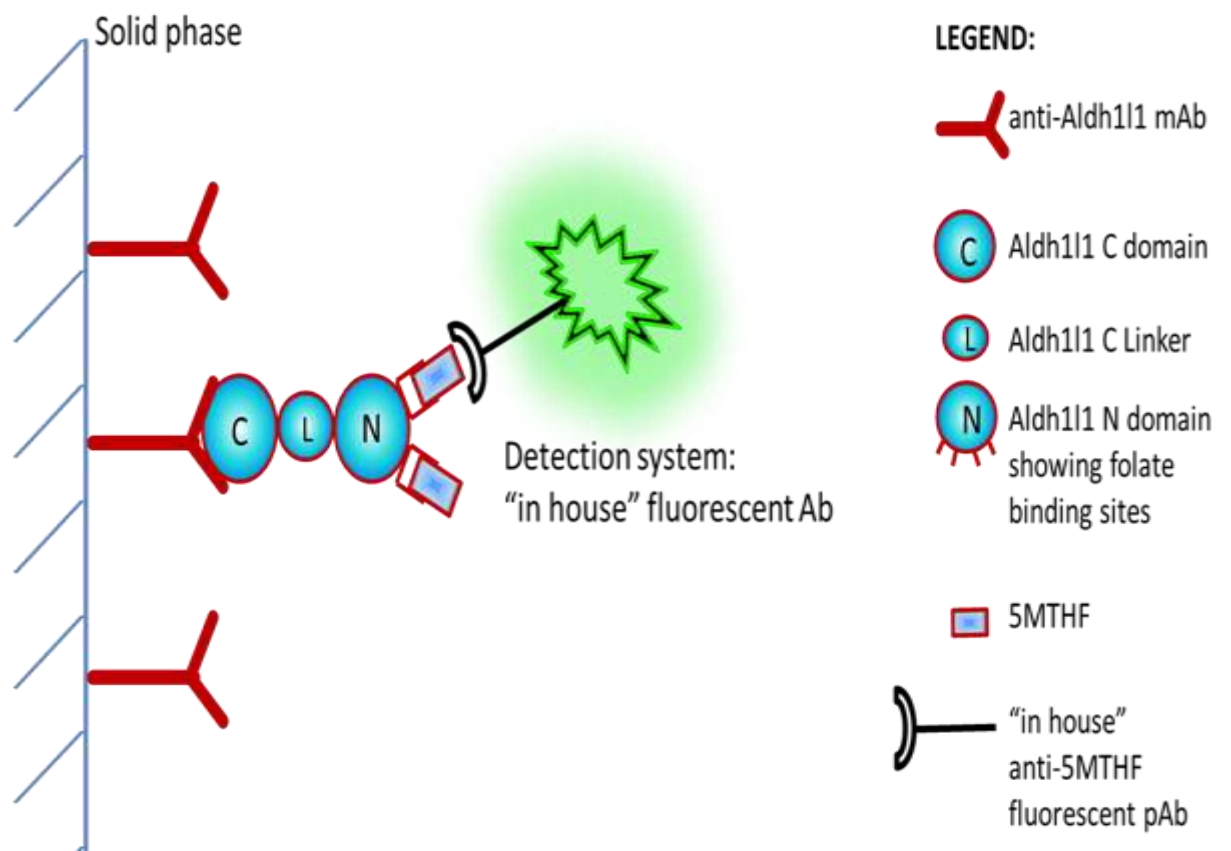


#### 2.2.4.2 Preparation of fluorescent 5mTHF antibody to be used in an “in house” fluorescent ELISA

Fluorescent 5mTHF antibody was prepared using the Lightning Link Cy3 conjugation kit following the manufacturer’s protocol (Novus Biologicals, USA).

#### 2.2.4.3 Determination of 5mTHF binding to FDH using an “in house” fluorescent ELISA .

A second ELISA was carried out in parallel to the production of FDH standard curves (paragraph 2.2.4.1.) Thus, the first step in this second experiment aimed to ensure binding of FDH to the solid phase using the conditions suggested in kit, i.e. incubation of solid phase with FDH for 2 hours at 37°C. FDH attached to the solid phase was then used to ensure detection of potential 5mTHF binding to the enzyme. Therefore, a second step in this experiment was to incubate FDH with 5mTHF overnight, while rocking at 600 rpm. 5mTHF was added at same concentration as FDH, i.e.  $2 \times 10^7$  pg/ml. A two fold serial dilution was performed to obtain a graph representing 5mTHF –FDH linking. 5mTHF and FDH concentration’s values chosen for the standard curve were decided according to FDH and 5mTHF data found in the literature for CSF (Cains et al 2009). Also, these values were decided accordingly to experiments performed by Dr. Krupenco using a ternary complex assay based on González-Segura studies in 1993 (data not published yet). After incubation, 5mTHF-FDH complexes were identified using an “in house” fluorescent anti-5mTHF Ab. See Figure 2.2 below for an “in house” 5mTHF-FDH ELISA system.



**Figure 2.2. "In house" ELISA assay to identify FDH-5mTHF complexes.**

## **2.2.5 FDH, 5mTHF and FR $\alpha$ immunolocalization in normal and hydrocephalic brain.**

### 2.2.5.1. Fluorescent dual immunostaining of coronal brain sections

Cryosections from gestational day 18 were probed with the following primary antibodies: rabbit anti-human FDH (a gently gift by Dr. S. Krupenco, mouse anti-rat 5mTHF (Millipore) and sheep anti-mouse FR $\alpha$  (R&D Systems) diluted at 1:1000, 1:2500 and 1:20 respectively in chicken serum. Sections were washed by immersion in PBS containing 0.1% Triton-X100 (VWR International, Lutterworth, UK) for 3 X 2 minutes and then antigen retrieved with sodium citrated buffer in microwave until boiling. Slides were allowed to cool and later washed 3 x 2 minutes in PBS. Afterwards, sections were carefully dried and an Immedge pen (Vector laboratories, Peterborough, UK) was used to draw a ring around every section to create a hydrophobic barrier around the edges ensuring this way blocking and Abs solution stayed over the section when added. Sections were blocked to avoid unspecific Ab bind to for 1 hour in a mixed of goat and donkey serum (Sigma Aldrich Company, Ltd, Dorset, UK) at 5% each serum in PBS-Triton-X100 0.1%. Blocking was carried out at room temperature in a humidity chamber. After blocking, 3 x 5 minutes washes in PBS Tween-20 1% sections were performed followed by incubation primary antibodies overnight. Double immunostaining was achieved by incubating FDH antibody either with 5mTHF or FR. After incubation, 3 x 5 minutes washes in PBS Tween-20 1% were carried out followed by incubation this time with secondary fluorescent Abs. All secondary antibodies were diluted at 1:200 in PBS Tween-20 1%. Green goat anti-rabbit antibody was chosen for FDH (Alexa 488 Sigma Aldrich Company Ltd. Dorset UK), red fluorescent sheep anti-mouse (Alexa fluor 594 Sigma Aldrich Company Ltd. Dorset UK) was chosen to detect 5mTHF and red fluorescent donkey anti-sheep for FR $\alpha$  location (Northern lights R&D Systems, UK). Negative controls were obtained by incubation with PBS instead of primary Abs. Secondary Abs were added to all slides and

incubated for 1 hour. Incubation was followed by 3 x 5 minutes washes in PBS Tween-20 1% before mounting slides in Vectashield with Propidium iodide (Vector laboratories, Peterborough, UK).

#### 2.2.5.2. Image analysis of sections captured by fluorescence microscopy

Tissue sections were captured on a Leica DMLB fluorescence microscope connected to a coolsnap digital camera (Princeton Scientific Instruments, Monmouth Junction, New Jersey, USA). The fluorophore chosen for FDH location (Alexa 488) was excited using the blue filter resulting in green light emission whereas fluorophores selected for 5mTHF and FR $\alpha$  location were excited using the green filter given rise to red fluorescence emission. Constant exposure times (500 milliseconds) were kept within and between stains. Images were analysed for level of fluorescence using Image J 1.36 b image processing software (National Institute of Health; <http://rsb.info.nih.gov/ij>). At least 10 images per experimental condition were imaged. The colour channel corresponding to the fluorophore used (green or red) from the source multichannel/composite image was selected, and the area of interest (fluorescent area) to be included in analysis was marked out using the "ROI" plugging. The "Threshold" plugging was used to determine the minimum and maximum signal/number of pixels in the region of interest and a value with intensity above the minimum threshold reading was chosen arbitrarily. The threshold value was maintained within and between stains. All regions of interest were counted and average using the tool ROI manager. Pixels were converted to area in microns squared (100x magnification, 1 micron=1 pixel). To avoid artificial inflation of positive staining in tissue, areas of fluorescence above the threshold value, but less than 10 $\mu\text{m}^2$  in area, were considered too small to be cells and were not included in the analysis. Total area above the threshold was calculated against a total area of analysis (10<sup>5</sup>  $\mu\text{m}^2$ ). Area/pixels above the threshold (area

positive) were recorded and expressed as density of positive staining within the total area analysed. Density was calculated using the formula shown below;

$$\text{Fluorescence density} = \frac{\text{Area positive (fluorescence above threshold)} \times 10^5 \mu\text{m}^2}{\text{Total area analysed}}$$

### 2.2.5.3 Fluorescent dual immunostaining and sequential detection by confocal microscopy

A Leica SP5 acousto-optical beam splitter confocal microscope with a 60x/0.75 numerical aperture Fluotar objective (Leica, Milton Keynes, UK) was used for sequential imaging to avoid spectral bleedthrough using the following settings: To locate FDH, a 495 nm laser line for Alexa 488 fluorophore excitation with green fluorescence emission detection at 519 nm was selected. In relation to 5mTHF and FR $\alpha$  identification, fluorophores Alexa 594 and Northern Lights respectively were excited using a 510 nm laser line for excitation and 590 nm for detection. Images of transmitted light were transferred to Image J software (version 1.37a; NIH, Bethesda, MA, USA). One 16 image “Z” stack was acquired per section. Sequential images were obtained, which involved exciting fluorophores on the tissue sections with only one laser at a time, and collecting fluorescent photons emitted by the excited fluorophores individually, in order to avoid cross-over of fluorescence emission of each specific channel. This approach was decided on the basis of the fluorophores broad bandwidths i.e.: 488-519 for fluorophore Alexa 488 and 510-590 for fluorophore Alexa 594 and Northern Lights.

## **2.2.6 Expression of FDH mRNA in normal and hydrocephalic brain.**

### 2.2.6.1 FDH mRNA location in normal and hydrocephalic brain using reverse transcription

#### “In situ” PCR.

Reverse transcription “in situ” PCR was performed in two steps: reverse transcription and cDNA amplification using PCR. The aim was further confirmation of ALDH1 mRNA expression in normal and abnormal brain and more importantly, the specific location of mRNA on tissue sections. A method was developed based on a modification of the technique elaborated by GJ Nuovo in 1997. The technique was optimized and adapted to our purposes using the following reagents, methodology and equipment:

#### **Reagents:**

All chemicals involved in this technique were molecular biology grade and treated with 0.1% DEPC for 12 hours, including distilled deionized water (ddw). The following buffers and solutions were prepared as described below:

-Blocking stock solution: A blocking reagent for nucleic acid hybridization and detection (Roche diagnostics, Mannheim, Germany) was solubilized in maleic acid buffer (100 mM maleic acid, 150 mM NaCl, pH 7.5, adjusted with Na OH to a final concentration of 10% (w/v) with shaking and heating in a microwave oven.

-Neutral buffered formalin (NBF): This buffer was prepared by dissolving 6.5 g of sodium phosphate dibasic and 4 g of sodium phosphate monobasic monohydrate in 500 ml of ddw, mix for 10 minutes, and then 100 ml of 4% paraformaldehyde were added and made up to 1 liter. pH was adjusted to 7.4 using sodium hydroxide.

-Phosphate buffer saline: This buffer was prepared by mixing 8g/L sodium chloride, 0.2 g/L potassium chloride, 1.42 g/L sodium hydrogen phosphate and 0.24 g/L potassium dihydrogen phosphate (pH 7.4).

-20 x sodium chloride-sodium citrate stock solution (SSC): 175.2 g sodium chloride and 88.2 g sodium citrate in ddw were mixed and then made up to 1 liter and solution adjusted to pH 7.0.

-Triton X-100 buffer: 0.1 M Tris-hydrochloric acid buffer (pH 7.4) containing 0.25% Triton X-100 (Sigma chemical Co. St. Louis, MO T-8787) and Igepal CA630 (Sigma, I-8896).

-RNase-Zap cleaning agent (Sigma, R2020).

-DNase I (RNase-free) and DNase buffer solution kit (New England Biolabs).

-Ribonuclease A (100µg/ml, Sigma)

-Maxima Reverse Transcriptase (Thermo scientific, EPO741) containing an RNA and DNA-dependent polymerase activity at 200U/µl (2000 U). The kit also contains 5X reverse transcription buffer and Ribolock RNase inhibitor (20 U).

-Oligo (dT)<sub>18</sub> primer (Thermo scientific, SO131)

- Jump-Start™ Taq DNA polymerase (Sigma, D4184) containing 10X reaction buffer without MgCl<sub>2</sub> which is provided separately at 25mM.

- Deoxynucleotides set solution (New England Biolab, UK limited) containing dATP, dCTP, dGTP and dTTP at 100 mM.

-Random primer Digoxigenin-11-2'-deoxy-uridine-5'-triphosphate alkali-labile (Roche diagnostics, Mannheim, Germany).

-FDH Genbank primer. Accession number: NM\_022547.1. Primers were designed using Roche ProbeFinder for rat version 2.49 ([www.rochediagnostics.qpcr.probefinder.com](http://www.rochediagnostics.qpcr.probefinder.com)).

Primers were selected from mRNA spliced sequences as these are uniquely in mRNA and we intend to amplify exclusively cDNA after reverse transcription from mRNA.

Therefore, gDNA synthesis in nuclei is in this avoided. Nevertheless, DNase treatment for inactivation of gDNA is also performed as described later in methodology (DNase digestion step).

Sense primer: **TCGACACTCAACACTTCAGGA.**

Antisense primer: **GGCTCCTGGGATGGGTAA**

- Anti-digoxigenin-rhodamine Fab fragments (Roche diagnostics, Mannheim, Germany).

### **Methodology:**

-Preparation and pretreatment of fresh brain and liver sections.

All surgical tools and microslides used for preparation of rat tissue sections were treated with 0.1% diethylpyrocarbonate (DEPC) for 12 hours at room temperature, then autoclaved aiming to eliminate any RNase activity and potential RNA polymerase damage.

All steps involved were handled with nitrile plastic gloves sprayed with RNase ZAP to remove RNase from gloves. Incubation and washes steps were performed at room temperature.

Control Sprague Dawley and hydrocephalic Texas pregnant rats were deeply anesthetized by intravenous injection with 50 mg/kg of sodium pentobarbital, and later euthanized by cervical dislocation. Rats at gestational day 19 were dissected and fetuses removed and euthanized while lay on ice for 15 minutes. Liver tissue was chosen as positive control, as



it is known is abundant in ALDHL1 protein and cDNA has been successfully isolated and characterized before in mammal liver (Min et al. 1988, Cook et al. 1991 and Hong et al. 1999). Embryonic brain, and maternal liver (“in situ” PCR tissue control), were removed quickly and frozen in isopentane cooled down by immersion on dry ice. All brains were stored at -70°C until use. Brains and liver were sectioned with a cryostat and 7µm thick sections were thaw-mounted onto the “In situ” PCR glass slides, two brain sections and one liver section (positive control) were arranged per microslide so that negative controls, positive controls and “test samples” were stained simultaneously. The sections were either store at -70 °C or transferred to the next step immediately.

The sections were fixed in NBF for 30 minutes at room temperature or overnight at 4°C, then, rinsed three times with PBS for 5 minutes each wash. After the washes, the slides were treated with 3% hydrogen peroxide in methanol for 15 minutes followed by two five minutes washes in PBS.

#### -DNase digestion

All sections were treated with 1U/µl of DNase I (RNase-free) solution before reverse transcription step to render gDNA template unavailable for DNA synthesis. Microslides were covered with incubation chambers RNase/ DNase free to prevent drying and incubated for 4 hours at 37°C. After incubation, the incubation chambers were removed and EDTA was included into the DNase I solution on slide at 5mM. Microslides were placed in incubator for 10 minutes at 75°C. After incubation with EDTA, slides were washed with DNase buffer for 5 minutes then rinsed in PBS-glycine (2% w/v), PBS and DEPC water for 5 minutes each. The washes were followed by treatment for 1 minute only with a graded series of ethanol (70- 100%) and air dried.

Positive control:

Rat liver tissue known to express FDH in high concentration was DNase treated, and used as positive control to assess the effectiveness of chosen FDH primers and suitability of experimental conditions for amplification of mRNA/cDNA using “In situ” PCR technique. One liver tissue section was placed per microslide along with negative control and “test section”.

Negative control:

One section per microslide was subjected to DNase treatment, and reverse transcription but, on this occasion, reverse primer or forward primer was omitted in the PCR master mix to demonstrate signal is due to amplification of cDNA by “In situ” PCR. For this reason, signal is not expected in negative controls.

Test sections:

One section per microslide is chosen as “test sections”, therefore, DNase treatment and RTPCR reagents are added to this section for reverse transcription of specific FDH mRNA to cDNA first, and later cDNA amplification with FDH primers. Positive staining (FDH mRNA/cDNA-Rhodamine labelled) was expected in cytoplasm of cells exclusively in these sections. This is due to the fact that all DNA, other than cDNA (mRNA), is inactivated by DNase treatment previously to reverse transcription. Furthermore and as aforementioned, gDNA synthesis is avoided by chosen primers from unique sequences of mRNA that are not present in gDNA as they occur after mRNA maturation and splitting, resulting in mRNA sequences with non-contiguous regions in the DNA.

-Reverse transcription. First step RT in situ PCR.

All reagents and microcentrifuge tubes were placed on ice, and a specific lab area was designated to perform the reaction. In a sterile microcentrifuge tube, the following reagents were assembled to cover just one test section:

Primer oligo (dt) <sub>15</sub> at 500µg/ml (stock)	3µl
dNTPs (each nucleotide at 10 mM)	3µl
RT maxima buffer (x1)	12µl
RNase inhibitor	1.5µl
RT maxima at 200 U/µl (stock)	1µl
H <sub>2</sub> O	60µl

50µl of reaction mixture was added per test section. To prevent sample dehydration during RT reaction, an incubation chamber was anchored to the slide before incubation on a thermal cycle block set at 50°C for 30 minutes followed by 85°C for 5 minutes. DEPC water was added to sections chosen on slide as controls.

-First SSC treatment.

After the reverse transcription step, all sections on the slide were washed twice with SSC buffer at room temperature for 10 minutes, followed by a final wash at 45°C for 10 minutes, and they were then air dried. CDNA amplification by PCR was carried out straight after SSC treatment.

-PCR. Second step RT in situ PCR.

In a sterile microcentrifuge tube, the following reagents were added in the following order to prepare 130  $\mu$ l of reaction mixture, enough to cover one slide i.e.: three sections.

Forward primer	5.2 $\mu$ l at 0.5 $\mu$ M (final concentration)
Reverse primer	5.2 $\mu$ l at 0.5 $\mu$ M (final concentration)
dATP	2.6 $\mu$ l at 200 $\mu$ M (final concentration)
dGTP	2.6 $\mu$ l at 200 $\mu$ M (final concentration)
dCTP	2.6 $\mu$ l at 200 $\mu$ M (final concentration)
dTTP	1.56 $\mu$ l at 100 $\mu$ M (final concentration)
DIG-11- dUTP	1.56 $\mu$ l at 1mM (stock)
Mg Cl <sub>2</sub>	20.8 $\mu$ l 25 mM (stock)
Blocking solution	13 $\mu$ l (10% w/v)
PCR buffer (x10)	13 $\mu$ l
Jump start enzyme	30.12 $\mu$ l (60 units/slide)
H <sub>2</sub> O	to 130 $\mu$ l

Each slide is coated with 130  $\mu$ l of PCR reaction mixture, covered with an incubation chamber, and finally placed on thermocycler set up to perform the thermal cycle series indicated on table 2.1 below:

Cycle number	Denaturation	Annealing	Polymerization
1	1 min at 94°C		
35	30 sec at 94°C	1 min at 55°C	1 min at 72°C
1			1 min at 72 °C

**Table 2.1. Thermocycler parameters used for “in situ” PCR i.e.: cDNA amplification.**

The newly formed cDNA was to be detected using the probe dig-11-dUTP after RT-PCR rather than by directed labelling.

-Second SSC treatment.

Slides were subjected to high stringency conditions by washing with 0.2 x SSC twice at 60C° for 10 minutes each, followed by rinsing in PBS for 5 minutes.

#### Equipment:

-A cryostat MicronHM 500 (Micron, Heidelberg, Germany) was used for obtaining tissue sections.

-A G-Storm GSI thermocycler (Labtech International/Tecan Ltd. Reading, UK) and CoverWell™ incubation chambers - RNase/ DNase free - were used, as well as microslides, superfrost ultraplus (VWR International Ltd.), for mRNA reverse transcription to cDNA and its amplification on brain tissue sections attached to microslides.

-A Leica DMLB fluorescence microscope coupled to a coolsnap digital camera (Princeton Scientific Instruments, Monmouth Junction, New Jersey, USA) was used to take images of transmitted light, as explained in paragraph 2.2.5.2. All images were transferred to Image J software (version 1.37a; NIH, Bethesda, MA, USA).

-A Leica SP5 acousto-optical beam splitter confocal microscope with a 60x/0.75 numerical aperture Fluotar objective (Leica, Milton Keynes, UK) was used for simultaneous imaging of DAPI and Rhodamine. 405/450 excitation/emission laser lines for DAPI and 510/590 excitation/emission laser lines for detection of FDH mRNA expression were used respectively. Images of transmitted light were transferred to Image J software (version 1.37a; NIH, Bethesda, MA, USA). One 16 image "Z" stack was acquired per section.

#### 2.2.6.2 FDH mRNA quantification in cerebral cortex tissue using real time quantitative PCR.

Real-time quantitative PCR (RTqPCR) was used to measure FDH mRNA expression in normal and hydrocephalic brain. Six normal and five hydrocephalic samples were analysed in parallel (each sample representing an individual cerebral cortex). Total RNA was extracted from whole fetal cerebral cortex using TRIzol reagent following the manufacturer's instructions (Invitrogen, UK). To synthesize cDNA, 2µg RNA was reverse transcribed using oligo (dT)<sub>15</sub> primers (Promega, UK) and Maxima Reverse Transcriptase (Thermo Scientific, UK). Rat liver total RNA, also extracted with TRIzol reagent in the same conditions as cerebral cortex, served as positive control. Omission of reverse transcriptase was used as negative control. cDNA at 400ng/µl was amplified using SYBR Green Jump Start master mix following the company's instructions (SIGMA). cDNA integrity was confirmed by b-actin amplification as described previously. Amplification of tyrosine 3-monooxygenase/tryptophan 5-monooxygenase activation protein (YWHAZ) mRNA (Table 2.2), a stable housekeeping gene expressed in brain, confirmed cDNA input was comparable between normal and hydrocephalic cerebral cortex samples. Specific primer sequences for cDNA amplification (Table 1) were designed from Gen-Bank sequences using Roche ProbeFinder for rat version 2.49 ([www.rochediagnostics.qpcr.probefinder.com](http://www.rochediagnostics.qpcr.probefinder.com)). mRNA expression was quantified using Step-One AB Applied Biosystems with normalization to positive control (liver) as internal calibrator. All reactions were run in triplicates using ROX as passive reference dye. PCR conditions were as follows: initial denaturation at 95°C x 15 min, followed by 40 PCR cycles of denaturation at 94°C X 15 sec, annealing for 30 sec at optimal annealing temperature (T<sub>a</sub> in Table 2.2) and extension at 72°C X 30 sec. PCR reaction efficiency approximated to 100% for all genes. Relative quantification of cDNA amplification

(mRNA expression) was carried out using the comparative method following Step-One AB Applied Biosystems software version 2.2 instructions.

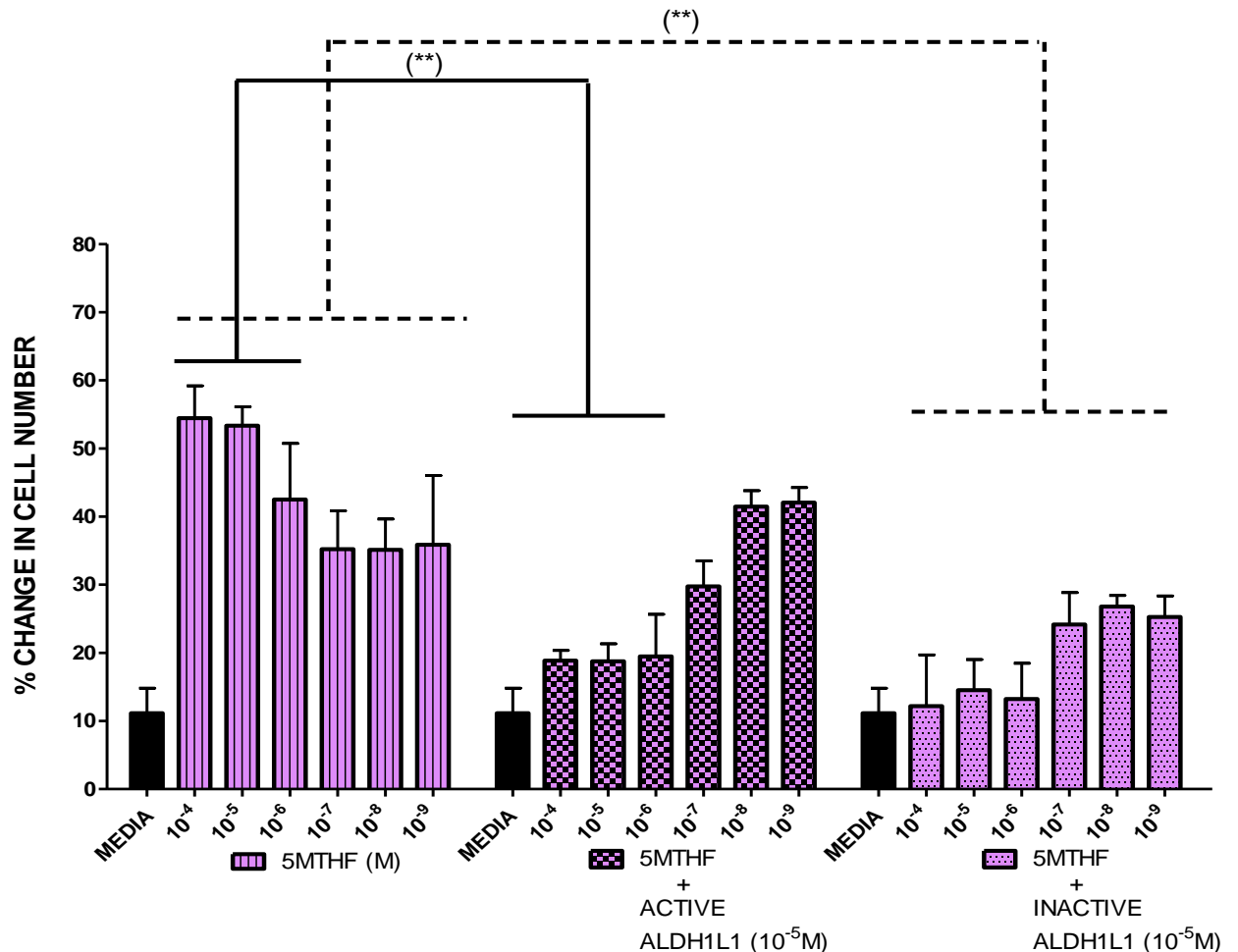
<b>Genes (rat)</b>	<b>Accession number</b>	<b>T<sub>a</sub> (°C)</b>	<b>Sense primer</b>	<b>Antisense primer</b>
<b>FDH</b>	<b>NM_022547.1</b>	<b>55</b>	<b>TCGACACTCAAC ACTTCAGGA</b>	<b>GGCTCC TGGGA TGGGTAA</b>
<b>BACTIN</b>	<b>NM_031144.2</b>	<b>60</b>	<b>CCCGCGAGTACA CCTTCT</b>	<b>CGTCATCCATGG CGAACT</b>
<b>YWHAZ</b>	<b>NM_01135699.1</b>	<b>55</b>	<b>CTACCGCTACTT GGCTGAGG</b>	<b>TGTGACTGGTC CACAATTCC</b>

**Table 2.2. Gene sequences and annealing temperatures (T<sub>a</sub>) for primers targeting FDH/ALDH1L1 and housekeeping genes.**

## 2.3 RESULTS

### 2.3.1 5mTHF in combination with FDH is detrimental for cell growth.

#### 2.3.1.1 Decreasing concentration of 5mTHF plus constant FDH



**Figure 2.3. Effect of decreasing 5mTHF and constant active and inactive FDH concentration on cell proliferation. MTHF alone (line pattern), 5mTHF + active FDH (square pattern) and 5mTHF + inactive FDH (dot pattern). Primary cortical cells from E19 Sprague- Dawley foetuses were incubated with the metabolite at 10<sup>-4</sup> - 10<sup>-9</sup> M, as illustrated in the graph, in the absence and presence of FDH at 10<sup>-5</sup> M. Cell bioavailability was measured using a fluorescence-based assay, as described in material and methods (2.2.1). Data are presented as mean percentages in cell change ± SEM obtained after normalization of relative fluorescence indexes (RFI) measurements (n=6). Analysis of variance (two-ways ANOVA) with Bonferroni post hoc test revealed significant differences in the indicated paired samples. Results are shown as: \*\*p < 0.01 for the effect on proliferation of 5mTHF alone versus 5mTHF in combination with FDH.**

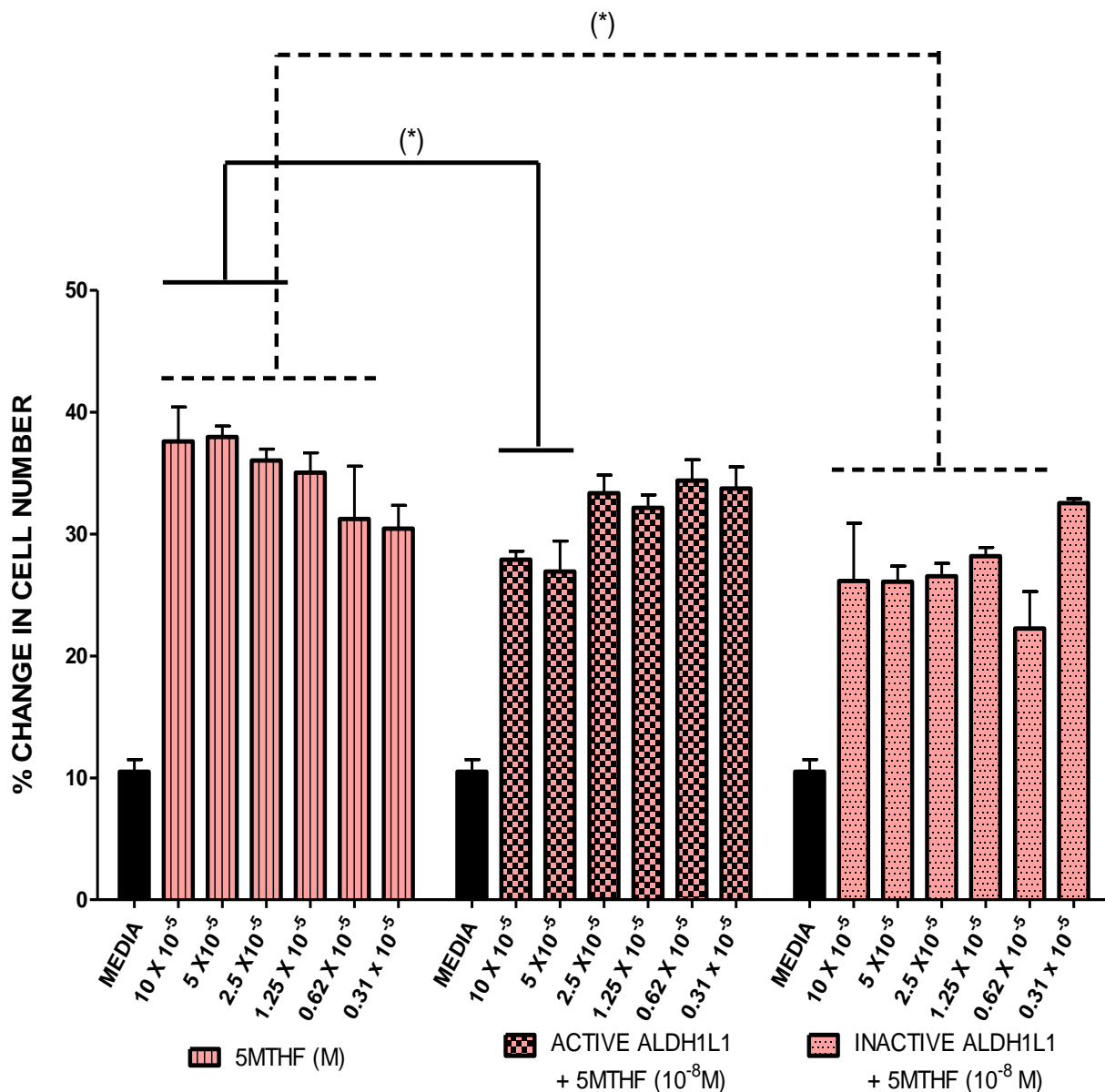


In order to determine the effect of constant FDH and decreasing 5mTHF concentration on cell growth, the metabolite was added to neurobasal media at concentration range  $10^{-4}$ -  $10^{-9}$  M, with and without active and inactive FDH at  $10^{-5}$  M. Control experiments showed that E19 cortical cells cultured in neurobasal media increased overall in cell number above media control levels (no folates) after 24 hours (Figure 2.3). The average percentage increases were of  $42.7 \pm 6$ ,  $28.38 \pm 3.08$  and  $13.84 \pm 4.34$  for media containing 5mTHF, 5mTHF plus active FDH, and 5mTHF plus inactive FDH respectively. Media with 5mTHF alone at a range of concentration  $10^{-4}$  –  $10^{-6}$  M caused a percentage increase in cell number of  $54.43 \pm 4.7$ ,  $53.34 \pm 2.7$  and  $42.50 \pm 8.2$ . These data show that cell proliferation was directly proportional to the concentration of 5mTHF in the media. By contrast, in general, the presence of FDH in combination with 5mTHF showed a clearly negative effect on cell growth with, both active and inactive protein. Thus, the addition of active FDH caused significant percentage decreases in cell number of  $35.59 \pm 1.31$ ,  $34.57 \pm 2.54$  and  $23.02 \pm 6.17$  when compared to media containing 5mTHF alone at  $10^{-4}$ ,  $10^{-5}$  and  $10^{-6}$  M respectively, ( $p < 0.01$ ). Moreover, the inhibitive effect of FDH on cell growth was null at 5mTHF  $10^{-8}$  and  $10^{-9}$  M, with percentage increase values of  $6.16 \pm 2.34$  and  $6.33 \pm 2.22$  respectively in the presence of active FDH. However, these results were not significant ( $p > 0.05$ )

In relation to inactive ALDH1L1, a generalized negative effect on growth at all 5mTHF concentrations occurred, with significant percentage decreases ( $p < 0.01$ ) as follows:  $42.23 \pm 7.51$ ,  $38.81 \pm 4.48$ ,  $29.26 \pm 5.20$ ,  $11.08 \pm 4.71$ ,  $8.32 \pm 1.61$  and  $10.60 \pm 3.07$ .

### 2.3.1.2 Decreasing concentration of FDH plus constant 5mTHF

Past Western blotting experiments allowed relative quantification of FDH in CSF of normal rats, revealing FDH in CSF is present at  $10^{-5}$ M (Cain et al. 2009). By contrast, a negligible signal was detected in hydrocephalic CSF. The experiments illustrated in figure 2.3 show some cell growth in the presence of ALDHL1 at  $10^{-5}$ M, along with 5mTHF at  $10^{-8}$ M, either with active or inactive FDH. These values were considered to further study the cell response to 5mTHF in combination with FDH but, on this occasion using FDH at concentration range  $10 - 0.31 \times 10^{-5}$  M and constant 5mTHF at  $10^{-8}$ M. Results from this experiment are shown in figure 2.4. This graph indicates that cortical cells cultured in neurobasal media with 5MTHF had a generalized increase in cell proliferation above media control levels following 24 hours growth at all concentrations. The average percentage increase was  $34.16 \pm 2.26$  with 5MTHF alone and  $16.46 \pm 3.32$  in the presence of 5mTHF plus active FDH. Cell proliferation was also slightly encouraged with 5mTHF plus inactive FDH, with an average percentage increase of  $20.91 \pm 4.03$ . In conclusion, 5MTHF alone without FDH led to the highest percentage increase in cell number.



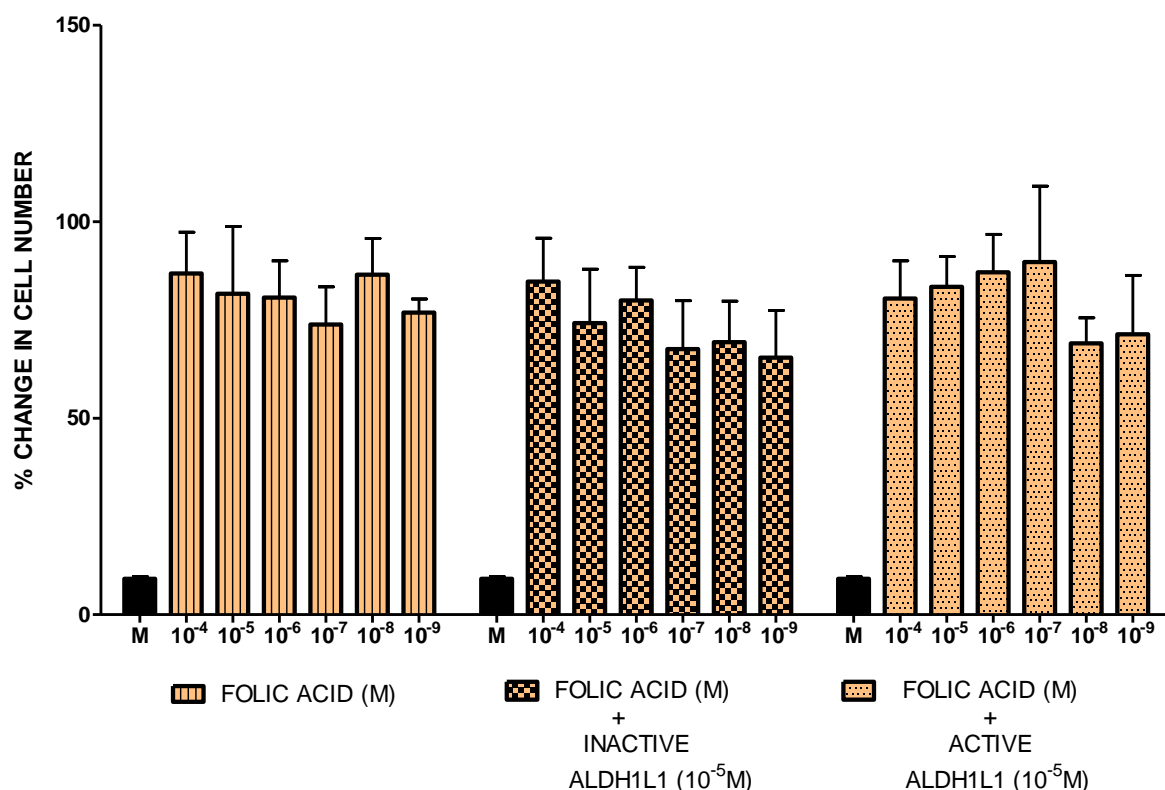
**Figure 2.4.** Effect on cell proliferation of decreasing 5mTHF alone, decreasing active FDH plus constant 5mTHF and decreasing inactive FDH plus constant 5mTHF. 5mTHF alone (line pattern), 5mTHF + active FDH (square pattern) and 5mTHF + inactive FDH (dot pattern). Cell bioavailability was measured using a fluorescence-based assay as described in material and methods (2.2.1). Data are presented as mean percentages in cell change  $\pm$  SEM obtained after normalization of relative fluorescence indexes (RFI) measurements (n=6). Analysis of variance (two-ways ANOVA) with Bonferroni post hoc test revealed significant differences in the indicated paired samples. Results are shown as: \*p < 0.05 for the effect on proliferation of decreasing 5mTHF alone versus constant 5mTHF in combination with decreasing active and inactive FDH.

Figure 2.4 also shows how 5mTHF at constant concentration in the presence of active FDH at  $10 \times 10^{-5}$  and  $5 \times 10^{-5}$  M reduced cell growth significantly with percentage decreases of  $9.73 \pm 0.75$  and  $11.04 \pm 2.58$  respectively (\* $p < 0.05$ ). However, the decrease in growth was less pronounced at FDH concentration of  $2.5 \times 10^{-5}$  and  $1.25 \times 10^{-5}$ , with percentage decreases of  $2.71 \pm 3.44$  and  $2.93 \pm 1.67$ . Finally, a relative percentage increase occurred at FDH concentration of  $0.62 \times 10^{-5}$  and  $0.31 \times 10^{-5}$  M with percentage increases values of  $3.15 \pm 1.69$  and  $3.33 \pm 1.76$ .

In relation to inactive FDH, there was a generalized decrease in cell number at concentration range  $10$ - $0.62 \times 10^{-5}$  M with percentage decreases of  $11.45 \pm 4.73$ ,  $11.86 \pm 1.27$ ,  $9.52 \pm 1.06$ ,  $6.85 \pm 0.70$  and  $9.12 \pm 3.04$  (\* $p < 0.05$ ). Similar to the results obtained from media treated with active FDH, a relative percentage increase of  $2.14 \pm 0.35$  was obtained at  $0.31 \times 10^{-5}$  M.

In summary, the positive effect on cell growth of 5mTHF can be perturbed by adding FDH to the media, and this effect is more intense in the presence of inactive FDH than active FDH. Importantly, FDH's inhibitory effect on cell growth is observed at high concentration in the range  $10$ - $5 \times 10^{-5}$  M, suggesting a concentration effect of FDH on cell growth.

### 2.3.2 Cell growth is not inhibited with folic acid in the presence of FDH

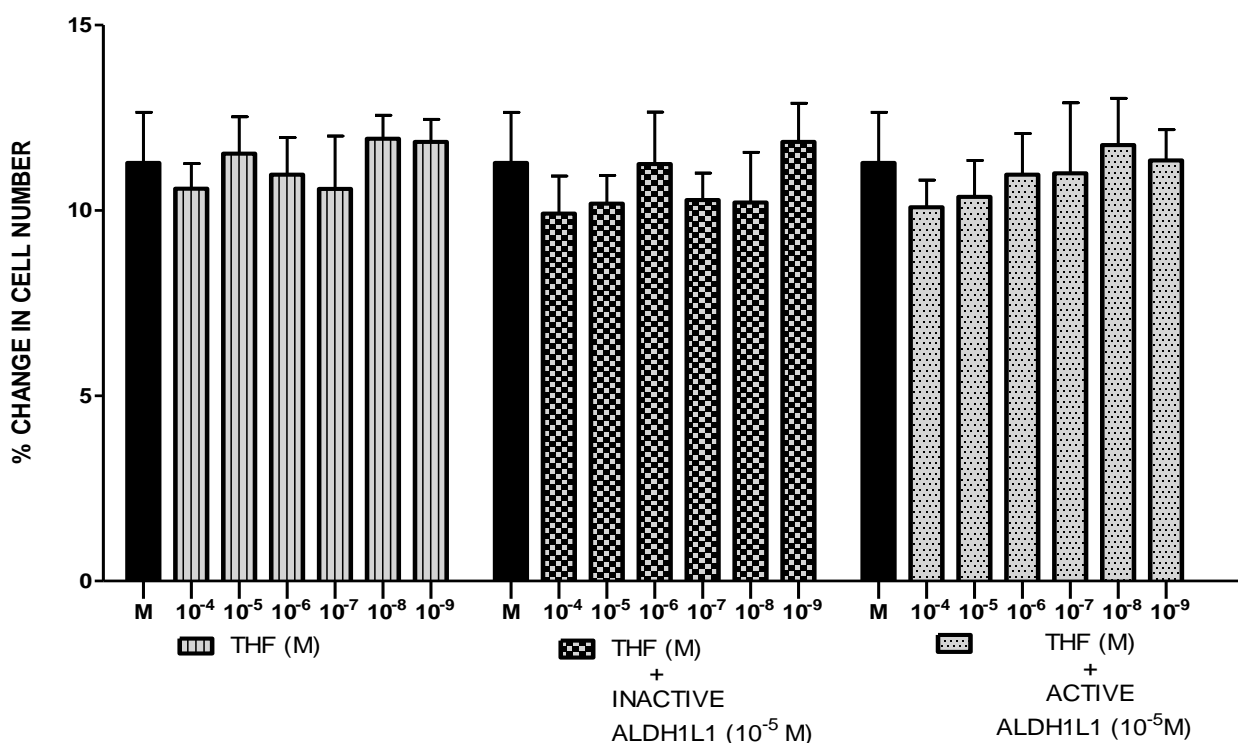


**Figure 2.5. Effect on cell proliferation of folic acid alone (line pattern), folic acid plus inactive ALDH1L1 (square pattern) and folic acid plus active FDH (dot pattern) all at decreasing concentrations. Cell bioavailability was measured using a fluorescence-based assay as described in material and methods (2.2.1). Data are presented as mean percentages in cell change  $\pm$  SEM obtained after normalization of relative fluorescence indexes (RFI) measurements (n=6).**

Folic acid is an artificial and stable folate commonly found within commercial media. The media control used throughout all experiments did not contain folic acid. Thus, folic acid was added to neurobasal media, and its effect on cell division assessed by comparison with media control in the presence and absence of inactive and active FDH. Figure 2.5 shows that cells in all conditions presented an average percentage increase above media control levels of  $82.43 \pm 7.75$ . On the other hand, media containing folic acid alone versus media with the folate in combination with either inactive or active FDH showed some small cell growth when FDH was present at specific concentrations. Thus, the average percentage

decreases due to FDH presence were  $8.86 \pm 3.57$  with inactive FDH and  $8.84 \pm 2.54$  with active FDH. In conclusion, FDH did not perturb cell growth in the presence of folic acid.

### 2.3.3 Commercial and unstable THF does not promote growth with or without FDH.

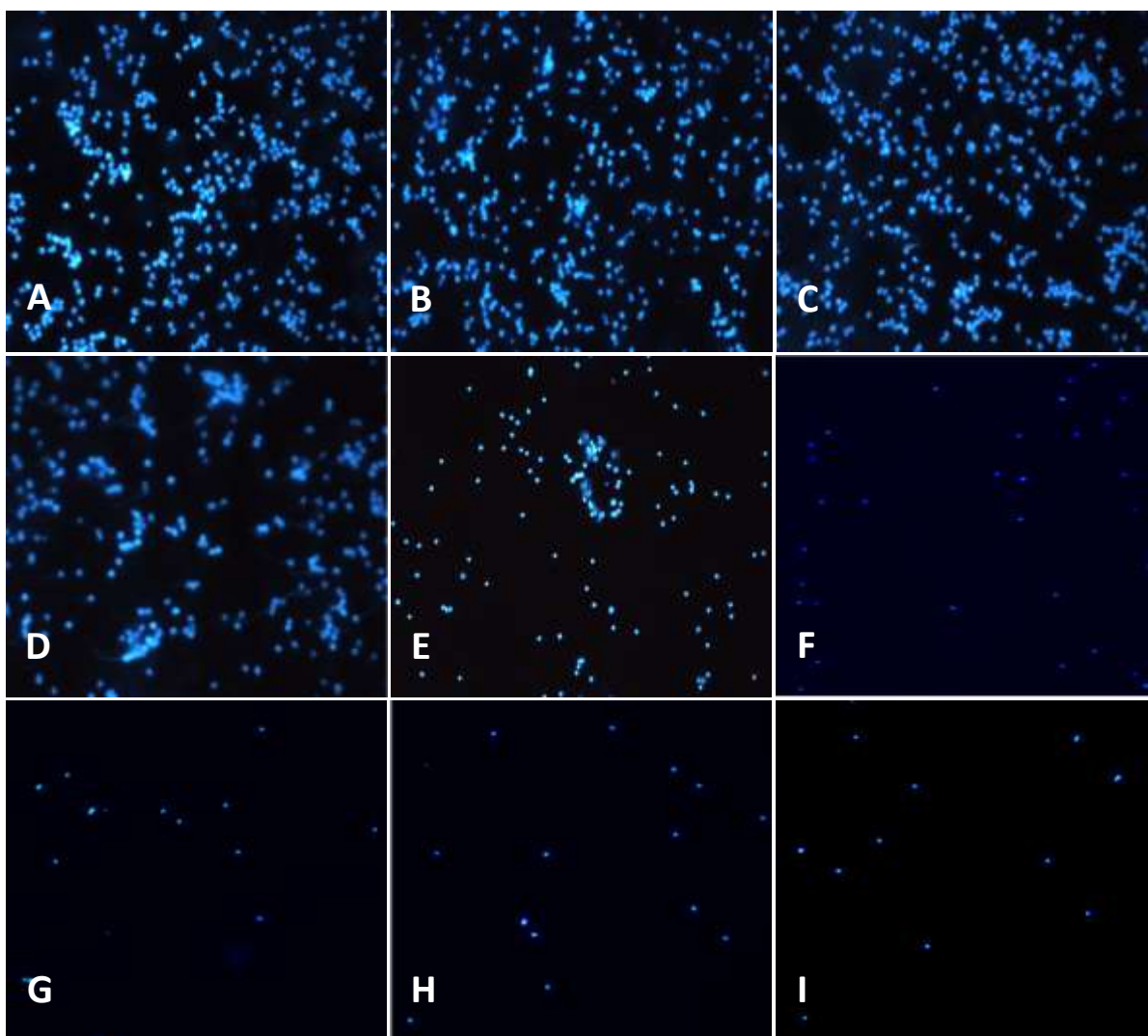


**Figure 2.6. Effect on cell proliferation of THF alone (line pattern), THF plus inactive ALDH1L1 (square pattern) and THF plus active ALDH1L1 (dot pattern) all at decreasing concentrations. Cell bioavailability was measured using a fluorescence-based assay as described in material and methods (2.2.1). Data are presented as mean percentages in cell change  $\pm$  SEM obtained after normalization of relative fluorescence indexes (RFI) measurements (n=6).**

THF is the product of FDH enzymatic reaction, and the effect of both molecules on cell division was determined by adding them to neurobasal media. Thus, THF alone, THF in combination with FDH and finally THF with active FDH were tested on cell growth. Cell growth was null or negligible in all conditions (Figure 2.6).

### 2.3.4 DAPI staining of cell cultures treated with folates and FDH

DAPI staining was carried out in parallel to folates effect on cell proliferation, which was described in section 2.2.2. DAPI staining results in the presence of specific folates with and without FDH are shown in Figure 2.7 below:



**Figure 2.7. DAPI nuclei staining snapshots of primary cell cultures in the presence of different types of folates ( $10^{-5}$  M) with and without FDH ( $10^{-5}$  M) as follows: folic acid (A), folic acid + inactive FDH (B), folic acid + active FDH (C), 5mTHF (D), 5mTHF + inactive FDH (E), 5mTHF + active FDH (F), THF (G), THF + inactive FDH (H) + active FDH (I), (x20) magnification.**

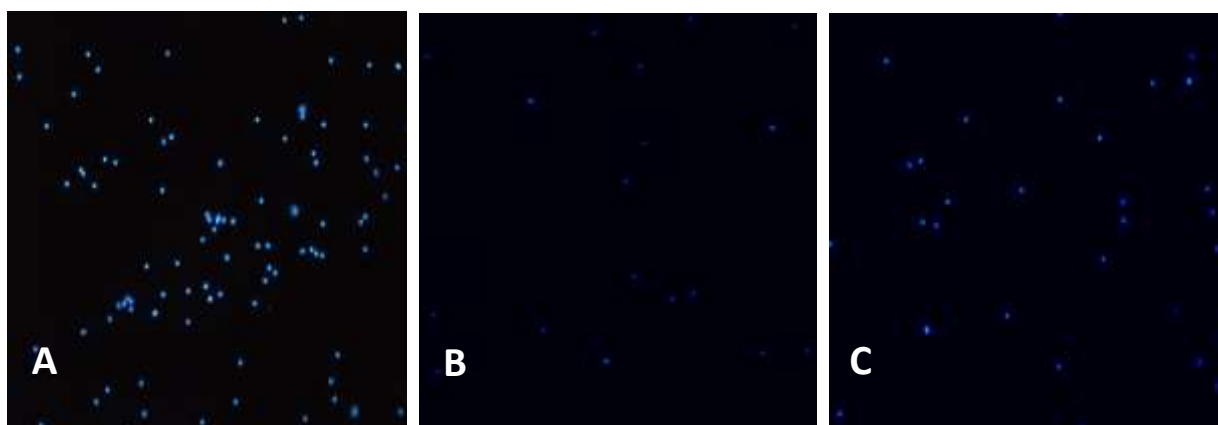
These results are in accordance with previous outcomes obtained from studies of folates' effects on cell proliferation (2.3.1, 2.3.2 and 2.3.3 sections) and visually demonstrate how

folic acid in the presence and absence of FDH exacerbates cell proliferation (Figure 2.7, A, B and C). In relation to DAPI staining of cells grown with 5mTHF, these results visually confirm how this folate potentiates growth when present alone in the media (Figure 2.7, D). Interestingly, this positive effect is compromised by the addition of inactive FDH (Figure 2.7, E) and active FDH (Figure 2.7, F). Finally, THF alone (Figure 2.7, G) and either in combination with inactive FDH (Figure 2.7, H) or active FDH (Figure 2.7, I) do not have any impact on cell growth.

### **2.3.5 THF conjugated to immunoglobulins (IgG) has a positive effect on cell growth.**

#### **2.3.5.1 DAPI staining of cell culture treated with IgG-THF.**

DAPI staining snapshots obtained from cell culture treated with IgG-THF are shown in figure 2.8 and DAPI fluorescent measurements are illustrated in figure 2.9. These results demonstrate that conjugated THF has a pronounced positive effect on cell growth in contrast to growth with commercially unstable THF alone or with no folate at all.



**Figure 2.8 shows DAPI nuclei staining snapshots of primary cell cultures in the presence of IgG-THF at  $10^{-5}$  M (A), THF at  $10^{-5}$  M (B) and media control (x 20 magnification).**



Accordingly, a 12.8 % increase in cell number occurred when cells were cultured in media with IgG-THF conjugates. This contrasts with minimal cell growth in cultures treated with media containing THF only.

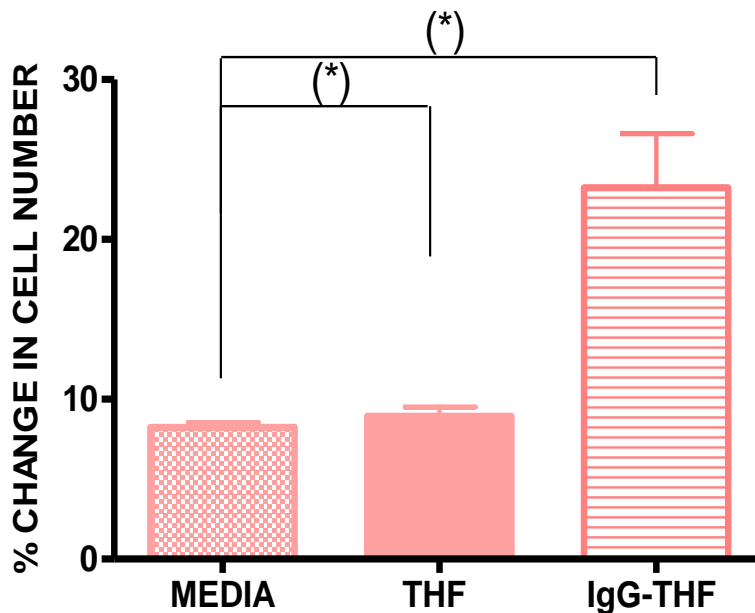
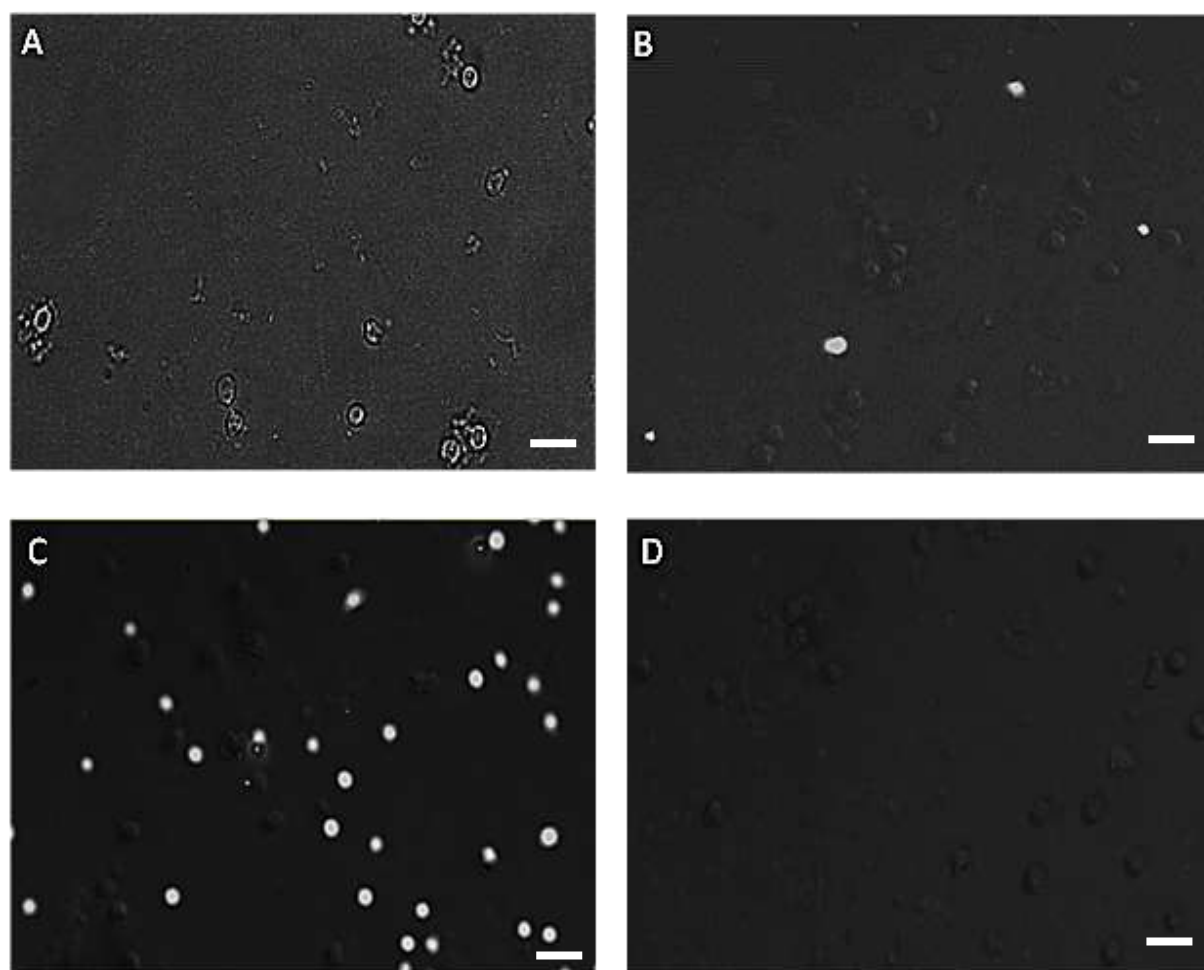


Figure 2.9 shows inhibitory effect of THF as opposed to IgG-THF's positive effect on cell growth of primary cerebral cortex cells at embryonic day 18. Cell growth was determined by measuring fluorescence due to DAPI-dsDNA complex formation using a fluorimeter set up at 358 nm excitation and 461 emission wavelengths. Data is presented as mean fluorescence readings  $\pm$  SEM (n=3). Analysis of data with Kruskal-Wallis test and post-test Dunn's multiple column comparison revealed significant differences. Results are indicated as  $*p < 0.05$ .

2.3.5.2 IgG-THF fluorescent tracking demonstrates THF is taken in by cerebral cortex cells.

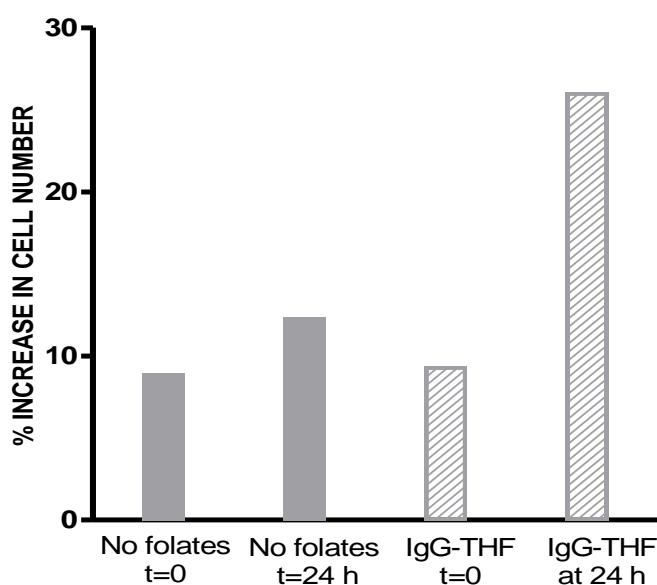


**Figure 2.10 Uptake of fluorescent THF-labelled IgG at  $10^{-5}$  M by cerebral cortex cells. Fluorescence microscope snapshots (x60) of cerebral cortex cells incubated with IgG-Cy3-THF (25 $\mu$ g/ml) were taken after 12 hours (A), 16 hours (B) and 24 hours (C). Cells incubated with IgG labelled to the same extent with Cy3 but lacking any conjugated THF are shown in D (negative control), (Scale bar = 100  $\mu$ m),**

The effect of THF in media deprived of any other folates and FDH was studied using THF conjugated to a monoclonal fluorescent THF antibody or immunoglobulin G type 1. Fluorescence inside cells was detected using an inverted fluorescence microscope which was set up at a maximum absorbance suitable for Cy3 (670 nm). The fluorescence signal was observed on the cell periphery after 12 hours growth when THF-conjugated Cy3 – labelled IgG was present in the media (Figure 2.10, A). THF entered the cells gradually over a period of 24 hours as cells divided (B and C). Cells growing in media without THF

but containing Cy3 –labelled IgG did not show any fluorescence, meaning that Cy3 labelled IgG was not accumulated by these cells. This suggests that attachment of fluorescent IgG to the folate promotes the uptake of THF-conjugated Cy3 –fluorescent IgG, as shown in photos A, B and C. These results showed that cerebral cortex cells were able to divide without the presence of FDH, and revealed that cell division can occur with THF only in the media. However, these results contradicted previous data (Figure 2.6) which suggested that unconjugated THF in cell culture leads to negligible growth. This finding emphasizes the importance of using stable THF in this type of cell culture study.

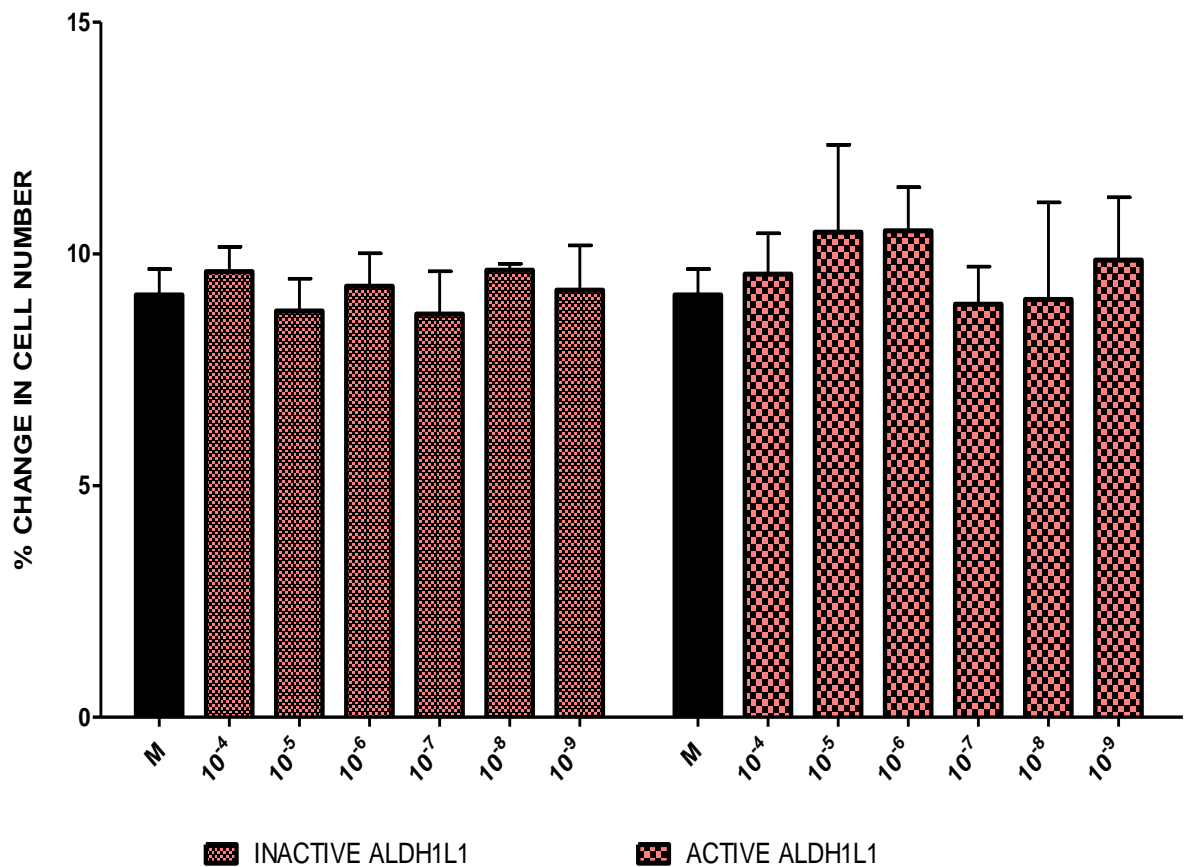
#### 2.3.5.3 Bioavailability studies suggest conjugated THF has a positive effect on cell growth.



**Figure 2.11 Effect on cell proliferation of THF (line pattern) versus no folates (plain pattern) at starting point (zero growth; t=0) and after 24 hours (t=24 h). Fluorescence was measured using a fluorescent PrestoBlue cell viability reagent kit as described in material and methods (2.2.3.3). Data are presented as percentage increases in cell number obtained after normalization of relative fluorescence indexes before and after 24 hours growth.**

Cell bioavailability was studied at the start ( $t=0$ ) and at the end of the experiment ( $t=24$ ) in the presence and absence of IgG-THF (Figure 2.11 above). Cell growth increase (14.4%) was obtained from cells cultured in the presence of IgG-THF after 24 hours, compared to growth with IgG-THF at the start of the experiment ( $t=0$ ). In contrast, minimal percentage increases occurred with cells grown in media without folates at  $t=0$  and  $t=24$ h. These results indicate a positive effect on cell growth by THF-IgG after 24 hours, and provide evidence about the suitability of immunoglobulins for the stabilization of oxygen sensitive vitamins like THF.

### 2.3.6 Negative FDH effect on cell growth depends on folate presence in the media.

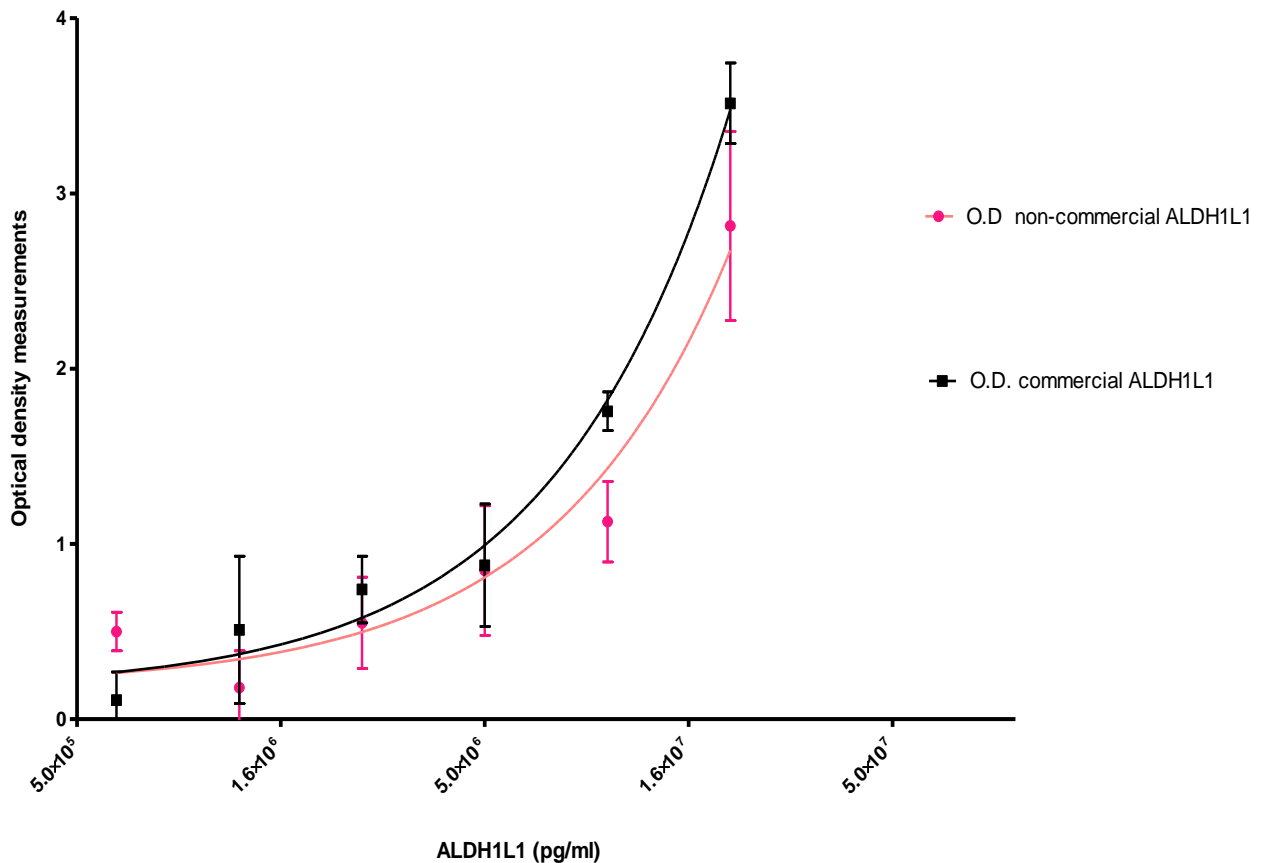


**Figure 2.12.** Effect on cell proliferation of active (small squares) and inactive ALDH1L1 (FDH) (large squares) Proliferation was measured using a fluorescence-based assay, as described in material and methods (2.2.1). Data are presented as mean percentages in cell change  $\pm$  SEM obtained after normalization of relative fluorescence indexes (RFI) measurements (n=6). Analysis of data with Kruskal-Wallis test and post-test Dunn's multiple column comparison revealed there was no effect of FDH on cell growth.

To assess the role of active and inactive FDH on the cerebral cortex, the folate binding protein was added to the media without any folates. Cortical cells cannot survive without folates and as expected, addition of FDH alone to neurobasal media led to a significant minimal average percentage increase of  $0.34 \pm 1.28$  when compared to the media control.

### 2.3.7 FDH shows affinity for 5mTHF.

2.3.7.1 Standard curves parallelism between non-commercial and commercial FDH is confirmed using a commercial FDH ELISA prior to development of an “in house” ELISA for detection of 5mTHF binding to FDH



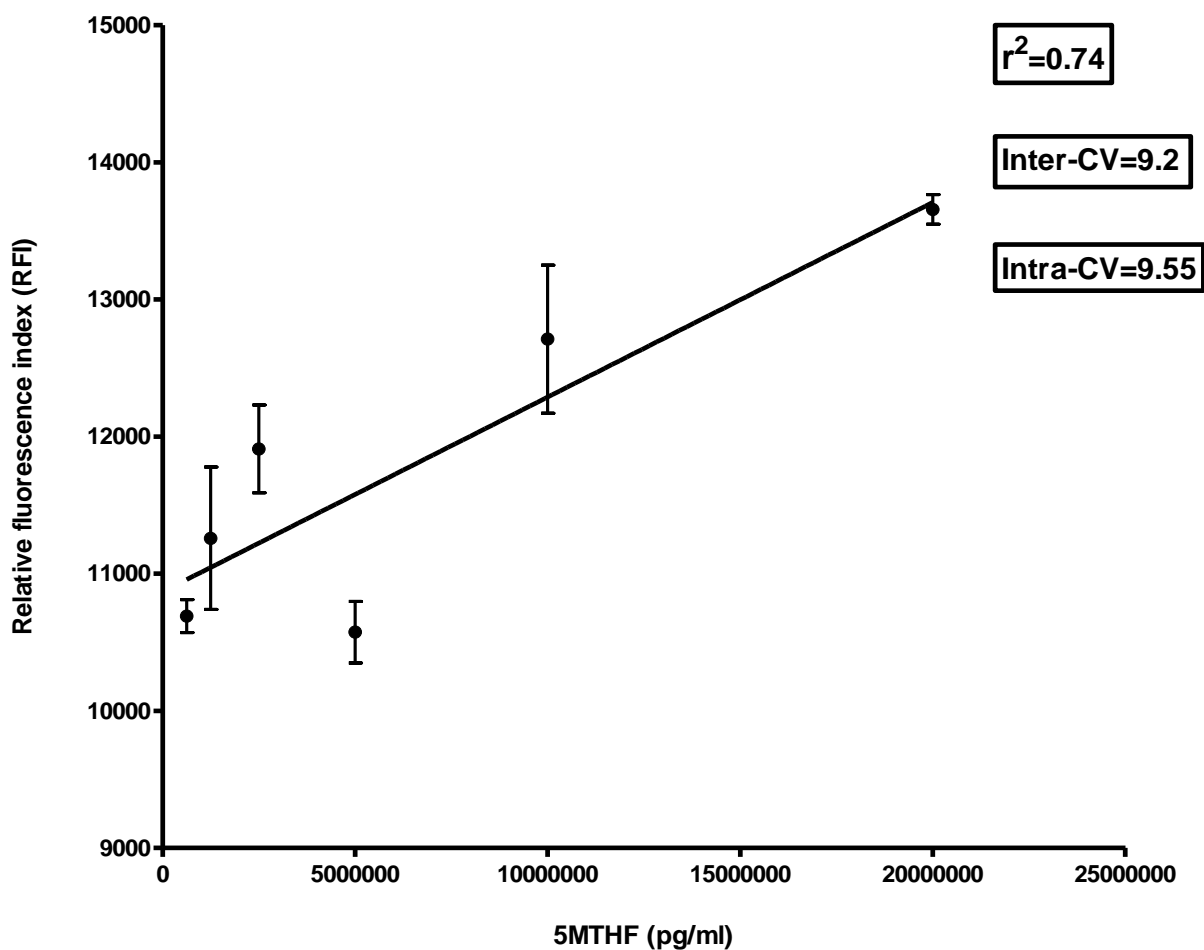
**Figure 2.13. Commercial and non-commercial (FDH) standard curves.** Standard curves were produced by plotting optical density measurements versus commercial kit standard FDH (black line) and non-commercial standard protein (pink line). Curves fits were compared using a non-parametric paired Wilcoxon rank test ( $p < 0.05$ ).

Standard curves were created in order to ensure FDH was bound to the ELISA kit solid phase using first the kit’s FDH standard protein and later the non-commercial FDH (Dr. Krupenco’s) which was used in all previous “in vitro” experiments. The aim was to demonstrate that non-commercial FDH behaves similarly to commercial protein. The kits

reagents and optimized experimental conditions recommended by the company were used to produce the standard curves. The kit's detection system, based on a colorimetric reaction (HRP-Avidin-TMB), allowed optical density measurements of FDH concentration. Optical density values were plotted versus FDH concentration to obtain the standard curves (Figure 2.13). The standard curves described a logarithmic trend and run in parallel, demonstrating that curve medians were not significantly different ( $p < 0.05$ ). In other words, the curves' paired values were significantly correlated, and therefore similar binding properties of commercial and non-commercial ALDHL1 to the monoclonal FDH antibody on the solid phase were established. These experiments helped to confirm the conditions needed to progress further towards the development of a fluorescent ELISA immunoassay that allows quantification of the potential binding between FDH and 5mTHF. An FDH standard curve was always run simultaneously to the fluorescent immunoassay to confirm FDH attachment to solid phase.

#### 2.3.7.2 "In house ELISA" using commercial FDH ELISA and fluorescent anti-5mTHF antibody shows FDH affinity for 5mTHF.

To assess whether there is affinity of FDH for 5mTHF, and therefore FDH-5mTHF complexes attached to the ELISA solid phase, plates were first coated with FDH, followed by incubation with 5mTHF. Equal concentrations of FDH and 5mTHF were added to the wells in order to achieve concomitant double serial dilutions for both molecules. Estimation of amount of 5mTHF bound to FDH was achieved by using an "in house" fluorescent 5mTHF antibody. There was a relative linear relationship between fluorescence and 5mTHF concentration, with  $r^2 = 0.74$ , demonstrating 5mTHF binds to FDH. Figure 2.14 below:



**Figure 2.14. “In house” Fluorescent ELISA assay. Study of potential FDH binding to 5mTHF was carried out using an “in house” fluorescent immunoassay. Fluorescent values were plotted versus 5mTHF concentration. A relative linear relationship with an  $r^2=0.74$  demonstrated FDH affinity for 5mTHF. The intervariation and intravariation coefficient of the assay was 9.2 and 9.55 respectively. N=3**

Fluorescence values were included only if their mean exceeded by more than two standard deviations the mean optical density given by the negative controls (buffer only), thereby establishing a cut-off value. Fluorescence values obtained from 5mTHF dilutions were all  $\geq$  than the cut-off value. Cut-off= Mean OD (-C) + 2SD= 136.

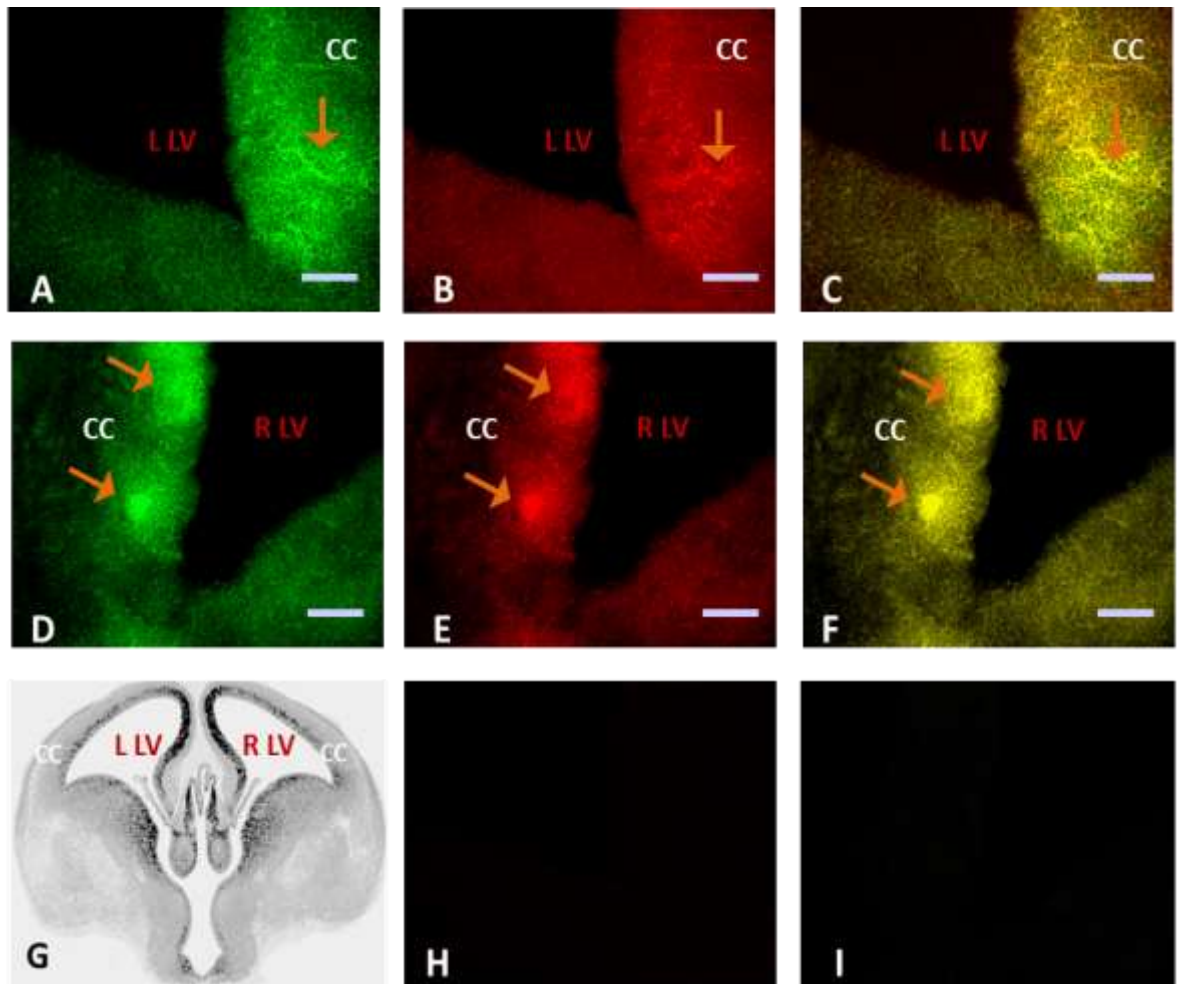


To study the variability of the method within the assay and between assays, intravariation and intervariation coefficients were calculated respectively. Top, middle and low standard curve values from different experiments were used to calculate both variation coefficients using the following formula:  $\text{Variation coefficient} = \text{SD} \times 100 / \text{mean}$ .

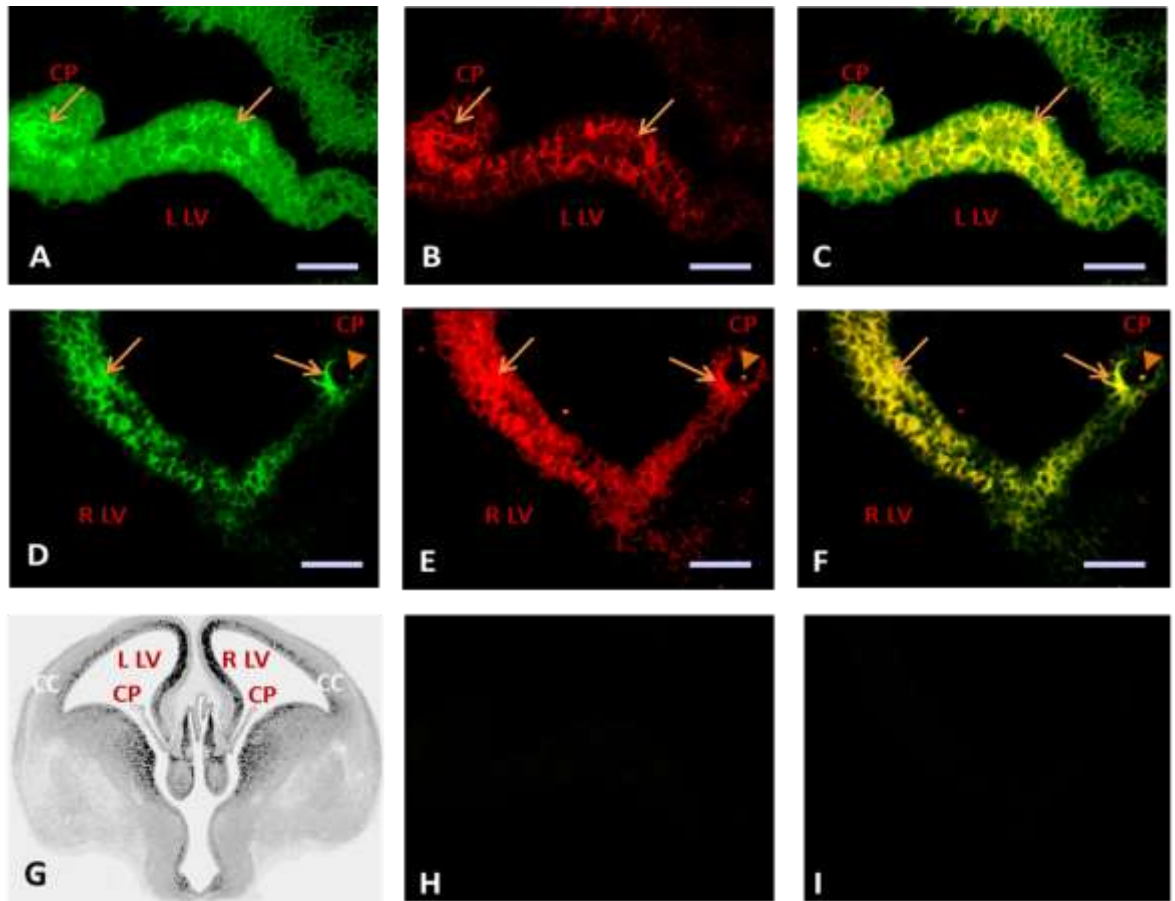
Intravariation coefficient (intra-CV) was 9.2 and intervariation coefficient (inter-CV) was 9.55. Finally, the graph end fluorescence measurement shows a value closed to the penultimate fluorescence reading, indicating that the assay may reach saturation at concentrations of 5mTHF higher than  $2 \times 10^7$  pg/ml.

### 2.3.8. FDH protein colocalizes with 5mTHF and FR $\alpha$

Representative photomicrographs of FDH and 5mTHF immunohistochemical localization in cerebral cortex (CC) and choroid plexus (CP) in normal and hydrocephalic brain (Figure 2.15 & Figure 2.16)



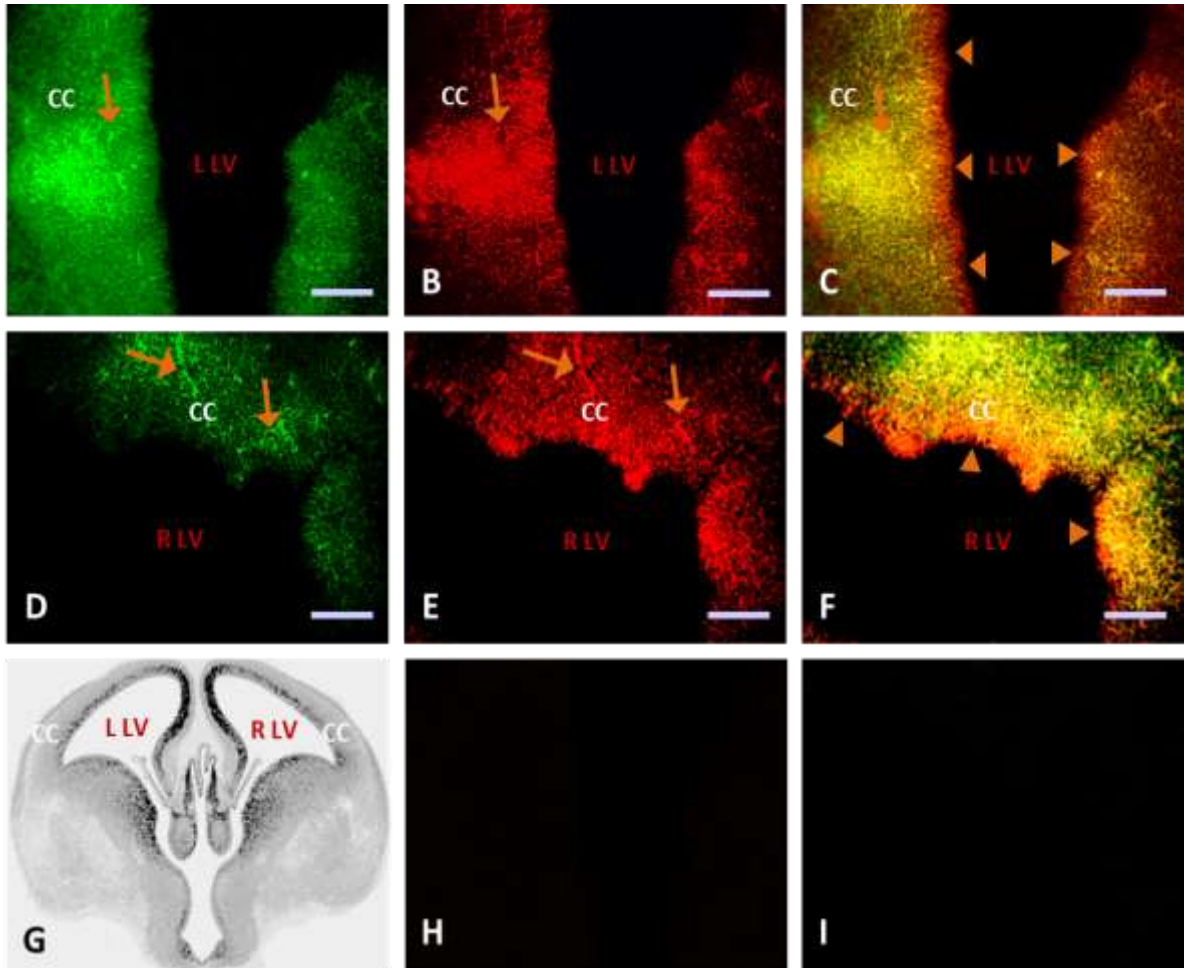
**Figure 2.15.** Fluorescence photomicrographs of coronal sections (15  $\mu\text{m}$ ) show immunolocalization and colocalization of FDH and 5mTHF in cerebral cortex (CC) of right (R) and left (L) lateral ventricle (LV) at gestational age 18. Positive staining for FDH (green) was found in CC of normal brain (A) and hydrocephalic brain (D). 5mTHF (red) was also identified in CC of normal (B) and abnormal brain (E). FDH and 5mTHF co-localization was evidenced by the generation of yellow color after merging green and red channels (yellow), as appears in images (C) and (F). Illustrative scheme of brain structures with positive staining (G), Normal brain negative controls merged (H), abnormal brain negative controls merged (I) (Scale bar = 100  $\mu\text{m}$ ), (x40 magnification), N=6.



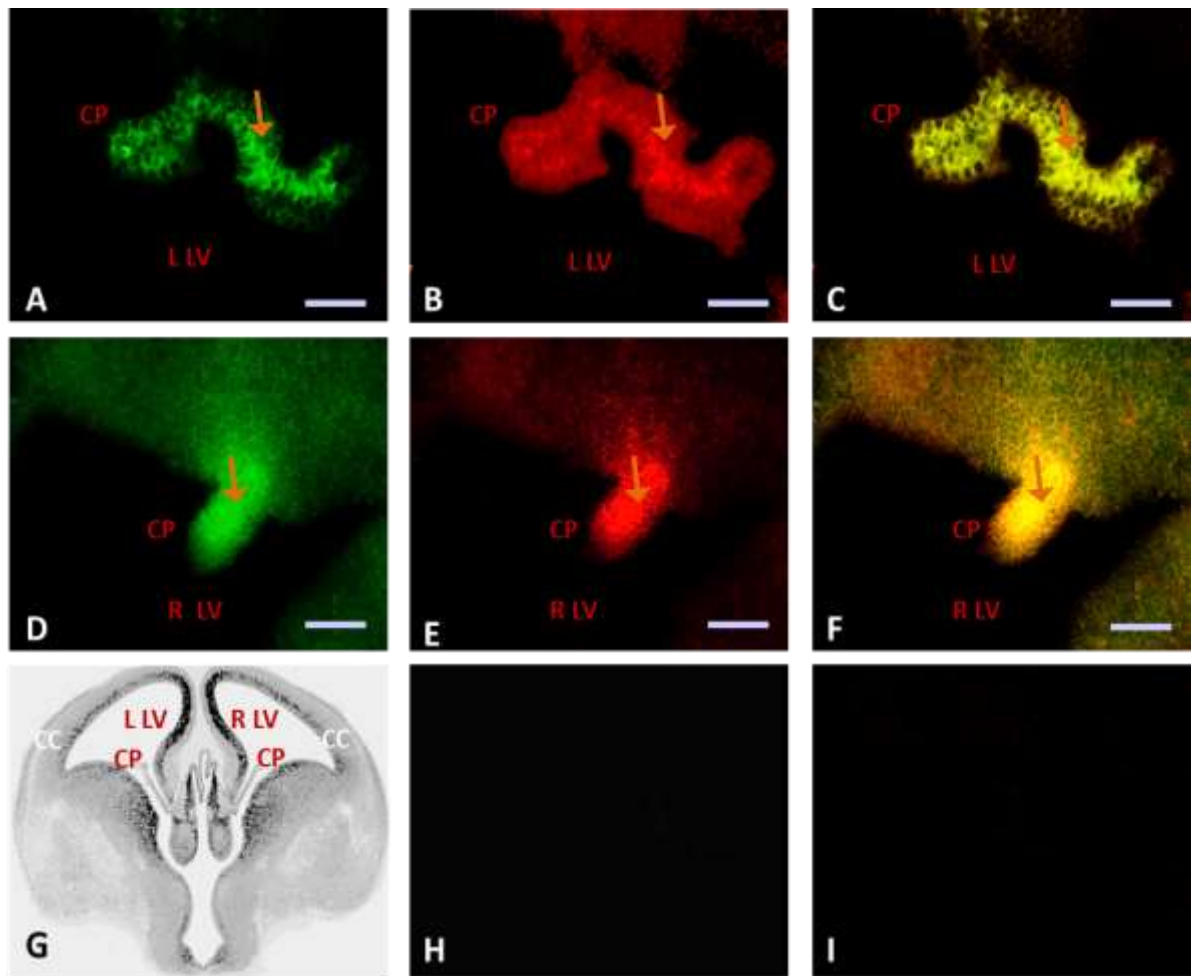
**Figure 2.16.** Immunofluorescence staining (arrows) of coronal sections (15  $\mu\text{m}$ ) identified FDH (green) in CP of normal (A) and abnormal brain (D) in left (L) and right (R) lateral ventricle (LV). Immunoreactivity was also detected for 5mTHF (red) in CP of normal (B) and hydrocephalic brain (E) at gestational age 18. FDH and 5mTHF co-localisation was visualized by green and red channels merging of normal (C) and abnormal (F) brain images (yellow color). Vesicles-like structures (arrowheads) were observed in (D and E) and colocalized as shown in (F). Illustrative scheme of brain structures representing immunoreactivity in images is shown in (G), Normal brain negative controls merged (H), abnormal brain negative control merged (I) (Scale bar = 100  $\mu\text{m}$ ), (x40 magnification), N=6.

Figure 2.15 shows heterogeneous FDH staining located on normal CC (A) and abnormal CC (D). A similar distribution is detected for 5mTHF in normal (B) and hydrocephalic brain (E). Surprisingly, and to our knowledge this was the first time it had been detected, choroid plexus showed FDH staining in normal brain (Figure 2.16 (B) and abnormal brain (E)). Co-localization between FDH and 5mTHF was also detected, and is shown in figure 2.15 and 2.16 images (C and F) in both CC, and CP of normal and abnormal brain

respectively. The specificity of all antibodies was confirmed by a lack of detectable stain in negative controls.



**Figure 2.17.** Immunohistochemical staining of coronal sections (15  $\mu$ m) identified FDH (green) in CC of normal (A) and abnormal brain (D) in left (L) and right (R) lateral ventricle (LV). Immunostaining was also positive for FR $\alpha$  (red) in CP of normal (B) and hydrocephalic brain (E) at gestational age 18. FDH and FR $\alpha$  colocalisation was exhibited by green and red channels merging of normal (C) and abnormal (F) brain images (yellow color). Illustrative scheme of brain structures showing immunoreactivity in images (G), Normal brain negative controls merged (H), abnormal brain negative control merged (I) (Scale bar = 100  $\mu$ m), (x40 magnification), N=6.

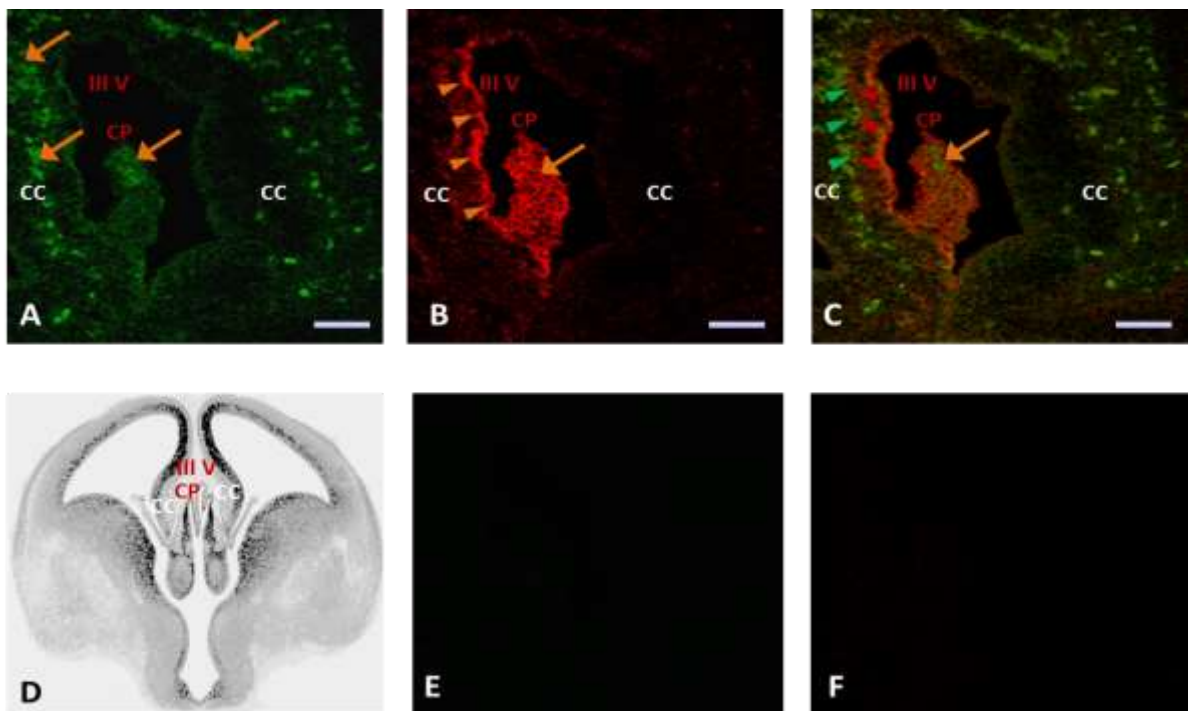


**Figure 2.18.** Immunohistochemical staining of coronal sections (15  $\mu\text{m}$ ) show discernible staining for FDH (green) in CP of normal (A) and abnormal brain (D) in left (L) and right (R) lateral ventricle (LV). Immunostaining appeared also positive for FR $\alpha$  (red) in CP of normal (B) and hydrocephalic brain (E) at gestational age 18. FDH and FR $\alpha$  co-localisation was shown by green and red channels merging of normal (C) and abnormal (F) brain images (yellow color). Illustrative scheme of brain structures showing immunoreactivity in images (G), Normal brain negative controls merged (H), abnormal brain negative control merged (I) (Scale bar = 100  $\mu\text{m}$ ), (x40 magnification).

In figure 2.17, discernible FDH and FR $\alpha$  staining was concentrated in specific areas, indicated with orange arrows on image A (normal brain) and D (abnormal brain) for FDH, as well as in images B (normal brain) and E (hydrocephalic brain) for 5mTHF. Figure 2.17 also clearly shows how FDH and FR $\alpha$  co-localize in CC in normal (C) and hydrocephalic brain (F). Interestingly, this pattern of distribution was similar to FDH and 5mTHF staining (Figure 2.15 and 2.16). Of notice, FR $\alpha$  staining was not only limited to staining in



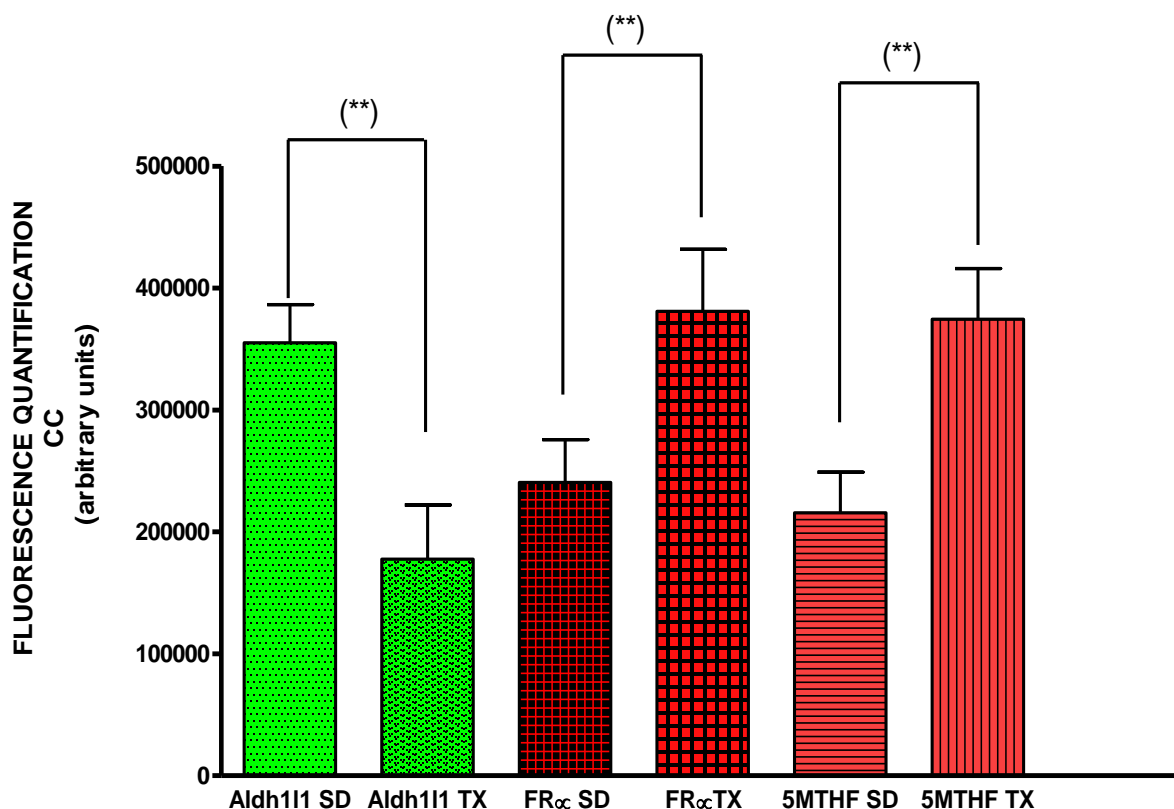
the form of clusters co-localizing with FDH but also diffusing along the neuroepithelia (arrow heads). This is shown in Figure 2.17 in normal brain (C) and hydrocephalic brain (F). The pattern of distribution for FDH and FR $\alpha$  in CP is illustrated in figure 2.18, where FDH and FR $\alpha$  staining is exhibited again in the form of clusters (orange arrows) in normal brain (A; FDH) and hydrocephalic brain (B; FR $\alpha$ ). A similar distribution is present in Texas rats' brain (D; FDH) and (E; FR $\alpha$ ). In relation to protein co-localization, FDH and FR $\alpha$  co-localize in C (normal brain) and F (abnormal brain). The specificity of all antibodies was confirmed by lack of detectable stain in negative controls as shown in Figure 2.17 (H; FDH and I; FR $\alpha$ ), and Figure 2.18 (H; FDH and I; FR $\alpha$ ).



**Figure 2.19. Confocal images of fluorescent immunohistochemical staining show coronal sections (15  $\mu$ m) of III normal brain ventricle (III V). FDH (green) is present in CC and CP (A, orange arrows) whereas FR $\alpha$  immunoreactivity (red) is exhibited in CC (B, red arrow heads) and CP (B, orange arrows). FDH and FR $\alpha$  proximity was shown by green and red channels merging (C; yellow color); see also arrow heads in green (FDH) and arrow heads in red (FR $\alpha$ ). Illustrative scheme of brain structures showing immunoreactivity in images (D); normal brain negative controls (E); abnormal brain negative control (F); (Scale bar = 100  $\mu$ m); (x40 magnification).**

Similar to results obtained from fluorescent microscopy images, confocal microscopy showed immunoreactivity for FDH in CC (A) and FR $\alpha$  in CP (B) of normal brain (Figure

2.19). However, this time the staining in CC (A) is punctuated and more dispersed, in contrast to the concentrated staining visualized on CP, which agrees with the FDH staining in aggregates detected in fluorescent micrographs (Figure 2.16 and 2.18). Noticeably, FR $\alpha$  on the contrary is identified marginally along the neuroepithelia of the CC (B, arrow heads) but located in the form of clusters in CP (B, arrow), which matches the results previously shown for FR $\alpha$  immunoreactivity in CP in fluorescent micrographs of normal and abnormal brain (Figure 2.15 and Figure 2.17). Importantly, after channels merge (C) FDH and FR $\alpha$  rather than co-localizing, they locate in close proximity, confirming confocal microscopy technology as a much more powerful tool for protein immunolocalization in fetal brain tissue. The specificity of all antibodies was revealed by the lack of detectable stain in negative controls (E; FDH) and (F; FR $\alpha$ ). Overall, FDH, 5mTHF and FR $\alpha$  staining between CC and CP from normal and abnormal brains was of different intensity, and measurements of fluorescence density variability between normal and hydrocephalic brain were determined and plotted in Figure 2.20.



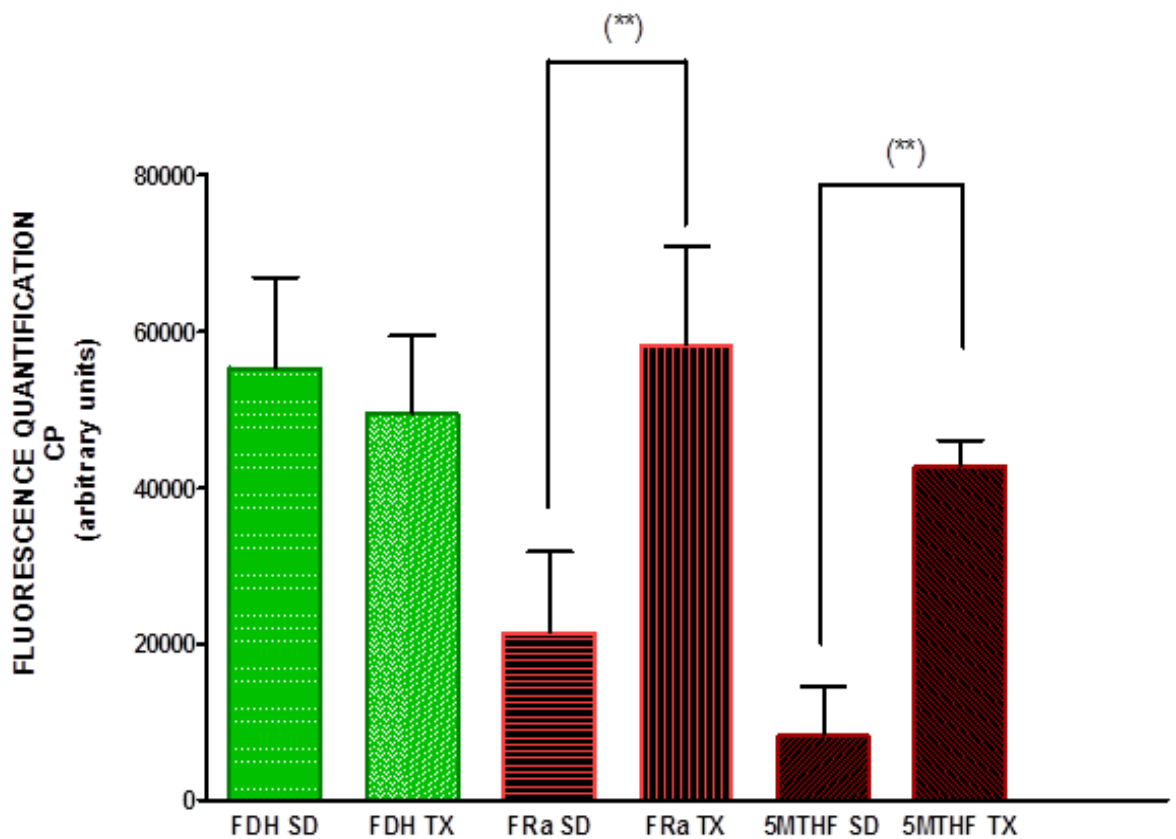
**Figure 2.20. Cerebral cortex (CC) immunohistochemical fluorescence quantification in Sprague Dawley controls (SD) and hydrocephalic rats. Fluorescence signal determination for FDH/ALDH1L1 (green), FR $\alpha$  (red squares) and M5THF (red lines) was assessed, as described in material and methods. The density of immunohistochemical staining was done per unit of area of section measured for CC in each group. Data from a minimum of 6 sections from each brain were averaged and recorded as mean  $\pm$ SEM for all embryos in each category, calculated from all litters. Analysis of variance revealed significant differences between the cerebral cortex of SD and Texas rats for FDH, FR $\alpha$  and M5HTF at  $p \leq 0.01$**

Fluorescence density measurements found in brain for FDH, FR $\alpha$  and 5mTHF were measured for CC and CP individually. Data from CC signal was pooled together and averaged. The mean values were compared across all SD and TX embryos as shown in figure 2.20. The differences between controls and hydrocephalic rats were determined using a two way-ANOVA analysis of variance. In general, FDH, FR $\alpha$  and 5mTHF staining presented differences in fluorescence density, when compared to staining between normal and abnormal brain. The comparative analysis revealed a mean fluorescence



density value for FDH staining significantly higher ( $281870 \pm 14403$ ) in SD sections (green dot pattern) than hydrocephalic rats ( $177630 \pm 44518$ ), (green and triangle pattern)  $p \leq 0.01$ . In relation to  $FR\alpha$  staining, and in contrast to FDH results, SD control rats presented a significantly lower mean fluorescence signal ( $240602 \pm 35195$ ), (red small square pattern) than TX rats ( $367626 \pm 65679$ ), (red large square pattern). Similar to  $FR\alpha$ , the 5mTHF staining average signal was less detectable in control rats than in hydrocephalic rats, with mean values of  $194988 \pm 38899$  and  $321013 \pm 95042$  in control brain and hydrocephalic brain respectively.

CP analysis was carried out following CC fluorescence measurements, using the same method to determine CC fluorescence signal. Detected density values were brought together and averaged resulting in a variety of differences, as shown in figure 2. 21below.



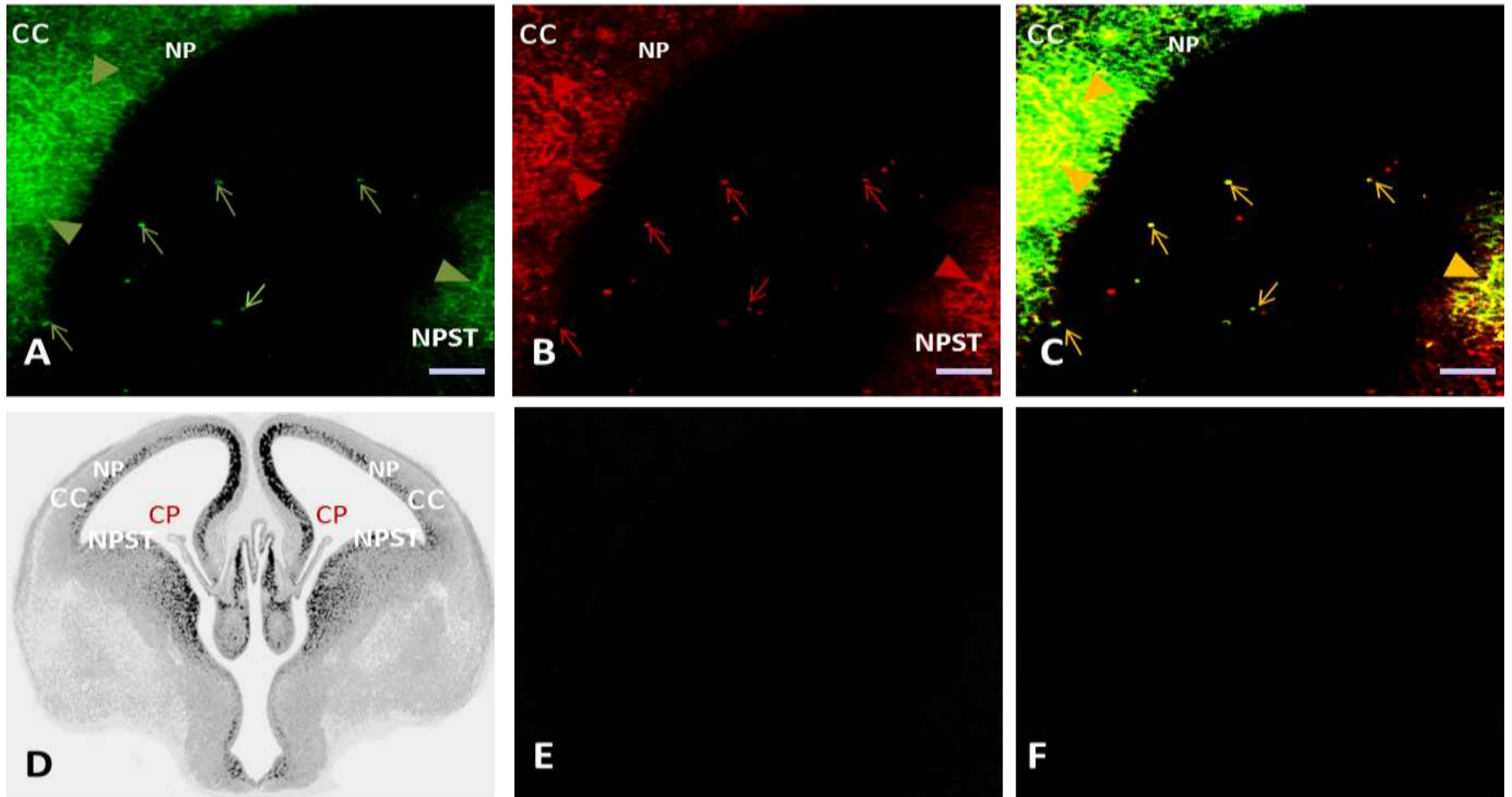
**Figure 2.21. Choroid plexus (CP) immunohistochemical fluorescence quantification in Sprague Dawley controls (SD) and hydrocephalic rats. Fluorescence signal measurement for FDH (green), FR $\alpha$  (red squares) and M5THF (red lines) was analysed as described in material and methods. The density of immunohistochemical staining was calculated per unit of area of section measured for CC in each group. Data from a minimum of 6 sections from each brain were averaged and presented as mean  $\pm$ SEM for all embryos in each category (6), calculated from all litters. Analysis of variance revealed significant differences between the cerebral cortex of SD and Texas rats for FR $\alpha$  and M5HTF at  $p \leq 0.01$**

Results from CP signal analysis in figure 2.21 show a minor decrease in FDH mean fluorescence when compared to normal ( $55326 \pm 11566$ ) and abnormal brain ( $50266 \pm 9807$ ). However, there was no statistically significant difference after analysis of variance ( $p \geq 0.01$ ). With regard to FR $\alpha$  staining, control rats showed a much lower mean density value ( $20605 \pm 10290$ ) than hydrocephalic rats ( $58438 \pm 11893$ ). Finally, 5mTHF staining in

control rats exhibited a remarkable decreased signal ( $8326 \pm 6244$ ) in comparison with abnormal rats ( $42717 \pm 3389$ ). Immunohistochemical staining revealed too fluorescence signal in small spherical structures, which were occasionally noticeable in histological sections of CP (previous Figure 2.16) and CC (Figure 2.22). An intense positive FDH staining (A, green arrows) and FR $\alpha$  signal (red arrows) were detected inside these structures, which interestingly also co-localize (C, yellow arrows).

Since FR $\alpha$  is a cell membrane marker itself, we can only suggest that these spheres are vesicles containing FDH and FR $\alpha$ -5mTHF complexes. Finally, green arrow heads indicate FDH staining in CC and neuroepithelia of the striatum (NPCT), (A). Red arrowheads represent FR $\alpha$  staining in CC and NPCT, (B) and yellow arrowheads FDH and FR $\alpha$  co-localization.

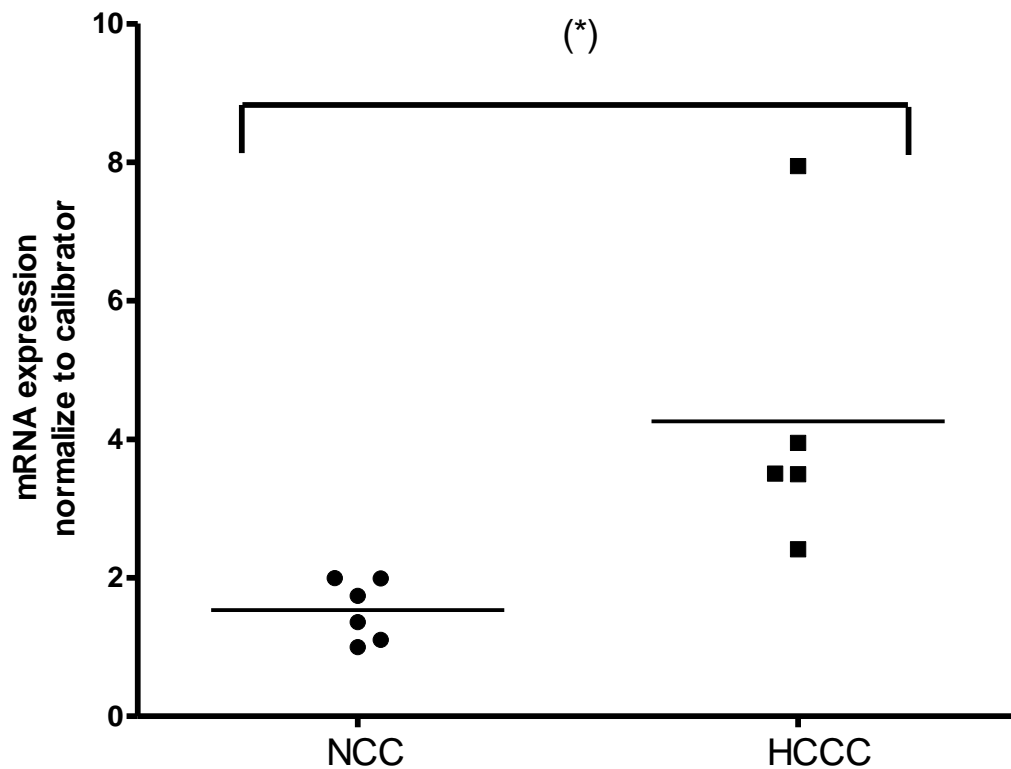
In conclusion, results from fluorescence immunostaining confirm location and extensive co-localization of ALDH1L, FR $\alpha$  and 5mTHF in cerebral cortex and choroid plexus, as well as differential density of signal when contrasting normal and abnormal brain. Of notice, FDH location in CP was unexpected, and this finding does not agree with previous immunostaining results in our lab, where FDH passed undetected in CP. However, FR $\alpha$  results agree with previous publications that localize FR $\alpha$  in CP, CC and vesicles (exosomes). Our results clearly demonstrate for the first time co-localization of FDH and FR $\alpha$  along with 5mTHF, which give us more insight into the FDH's role in brain folate handling and interrelationships with folate transporters such as FR $\alpha$ .



**Figure 2. 22. Representative fluorescence micrographs of FDH and FR $\alpha$  positive staining in CC, neuroepithelia of the striatum (NPST) and vesicle-like structures in LV. Green arrowheads show FDH staining in CC and NPST and green arrows indicates FDH in vesicle-like structures (VLS) (A). Red arrowheads point to FR $\alpha$  signal in CC/NPST and red arrows in VLS (B). FDH and FR $\alpha$  co-localization in CC and NPCT is shown as yellow staining (arrowheads) as well as co-localization of FDH and FR $\alpha$  inside vesicles which is indicated with yellow arrows (C). Scale bar 100 $\mu$ m.**

### 2.3.9 FDH is significantly overexpressed in CC of the hydrocephalic brain.

A relative quantification of FDH mRNA transcripts was carried out using traditional RTPCR technique, as described in material and methods, in normal and abnormal CC. This was done in order to elucidate, first, if there is a variation in FDH gene expression between normal and hydrocephalic CC, second, to assess whether FDH protein and mRNA coincide in location within the cerebral cortex, meaning CC synthesize FDH, and third, to determine whether changes in FDH protein levels correlate with changes in mRNA levels.



**Figure 2.23.** Expression of FDH mRNA in normal cerebral cortex (NCC), indicated as circles; n=6 and hydrocephalic cerebral cortex cells (HCCC) represented with squares; n=5). mRNA expression was normalized to calibrator. Data are shown as a scatter plot with the median represented by the horizontal line \*p < 0.05 (Mann-Whitney test).

mRNA analysis for FDH and YWHAZ (reference gene) in normal and abnormal cerebral cortex cells, as well as liver (internal calibrator and positive control), was carried out in

parallel. All samples were amplified for b-Actin (housekeeping gene) to ensure cDNA integrity was not compromised.

Expression of mRNA for FDH was detected in all normal and hydrocephalic cerebral cortex cells examined with comparable expression between them (Figure 2.23). ALDHL1 expression in hydrocephalic cells was significantly higher than in normal cells \* $p < 0.05$ , with Ct values in the range 29-30 and 27-28 for normal and hydrocephalic samples respectively. Ct value for liver was 27. A relative quantification using the comparative method was used to calculate the fold changes represented in graph (Figure.23) using the formula  $2^{-\Delta Ct}$ . Fold change is directly proportional to mRNA expression and hence the higher values in fold change were displayed in hydrocephalic samples also exhibiting the most variable pattern of expression between individual samples with fold changes in the range (2-8). By contrast, fold changes for normal samples were lower than for abnormal samples, with fold change values in the range (1.5-2). This outcome was unexpected as it was thought FDH protein synthesis should positively correlate with FDH mRNA transcription. However and contrary to our expectations, FDH was significantly overexpressed in fetal rat hydrocephalic brain.

Due to the particularly small size of fetal CP structures, it was impossible to obtain enough concentration of CP tissue to study ALDHL1 gene expression using the traditional RTPCR technique, and for this reason FDH mRNA in CP was assessed using “in situ” PCR instead.

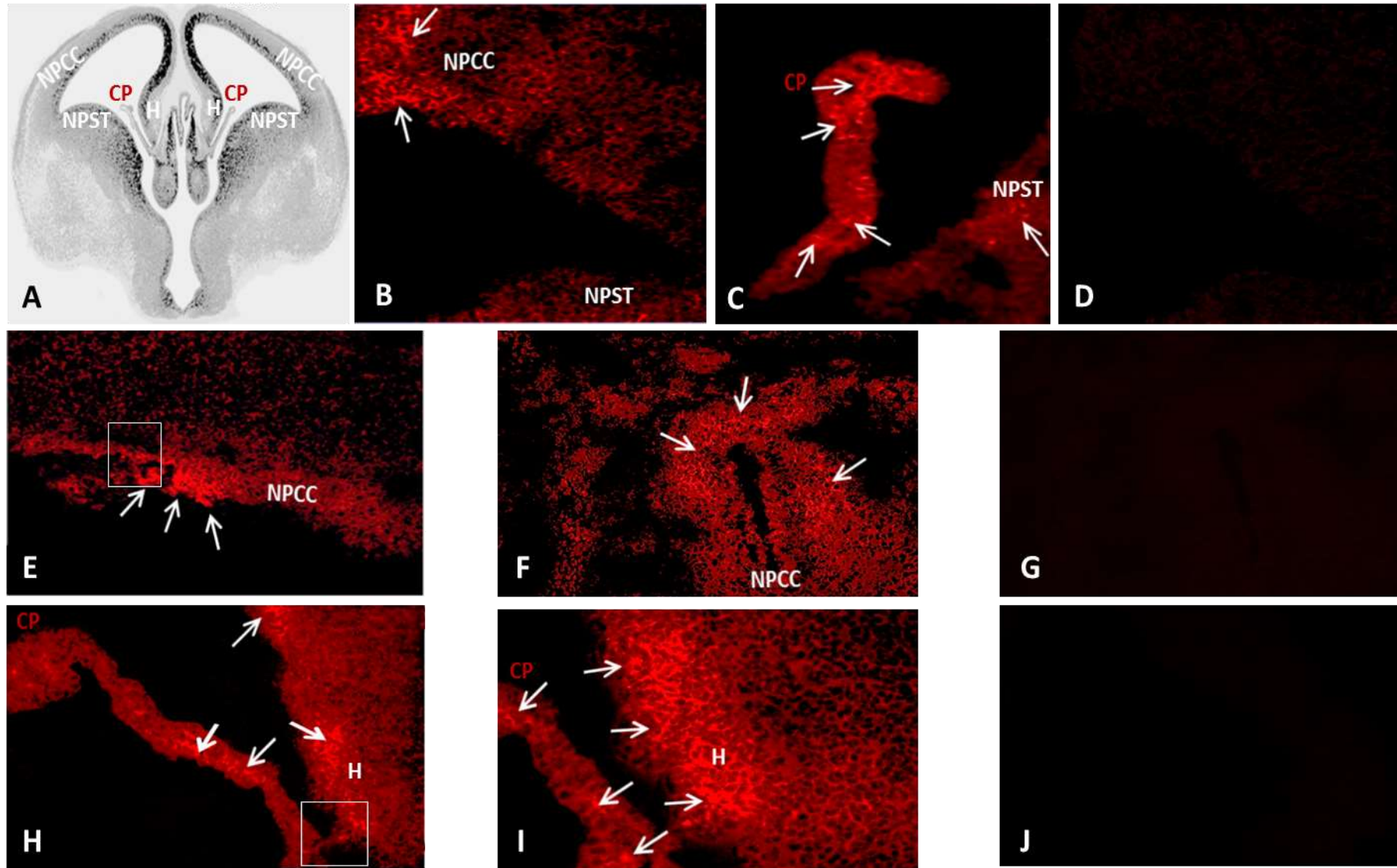
### 2.3.10 FDH mRNA is expressed in CC and CP in normal and hydrocephalic brain.

According to our results from RTPCR, where ALDH1L mRNA were identified in cerebral cortex tissue, we proposed that FDH mRNA and protein location may also coincide in other regions of the brain, such as CP and vesicles. To ascertain if this was the case, and even more importantly, to verify if cerebral cortex relies on vesicles to acquire FDH and 5mTHF, a fluorescence technique suitable to identify mRNA rather than protein was chosen. This technique, called “in situ” RTPCR, was performed following the protocol described in material and methods for “in situ” PCR, to identify FDH mRNA transcripts in the entire brain. This technique allowed us to corroborate further the location of FDH in CC of normal and abnormal fetal brain, as well as to visually confirm gene expression of FDH in CP. As explained earlier, technical difficulties made it impossible to perform traditional RTPCR on CP tissue. This demonstrates the convenience of “in situ” PCR rather than the RTPCR technique to study FDH mRNA expression and location in fetal brain.

Figure 2.24 below shows a diffused and punctuated pattern of FDH mRNA staining (red color/Rhodamine, white arrows). Red signal is observed in the differentiating neuroepithelium of normal CC (NPCC), (B) and normal CP (NPCC, C). Some minimal but still positive staining is also observed in neuroepithelium of striatum (NPST), (C). In relation to hydrocephalic brain, a noticeable staining even at low resolution (x10) is identified marginally at the level of the NPCC (E). Signal in abnormal NPCC is also discernible in selected regions (square) as shown in image F (X40). Hydrocephalic CP presents a dispersed positive staining (H, x20), which can be seen more in detail in magnified selected region (square) in image I (x40). Staining is also localized in the differentiating hippocampal region (H) as indicated in images H and I. Negative controls

for normal brain (D) and abnormal brain (G and J) lack either forward or reverse primers, and there is no signal.

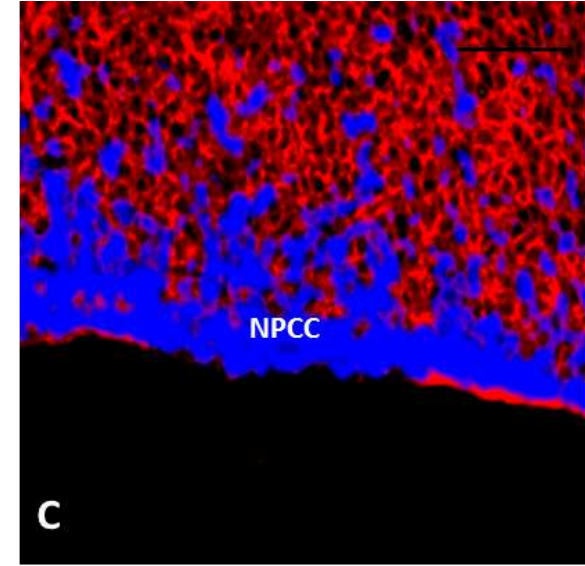
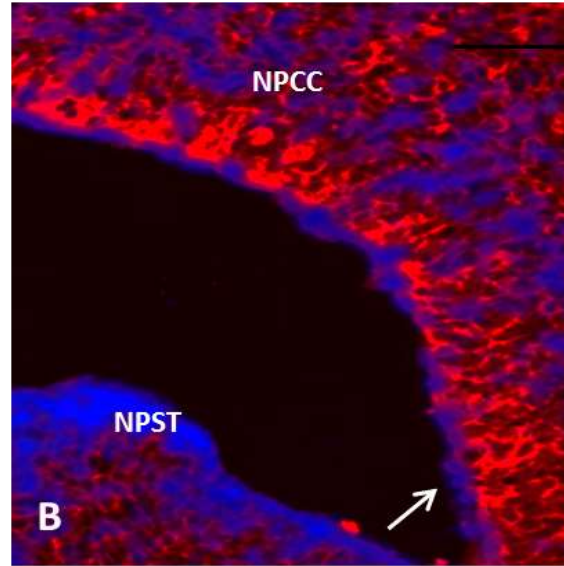
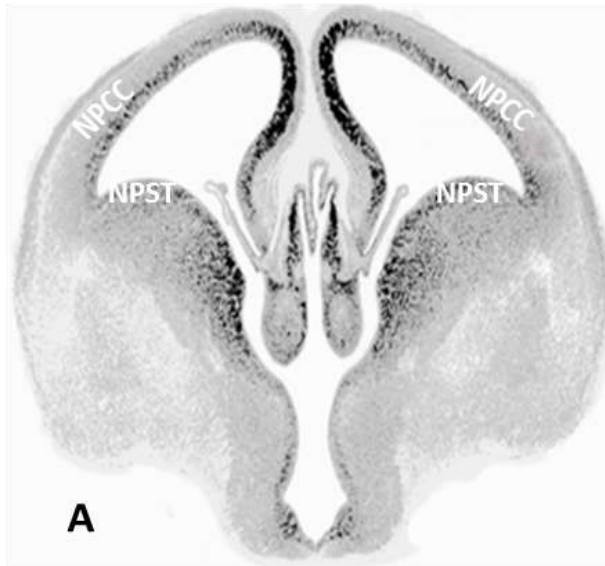




**Figure 2.24.** Representative fluorescence (Rhodamine) micrographs of FDH mRNA tissue distribution in neuroepithelia of CC (NPCC) and CP (NPCP) in LV. First illustration shows scheme describing brain structures shown in micrographs (A), positive labelling in NPCC and CP of normal brain (B) and (C) respectively (X40). Fluorescence signal was also detected in NPCC of hydrocephalic brain (E, x10) and selected magnified area (square) in F (x40) as well as in hydrocephalic CP (H, X20) and magnified area (square) in I, X40. Negative controls lacked forward or reverse primer as shown in (D) for normal brain, and G and J for abnormal fetal brain.

To demonstrate that the red signal in the images is due to PCR amplification of cDNA, rather than genomic DNA (gDNA), previously imaged brain sections (Figure 2.24) were subjected to DAPI staining and imaged again using confocal microscopy as described in material and methods. Blue nuclei can be observed in Figure 2.25 confirming the authenticity of the “In situ” PCR using primers designed uniquely to amplify FDH mRNA/cDNA, as also shown in figure 2.25. The FDH-mRNA/cDNA-Rhodamine labelled is exhibited in Figure 2.25 as intense red in B (normal brain) and C (hydrocephalic brain). On the other hand, the lack of red staining in nuclei revealed by blue DAPI staining confirms the suitability of the parameters chosen for the DNase treatment in our optimized protocol.

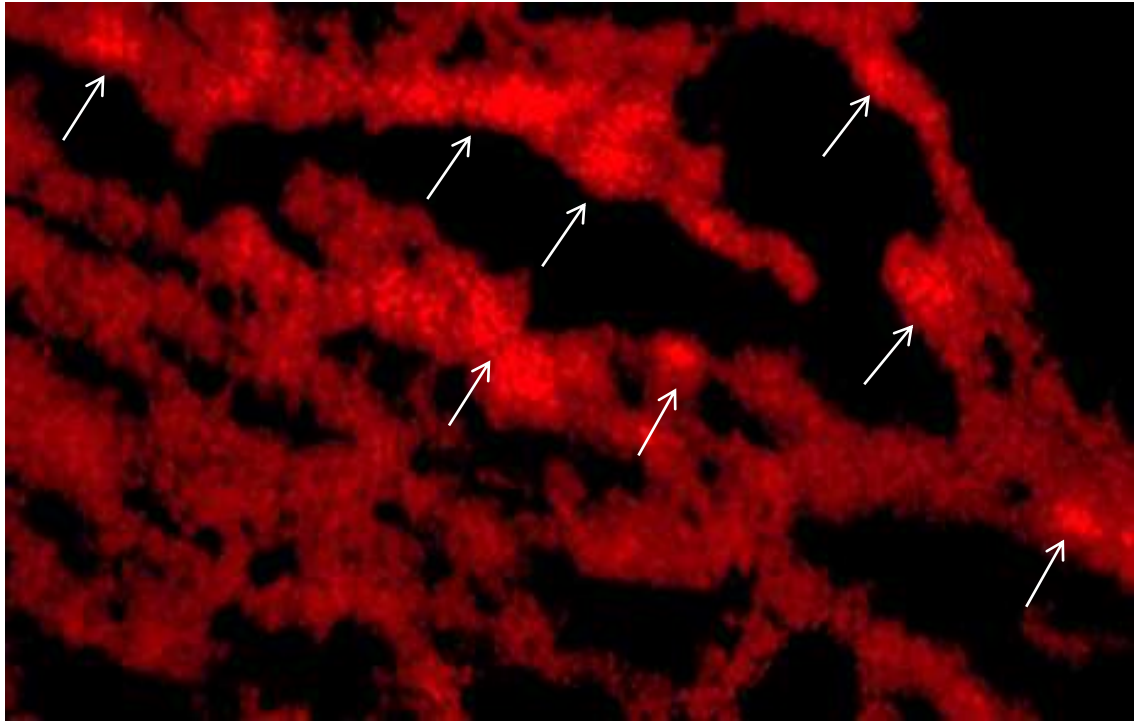
In conclusion, mRNA/cDNA location in normal and hydrocephalic brain demonstrates that fetal CC can synthesize its own FDH, and seems not to depend on vesicles coming from CP to obtain this enzyme. However, with this finding we do not exclude the possibility that fetal brain may also rely on FDH function as a folate binding protein and potential folate transporter to provide the CC with 5mTHF in the form of 5mTHF-FDH complexes, shuttled in vesicles coming from CP. This may take place in a similar fashion to FR $\alpha$ , a known folate transporter in charge of 5mTHF supply to the cerebral cortex through exosomes.



**Normal brain.** Image B clearly illustrates blue nuclei (DAPI staining) in NPST and NPCC. Blue nuclei is partially surrounded by Rhodamine staining (intense red) representing ALDH1L1 mRNA/cDNA in cytoplasm cells of NPST and NPCC. Vesicle-like formations are suggested in NPCC and NPST (white arrow). Scale bar (100  $\mu$ )

**Abnormal brain.** Image C shows intense blue stained (DAPI) in nuclei cells of NPCC. Rhodamine staining (red) reveals ALDH1L1 mRNA/cDNA production in cytoplasm cells of cerebral cortex. Scale bar (100  $\mu$ )

**Figure 2.25.** Confocal images of double staining (DAPI+FDH mRNA/cDNA rhodamine labelled) on coronal brain sections (LV) treated with DNase (gDNA inactivation). Image A shows brain structures stained with DAPI (blue) and rhodamine (red) in normal brain (B) and abnormal brain (C). Positive control is shown below.



**Figure 2. 26. Fluorescence micrograph of liver, positive control for FDH mRNA/cDNA-rhodamine labelled amplification by “In situ” PCR. Image shows positive staining in hepatocytes indicated with white arrows (intense red), x40**

## 2.4. CONCLUSIONS-DISCUSSION

Previous research in our laboratory utilizing a combination of liquid chromatography and mass spectrophotometry (LC/MS) for rat CSF analysis identified differences in protein composition between normal and hydrocephalic CSF (Nabiuni, M. 2006). More than one thousand proteins were not present in hydrocephalic CSF when compared with normal CSF. One of the proteins missing in the abnormal CSF was the multicomplex and multifunctional folate enzyme FDH. This enzyme has been described in the past to have a role in human neural tube defects (Antony & Heintz, 2007) and it is associated with heritable folate deficiency in rodents (Champion et al. 1994). On the other hand, FDH is involved in the folate cycle, a major metabolic pathway dedicated to producing nucleotides among other important molecules in metabolism. Therefore, a lack of folate enzymes such as FDH in CSF also implies folate imbalance leading to nucleotide deficit followed by low DNA synthesis and diminished cerebral cortex growth (Nabiuni et al. 2006 and Cain et al. 2009).

In this study we investigated first the role of key folates in the presence and absence of FDH on cerebral cortex cells by means of “in vitro” cell culture experiments, cell bioavailability fluorescence quantification comparison between media conditions, and cell growth visualization by fluorescence DAPI staining. These experiments focused on 5mTHF, also called folic acid in its oxidized synthetic form (Powers, 2007), as 5mTHF is a key vitamin for cell growth “in vitro”, as well as for the general development of the central nervous system in the first trimester of pregnancy (Scholl et al. 1996 and Darnton-Hill et al. 2015). As expected, results from cell cultures exposed to single 5mTHF showed a positive correlation between 5mTHF concentration and cell division. However, cell response to media containing 5mTHF and FDH was complex and strictly dependent on

concentration levels of each molecule. When the active form of the enzyme was added at normal rat CSF concentration levels ( $10^{-5}$  M), and 5mTHF was present at high concentration in the range  $10^{-4}$ - $10^{-6}$  M, cells proliferated significantly ( $p < 0.01$ ). In contrast, active FDH promoted growth when 5mTHF was at low concentration ( $10^{-7}$ - $10^{-9}$  M), although this result was not statistically significant ( $p > 0.05$ ). In view of this outcome, it is proposed that active FDH binds to 5mTHF when present at high concentration, storing it for later use when needed. On the other hand, when 5mTHF is at low concentration, both 5mTHF and active FDH are free to enter the cells and activate the folate metabolic cycle, encouraging cell growth.

We also worked with an inactive form of the FDH (point deletion in intermediate domain) to study its folate binding properties in isolation and its effect on growth in the presence of 5mTHF. On this occasion, FDH at the same concentration as previous experiments ( $10^{-5}$ ) was significantly detrimental for cell growth ( $p < 0.01$ ) when 5mTHF was present at nearly all concentrations in the range ( $10^{-4}$ - $10^{-9}$ ). These results were similar to results obtained with active FDH and 5mTHF at high concentration, which suggests that inactive FDH sequesters 5mTHF, acting as a 5mTHF extracellular reservoir, and impeding 5mTHF access into the cells, thus leading to a generalized decrease in cell growth.

Similar results were obtained from experiments with media containing constant 5mTHF ( $10^{-8}$  M) and active FDH at high concentration ( $10^{-5} \times 10^{-5}$ ), where a relatively significant percentage decrease (12%) ( $*p < 0.005$ ) in cell growth occurred. Yet, this decrease in cell proliferation was less remarkable under these conditions than the reduction in cell growth seen with experiments using constant active FDH and high 5mTHF concentration, where the percentage decrease in cell proliferation was greater than 40% when compared to the

media control. Finally, an overall reduction in cell growth was also observed with inactive FDH at all concentrations in the presence of constant 5mTHF  $p < 0.005$ .

In conclusion, “in vitro” experiments for the study of 5mTHF’s effect along with FDH on cell proliferation suggested that FDH has affinity for 5mTHF, and this affinity depends on the specific FDH and 5mTHF concentration in the extracellular media.

In view of previous results, a sandwich ELISA was developed to investigate further whether or not there is affinity of FDH for 5mTHF. This approach aimed to clarify the suspected linkage between the enzyme and the folate 5mTHF in “in vitro” cell culture experiments. Sandwich ELISA immunoassays have proven a valuable asset for the detection of analytes of interest in body fluids. To investigate the potential affinity of FDH for 5mTHF further, an “in house” fluorescent immunoassay was developed. The immunoassay was able to detect FDH-5mTHF binding in all serial dilutions, producing a decrease in signal directly proportional to FDH and 5mTHF concentration. The intra and inter variation coefficient results were also relatively high, at 9.2 and 9.55 respectively, confirming the need for further optimization of the assay. For instance, polyglutamated 5mTHF may be used instead of the non-glutamated 5mTHF used in this assay as it is known FDH is affected by the degree of folate polyglutamation (Kim, D.W. et al. 1996 and Anguera M.C. et al 2006). In spite of the need for assay refinement, the Sandwich ELISA was adequate to confirm FDH affinity for 5mTHF. This outcome suggests a new role for ALDH1 as a 5mTHF binding protein, similar to  $FR\alpha$ , a membrane receptor with a high affinity for reduced folates such as 5mTHF (Steinfeld, R. et al. 2009, Cains, S et al. 2009 and Zhao et al. 2011).



Furthermore, the confirmation of FDH affinity for 5mTHF suggests the potential ability for this enzyme to pool free extracellular and intracellular 5mTHF, and agrees with previous publications about a possible function for FDH in the regulation of folate storage (Anguera et al. 2006). In this respect, a lack of FDH in CSF can be detrimental for regulation of 5mTHF concentration, having a negative knock-on effect on different areas of the brain. Importantly, this outcome also indicates that FDH may have a role in methylation, providing methyl groups for DNA modifications and SAM production, SAM being a methyl donor which is involved in more than 100 metabolic reactions. Interestingly, it is known that altered homocysteine and methionine levels are associated with the narrowing of blood vessels, such as the carotid arteries in the brain and blood vessels in the placenta, leading to abruption and pre-eclampsia (Solansky et al. 2010). Also, recently, high homocysteine levels in plasma have been linked to blood vessel global hypomethylation (Yang et al. 2014). Because methionine production is dependent on methyl group provision to the folate metabolic cycle through 5mTHF, we suggest that the low FDH levels observed in hydrocephalic CSF also mean that 5mTHF deficit and perturbed balance between methionine and homocysteine plasma levels put pregnancies and fetal development at risk.

In addition, 5mTHF is a substrate for the ubiquitously produced methionine synthase (MTR) ([www.genecards.com](http://www.genecards.com)), which is responsible for the conversion of 5mTHF into THF. THF is a folate at the core of the folate metabolic cycle, needed among other functions for nucleotide production and concomitant production of methionine (Refsum et al. 2001) an amino acid which is vital for fetal brain development (Davis et al. 2004 and Dauncey, MJ et al. 2012). Nevertheless, THF is also FDH's product of reaction (Schirck et al. 1994 and Kim et al. 1996), for which FDH has an affinity greater than for its substrate



(Schirch et al. 1994). For this reason, THF's effect on cell proliferation was also analysed in the presence and absence of FDH. Results from these experiments were contradictory; whilst THF with and without FDH in the media did not have any significant impact on cell division, experiments using THF conjugated to a THF fluorescent IgG led to an increase in cell proliferation. The differences in cell growth impact by single THF compared to THF linked to immunoglobulins were due to the unstable nature of this vitamin. Single THF reacts with oxygen especially in neutral or alkaline solutions at room temperature, rendering it inactive because of degradation after oxygen binding and loss of protons, causing a change in THF chemical properties and structure. In this regard, we minimized THF degradation by purging THF solutions with Argon, a gas which is able to remove oxygen and therefore prevent inactivation. However, THF's contact with oxygen was unavoidable once added to the media which was included in cell cultured plates, which were in contact with air at room temperature. Due to cell culture media air exposure in the incubator, THF must have degraded after 24 hours of growth, as it is known to become 10% inactive after 5 minutes at 37°C and 25% inactive after 45 minutes in the presence of oxygen (Young, D. W. et al. 1969). Interestingly, fluorescent IgG conjugated to THF potentiated cell growth in comparison with negative control media, as seen in fluorescent IgG-THF tracking experiments. These results strongly support the suitability of immunostabilized THF for prevention of oxidation, encouraging cerebral cortex cell growth "in vitro", which was confirmed by fluorescence quantification assay and DAPI staining of primary cell cultures containing the IgG-THF complex. Nevertheless and in spite of acknowledging that DAPI staining does not allow assessment of cell bioavailability, we argue that in primary cell cultures the majority of cells are alive and therefore fluorescence quantification assay of cell growth and the DAPI staining exhibited by the cells nuclei represents cell bioavailability (Davis, J. 2009).

In conclusion, the “in house” fluorescent IgG-THF conjugate and its positive effect on cell growth foresee a potential folate treatment for congenital hydrocephalus and prevention of the cortical plate gross reduction described in fetal brain during this condition. This outcome is also in accordance with previously published research in our lab, where THF in combination with folinic was also beneficial to increase cerebral cortex growth “in vivo” (Cain et al. 2009). Because folates are thought to be transported bound to their enzymes or their receptors in plasma and CSF (Jones et al. 2002), it is not surprising that stabilized THF had a better impact on cell growth than unstable THF, demonstrating the inability for natural THF to be active freely in body fluids. In this scenario, these results also provide evidence that THF may be transported bound to FDH in CSF, a consideration, as mentioned in the introduction to this research, which is also plausible for 5mTHF. In any case, a more extensive investigation needs to be carried out to study the potential use of THF-IgG complex as a folate supplement for congenital hydrocephalus “in vivo”.

With regard to folic acid, cell proliferation with media enriched with the artificial folate alone had the greatest positive effect on cell growth, with percentage increases higher than 80% when compared to the media control. The cell response was similar with folic acid in combination with FDH. Surprisingly, these results were opposite to results from previous research “in vivo” in our lab group, where folic acid supplementation to the hydrocephalic mother was unsuccessful to treat congenital hydrocephalus. This highlights that “in vitro” results do not always coincide with “in vivo” results. Nevertheless, “in vitro” experiments were chosen as a first step for the purposes of our studies.

To clarify whether FDH is either located and biosynthesized in cerebral cortex, or transported in vesicles from choroid plexus within exosomes in a similar fashion to FR $\alpha$

transport system (Grapp et al. 2013), or both, fluorescence FDH protein and mRNA location, as well as gene expression studies, were carried out on fetal brain at embryonic day 18, when CSF blockage and accumulation is established in the hydrocephalic brain.

Since immunohistochemical studies localized ALDHL1 with 5mTHF and FR $\alpha$  in choroid plexus, as well as in cerebral cortex, we can only suggest that FDH and FR $\alpha$  are interrelated and share a common transport function, which is the handling and provision of 5mTHF to the different areas of the brain. With regard to the vesicles identified in some brain sections, these were detected thanks to FR $\alpha$  being a membrane marker itself. These vesicles too showed colocalization of FDH with 5mTHF and FR $\alpha$  in the LV in proximity to choroid plexus and neuroepithelia of areas in the process of differentiation. Previous work published by Bachy et al. in 2008 and Harrington et al. in 2009 supports these findings. In addition, it is known that differentiation is an on-going process at embryonic day 18, and for this reason it is not surprising that these vesicles appear close to the neuroepithelia of the cerebral cortex and the striatum, confirming a need for 5mTHF in both regions of the brain which are in the process of differentiation. Furthermore, these findings also provide evidence of a role for vesicles in the transport for FDH-5mTHF and FR $\alpha$ -5mTHF complexes to different areas of the brain, and concur with Grapp et al.'s research in 2013 and their discovery of vesicles (exosomes) with a role in transporting FR $\alpha$ -5mTHF complexes from choroid plexus to cerebral cortex.

Based on the assumption that ALDHL1 protein and mRNA should coincide in location, “in situ” RTPCR was performed to identify mRNA in normal and abnormal brain. A noticeable staining was exhibited by the choroid plexus and cerebral cortex in both normal

and abnormal brain. However, time restrictions to the duration of this project did not allow gene expression analysis and location of FR $\alpha$  mRNA. In any case, the Steinfeld research group in 2009 published their studies about mRNA expression of folate transporters in human brain tissue finding high levels of FR $\alpha$  mRNA expression in choroid plexus of the adult brain, but not in fetal brain. In view of their results and our findings, we propose that the cerebral cortex relies on FR $\alpha$  for the provision of 5mTHF. However, FR $\alpha$  is only responsible for 50% of the folate transport in the brain (Wollack et al. 2008) and in spite of other brain folate transporters such as Reduce Folate carrier (RFC) (Wang et al. 2001) and Proton coupled folate transporter (PCFT), known to be involved in transport (Ganapathy et al 2004, Wollack et al. 2008), only FR $\alpha$  and FR $\alpha$ -PCFT dependent transport has been proven as the main folate transports in the brain (Grapp et al. 2013). Taking into account these findings and our results about FDH affinity for 5mTHF and its co-localization with FR $\alpha$  and 5mTHF, we can only conclude that FDH is involved along with FR $\alpha$  in the transport of 5mTHF from choroid plexus to cerebral cortex through vesicles (exosomes) formed in the choroid plexus and floating in CSF (Bachy et al. 2008). On the other hand, FDH mRNA expression analysis by traditional RTPCR and “in situ” RTPCR confirmed that FDH is produced in choroid plexus and cerebral cortex, suggesting that cerebral cortex acquires FDH through vesicles, as well as being able to produce the enzyme “in situ”. Going back to our “in vitro” experimental results using media containing FDH and 5mTHF, we proposed that FDH acts as a folate transporter binding to 5mTHF in situations of high 5mTHF concentration. Therefore, FDH seems to act as a folate binding protein to either transport 5mTHF or store it when present in excess at extracellular level in body fluids, such as CSF, as well as intracellularly. This possibility was also considered by Krupenco’s research group in 2010.

With regard to differences in fluorescence density analysis of FDH staining between normal and abnormal brain, it should be emphasized that FDH protein levels in abnormal brain were lower than in normal brain ( $p \leq 0.01$ ), and this result did not correlate with mRNA expression in cerebral cortex. On the contrary, FDH mRNA expression was higher in hydrocephalic brain than normal brain ( $p \leq 0.05$ ). A plausible explanation for this outcome is that gene expression and protein levels do not always correlate. This is due to differences between enzymes and mRNA stability; whereas protein half-life can be hours or days, mRNA degradation is limited to 2-7 hours. Furthermore, mRNA transcription rate and protein translation rate do not always correlate either, and normally only when the protein is highly abundant is mRNA also highly expressed. Finally, there are mRNA posttranscriptional modifications and protein posttranslational changes that contribute to variations in the total level of mRNA and protein leading to uncorrelated results (Vogel et al. 2012).

With regard to FDH immunohistochemical studies, it was found that there is a protein deficit at tissue level in the hydrocephalic brain, which is in agreement with results from previous research where hydrocephalic CSF was devoid of FDH. Even more importantly, results from FDH gene expression analysis showed high mRNA expression in abnormal cerebral cortex, which we argue may be a response to low FDH concentration in CSF. Interestingly, this is the case for  $FR\alpha$  regulation of gene expression where biosynthesis of  $FR\alpha$  is activated in situations of low extracellular folate by negative feedback (Anthony 1996). Negative feedback may be followed by problems at transcriptional or translational level, causing low synthesis of FDH intracellular and/or extracellularly.

With respect to FR $\alpha$  and 5mTHF, fluorescence density analysis of staining showed major protein expression in abnormal brain when compared to normal  $p \leq 0.01$ . This agrees with previous publications of our work where the Dot Blot technique showed that 5mTHF was significantly more abundant in hydrocephalic fetal CSF than in normal brain at embryonic day 20. Interestingly, the level of 5mTHF in the mothers' serum was significantly lower in Texas rats than in normal rats (Cain et al. 2009). Considering that FR $\alpha$  is not produced in the fetal brain (Steinfeld et al, 2009), we can only argue that FR $\alpha$ -5mTHF complexes come from blood circulation in contact with the highly irrigated choroid plexus (Dziegielewska et al 2001 and Hartwig et al. 2010), and that FR $\alpha$  gene expression control and protein production happen somewhere else upstream, rather than in the brain. For instance, regulation of FR $\alpha$  protein expression may be controlled by the placenta, an auxiliary organ known as an important source for FR $\alpha$  synthesis during pregnancy (Henderson et al. 1995, Elnakat & Ratnam 2001 and Solansky et al. 2010). From this point on, we argue that the placenta rather than fetal brain may be responsible for the differences in FR $\alpha$ , and hence, the 5mTHF differences in concentration seen between hydrocephalic and normal brain. We therefore propose the hydrocephalic placenta as an organ for future folate-transport investigation. The role of placenta in maternal-fetal vitamin transport in humans was established by Baker et al in 1981.

Furthermore, since 5mTHF is a ligand for FR $\alpha$  and, as suggested in this study, also a ligand for FDH, and taking into account the binding ratio should be 1:1, higher levels of 5mTHF were expected to be found in both normal and abnormal brain. Therefore, not all FR $\alpha$  and FDH molecules bound to 5mTHF, which suggests that competition led to a low rate of binding. This is commonly observed in receptor-bivalent ligand binding studies (Urbana, 1993 and Xie et al. 2005).

Finally, our findings reveal high concentration of FR $\alpha$  and low FDH protein in Texas rats at tissue level. Increased levels of FR $\alpha$  may lead to exacerbated 5mTHF provision from choroid plexus to cerebral cortex. At the same time, FDH is considered to be a regulatory protein with a role in creating folate pools in situations of high intracellular concentration, storing them for later use in the case of high demand (Anguera et al. 2006 and Krupenco et al. 2002 and 2010). Consequently, our findings (low FDH protein levels) mean free one-carbon folate molecules and folate excess in CSF, as well as intracellularly, leading to CSF folate imbalance and homeostasis disruption, all of which have negative consequences for CNS development as a whole. Accordingly, a role for folate receptors in homeostasis has been established in the past (Weitman et al. 1992 and Johansson et al. 2008).

In conclusion, there are three functional implications for congenital hydrocephalus arising from these studies. First, FDH affinity for 5mTHF outcomes suggests FDH is able to bind to 5mTHF. This finding means that at extracellular level, FDH may transport 5mTHF into vesicles, providing the cerebral cortex with this key folate. At intracellular level, FDH binding to 5mTHF may have a regulatory function in that it aims to store 5mTHF in situations of high 5mTHF concentration. Our findings also revealed low concentration of FDH at tissue levels, which implies low regulation of 5mTHF concentration and folate cell homeostasis disruption. This may also be the case in situations of low FDH in hydrocephalic CSF. Secondly, FDH mRNA overexpression by hydrocephalic cerebral cortex cells did not correlate with the levels of protein found. Based on these results, we conclude that FDH mRNA transcription and/or translation processes may also be altered in congenital hydrocephalus, resulting in low FDH protein expression. On the other hand, the low concentration of FDH in hydrocephalic CSF found in previous published studies, and the high mRNA expression in cerebral cortex seen in our studies, suggest that a negative

feedback loop is occurring to compensate for the low levels of FDH present extracellularly. Thirdly, we argue that the high levels of FR $\alpha$  and 5mTHF observed in choroid plexus and cerebral cortex come from the blood supply irrigating the choroid plexus, as FR $\alpha$  is not expressed in either choroid plexus or cerebral cortex. In this regard, we propose that the placenta is also impaired in hydrocephalus, resulting in FR $\alpha$  gene overexpression. Finally, our results in relation to stabilized THF's positive effect on cell proliferation suggest new avenues for the development of a safe treatment for congenital hydrocephalus, instead of the life-threatening invasive surgery (shunting) commonly used these days.



## 2.5 REFERENCES

- Anguera, M.C. et al. (2006). Regulation of folate-mediated one-carbon Metabolism by 10-FormylTHF Dehydrogenase. *J. Biol. Chem.* 281/27: 18335-18342.
- Antony, T.E. and Heintz, N. (2007). The folate metabolic enzyme FDH is restricted to the midline of the early CNS, suggesting a role in human neural tube defects. *J. Comp. Neurol.* 500: 368-383.
- Antony, A.C. (2007). In utero physiology: role of folic acid in nutrient delivery and fetal development. *Am. J. Clin. Nutr.* 85: 5985-6035.
- Antony, A. C. (1996). Folate receptors. *Annu. Rev. Nutr.* 16, 501–521
- Bachy , I. et al. (2008). The particles of the embryonic cerebrospinal fluid: How could they influence brain development? *Brain Res Bull.* 75: 289-94.
- Baker, P. et al (1981). Role of placenta in maternal-fetal vitamin transfer in humans. *Am. Obstet. Gynecol.* 141: 792-6.
- Blehaut, H. et al. (2010). Effect of Leucovorin (Folinic Acid) on the Developmental Quotient of Children with Down's Syndrome (Trisomy 21) and Influence of Thyroid Status. *PLoS ONE* 5 / 1: e8394
- Cains, S et al. (2009). Addressing a folate imbalance in fetal cerebrospinal fluid can decrease the incidence of congenital hydrocephalus. *J. Neuropathol.* 68: 404-416.
- Champion, K. M., Cook, R. J., Tollaksen, S. L., and Giometti, C. S. (1994). Identification of a heritable deficiency of the folate-dependent enzyme 10-formyltetrahydrofolate dehydrogenase in mice. *Proc. Natl. Acad. Sci. U.S.A.* 91: 11338–11342.
- Cook, R. J., Lloyd, R. S., and Wagner, C. (1991). Isolation and characterization of cDNA clones for rat liver 10-formyltetrahydrofolate dehydrogenase. *J. Biol. Chem.* 266: 4965–4973.
- Chen, L., Qi, H., Korenberg, J., Garrow, T. A., Choi, Y. J., and Shane, B. (1996). Purification and properties of human cytosolic folylpoly- $\gamma$ -glutamate synthetase and organization, localization, and differential splicing of its gene *J. Biol.Chem.* 271.
- Darnton-Hill, I et al. 2015. Micronutrients in pregnancy in low-and-middle-income countries. *Nutr.* 7, 1744-1768.
- Dauncey M.J (2012). Recent advances in nutrition, genes and brain health. *Proc. Nutr. Soc.* 71(4):581-91.
- Davis, J. (2009). *Animal cell culture: Essential methods.* Willey online library. John Wiley & Sons. Ltd.

Davis, S., Stacpoole, P., Williamson, J., Kick, L., Quinlivan, E., Coats, B., Shane, B., Bailey, L., and Gregory III, J. F. (2004). Tracer-derived total and folate-dependent homocysteine remethylation and synthesis rates in humans indicate that serine is the main one-carbon donor. *Am. J. Physiol.* 286: E272–E279..

Dziegielewska, K.M. et al. (2001). Development of the choroid plexus. *Microsc. Res. Tech.* 52: 5-20.

Elnakat, H., Ratnam, M. (2004). Distribution, functionality and gene regulation of folate receptor isoforms: implications in targeted therapy. *Adv. Drug Deliv. Rev.* 56: 1067–84.

Fu, T.-F., Maras, B., Barra, D. and Schirch, V. (1999). A Noncatalytic Tetrahydrofolate Tight Bind to Site Is on the Small Domain of 10-Formyltetrahydrofolate Dehydrogenase. *Arch. Biochem. Biophys.* 367.

Ganapathy et al. (2004). SLC19: the folate/thiamine transporter family. *Plfugers Arch.* 447: 641-6.

Geraldine, G. et al. (2007). Symposium on ‘Micronutrients through the life cycle’. Folate and vitamin B12: friendly or enemy nutrients for the elderly. *Proc. of the Nutr, Soc.* 66: 548–558.

Grapp, M. et al. (2013) Choroid Plexus transcytosis and exosome shuttling deliver folate into brain parenchyma. *Nat.* 2123: 589-93.

Greenberg, M.S. (2001). *Handbook of Neurosurgery*. 5<sup>th</sup> ed. New York: Thieme Medical Publishers.

Geller, J. et al. (2002). Hereditary folate malabsorption: family report and review of the literature. *Medicine (Baltimore)* 81: 51–68.

Hansen, F.J. and Blau, N. (2005). Cerebral folate deficiency: Life-changing supplementation with folinic acid. *Mol. Genet. Metab.* 84: 371-73.

Harrington, M.G. et al. (2009). The morphology of nanostructures provides evidence for synthesis and signalling functions in human cerebrospinal fluid. *Cerebrospinal Fluid Research* doi: 10.1186/1743-8454-6-10.

Hartwig, W. and Wernes, P. (2010). Choroid plexus. *Biol. and Pathol.* 119: 75-78.

Henderson et al. (1995). Maternal-to-fetal transfer of 5-methylTHF by the perfused human placental cotyledon: evidence for a concentrative role by placental folate receptors in fetal folate delivery. *J. Laboratory. Clin. Med.* 126: 184-203.

Hong, M., Lee, Y., Kim, J.W., Lim, J.-S., Chang, S.Y., Lee, K.S., Paik, S.-G., and Choe, I.S. (1999). Isolation and characterization of cDNA clone for human liver 10-formyltetrahydrofolate dehydrogenase. *Biochem. Mol. Biol. Int.* 47: 407–415.

- Hyland, K. et al. (2010). Cerebral folate deficiency. *J. Inherit Metab. Dis.* 33: 563-570.
- Johanson et al. 2008. Multiplicity of cerebrospinal fluid functions: new challenges in health and disease. *Cerebrospinal fluid res. Review.* 5:10
- Jones, H.C. et al. (1997). Aqueduct stenosis in animal models of hydrocephalus. *Child. Nerv. Syst.* 13: 503-4.
- Kamen, B.A., Smith, A.K. (2004). A review of folate receptor alpha cycling and 5-methylTHF accumulation with an emphasis on cell models in vitro. *Adv. Drug Deliv. Rev.* 56: 1085–97.
- Krebs, H.A., Hems, R., and Tyler, B. (1976). The regulation of folate and methionine metabolism. *Biochem. J.* 158: 341–353.
- Khon, D.F. et al. (1981). A new model of congenital hydrocephalus in the rat. *Acta Neuropathol. (Berl.)* 54: 211-218.
- Kim, D.W., Huang, T., Schirch, D., and Schirch, V. (1996). Properties of Tetrahydropteroylpentaglutamate bound to FDH. *Biochem.* 35: 15772–15783.
- Krupenko, S.A. and Oleinik, N.V. (2002). 10-formyltetrahydrofolate dehydrogenase, one of the major folate enzymes, is down-regulated in tumor tissues and possesses suppressor effects on cancer cells. *Cell growth & Differ.* 13: 227-236.
- Krupenko, S.A. (2009). FDH: An aldehyde dehydrogenase fusion enzyme in folate metabolism. Minireview. *Chem.-Biol. Interact.* 178: 84-93.
- Leamon & Low (1991). Delivery of macromolecules into living cells: a method that exploits folate receptor endocytosis. *PNAS.* 8: 5572-6.
- Mashayekhi, F. et al. (2002). Deficient cortical development in the hydrocephalic Texas (H-Tx) rat: a role for CSF. *Brain* 125: 1859-1874.
- Min, H., Shane, B., and Stokstad, E.L.R. (1988). Identification of 10-formyltetrahydrofolate dehydrogenase-hydrolase as major folate bind to protein in liver cytosol. *Biochem. Biophys. Acta* 967: 348–353.
- Miyan, J.A. et al. (2003). Development of the brain: a vital role for CSF. *J. Physiol. Pharmacol.* 81: 317-328.
- Molloy, A.M., and Scott, M.J. (2001). Folates and prevention of disease. *PHN.* 4: 601-609.
- Moretti, P. et al. (2005). Cerebral folate deficiency with developmental delay, autism, and response to folinic acid. *Neurol.* 64: 1088-90.
- Nabiuni, M. Analysis of protein content of cerebrospinal fluid in developing hydrocephalic texas rat. Faculty of Life Sciences. Manchester, UK: The University of Manchester, 2006

Oleinik, N.V. and Krupenko, S.A. (2003). Ectopic expression of 10-formyltetrahydrogenase in A549 cells induces G1 cell cycle arrest and apoptosis. *Mol. Cancer Res.* 1: 577-588.

Oleinik, N. V. et al. (2005). Cancer cells activate p53 in response to 10-formyltetrahydrofolate dehydrogenase expression. *Biochem. J.* 391: 503-511.

Owen-Lynch, P.J. et al. (2003). Defective cell cycle control underlies abnormal cortical development in the hydrocephalic Texas rat. *Brain* 126: 623-631.

Powers, H.J. (2007) Folic acid under scrutiny. *Br. J. Nutr.* 98 (4):665-6.

Pietrzik, K et al. (2010). Folic acid and L-5-Methyltetrahydrofolate. *Clin. Pharmacokinet.* 49: 535-548.

Ramaekers, V.R. et al. (2004). Cerebral folate deficiency. *Dev. Med. Child Neurol.* 46: 843-51.

Refsum, H. (2001). Folate, vitamin B12 and homocysteine in relation to birth defects and pregnancy outcome. *J. Br. Nutr.* 85 (Suppl. 2): S109-13.

Schirck et al. (1994). Domain structure and function of 10-Formyltetrahydrofolate dehydrogenase. *J. Biol. Chem.* Vol. 269 (40) 24728-24735.

Selhub, J., Franklin, W.A. (1984). The folate-binding protein of rat kidney. Purification, properties, and cellular distribution. *J. Biol. Chem.* 259: 6601-6.

Solansky, N. et al. (2010). Expression of folate transporters in human placenta and implications for homocystein metabolism. *Plac.* 31: 134-143.

Steinfeld, R et al. (2009). Folate receptor alpha defect causes cerebral folate transport deficiency: A treatable neurodegenerative disorder associated with disturbed myelin metabolism. *Am. J. Hum. Genet.* 85: 354-363.

Urbana, D.A. (1993). *Receptors: Models for trafficking and signalling.* Oxford University Press. USA.

Vogel, C et al. (2012). Insights into the regulation of protein abundance from proteomics and transcriptomic analyses. *Nat. Rev. Genet.* 13: 227-232.

Wang, Y., Zhao, R., Russell, R.G., Goldman, I.D. (2001). Localization of the murine reduced folate carrier as assessed by immunohistochemical analysis. *Biochim. Biophys. Acta* 1513: 49-54

Weitman, SD et al. 1992. Cellular localization of the folate receptor: potential role in drug toxicity and folate homeostasis. *Cancer Res.* 52: 6708-11.

Wollack, J.B. et al. (2008). Characterization of folate uptake by choroid plexus epithelial cells in a rat primary culture model. *J. Neurochem.* 104: 1494-1503.

Yang, XL. Homocysteine induces blood vessels global hypomethylation mediated by LOX-1. *Genet. Mol. Res.* 13: 3787-3799.

Zhao, R. et al. (2011). Mechanisms of membrane transport of folates into cells across epithelia. *Annu. Rev. of Nutr.* 31: 177-201.

## **CHAPTER 3**

### **FOLATES ARE CRUCIAL FOR FETAL MENINGEAL ARACHNOID CELL GROWTH: IMPLICATIONS FOR CONGENITAL HYDROCEPHALUS.**

#### **ABSTRACT**

Past investigations revealed an association between reduction in the CSF concentration of the folate binding enzyme 10-formyltetrahydrofolate dehydrogenase (FDH), reduced cerebral cortex development and hydrocephalus. We propose that FDH and folates are also crucial for the development of a functional arachnoid, which is in charge of normal CSF drainage and brain CSF outflow. Impediment of normal folate transport caused by low FDH levels in CSF, and therefore low folate provision to the arachnoid tissue, may lead to arachnoid dysfunction and consequently CSF flow blockage and congenital hydrocephalus. The present study aims to investigate the role of FDH in folate transport and its contribution to the development of the arachnoid tissue in the fetal brain.

### **3.1 INTRODUCTION**

The arachnoid is a secondary blood-cerebrospinal fluid barrier, and one of the three layers of connective tissue (meninges) enclosing the brain and the spinal cord. The arachnoid matter starts developing at embryonic day 13.5 and is made up of fibrous tissue linked by tight- junctioned epithelial cells (Bhavaya et al. 2007). Contiguous to the arachnoid runs another meningeal layer, the Piamater, a meninge also made of arachnoid tissue with strands connecting with the arachnoid membrane and forming a three-dimensional web (Kida et al. 1988). The space between the arachnoid and the pia is known as the subarachnoid space and is filled with cerebrospinal fluid (Boulton et al. 1999). At gestational day 18, CSF synthesis commence in the primary blood-cerebrospinal brain barriers, the choroid plexuses, which are small structures situated inside the brain ventricles (Oi et al. 1996). CSF is constantly produced and flows from ventricles to the SAS, leaving the brain mainly through the arachnoid villi in the arachnoid (Xin et al. 2010). Despite over 100 years of research into the arachnoid tissue, its involvement in CSF flow and its role in drainage are still poorly understood (Glimcher et al. 2008 and Holman et al. 2010). A great deal of importance has been attributed to specific structures in the mature arachnoid (arachnoid granulations) in terms of their role in molecule transport and in allowing small molecules to be drained into blood, whilst preventing large molecules in CSF from unloading into the venous sinuses in contact with the arachnoid tissue (Grzybowski et al. 2006 and Glimcher et al. 2008). It is known that blockage of CSF absorption in the arachnoid can give rise to an altered flow and CSF accumulation, leading to congenital hydrocephalus. Thus, congenital hydrocephalus has been associated with arachnoid development impairment and dysfunction due to abnormal morphology and altered differentiation of this meningeal tissue (Vivatbutsiri et al. 2008). However, the specific pathology of congenital hydrocephalus remains unclear, and the condition has

been reported to be more than just an alteration in CSF flow and mechanical phenomena. Children born with hydrocephalus present with neuroepithelia denudation, leading to Sylvius Aqueduct obliteration and CSF obstruction, impairment of the cerebral cortex and cognitive deficit. These events are thought to be caused by abnormal development of certain cerebral neuron's populations and abnormalities of the subcommissural organ, which in turn results in changes in CSF composition, severe alterations of the hypothalamus and neuroendocrine deficiencies (Miyan et al. 2003 and Rodriguez et al. 2006).

CSF contains folates; these are polyglutamated derivatives that function as co-enzymes in metabolic reactions of the folate cycle providing carbon groups for the production of purine rings. (Wagner 1995). The folate metabolic cycle is also needed for production of thymidylate and remethylation of homocysteine to methionine (Molloy and Scott 2001). At the same time, methionine is critical for the synthesis of the methyl donor S-adenosylmethionine (SAM), which is involved in key methylation reactions including DNA, RNA and protein methylation (Shane 1995 and Anguera et al. 2006).

Deficiencies in folate have been associated with neural tube defects and neurological disorders in children due to impaired biosynthesis of SAM, dTMP and methionine, leading to DNA hypomethylation (Suh et al. 2001). These facts highlight the importance of keeping intracellular and extracellular folate levels for an adequate DNA biosynthesis and expression. Folate levels depend on folate transport, bioavailability, polyglutamation state, cell turnover and folate binding protein concentration (Suh et al. 2001 and Anguera et al. 2006). In view of our results, we propose that the folate binding protein and enzyme FDH may have a key role in maintaining cellular folate concentration, binding to folates such as 5mTHF, the most abundant folate in CSF, and storing it in situations of 5mTHF excess.



This view concurs with the discoveries of Champion et al. (1994) describing FDH knock-out rodents as unable to re-establish their normal extracellular and intracellular folate levels, in spite of being supplemented with folates.

The present study reveals a close association between folate imbalance (raised levels of extracellular 5mTHF) and abnormal arachnoid tissue growth. Thus, we suggest that the positive correlation observed in our “in vitro” experiments between arachnoid cell proliferation and increased 5mTHF is due to a critical dependence of arachnoid tissue on 5mTHF levels in CSF for cell division and differentiation. It is known that 5mTHF levels are high in CSF (Cains et al. 2009) and that folate concentration in CSF is regulated by FDH (Anguera et al. 2006). Therefore, and in accordance with our “in vitro” work, we hypothesize that congenital hydrocephalus is triggered by extracellular 5mTHF accumulation in response to low FDH levels, and consequently folate concentration deregulation, leading to excessive arachnoid cell division. In conclusion, our results imply that cell growth hyperstimulation caused by altered high 5mTHF levels in CSF in congenital hydrocephalus may render the arachnoid tissue unable to exert its functions of controlling and maintaining the CSF out-flow required for the correct development of the fetal brain.

## **3.2 MATERIAL AND METHODS**

### **3.2.1 Animals**

Animal experiments were performed at the Biological Services Unit at the University of Manchester following the Home Office animal procedures. Rats from the strain of Sprague-Dawley were used and they will be the animal control of choice for future experiments to investigate congenital hydrocephalus. The Sprague- Dawley is suitable for our studies as it has the same period of gestation (21 days) as the rat model for congenital hydrocephalus; the inbred Hydrocephalic Texas strain.

Sprague-Dawley rats were kept in a 12h: 12h light: dark cycle, and had free access to food and water. Their diet was based on a standard BK universal rat and mouse diet which contains folic acid at 3.2 mg/kg.

### **3.2.2 Matings**

Timed matings were arranged to produce age specific fetuses. Generation of timed matings was achieved by housing males and females in the same cage. These cages have a tray attached where vaginal plugs can be found if there is a successful mating. The day on which the vaginal plug is found is considered day zero.

### **3.2.3 Collection of fetal brains and dissection**

Fetuses were collected on embryonic day 18. Schedule 1 was performed on designated pregnant rats by specialized technicians in the animal unit. Death was confirmed through a lack of reflexes in eyes and tail. Dissection was always undertaken using sterile tools. The lower abdomen was opened and the uterus taken out and placed on ice to ensure fetal euthanasia. Fetal heads were removed and later soaked in the corresponding culture media.

### **3.2.4 Arachnoid tissue processing and identification**

#### 3.2.4.1 Arachnoid tissue processing

Fetal brains were positioned in a dissecting plate using sterile tools and adequate equipment. The fetal arachnoid membrane, a transparent, vascularized and elastic layer situated immediately in contact with the surface of cerebral cortex, was removed and isolated under the dissecting microscope. The membrane was submerged into Dulbecco's modified Eagle's medium (DMEM), (Invitrogen, Paisley, UK) containing 0.05% insulin and 20% FBS (Sigma Aldrich Company, Ltd, Dorset, UK). The leptomeninge was cut into 3 mm fragments and plated in 25-cm<sup>2</sup> flasks (Corning Ltd, UK) with complete medium (DMEM with supplements). The flasks were kept at 37°C in an incubator with 5% CO<sub>2</sub> atmosphere. The medium was replaced every 2 days. Arachnoid cells were transferred after 72 hours from the bottom of the flask to 24 well plates containing a 10 mm coverslip/well. The media was removed from flasks, and cells were washed with Hanks' buffer and digested in 1:1 (v/v) dilution with 0.25 % (w/v) trypsin and 0.02 (w/v) ethylenediamine tetra-acetic acid (EDTA) for 15 minutes. Complete media was added to stop digestion, and

arachnoid cells were suspended and then mechanically separated and triturated by up and down pipette aspiration. Dissociated cells were counted using a haemocytometer in the presence of 50% Trypan blue (Sigma Aldrich Company Ltd, Dorset, UK) to ensure that the cells to be cultured were all viable. The cell suspension was diluted to achieve a cell concentration of  $4 \times 10^5$  cells/ml, and was used for subcultivation in 24 well plates with each well containing 100  $\mu$ l of cell suspension.

#### 3.2.4.2 Arachnoid cell-type identification

Cytokeratin 18 and zone occludens (ZO-1) are cell markers of arachnoid cells, as previously described in published protocols for identification of mammal arachnoid cells (Xin et al. 2010). Tissue isolated from the brain was cut into 3 mm fragments and fixed with 4% paraformaldehyde in PBS. The cells were permeabilized with 0.5% TritonX-100 also in PBS for 5-7 minutes, and washed 3 x 5 minutes with a washing solution containing 10% FBS and 0.2% Tween-20 in PBS, before application of primary antibodies. Double staining with mouse anti-human Cytokeratin 18 (Abcam, Cambridge, UK) and rabbit anti-human ZO-1 (Invitrogen, Paisley, UK) was performed sequentially as it is required when using species-specific primary antibodies. Cells were incubated with primary antibodies for 1 hour, washed with washing solution, and incubated with secondary antibodies Alexa Fluor 488 conjugated anti-rabbit or Alexa Fluor 594 anti-mouse (Invitrogen, Paisley, UK) at 1:500 dilution for 1 hour. Finally, cells were washed with washing solution, counterstained with 4',6-diamidino-2-phenylindole (DAPI), and mounted with antifade reagent (Prolong Gold, Invitrogen, Paisley, UK). Images from immunostained arachnoid cells were captured at 300 milliseconds exposure on a Leica DMLB fluorescence microscope connected to a Coolsnap digital camera.

### 3.2.5 Primary arachnoid cell culture treated with folates and FDH

Primary arachnoid cell culture were maintained at 37 °C in 5% carbon dioxide for 48 hours to study the cells' response to media containing 5mTHF, THF and folic acid at concentration range ( $10^{-4}$ - $10^{-9}$  M), with and without inactive ALDHL1 (point mutation in intermediate domain) and active FDH (intact intermediate domain) at constant concentration ( $10^{-5}$  M). The FDH concentration range was chosen according to the estimated value obtained in previous Western blots studies for FDH in normal rat CSF (Cain et al. 2009). Inactive and active FDH was kindly provided by Dr. S Krupenco, Department of Biochemistry and Molecular Biology, Medical University of South Carolina, Charleston, SC. Inactive FDH was used to study exclusively its folate binding properties in isolation of its enzymatic function. Hence, only the tight bind N domain was active to bind to folates (Fu et al. 1999). Media without folic acid was used as negative control. Cell proliferation was measured using the fluorescent PrestoBlue cell viability reagent kit following the company's protocol (Invitrogen, Paisley, UK). Briefly, PrestoBlue reagent was 1/10 diluted in deionized water and 10 $\mu$ l of solution was added to 100 $\mu$ l media per well. This step was followed by 30 minutes incubation at 37°C. Fluorescence signals due to enzymatic activity, and therefore cell division, were measured on a Magellan 200 fluorimeter (TECAN, UK), set up at 535 nm and 615 nm for wavelength excitation and emission respectively. All folate solutions were purged with Argon before being added to the arachnoid media in order to avoid folates oxidation, which would render folates unstable and inactive.

### **3.2.6 DAPI staining of primary arachnoid cell cultures treated with folates and FDH**

DAPI staining was performed for imaging and visualization of cultured arachnoid cells exposed to FDH and folates. Blue-fluorescent DAPI nucleic acid stain (Invitrogen, Paisley UK) was carried out following the company's instructions. Cells plated in poly-D lysine-coated 24-well plates containing 10 mm glass round coverslips (VWR International, Ltd.), and cells attached at an initial density of  $4 \times 10^5$  cells/ml, were washed with washing solution, counterstained with 4',6-diamidino-2-phenylindole (DAPI) and mounted with antifade reagent (Prolong Gold, Invitrogen, Paisley, UK). Images from DAPI stained arachnoid cells were captured at 300 milliseconds exposure on a Leica DMLB fluorescence microscope connected to a Coolsnap digital camera. DAPI stains dsDNA preferentially, giving rise to fluorescence enhancement that can be detected with a violet filter.

### **3.2.7 CSF treatment**

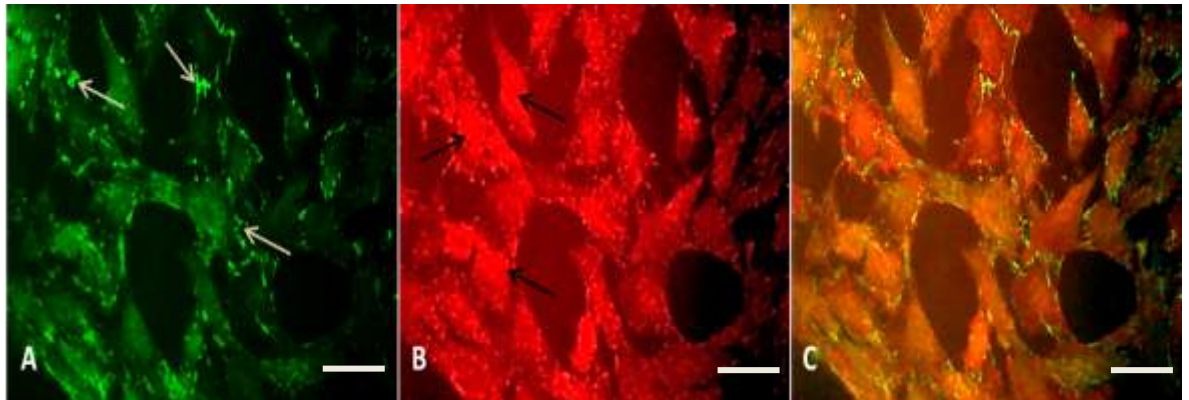
After 48h growth, cells in the 24 well plates were treated with 50% normal and abnormal CSF diluted in complete media. After treatment, the cells were left to grow for another 24h in order to investigate their effect on cell proliferation. Cell growth was determined using the colorimetric assay MTT (Tetrazolium dye cell viability kit (R& D Systems, UK). This assay assesses cell metabolic activity by measuring changes in color (optical density) after reduction of MTT by enzymes which turn the yellow MTT dye into a purple color. Optical density is directly proportional to the number of viable cells in the media.

### **3.2.8 Statistical analysis**

Cell culture experimental data from the effect of folate and FDH supplementation on cell proliferation was analysed by two-way ANOVA. In regard to CSF, its impact on cell proliferation, as well as its effect on cell death was assessed by one-way ANOVA.

### 3.3 RESULTS

#### 3.3.1 Immunocytological assessment

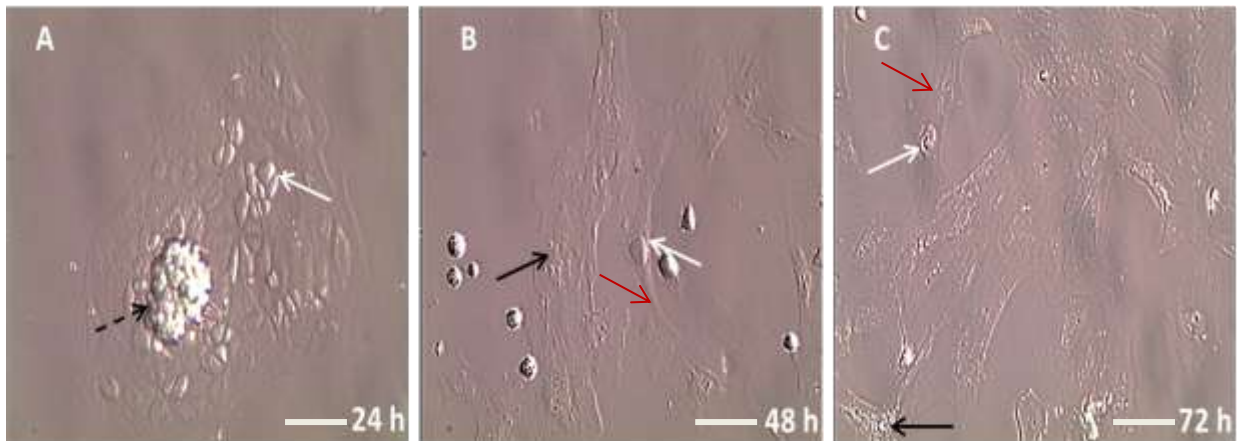


**Figure 3.1.** Fluorescent immunohistochemical staining of arachnoid tissue at embryonic day 18. The staining shows mesenchymal polygonal cells linked together by junctions (zone occludens-1) identified as green fluorescence and pointed with white arrows in image A. Staining of cell marker cytokeratin 18 in cytoplasm (fluorescent red, black arrows) is shown in image B. Image C represents A and B merging, N=6, scale bar: 50  $\mu$ m.

Fetal meningeal arachnoid tissue was isolated and attached to fibronectin-coated coverslips. Arachnoid cell phenotype was confirmed and characterized by using arachnoid-specific primary antibodies to detect junction arachnoid cell markers (Zone occludens-1 (ZO-1)) and cytoplasmic-specific protein (Cytokeratin 18). Primary antibody expression was visualized by labelling the cells with secondary antibodies conjugated to fluorescent molecules. Secondary antibodies were anti-IgG FITC (green) for localization of ZO-1 and Alexa fluor 555 (red) for identification of cytokeratin 8. Fetal arachnoid cells exhibited a polygonal shape with junctions or ZO-1 (green staining) between cells (Figure 3.1, A). The cells' cytoskeleton presented dense clusters of arachnoid-specific cytokeratin which was revealed with red fluorescence (B, black arrows). Images A and B were merged (C) to visualize location of ZO-1 junctions in relation to cytokeratin 18. Once arachnoid tissue was confirmed by specific cell markers, and the tissue was “in vitro” cultured for production of subsequent primary cell cultures to be used for folate effect studies.



### 3.3.2 Morphological and confluency assessment



**Figure 3.2 Cultured arachnoid cells micrographs using bright-field microscopy show cell appearance and confluency after 24 hours (A), 48 hours (B) and 72 hours (C), N:6, scale bar: 50  $\mu$ m.**

Fetal arachnoid fragments (Figure 3.2, A, dashed black arrow) were used for production of primary cell cultures. These attached to the bottom of flasks creating tissue-like structures or scaffolds distributed as a monolayer of polygonal cells with large nuclei (Figure. 3, A, B and C, white arrows) and many granules in cytoplasm (Figure. 3 B and C, black arrows). Also, the cells attach together forming sheets that bridge together (Figure. 3 B and C, red arrows). This agrees with characteristics described for this cell-type in previous publications (Murphy et al. 1991). Cell proliferation increased progressively at 24 hours growth to achieve total confluency after 72 hours.

3.3.3 FDH is counterproductive for arachnoidal cell growth in the presence of 5mTHF.

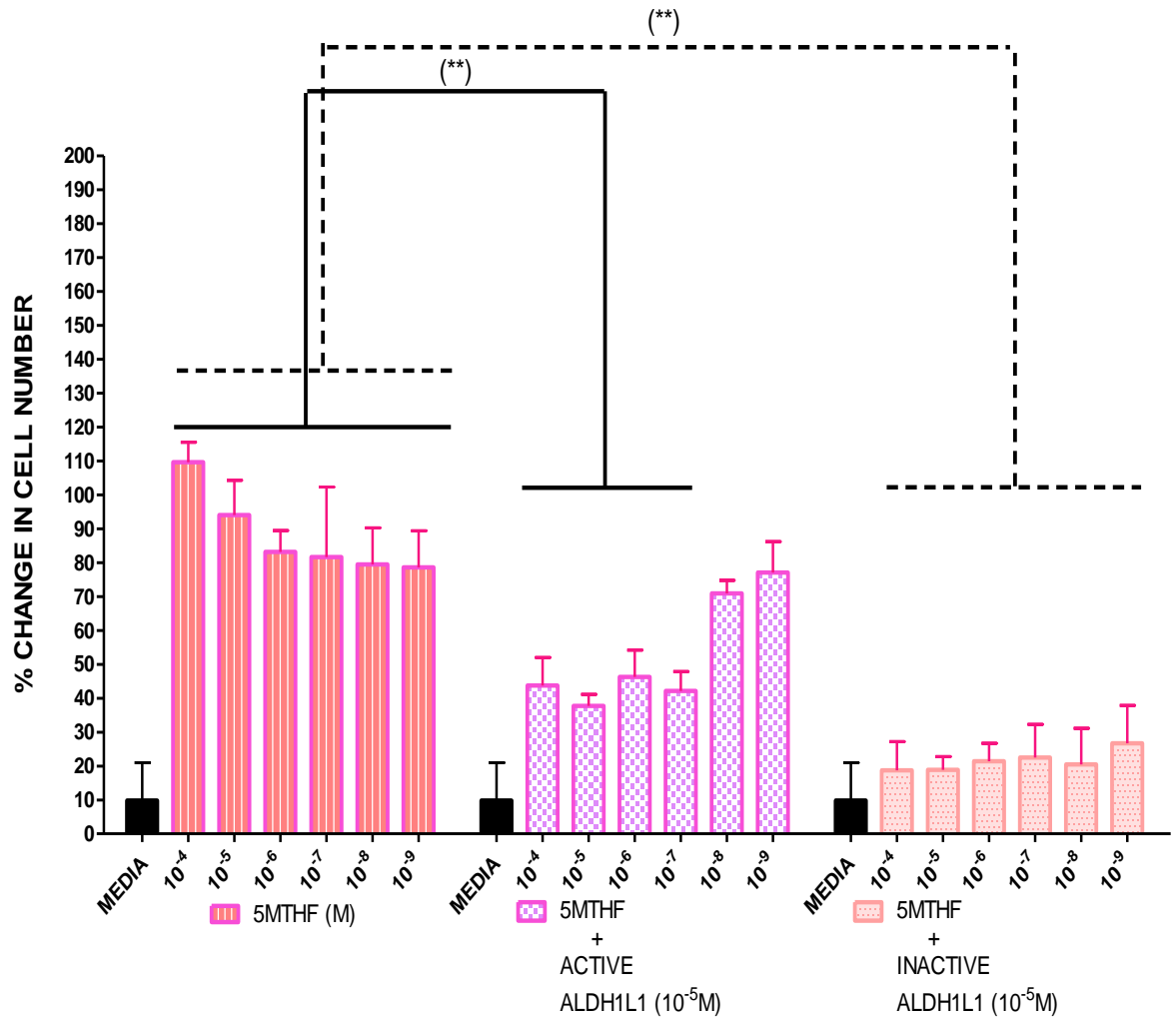


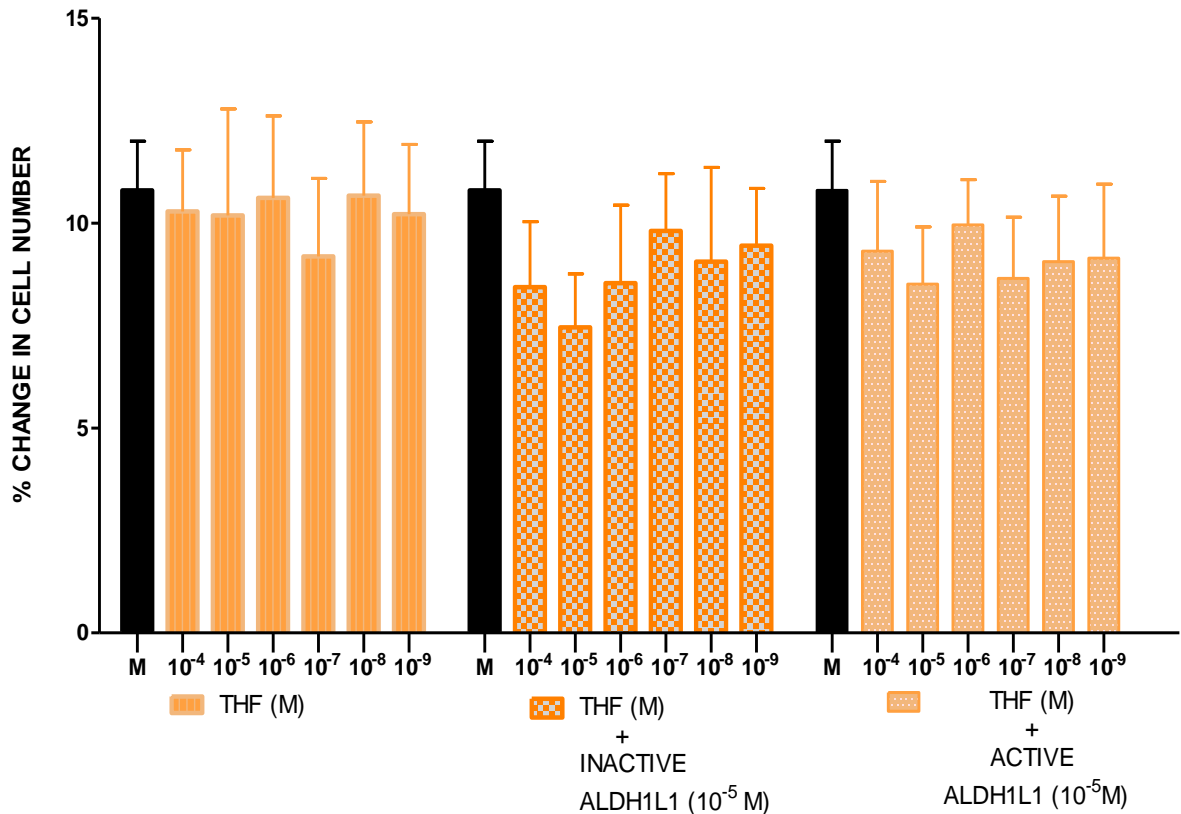
Figure 3.3. Effect of decreasing 5mTHF and constant active and inactive FDH/ALDH1L1 concentration on cell proliferation. MTHF alone (line pattern), 5mTHF + active FDH (square pattern) and 5mTHF + inactive FDH (dot pattern). Arachnoid cells from E19 Sprague- Dawley foetuses were incubated with metabolites in the range 10<sup>-4</sup> - 10<sup>-9</sup>M in the absence and presence of FDH at 10<sup>-5</sup> M. Cell bioavailability was measured using a fluorescence-based assay as described in material and methods (paragraph 3.2.5). Data are presented as mean percentages in cell change ± SEM obtained after normalization of relative fluorescence indexes (RFI) measurements (n=6). Analysis of variance with post hoc test revealed significant differences in the indicated paired samples. Results are shown as: \*\*p < 0.01 for the effect on proliferation of 5mTHF alone versus 5mTHF in combination with FDH.

To assess the effect of constant FDH and decreasing 5mTHF concentration on cell growth, the metabolite was added to the arachnoid media at concentration range ( $10^{-4}$  -  $10^{-9}$  M) with and without active and inactive FDH at  $10^{-5}$  M (Figure 3.3). Overall, control experiments showed that E18 arachnoid cell cultured in folate supplemented DMEM media showed an increase in cell number above media control levels (Figure 3.3, media columns; no folates/black columns) after 72 hours growth. Thus, the average percentage increases were of  $87.80 \pm 12.07$ ,  $52.98 \pm 16.62$  and  $21.52 \pm 2.86$  for media containing 5mTHF alone (Figure 3.3, first set of columns), 5mTHF plus active FDH (Figure 3.3, second set of columns) and 5mTHF plus inactive FDH (Figure 3.3, third set of columns). Interestingly, media containing just 5mTHF cell growth was exacerbated at all concentrations and peaked at  $10^{-4}$  M with percentage increases in cell number as follows: 109.63 ( $10^{-4}$  M), 94.2 ( $10^{-5}$ ), 83.19 ( $10^{-6}$ ), 81.69 ( $10^{-7}$ ), 79.49 ( $10^{-8}$ ), 78.61 ( $10^{-9}$ ). These data clearly demonstrate that cell proliferation was directly proportional to the concentration of 5mTHF in the media. In contrast, the presence of FDH in combination with 5mTHF had a significant detrimental effect on cell growth with both active and inactive protein ( $p < 0.01$ ).

In conclusion, these data confirm that the addition of active FDH in the folate (5mTHF) supplemented media caused significant decreases in growth percentage with cell cultures presenting a reduction in cell proliferation of 65.89% ( $10^{-4}$  M), 56.47% ( $10^{-5}$  M), 36.93% ( $10^{-6}$  M), 39.51% ( $10^{-7}$  M), 8.54% ( $10^{-8}$  M) and 2.55% ( $10^{-9}$  M) when compared to media containing 5mTHF alone. This reduction was significantly more pronounced in the presence of inactive FDH ( $p < 0.01$ ), with decreases in growth as follows: 90.91% ( $10^{-4}$  M), 74.8% ( $10^{-5}$  M), 60.79% ( $10^{-6}$  M), 60.19% ( $10^{-7}$  M), 59.04% ( $10^{-8}$  M) and 51.92% ( $10^{-9}$  M). These data indicate that FDH has a generalized negative effect on cell growth in the presence of 5mTHF, which correlates with decreasing 5mTHF concentration in the media.

Interestingly, with active FDH, the negative impact on cell growth is less apparent when 5mTHF was at  $10^{-8}$  M and  $10^{-9}$  M, indicating that FDH effects on growth depends on its specific concentration in the media.

### 3.3.4 THF with or without FDH does not potentiate cell arachnoid growth.

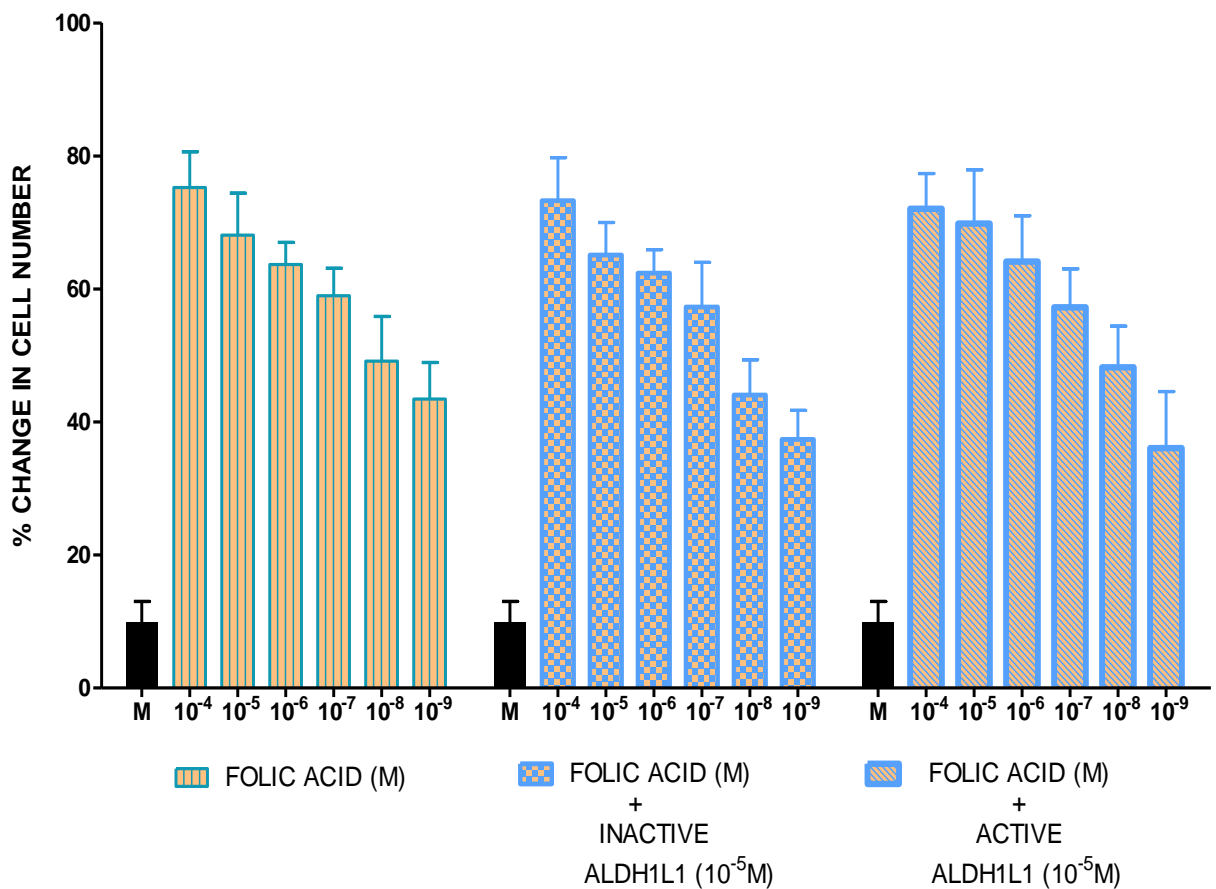


**Figure 3.4. Effect on cell proliferation of THF alone (line pattern), THF plus inactive ALDH1L1 (FDH) (square pattern) and THF plus active ALDH1L1 (FDH) (dot pattern) at decreasing concentrations. Cell bioavailability was measured using a fluorescence-based assay as described in material and methods (paragraph 3.2.5). Data are presented as mean percentages in cell change  $\pm$  SEM obtained after normalization of relative fluorescence indexes (RFI) measurements (n=6). Analysis of data with Kruskal-Wallis test and post-test Dunn's multiple column comparison revealed THF had no effect on cell proliferation with or without ALDH1L1 (FDH).**

FDH has a high affinity for THF, a product of its enzymatic reaction. Taking this fact into consideration, the effect of both molecules on cell division was determined by adding to arachnoid media THF alone, THF in combination with FDH and finally THF with active FDH. Cells in all conditions had a growth percentage below media control levels (M) (10.8%) after 72 hours growth (Figure 3.4). This reduction in growth was relatively less intense in arachnoid cells co-cultured with inactive FDH and THF, when compared to

growth in the presence of THF alone, with an averaged reduction in growth of 8.7% and 10.1% respectively (Figure 3.4, second set of columns). With regard to active FDH and 5mTHF, the average reduction in percentage cell growth values was 9.06%, which was also lower than controls (M) in Figure 3.4, (third set of graphs). In conclusion, these data indicate that THF alone, as well as along with FDH in the media, may not be beneficial for arachnoid cells, although these data were not statistically significant ( $p \geq 0.05$ ).

### 3.3.5 Folic acid exacerbates growth with and without FDH

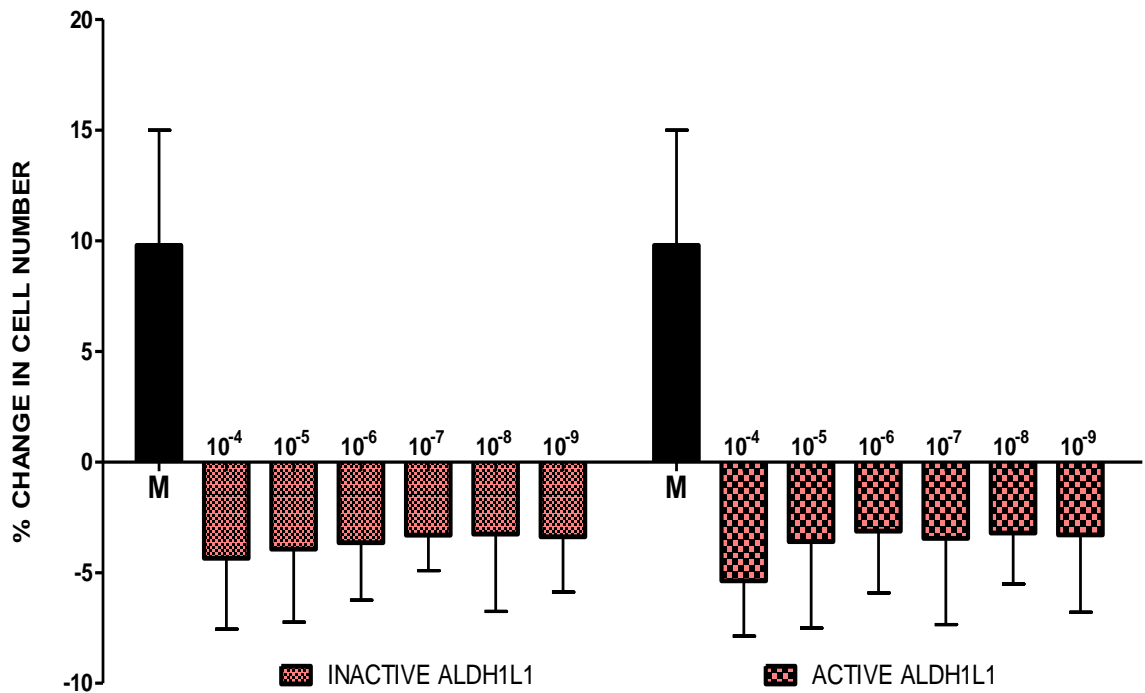


**Figure 3.5. Effect on cell proliferation of folic acid alone (line pattern), folic acid plus inactive ALDH1L1 (FDH), (square pattern) and folic acid plus active ALDH1L1 (FDH), (dot pattern) at decreasing concentrations. Cell bioavailability was measured using a fluorescence-based assay as described in material and methods (3.2.5). Data are presented as mean percentages in cell change  $\pm$  SEM obtained after normalization of relative fluorescence indexes (RFI) measurements (n=6). Analysis of data with Kruskas-Wallis test and post-test Dunn's multiple column comparison revealed FDH did not have a positive effect on cell growth and the average cell growth was similar at all conditions in the presence of folic acid with and without FDH**

Folic acid is a biosynthetically artificially produced folate, which is normally present in commercial media. For this reason, only DMEM media depleted of folic acid was used as the control media throughout all experiments. Folic acid was added to DMEM media to study its effect on cell division, which was subsequently assessed by comparison with media control (no folates). Folic acid's effect on cell division was also determined in the presence and absence of inactive and active FDH. Figure 3.5 shows that cells in all conditions presented a similar average percentage increase above media control levels of  $59.77 \pm 11.86$  for folic acid alone,  $57.93 \pm 13.5$  for folic acid + inactive FDH and  $56.58 \pm 13.7$  for folic acid + active ALDH1L. In conclusion, FDH does not significantly interfere with cell growth in the presence of folic acid and cell division remains similar to media containing folic acid only ( $p > 0.05$ ).



### 3.3.6 FDH effect on arachnoidal cell growth depends on folate presence in media

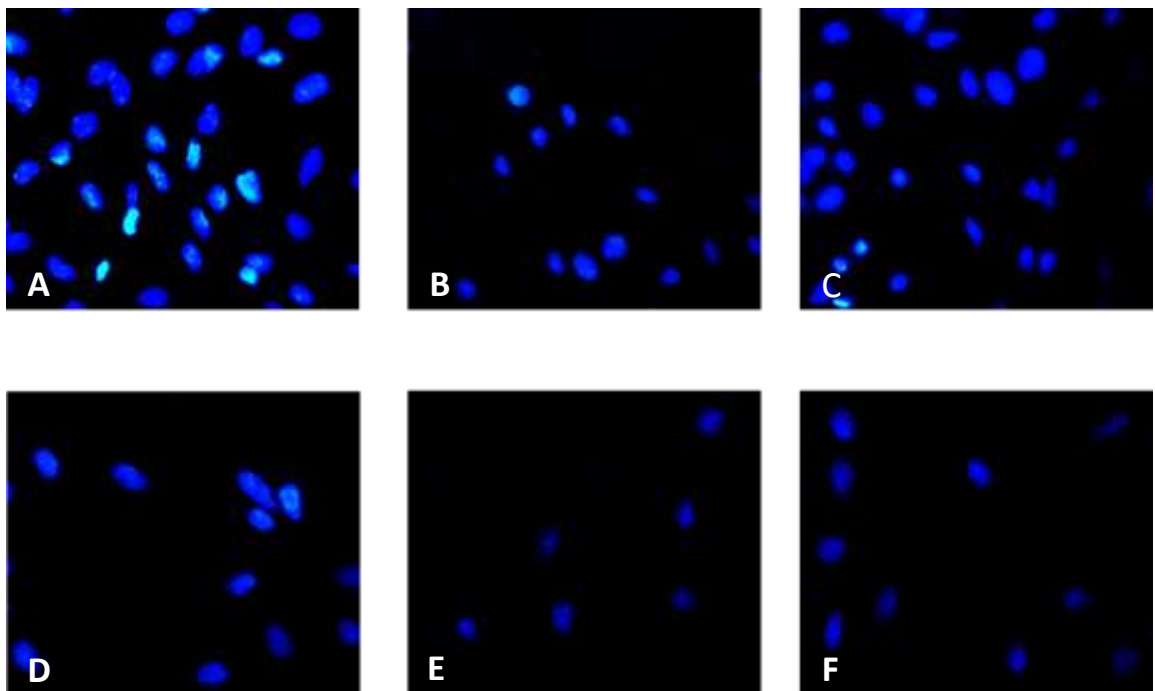


**Figure 3.6. Effect on cell proliferation of active (small square) and inactive FDH (large square). Proliferation was measured using a fluorescence-based assay as described in material and methods (3.2.5). Data are presented as mean percentages in cell change  $\pm$  SEM obtained after normalization of relative fluorescence indexes (RFI) measurements (n=6). Analysis of data with Kruskal-Wallis test and post-test Dunn's multiple column comparison revealed no change in cell growth either with inactive or active FDH.**

In order to study whether there is any effect of active and inactive FDH alone on arachnoid cells, the folate binding protein was added to the media without any folates. Arachnoid cells cannot survive without folates, and as expected, addition of single FDH to a media depleted of folates resulted in an overall negative growth at all concentrations (Figure 3.6 above).

### 3.3.7 DAPI staining reveals different effects on growth of arachnoidal cells co-cultured with folates and FDH.

DAPI staining was performed on cell cultures treated with folates and FDH to study their effect on cell proliferation visually. As expected, these results agreed with fluorescence quantification analysis of cell division after treatment with folates and FDH using the fluorescence based assay (Presto Blue), (paragraph 3.2.6). DAPI staining results in the presence of specific folates at  $10^{-5}$  M with and without FDH also at  $10^{-5}$  M are illustrated in Figure 3.7 below:

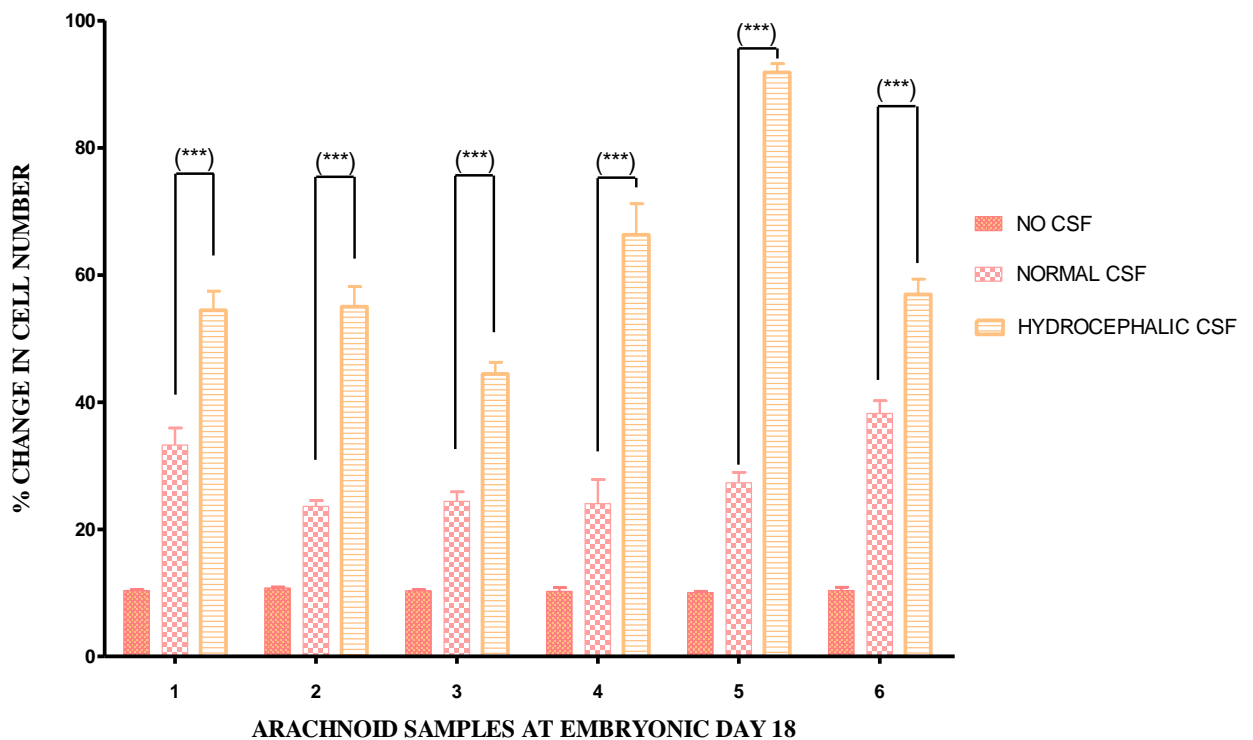


**Figure 3.7. DAPI nuclei staining snapshots of primary cell cultures in the presence of different types of folates with and without FDH as follows: 5mTHF (A), 5mTHF + ACTIVE FDH (B), FOLIC ACID (C), THF(D), THF + ACTIVE FDH (E) and negative control (NO FOLATES), (F), (x20) magnification.**

Figure. 3.7 shows how 5mTHF potentiates cell division (A), whereas the presence of FDH results in a negative effect on cell growth (B). In a similar fashion to 5mTHF, folic acid also encouraged cell proliferation (C). On the other hand, growth with THF had a negative impact on cell division with and without FDH (D) and (F) respectively, with cell growth similar to negative controls. This suggested a halt in cell division in the presence of THF.

### 3.3.8. CSF effect on arachnoid cell growth

In past studies, normal CSF was shown to have a beneficial effect on cell growth of cerebral cortex cells, whilst hydrocephalic CSF was found to be detrimental. In order to investigate whether there is a role for CSF in the proliferation and development of arachnoid cells, this body fluid was placed in arachnoid media depleted of folates and FDH. After 24 hours growth with arachnoid media enriched at 50% CSF, cell bioavailability was measured using a colorimetric assay (MTT assay) as described in material and methods. Optical density was quantified, and this data was used to calculate percentage cell changes with and without CSF. Percentage cell increases are represented versus arachnoid samples, as shown in Figure 3.8 below:



**Figure 3.8. CSF effect on arachnoid cell proliferation.** Dot bars represent CSF-untreated cultures, cultures enriched with normal 50% CSF (squares) and cultures enriched with 50% hydrocephalic CSF (horizontal lines). Analysis was performed on six different arachnoid samples. Data are presented as mean percentages in cell change  $\pm$  SEM obtained after normalization of optical density measurements. Analysis of variance (two-ways ANOVA) with Bonferroni post hoc test revealed significant differences in all indicated paired samples,  $N=6$ . Results are shown as: \*\*\* $p < 0.001$  for the effect on proliferation of normal CSF versus hydrocephalic CSF.

Figure 3.8 shows that the presence of normal and hydrocephalic CSF clearly encouraged arachnoid cell division when compared to media devoided of CSF. Surprisingly, this outcome contradicted the results of previous published research using cerebral cortex cells, which after exposure to hydrocephalic CSF resulted in cell arrest in the S phase of the cell cycle. In this study, all samples exposed to normal CSF show an average 17.77% increase in cell growth with respect to media without CSF. With regard to samples treated with hydrocephalic CSF, the average percentage increase was 50.78% when compared to untreated samples. This percentage increase also meant that hydrocephalic CSF stimulated growth even more than normal CSF, with 33% more growth due to the presence of abnormal CSF in the media after 24 hours ( $p < 0.001$ ). Finally, figure 3.8 also shows variability between samples with the same treatment. For instance, sample 5 and sample 3, which were both treated with hydrocephalic CSF, presented very different percentage increases, with the sharpest percentage increase (92.2%) for sample 5 in contrast with sample 3 (46.56%). A more similar trend in percentage change was shown by samples treated with normal CSF, with sample 6 presenting the highest percentage increase (35.9%) and sample 1 the lowest (22.5%).

### 3.4 CONCLUSION-DISCUSSION

The adequate development of fetal arachnoid tissue is crucial for cerebrospinal fluid egress and the failure of that function leads to fluid build-up and congenital hydrocephalus (Cornelius et al. 2011). In this study, morphological and immunocytological assessment allowed characterization of cytoskeletal protein expression and intercellular junctional proteins typical in tissues with a function in fluid flow regulation (Bhavya et al. 2007). Morphological and immunocytological assessment were also critical in order to confirm arachnoid tissue phenotype for later production of primary cell cultures, and to ultimately determine the effects of folate, and normal and abnormal CSF on arachnoid cell growth.

In previously published studies (Cain et al. 2009), folates such as THF, in combination with folinic acid, encouraged cerebral cortex growth and differentiation “in vivo” and “in vitro”. In this study, folates’ effect on cell division was also assessed, but on this occasion on arachnoid primary cell cultures. Results from this investigation revealed 5mTHF as the only folate able to potentiate cell arachnoid division and subsequent production of tissue-like sheets that distribute as monolayer of polygonal cells at the bottom of flasks. These characteristics are typical in arachnoid cell growth “in vitro”, and meant that 5mTHF contributes to the production of cell to cell connections, allowing flow regulation. This outcome also indicates that 5mTHF is the key folate for arachnoid cell growth, and suggests that this folate may be also crucial for the correct development of a functional fetal arachnoid in early pregnancy. In contrast, 5mTHF co-culture with active FDH was counterproductive for cell growth at specific concentrations of 5mTHF and FDH. For instance, when 5mTHF was present at concentration range ( $10^{-4}$ – $10^{-9}$  M) and active FDH at concentration present in normal CSF ( $10^{-5}$  M), ( $p \leq 0.05$ ).

FDH binds to 5mTHF and limits arachnoid cells' capability to use the folate for cell division. This finding also agrees with results from experiments with cerebral cortex cells cultured with 5mTHF and FDH where cell division was also negatively affected by the presence of FDH in the media at pre-determined concentrations. In contrast, active FDH at the same concentration ( $10^{-5}$  M) and 5mTHF at small concentrations ( $10^{-8}$ - $10^{-9}$  M) potentiated cell growth. However, this result was non-statistically significant, and we argue that a more extensive dose response study is needed to clarify this result. Nevertheless, once more, our experiments suggest that FDH is a folate binding protein responsible for folate regulatory function in CSF, making it available to cells or sequestering it instead depending on 5mTHF specific concentration in CSF. Our findings also agree with the research of Anguera et al. (2006) describing FDH as an enzyme that is able to pool folates in situations of high folate concentration. In addition, it is known that folates like 5mTHF can be trapped in situations of cobalamine deficiency (Krumdieck et al. 1978) impeding its conversion into THF. This is important, as THF is a key folate that cells need for DNA methylation and DNA synthesis in the folate metabolic cycle. THF is also needed for the production of S-Adenosyl-L- methionine (SAM) a common substrate involved in methyl group transfers and crucial for more than 100 metabolic reactions in the body (Roje, 2006).

In the hydrocephalic brain, CSF lacks FDH, which suggests that folate concentration in CSF is not regulated by the enzyme. Therefore, 5mTHF may be accumulated in the body fluid, leading downstream to an exacerbation of arachnoid tissue proliferation, as observed in our "in vitro" experiments in situations of high levels of 5mTHF in the presence of active FDH. Our experiments also showed that arachnoid primary cell culture treatment with hydrocephalic CSF stimulates arachnoid cell division, and this effect was much more noticeable when contrasting cell cultures treated with hydrocephalic CSF with cell cultures

without CSF or cultures with just normal CSF. These findings agreed with past studies on analysis of hydrocephalic CSF, which showed higher levels of 5mTHF in hydrocephalic CSF than normal CSF (Cains et al. 1989). Our results also agree with Gonzalez et al. experiments in 2006, describing CSF from hydrocephalic rats as a promoter of neuronal and glial differentiation.

Whilst brain alterations in congenital hydrocephalus are mainly related to brain loss, there are also mechanisms by which the hydrocephalic brain compensates for brain damage by repairing with exacerbated cell proliferation. For instance, certain subpopulations of astrocytes respond to neuroepithelia denudation by increasing the cell division rate and by creating ependymal-like new barriers in the affected areas (Rodriguez et al. 2006). Hereby, our studies suggest that the arachnoid tissue responds to hydrocephalic CSF and its changes in composition (high levels of 5mTHF and low levels of FDH) by encouraging cell division.

In conclusion, we propose that FDH is a regulatory folate binding protein, and its depletion in hydrocephalic CSF is the cause of increased 5mTHF levels leading to abnormal arachnoid development and dysfunction.

Furthermore, it is known that a lack of FR $\alpha$  (5mTHF transporter) in the brain, leads to brain deficits (Steinfeld et al. 2009). Similar to FR $\alpha$ , FDH is a folate binding protein in brain CSF that is able to bind to 5mTHF. Consequently, its absence in CSF may account



not only for congenital hydrocephalus but also for other fetal brain disorders related to 5mTHF deficit in CSF.

### 3.5 REFERENCES:

- Anguera, M.C. et al. (2006). Regulation of folate-mediated one-carbon Metabolism by 10-FormylTHF Dehydrogenase. *The J. Biol. Chem.* 281/27: 18335-42.
- Bhavya C. M. et al. (2007). Characterization of arachnoidal cells cultured on three-dimensional Nonwoven PET matrix. *Tissue engineering.* (13): Number 6: 1-11.
- Blomquist, H.K. et al. 1986. Cerebrospinal fluid hydrodynamic studies in children. *J. Neurol. Neurosurg. Psychiatr.* (49): 536-40.
- Boulton, M. et al. (1999). Contribution of extracranial pressure in lymphatics and arachnoid villi to the clearance of a CSF tracer in the rat. *Am. J. Physiol.* (276): 818-20.
- Burtis, C.A. et al. (2012). *Clinical Chemistry and Molecular Diagnostics. Tietz textbook.* 5<sup>th</sup> edition. Elsevier.
- Champion K.M. et al. 1994 Identification of a heritable deficiency of the folate-dependent enzyme 10-formyltetrahydrofolate dehydrogenase in mice. *Proc. Natl. Acad. Sci. USA.* (91): 11338-42.
- Cornelius et al. (2011). Arachnoid Cells on Culture Plates and Collagen Scaffolds: Phenotype and Transport Properties. *Tiss. Eng.: Part A.* (17): 1759- 66.
- Friden, H.G & Ekstedt, J. (1983). Volume/pressure relationship of the cerebrospinal space in humans. *Neurosurgery.* (13): 351-62.
- Glimcher, S.A. et al. (2008). Ex vivo model of cerebrospinal fluid outflow across human arachnoid granulations. *Invest. Ophthalmol. Vis. Sci.* (49): 4721-28.
- Glish, GL and Vacher, RW. (2003). The basics of mass spectrometry in the twenty-first century. *Nat. Rev. Drug Discov.* 2: 140-150.
- Gonzalez, C et al. (2006). The CSF of H-Tx rats promote neuronal and glial differentiation from neurospheres. *Cerebrospinal fluid Res. (Suppl. 1).* S10.
- Grzybowski, D.M. et al. (2006). In vitro model of cerebrospinal fluid outflow through human arachnoid granulations. *Invest. Ophthalmol.* (47):8-12.
- Holman, D.W. et al. (2010). Cerebrospinal fluid dynamics in the human cranial subarachnoid space: an overlooked mediator of cerebral disease. II. In vitro arachnoid outflow model. *J. R. Soc. Interface* 7, 1205-18.
- Hyland, K. & Surtees, R. (1992). Measurement of 5-methyltetrahydrofolate in cerebrospinal fluid using hplc with coulometric electrochemical detection. *Pteridines Vol.* (3): 149-150.

- Kida, S. et al. (1988). Light and electron microscopic and immunohistochemical study of human arachnoid villi. *J. Neurosurg.* (69): 429-35.
- Krumdieck et al. (1978). A long-term study of the excretion of folate and pterins in a human subject after ingestion of <sup>14</sup>C folic acid, with observations on the effect of diphenylhydantoin administration. *Am. J. Clin. Nutr.* Vol (31): 88-93.
- Mason, J.B. (1990). Intestinal transport of monoglutamyl folates in mammalian systems. In: Picciano MF et al. *Folic acid metabolism in health and disease*. Editorial Wiley-Liss. New. York. 47-64.
- Mehta B.C., Holman & D.W. et al. (2007). Characterization of arachnoid cells cultured on three-dimensional nonwoven PET matrix. *Tiss. Eng.* 13, 1269-73.
- Miyan et al. (2003). Development of the brain: a vital role for cerebrospinal fluid. *J. Phys. Pharmacol.* (81): 317-28.
- Molloy, A.M., and Scott, M.J. (2001). Folates and prevention of disease. *Public Health Nutrition* 4 (2B): 601-09.
- Murphy, M. et al. (1991). Establishment and characterization of a human leptomeningeal cell line. *J. Neuro. Res.* 30 (3):475-83.
- Oi et al. (1996). Experimental models of congenital hydrocephalus and comparable clinical problems in the fetal and neonatal periods. Review. *Child Nerv. Syst.* (12): 292-302.
- Rodriguez E.M. et al. (2006). Long-lasting hydrocephalus in HYH mutant mice: gain and loss of a brain surviving hydrocephalus. *Cerebrospinal Fluid Res.* 3 (1): S15.
- Roje, S. (2006). "S-Adenosyl-L-methionine: beyond the universal methyl group donor". *Phytochem.* 67 (15): 1686-98
- Sainte-Rose, C. (1990). Hydrocephalus in childhood. Youmans, J.R. ed. *Neurological Surgery* 4th ed. Vol. 2. Philadelphia, PA: W.B. Saunders Co., 890-95
- Sanderson et al. (2003). Folate bioavailability: UK Food Standards Agency workshop report. *Br. J. Nutr.* (90): 473-79.
- Shane, B. (1995). Folate in Health and Disease (Bailey, L. B., ed) pp. 1–22, Marcel Dekker, Inc., New York.
- Steinfeld, R et al. (2009). Folate receptor alpha defect causes cerebral folate transport deficiency: A treatable neurodegenerative disorder associated with disturbed myelin metabolism. *Am. J. Hum. Gen.* (85): 354-363.
- Suh et al. (2001). New perspectives on folate catabolism. *Annu. Rev. Nutr.* (21):255–82
- Upton, M.L. & Weller, R.O. (1985). The morphology of cerebrospinal fluid drainage pathways in human arachnoid granulations. *J. Neurosurg.* (63): 867-72.
- Xin et al. 2010. Arachnoid cell involvement in the mechanism of coagulation-initiated inflammation in the subarachnoid space after subarachnoid haemorrhage. *Biomed. & Biotechno.* 11(7):516-523

Van der Put, N.M.J. et al. 2001. Folate, homocysteine and neural tube defects: an overview. *Exp. Biol. Med.* Vol. 226: (4) 243-270.

Vivatbutsiri et al. (2008). Impaired meningeal development in association with apical expansion of calvarial bone osteogenesis in the *Foxc1* mutant. *J. Anat.* (212): 603-11.

Wagner, C. (1995) in *Folate in Health and Disease* (Bailey, L. B., ed.) 23–42, Marcel Dekker, Inc., New York

## **CHAPTER 4**

# **INGENUITY PATH ANALYSIS OF NORMAL VERSUS HYDROCEPHALIC CSF'S PROTEIN PROFILES IDENTIFIED BY LCMS.**

### **ABSTRACT:**

Congenital hydrocephalus is triggered during the first trimester of pregnancy and begins with increased intracranial pressure due to cerebrospinal fluid (CSF) build-up. This is followed by variations in CSF constituents related to the folate metabolic cycle, and reduced thickness of the cortical plate. These events result in mental retardation, intellectual disability and abnormal CSF proteome.

In this investigation, LCMS analysis was performed to identify differences in CSF protein profiles expressed during normal and hydrocephalic conditions, focusing on the presence and absence of proteins in normal and abnormal CSF. Variations in LCMS protein profiles were analysed, first using Microsoft Excel to filter LCMS data and select the proteins unique to each type of CSF, and subsequently by a second analysis of Excel datasets using a bioinformatic tool called Ingenuity Path Analysis (IPA). IPA allows protein matching with metabolic pathways exclusively represented in hydrocephalic CSF and missing in normal CSF, and vice versa. The ultimate aim is to help in the discovery of key metabolites, which are either missing or in excess in hydrocephalic CSF, that may be good candidates for the development of novel therapies. Furthermore, the present study may give some insights into the pathology of congenital hydrocephalus, which has not yet been fully characterized, and open new avenues for an alternative treatment to shunting, the current treatment, which is associated with a high risk of infection and technical failures.

## 4.1 INTRODUCTION

Brain CSF is a nutritional fluid vital for CNS development. It is secreted by the choroid plexuses in the brain ventricles where it accumulates if bulk flow is interrupted. CSF obstruction is caused either by obstruction of the cerebral aqueduct or by abnormal absorption within the arachnoidal villi in contact with the general blood circulation where CSF is drained. CSF blockage leads to enlarged ventricles also called hydrocephalus (water in the brain). Congenital hydrocephalus begins early in pregnancy and starts with increased intracranial pressure caused by CSF accumulation leading to intellectual impairment as well as CSF compositional changes. These events suggest that normal and hydrocephalic CSF presents a differential protein spectrum. Based on this assumption, past studies relied on LCMS analysis (Nabiuni et al. 2006) to identify the specific protein profile corresponding to normal and abnormal CSF. LCMS is a powerful analytical technique used in the clinical diagnosis of neurological and metabolic disorders (Grebe et al. 2011, Johnson et al. 2005). The technique combines physical separation of chemical molecules by liquid chromatography (LC) with mass analysis by mass spectrometry (MS) of proteins previously fragmented by enzymatic digestion (Glish and Vacher, 2003). LC generates a peptide fragmentation pattern, and MS allows sensitive peptide detection based on molecular mass and particle charge once peptides are ionized with electron beams that render the peptides positively charged. After ionization, molecules are separated according to their mass-to-charge ratio by means of electromagnetic fields in a built-in analyser. MS includes ion detectors that allow protein identification at the same time as protein quantification. The resulting MS data can be further analysed with Mascot software, a database that further identifies proteins according to their peptides' molecular weight patterns and amino acid sequences. The end result is a list of proteins with an assigned

accession number and corresponding chemical names (Arpino, 1992, Glish and Vacher, 2003).

In past investigations, we examined the CSF protein profile in normal and hydrocephalic fetal rodents using LCMS followed by Mascot software for identification of proteins related to the folate metabolic cycle. Deficiencies in folate enzymes and folate transporters in the brain are linked to neural tube defects and severe developmental regression (Antony, 2007 and Steinfeld et al. 2009). In our previous study, two lists of proteins were generated by LCMS, one corresponding to normal CSF and a second one corresponding to abnormal CSF. The LCMS protein profile analysis gave evidence of differences in CSF composition between normal and hydrocephalic CSF. These differences were clear in terms of folate enzymes where hydrocephalic CSF appeared to be devoid of the enzyme formyl-tetrahydrofolate dehydrogenase, a key enzyme in the folate metabolic cycle involved in the production of tetrahydrofolate (THF) from formyl-tetrahydrofolate. THF is crucial in brain development as this co-enzyme, which is at the core of the folate metabolic cycle, is responsible for the synthesis of the methyl donor S-adenosyl-L-methionine (SAM). SAM is responsible for more than 100 metabolic reactions in the body and it is crucial for DNA methylation and production of methionine (Mischoulon and Maurizio, 2002); hence the importance of maintaining normal concentrations of FDH in CSF for the correct development of the fetal brain.

In the present study, we focus not only on folate enzymes but on the global protein profile obtained previously from LCMS analysis of CSF. Thus, all LCMS datasets were first grouped using the Microsoft Excel in order to filter the information and to identify differences between normal and hydrocephalic CSF. Each LCMS listed protein

corresponding to normal and hydrocephalic CSF respectively was allocated an identification number used for later comparison searches in the LCMS lists. Normal protein identification numbers which were missing in abnormal CSF were assigned a specific value that was later captured by means of the Excel tool autofilter. The Excel analysis resulted in two protein profiles, one representing exclusively proteins found in normal CSF, and a second list representing the proteins exclusively found in hydrocephalic CSF. Proteins common to normal and hydrocephalic CSF were excluded. In the present study we also carried out a further analysis of LCMS protein profiles utilizing a bioinformatic tool called Ingenuity Path Analysis (IPA). IPA creates associations between the proteins identified by LCMS and the metabolic pathways where related proteins may fall.

We speculate that proteins present in abnormal CSF but missing in normal CSF may be potential biomarkers of congenital hydrocephalus. Thus, a comparative analysis was performed in order to determine the specific metabolic pathways represented in the normal CSF and abnormal CSF. IPA differential metabolic pathway identification for normal and hydrocephalic CSF implied, in our opinion, the activation of genes involved in the metabolic pathways found by IPA, and downregulation of the genes that passed undetected.

IPA analysis is based on p-value measurements for a given process. These are calculated taking into account the specific number of genes found in our dataset, which are known to be linked to that process, and a reference total set of genes recognized by IPA databases as part of biological processes associated to the specific canonical pathway ([www.ingenuity.com](http://www.ingenuity.com)). Therefore, on this occasion, the p-value is a measure of the



probability that the IPA relationships between LCMS focus genes and a given metabolic pathway or biological process is due only to random chance.

In conclusion, we performed IPA analysis to identify genes which are not represented in hydrocephalic CSF, as they may be indicative of inactivation of specific metabolic routes. On the other hand and regarding the genes exclusively detected in hydrocephalic CSF, we propose that they must be activated, thus explaining their absence in normal CSF. Based on these assumptions, the aim of this study is to discover the canonical pathways and associated biological processes that are suspected to be active in abnormal CSF in contrast with normal CSF, and to shed some light on the complex pathology of a disorder which is still not fully understood. We also intend to draw attention to aspects of the disorder other than the impairment of the folate metabolic cycle and contribute to the identification of biomarkers and novel drugs for a better treatment and prevention.

## **4.2 MATERIAL AND METHODS**

### **4.2.1. EXCEL analysis**

LCMS protein profile analysis was performed as described by Nabiuni and colleagues in 2009. LCMS protein lists corresponding to normal and abnormal CSF respectively were entered into EXCEL spreadsheets. The analysis started with the assigning of a specific numerical value to each protein within the protein list pertaining to normal CSF (reference list). For instance, protein A was given the value “1” in order to identify it in the list of proteins representing abnormal CSF, if present. Of notice, the assigned number also gives information about order and position in the list. When a protein is missing in the abnormal CSF a, “-1” value is assigned, which means “error”. This is achieved by using the “if error” formula. This formula allows the error to be tracked, and a “-1” number will be displayed in the cell. Therefore, proteins that do not match between lists i.e. proteins missing will have the value “-1”. The command “autofilter” was also used to select the proteins to be displayed. For example, we can obtain a list with all proteins missing in abnormal CSF by “autofiltering” all cells that contain values other than “-1” in the list of proteins from normal CSF (reference list). Three lists of proteins were obtained using the corresponding “autofilters”: list of proteins unique to normal CSF, proteins unique to abnormal CSF and list of common proteins for both normal and abnormal CSF.

#### 4.2.2 LCMS protein analysis.

The majority of diseases and biological processes manifest at the protein level. Since there is not always a good correlation between protein and gene expression, protein expression profiles produced by LCMS technology can be useful as an alternative and complementary approach to genomics (Wang 1999, Uriarte 2008, Dai et al. 2009).

Past studies in our laboratory showed that LCMS is a suitable tool for identification of protein sequences in normal and hydrocephalic CSF using Mascot search software for the MS data. This computer program integrates data based on molecular weight and amino acid sequence, and specific fixed modifications (Carbamidomethyl of C) and variable modifications (Oxidation of M) were considered in the Mascot search engine for protein identification. A confidence limit was also chosen based on the peptide fragmentation pattern obtained after previous enzymatic digestion of every single protein, as well as the unequivocal identification of every peptide fragment (Glish and Vachet, 2003). The LCMS data obtained after Mascot search consisted of two lists of proteins, corresponding to normal and abnormal CSF respectively. Each identified protein was accompanied by its equivalent accession numbers and biochemical name (Nabiuni 2006). Both lists of proteins were contrasted, and special attention was given to proteins involved in the folate metabolic cycle and present in normal CSF but absent in abnormal CSF. The logic behind this approach was decided on the basis that folates played a vital role in the development of the cerebral cortex in Texas rats. Past studies, demonstrated how CSF enriched with thymidine (nucleoside), and folates (THF and folic acid) significantly encouraged cerebral cortex cell proliferation “in vivo” (Cain et al 2009) reducing, hereby, the

incidence of congenital hydrocephalus. On this scenario, this study concentrates on investigating the composition of hydrocephalic CSF in contrast to normal CSF in order to investigate what proteins and associated metabolic pathways are missing in CSF, but present in normal CSF, and vice versa.

#### 4.2.3 IPA analysis.

Ingenuity path analysis (IPA) is a bioinformatic tool that makes use of databases containing the knowledge available in the literature about protein and gene information, as well as protein-protein and protein-gene interactions. IPA analysis needs list of proteins with recognizable identifiers or accession numbers, and match the protein identification number with the gene accession number. After protein-gene matching, the IPA tool performs a core analysis to predict what proteins/genes are associated with a specific biological function or disease, and with canonical pathways ([www.ingenuity.com](http://www.ingenuity.com)) The greater the number of proteins associated to a specific biological function, the greater the possibility of that function being activated. However, the predictive value of the IPA tool is low, and does not give any information about the directionality of the activated process, unless it is accompanied by gene or protein quantification. Nevertheless, protein expression profiling lists produced by LCMS can be uploaded to the IPA server. Lists of proteins can then be core analysed as a starting point in any research that aims to predict the molecular interactions between proteins, and its involvement and association with specific cell functions or diseases (Calvano et al. 2005, Dai et al. 2009).

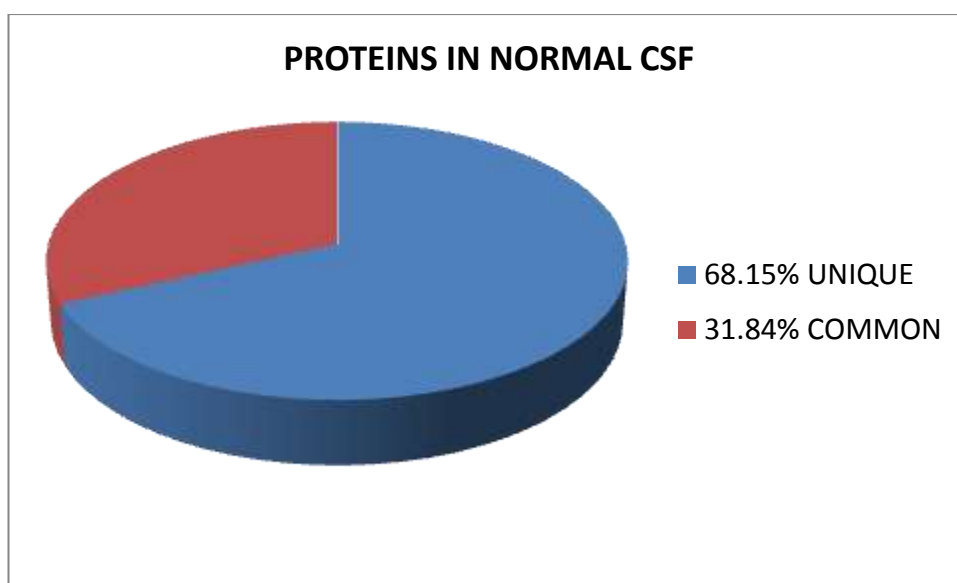
A global canonical pathway analysis (GCP) was carried out on EXCEL categories (protein lists). P-value measurements obtained from GCP analysis were equivalent to the relationships found between related genes in the EXCEL categories and their associated metabolic pathways or biological processes. The greater the number of genes involved in a pathway or process, the more likely it is that the association between focus genes and metabolic pathway is not due to mere chance. P-values were calculated using the right-tailed Fisher Exact Test, which is already built into the IPA software. P-values less than

0.05 mean results are statistically significant and non-randomly associated. Ratios are also calculated by IPA, and represent the number of molecules found in a metabolic pathway in relation to the total number of molecules included in the metabolic pathway. A threshold ratio  $\geq 0.1$  is normally chosen, and the higher ratio value is 1.

## 4.3 RESULTS

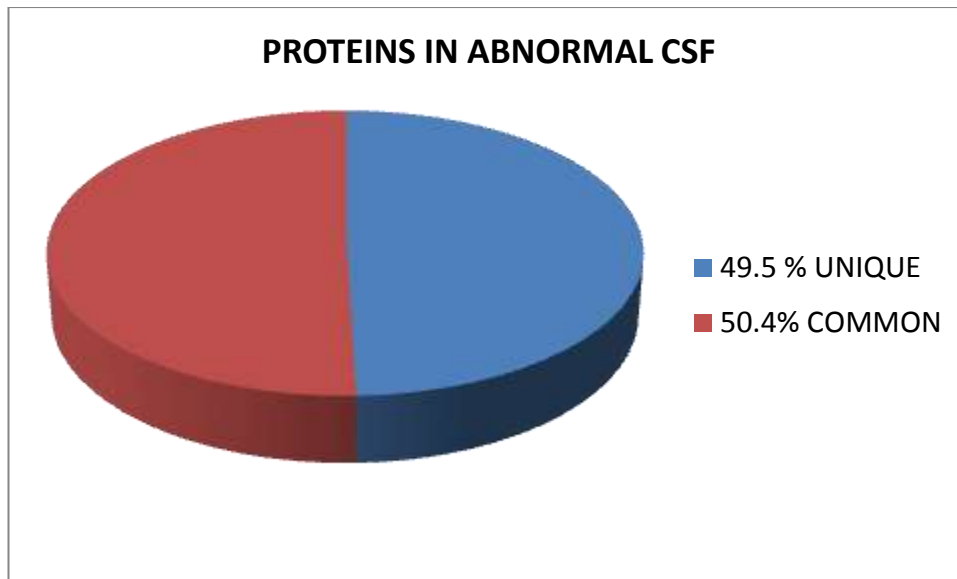
### 4.3.1 EXCEL analysis

A total number of 1036 proteins in normal CSF, previously identified by LCMS, were included in the EXCEL analysis. This analysis showed that only 31.84% of proteins were common to abnormal CSF whilst 68.15% were unique to normal CSF (Figure 4.1).



**Figure 4.1. Percentage of proteins presents only in normal CSF versus percentage common to abnormal CSF.**

In contrast, EXCEL analysis demonstrated that the LCMS protein profile from abnormal CSF analysis included a total number of 959 proteins presenting a higher content in proteins common to normal CSF (50.4%) when compared to normal CSF (31.84%). Further, the number of unique proteins to abnormal CSF was smaller with 49.5% of proteins unique to abnormal CSF versus 68.15% found in the normal CSF, (Figure 4.2).



**Figure 4.2. Percentage of protein presents only in abnormal CSF versus percentage common to abnormal CSF.**

Two lists of proteins were produced by EXCEL analysis. They are shown in table 4.1 and table 4.2. Table 4.1 represents proteins found in normal CSF only whereas table 4.2 indicates proteins only found in abnormal CSF. Table 4.1 shows 1036 proteins unique to normal/control CSF out of 1520 total number of proteins analysed. On the other hand, table 4.2 shows how only 475 proteins were unique to abnormal CSF out of 959 total numbers of proteins analysed from abnormal CSF. All tables describe accession numbers (Swisspro database) followed by their chemical names.



**TABLE 4.1. Proteins in normal CSF not present in abnormal CSF**

<b>PROTEIN ID</b>	<b>CHEMICAL NAME</b>
Q9QUT6	Beta 1 globulin - Rattus sp.
Q9QW91	Beta 2 globulin.- Rattus sp.
A25747	haemoglobin beta III-1/III-2 chain - rat
S00840	Haemoglobin beta chain. minor - rat
Q91V15	Alpha-2-globin chain (2-alpha globin).- Rattus norvegicus - (Rat).
Q80XV2	Alpha-globin (Fragment).- Rattus sp.
AAA40756	RAT Apolipoprotein E gene, complete CDS - Rattus norvegicus
AAC60703	S76779 NID: - Rattus sp.
B90284	haemoglobin alpha-2 chain - rat (tentative sequence) (Fragments)
BAA01101	RATBSP NID: - Rattus norvegicus
AAF63196	AF227534 NID: - Rattus norvegicus
A36579	inositol 1,4,5-triphosphate receptor 1 - rat
AAF07822	AF138789 NID: - Rattus norvegicus
AAR95660	AY480027 NID: - Rattus norvegicus
AAR95665	AY480032 NID: -Rattus norvegicus
BAA32699	AB008551 NID: - Rattus norvegicus
AAH62238	BC0662238 NID: - Rattus norvegicus
S53611	MIBP1 protein - rat
AAG28596	AF225960 NID: - Rattus norvegicus
A24903	tubulin alpha-1 chain - Chinese hamster
Q923K6	Calcium channel isoform alpha1E7.- Rattus norvegicus - (Rat).
P70570	Laminin-5 alpha 3 chain.- Rattus norvegicus - (Rat).
A60560	formyltetrahydrofolate dehydrogenase (EC 1.5.1.6) Rat

AAQ02380	AY238344 NID: - Rattus norvegicus
Q99P38	Synaptotagmin VIII - Rattus norvegicus - (Rat).
Q810E4	ATP-binding cassette protein C1.- Rattus norvegicus - (Rat).
K6PF RAT	6-phosphofructokinase, muscle type (EC 2.7.1.11) (Phosphofructokinase 1)
Q9QYE7	Alpha D integrin.- Rattus norvegicus - (Rat).
KGRTT1	T-kininogen I precursor- rat
A35007	ATP citrate (pro-S)-lyase (EC 4.1.3.8) - rat
Q9JIF2	Kalirin-9a.- Rattus norvegicus - (Rat).
CAE83934	BX883042 NID: - Rattus norvegicus
AAR89949	AY499658 NID: - Rattus norvegicus
Q8CG09	Multidrug resistance-associated protein 1.- Rattus norvegicus - (Rat).
CHRTM1	Sodium channel protein mu1 alpha chain. skeletal muscle - rat
Q811U3	CAST2.— Rattus norvegicus - (Rat).
Q9QUG4	ATPase 7B.- Rattus norvegicus - (Rat).
AAA42014	RATRBB1 NID: - Rattus norvegicus
A45386	omega-conotoxin-sensitive calcium channel alpha-1 subunit rbB-I - rat
AAQ96221	AY383663 NID: - Rattus norvegicus
AAS90634	AY530298 NID: - Rattus norvegicus
Q9ERH3	TGF-beta resistance-associated protein.- Rattus norvegicus - (Rat).
Q7TP24	Bal -667.- Rattus norvegicus - (Rat).
AAD41775	AF121217 NID: - Rattus norvegicus

T32731	PAR interacting protein - rat
Q63581	Rat T-kininogen (T-KG) - Rattus norvegicus - (Rat).
O70611	Rat skeletal muscle type I voltage-gated sodium channel (rSkM1 ) variant.
AAG35188	AF290214 NID: — Rattus norvegicus
BAB78470	AB049473 NID: - Rattus norvegicus
AAQ96270	AY383712 NID: - Rattus norvegicus
AAF61375	AF133301 NID: - Rattus norvegicus
A53165	dynamin II isoform aa - rat
CAA10946	RNDPDELTA NID: - Rattus norvegicus
T17101	probable voltage-activated cation channel - rat
QTP75	Aa2-066.- Rattus norvegicus - (Rat).
AAR23149	AY462245 NID: - Rattus norvegicus
OYRTHX	Heat-stable enterotoxin receptor precursor - rat
AAS66223	AY539883 NID: - Rattus norvegicus
AAD04569	AF102855 NID: - Rattus norvegicus
AAO74586	AY188179 NID: - Rattus norvegicus
Q7TPL1	Ac1-163.- Rattus norvegicus - (Rat).
A49128	cell-fate determining gene Notch2 protein - rat
AAF61445	AF139055 NID: - Rattus norvegicus
ATB3 RAT	Plasma membrane calcium-transporting ATPase (EC 3.6.3.8) (PMCA3)
AAC68900	AF086624 NID: - Rattus norvegicus
AAB39764	RATADCYA NID: - Rattus norvegicus

A32827	fetuin precursor- rat
CAE83998	BX883046 NID: - Rattus norvegicus
T42216	multidrug resistance-associated protein homolog MLP-1 - rat
ATRTC	actin beta - rat
AAC52782	RNU67309 NID: - Rattus norvegicus
AAA41713	RATNMCA2C NID: - Rattus norvegicus
CAE83981	BX883045 NID: - Rattus norvegicus
O54892	Mutant type II hexokinase. - Rattus norvegicus - (Rat).
BAA07283	RATRCACN4B NID: - Rattus norvegicus
BAB61904	AB053447 NID: - Rattus norvegicus
A34736	nestin - rat
WNK4 RAT	Serine/threonine-protein kinase WNK4 (EC 2.7.1.37)
AAD42975	AF159046 NID: - Rattus norvegicus
Q99P37	Synaptotagmin VIIa.- Rattus norvegicus - (Rat).
A45669	neurofilament triplet M protein - rat
BAA13016	D86086 NID: - Rattus norvegicus
HHRT60	chaperonin groEL precursor - rat
BAA02499	RATNMDARC NID: - Rattus norvegicus
T140050	protein kinase (EC 2.7.1.37) beta. myotonic dystrophy-associated - rat
CAF33425	AJ629845 NID: - Rattus norvegicus
AAS66670	AY548105 NID: - Rattus norvegicus
AAQ67738	AY357891 NID: - Rattus norvegicus
T17198	CL3BA protein - rat

Q7TP27	Bal 651. - Rattus norvegicus
SUIS RAT	Sucrase-isomaltase, intestinal Contains: sucrase (EC 3.2.1.48)
A345439	myosin I Heavy chain - rat
AAS66285	AY539945 NID: - Rattus norvegicus
A41541	adenylate cyclase (EC 4.6.1.1) II - rat
SYJ1 RAT	Synaptojanin 1 (EC 3.1.3.36)
Q9ERQ2	ABC50 (Fragment).- Rattus norvegicus - (Rat).
T43275	neurabin - rat
AAN72415	AY149995 NID: - Rattus norvegicus
AAD16999	AF110477 NID: - Rattus norvegicus
O88421	Voltage-gated sodium channel variant rPN4a.- Rattus norvegicus - (Rat).
O08562	voltage-dependent sodium channel PN1 (Fragment).- Rattus norvegicus - (Rat).
AAS45402	AY535015 NID: - Rattus norvegicus
AAS65873	AY555273 NID: - Rattus norvegicus
CAA44680	RNFASDNA NID: - Rattus norvegicus
CAA31780	RNFAS NID: - Rattus norvegicus
AAQ05020	AF466694 NID: -Rattus norvegicus
Q99P36	Synaptotagmin VIIb.- Rattus norvegicus - (Rat).
A41015	Dihydrolipoamide S-succinyltransferase (EC 2.3.1.61) precursor - rat
T14324	alpha-latrotoxin receptor, Calcium-independent - rat
Q9R1R4	Tudor repeat associator with PCTAIRE 2.- Rattus norvegicus - (Rat).

AAR16316	AE017191 NID: - Rattus norvegicus
AAA41490	L29429 NID: - Rattus norvegicus
AAN75376	AY149902 NID: - Rattus norvegicus
CAE84039	BX883048 NID: - Rattus norvegicus
T31669	neural zinc finger protein MyT3 - rat
S65440	Nitric-oxide synthase (EC 1.14.13.39) - rat
AAB06393	RNU59245 NID: - Rattus norvegicus
AAC52946	RNU70050 NID: - Rattus norvegicus
AAA74950	RNU314663 NID: - Rattus norvegicus
S46264	microtubule-associated protein - rat
A41939	G protein-coupled glutamate receptor - rat
AAR95632	AY435131 NID: -Rattus norvegicus
Q7TT47	Paraplegin.- Rattus norvegicus - (Rat).
AAR95630	AY435129 NID: - Rattus norvegicus
Q35774	75 kDa fibrous sheath protein, - Rattus norvegicus
AAO18238	AY187039 NID: - Rattus norvegicus
AAC37646	RATNR2DA NID: Rattus norvegicus
JC4166	Protein tyrosine kinase (EC 2.7.1.112) tyro3 precursor - rat
S46217	Protein tyrosine-phosphatase (EC 3.1.3.48). Type sigma precursor - rat
AAO38858	AY192567 NID: - Rattus norvegicus
Q8CJG5	DLST dihydrolipoamide succinlytransferase. exon I5 and complete cds.- (Rat).
Q9WV40	Munc13-2 protein.- Rattus norvegicus - (Rat).

Q63557	Fatty acid Synthase Rattus norvegicus - (Rat).
BAA12319	RATNAP1P NID: - Rattus norvegicus
CAA60264	RNFLFIB NID: - Rattus norvegicus
A31887	testosterone 7alpha-monooxygenase (EC 1.4.14.-) cytochrome P450 2A2 - rat
AAF62176	AF247453 NID: - Rattus norvegicus
A34337	propionyl-CoA carboxylase (EC 6.4.1.3) alpha chain precursor - rat (fragment)
CAE83972	BX883045 NID: - Rattus norvegicus
Q91ZD9	Synaptojanin 2B1- Rattus norvegicus - (Rat).
AAD24587	AF136943 NID: - Rattus norvegicus
CAA50871	RNMYR4 NID: - Rattus norvegicus
JC2486	3',5'-cyclic-nucleotide phosphodiesterase (EC 3.1.4.17). cGMP- stimulated - rat
AAL78956	AF455050 NID: - Rattus norvegicus
Q8CIN3	Receptor-like protein tyrosine phosphatase gamma A-type isoform.- Rat
CAB09536	RNZ96106 NID: - Rattus norvegicus
AAF81653	AF199331 NID: - Rattus norvegicus
AAR89918	AY496443 NID: - Rattus norvegicus
T31673	N-acetylglucosaminyltransferases (EC 2.4.1.-). chain p1 10 - rat
BAA06340	RATACYLCOA NID: - Rattus norvegicus
JC5028	nitric-oxide synthase (EC 1.14.13.39) L - rat
Q9JHS0	Conjugate export pump protein (Fragment).- Rattus norvegicus -

	(Rat).
Q8JZS5	Filamin-interacting protein S-FILIP.- Rattus norvegicus - (Rat).
AAP43670	AY211532 NID: - Rattus norvegicus
S18188	notch protein homolog, - rat
AAA18905	RATRBCII NID: - Rattus norvegicus
S58400	cellutagmin II sytVII - rat
I60598	Fit-1 tyrosine kinase receptor - rat
Q8R4C1	Putative secretory pathway Ca-ATPase SPCA2.- Rattus norvegicus - (Rat).
CAC07697	Sequence 1 from Patent WO9947670.- Rattus norvegicus - (Rat).
D3HI RAT	3-hydroxyisobutyrate dehydrogenase. mitochondrial precursor (EC 1.1.1.31)
AAG17548	AF218826 NID: - Rattus norvegicus
AAQ94494	AY394725 NID: - Rattus norvegicus
AAR95631	AY435130 NID: - Rattus norvegicus
AAA40678	RATADCYB NID: - Rattus norvegicus
AAB63955	RATMATRIN3 NID: - Rattus norvegicus
AAA02857	RATNIIIA NID: - Rattus norvegicus
S54357	plasma membrane Ca <sup>2+</sup> -ATPase isoform 4 rat
BAA28174	AB001453 NID: - Rattus rattus
JS0306	microtubule-associated protein tau - rat
Q8R4D0	RNA-binding protein staufen splice form A. - Rattus norvegicus - (Rat).
AAA02874	RATGLUR52A NID: -Rattus norvegicus



AAD53121	AF176688 NID: -Rattus norvegicus
S19808	glutamate receptor GluR5-1 chain precursor - rat
A38306	alpha-mannosidase (EC 3.2.1.24) - rat
AAH61793	BC061793 NID: - Rattus norvegicus
AAA41030	RATCYP45F NID: - Rattus norvegicus
Q8K1M7	BMP retinoic acid-inducible neural-specific protein-3 - Rattus norvegicus
BAA07504	RATF3A NID: - Rattus norvegicus
CAA11465	RNO223599 NID: - Rattus norvegicus
BAA88897	AB020209 NID: - Rattus norvegicus
NOS2 RAT	Nitric oxide synthase, inducible (EC 1.14.13.39) (NOS, type II)
S37032	gene LL5 protein - rat
AAB37571	RNU61266 NID: - Rattus norvegicus
Q9R0L5	TIP120-family protein TIP120B.- Rattus norvegicus - (Rat).
AAP72019	AY237644 NID: - Rattus norvegicus
Q8CF82	ATP-binding cassette protein 5.- Rattus norvegicus - (Rat).
Q63724	Microtubule-associated protein 2.- Rattus rattus (Black rat).
BAA013138	RATVSMNOS NID: - Rattus norvegicus
AAC53338	AF016297 NID: - Rattus norvegicus
AAD30271	AF127798 NID: - Rattus norvegicus
Q8VHE9	Hypothetical protein.- Rattus norvegicus - (Rat).
AAS66226	AY539886 NID: - Rattus norvegicus
AAA84964	RNU38179 NID: - Rattus norvegicus
AAS66282	AY539942 NID: - Rattus norvegicus

BAA02500	RATNMDARD1 NID: - Rattus norvegicus
S57833	transmembrane protein HEM2 - rat
AAP82454	AY330294 NID: - Rattus norvegicus
CAE83957	BX883044 NID: - Rattus norvegicus
AAR95633	AY435132 NID: - Rattus norvegicus
CGRT1S	collagen alpha 1(I) chain - rat (tentative sequence) (fragments)
CA11 RAT	Collagen alpha 1(I) chain (Fragments) -Rattus norvegicus
AAD42976	AF159047 NID: - Rattus norvegicus
T14124	neural zinc finger factor 3 - rat
BAD15356	AB176831 NID: - Rattus norvegicus
AAF81646	AF199324 NID: - Rattus norvegicus
AAA70429	RAT10HCO NID: Rattus norvegicus
PIB4 RAT	1-phosphatidylinositol-4,5-bisphosphate phosphodiesterase beta 4
AAS18426	AY495696 NID: - Rattus norvegicus
A38235	microtubule-associated protein. 110K tau - rat
Q55166	ARE1-Rattus norvegicus
Q4RTV3	vitamin D3 25-monooxygenase (EC 1.14.14.-) cytochrome P450 27 precursor.
Q7TPJ1	Ac2-233 - Rattus norvegicus - (Rat).
AAQ16157	AY273816 NID: -Rattus norvegicus
P97949	TAP1 protein.- Rattus norvegicus - (Rat).
A40170	glutamate receptor A precursor- rat
Q63555	SP120.- Rattus norvegicus (Rat).
BAA07994	RATNWUT NID: - Rattus norvegicus

AAA41096	RATDPP NID: - Rattus norvegicus
Q9JMK8	Vps541-like protein.- Rattus norvegicus - (Rat)
A34272	testosterone 7alpha-hydroxylase (EC 1.14.14.-) cytochrome P4502A1 - rat
Q7TP38	Ab2-371 - Rattus norvegicus - (Rat).
JC5029	nitric-oxide synthase (EC 1.14.13.39) U - rat
JH0592	glutamate receptor chain KA-2 precursor - rat
CAA56333	RNHEM2 NID: - Rattus sp.
AAS18425	AY495695 NID: - Rattus norvegicus
I56555	Sodium channel protein 6 - rat
A37180	chromogranin/secretogranin-like vesicle protein precursor - rat
JC7365	septin-like protein-a - rat
AAD46653	AF164486 NID: - Rattus norvegicus
O88600	Ischemia responsive 94 kDa protein - Rattus norvegicus - (Rat).
A53588	adenylate cyclase (EC 4.6.1.1) VIII - rat
O54728	Phospholipase B.- Rattus norvegicus - (Rat).
AAB60525	U45479 NID: - Rattus norvegicus
AAA40813	RATBG NID: - Rattus norvegicus
I57961	glucuronosyltransferase (EC 2.4.1.17) precursor - rat
A54142	nucleoporin NUP107 - rat
CAD89523	RNO557016 NID: - Rattus norvegicus
AAH61999	BC061999 NID: - Rattus norvegicus
A39914	dipeptidyl-peptidase IV (EC 3.4.14.5). membrane-bound form precursor - rat

OYRTR	atrial natriuretic peptide receptor A precursor - rat
Q9ERZ8	Vanilloid receptor-related osmotically activated channel.- Rattus norvegicus
AAD09246	RNU90725 NID: - Rattus norvegicus
Q63643	Aryl hydrocarbon receptor nuclear translocator 2 (Fragment).- Rat
AAC13318	RNU61772 NID: - Rattus norvegicus
AAQ96246	AY383688 NID: - Rattus norvegicus
AAC52693	MMU58203 NID: -Mus musculus
AAS66255	AY539915 NID: - Rattus norvegicus
O54755	MIPP65 - Rattus norvegicus - (Rat).
AAA17833	RNU08260 NID: - Rattus norvegicus
AAD50906	PAIRED 1G-LIKE RECEPTOR-A2.- Rattus norvegicus - (Rat).
AAO91938	AY191271 NID: - Rattus norvegicus
JC4391	pyruvate carboxylase (EC 6.4.1.1) precursor - rat
AAF25004	AF156982 NID: - Rattus norvegicus
Q9QW24	TIE-2 =RECEPTOR-like tyrosine kinase - Rattus sp.
Q9EPI7	Putative MAGE-like protein.- Rattus norvegicus
AAQ88212	AY382879 NID: - Rattus norvegicus
AAH59165	BC059165 NID: - Rattus norvegicus
AAH61865	BC061865 NID: - Rattus norvegicus
CAE83974	BX883045 NID: - Rattus norvegicus
AAA40844	RATCACAI NID: - Rattus norvegicus
BAC36835	AK077507 NID: - Mus musculus
S70642	ubiquitin ligase Nedd4 - rat (fragment)

Q7TSP2	Kinesin-like protein KIF15.- Rattus norvegicus - (Rat).
JC6124	diacylglycerol kinase (EC 2.7.1.107) IV - rat
AAB96342	RNU82626 NID: - Rattus norvegicus
S68443	double-stranded RNA-specific adenosine deaminase (EC 3.5.4.-) - rat
Q923K9	APOBEC-1 complementation factor long isoform.- Rattus norvegicus - (Rat).
AAA41240	RATGLUR2A NID: - Rattus norvegicus
AAD34012	AF149118 NID: - Rattus norvegicus
PLD1 RAT	Phospholipase D1 (EC 3.1.4.4) (PLD 1) (Choline phosphatase 1)
T13725	phospholipase D (EC 3.1.4.4) 1a - rat
A24600	glucuronosyltransferase (EC 2.4.1.17) precursor - 3-methylcholanthrene-inducible
Q63283	LMW T-kininogen I.- Rattus norvegicus - (Rat).
A57112	contactin precursor - rat
T17199	CL3BB protein - rat
CAB44314	RNO131899 NID: - Rattus norvegicus
AAB96356	RNU40603 NID: - Rattus norvegicus
Q8VD43	UDP-glucuronosyltransferase 1A7.- Rattus norvegicus - (Rat).
AAC33405	RNU95177 NID: - Rattus norvegicus
P97561	Tap1 protein.- Rattus norvegicus - (Rat).
Q925T1	RGPR-p1I7.- Rattus norvegicus - (Rat).
AAH61722	BC061722 NID: - Rattus norvegicus
CAA09720	RNO011605 NID: - Rattus norvegicus

AAC33291	AF083330 NID: - Rattus norvegicus
Q7TQP6	Cardiac ankyrin repeat kinase.- Rattus norvegicus - (Rat).
S13426	multidrug resistance protein homolog - rat
AAH61738	BC061738 NID: - Rattus norvegicus
AAF81655	AF199333 NID: - Rattus norvegicus
O88763	phosphatidylinositol 3-kinase Rattus norvegicus - (Rat).
NAL6 RAT	NACHT-. LRR- and PYD-containing protein 6
Q9R174	Glutamate receptor subunit GluR2-flip precursor - Rattus norvegicus - (Rat).
B28065	Ca <sup>2+</sup> transporting ATPase (EC 3.6.3.8) 2 - rat
GEPH RAT	Gephyrin (Putative glycine receptor-tubulin linker protein).- Rat
Q91XQ4	Putative ionotropic glutamate receptor GLURR-F11694B.- Rat
Q9JE0	MHC class II transactivator type I.- Rattus norvegicus - (Rat).
BAA12144	D83948 NID: - Rattus norvegicus
A44097	methylmalonate-semialdehyde dehydrogenase (acylating) (EC 1.2.1.27) - rat
AAA02853	RATNIIIA NID: - Rattus norvegicus
A29953	alpha-I proteinase inhibitor III. hepatic clone AF7 - rat (fragment)
AAF81644	AF199322NID: - Rattus norvegicus
T00025	PSD-95 binding protein - rat
Q9R0T3	Protein kinase Inhibitor p58.- Rattus norvegicus (Rat).
JC6329	yeast secretory protein homolog rsec6/8 complex - rat
BAA09460	RATTESK1B NID: - Rattus norvegicus
BAA23672	D89093 NID: - Rattus norvegicus

AAD16009	AF120492 NID: - Rattus norvegicus
Q9JL97	GPI-anchored ceruloplasmin.- Rattus norvegicus - (Rat).
A39667	brain-derived neurotrophic factor receptor precursor - rat
Q8VD44	UDP-glucuronosyltransferase 1A8.- Rattus norvegicus - (Rat).
S34719	haemoglobin beta-2.0 chain - rat
AAH58502	BC058502 NID: - Rattus norvegicus
JC5953	inter-alpha-inhibitor HP4 heavy chain - rat
AAS21244	AY462092 NID: - Rattus norvegicus
AAR01113	AY333961 NID: - Rattus norvegicus
AAK56958	AF375463 NID: - Rattus norvegicus
S41067	collagen alpha 1(III) chain - rat
Q9R0W3	Plasminogen protein precursor (EC 3.4.21.7).- Rattus norvegicus - (Rat).
AAS66221	AY539881 NID: - Rattus norvegicus
AAR95634	AY435133 NID: - Rattus norvegicus
A53731	translation initiation factor eIF-2 alpha chain kinase (EC 2.7.1.-) - rat
CAA90600	RNPTPASE NID: - Rattus norvegicus
BAA23523	AB008803 NID: - Rattus norvegicus
BAA75254	AB011821 NID: - Rattus norvegicus
S01713	tubulin beta-7 chain - chicken
A35781	hippocampus-derived neurotrophic factor precursor - rat
Q924K3	APOBEC-1 complementation factor short isoform.- Rattus norvegicus - (Rat).

AAB09537	RNU63288 NID: - Rattus norvegicus
Q35850	Carboxypeptidase D precursor- Rattus norvegicus - (Rat).
Q9JIZ3	Cenexin 2.- Rattus norvegicus - (Rat).
Q62965	Glycine-, glutamate-, thienylcyclohexylpiperidine-binding protein.- Rat
PC6300	synaptotagmin X - rat (fragment)
Q9R0L3	TIP120-family protein TIP120B, short form.- Rattus norvegicus - (Rat).
P97560	Tap1 protein.- Rattus norvegicus - (Rat).
Q8K3M6	Cytomatrix protein p110 - Rattus norvegicus - (Rat).
Q7TP87	AB1-233.- Rattus norvegicus - (Rat).
S25576	probable transport protein mt2 - rat
AAC52289	RNU24150 NID: - Rattus norvegicus
AAA63911	RATOSTP NID: - Rattus norvegicus
AAF34909	AF221622 NID: - Rattus norvegicus
Q80WI4	Phospholipase C delta.- Rattus sp.
CAA67021	RNKISRNA NID: - Rattus norvegicus
BAD05181	AB118026 NID: - Rattus norvegicus
CAB56206	RNO245646 NID: - Rattus norvegicus
I77467	serotonin receptor ID - rat
Q811A4	Procollagen-lysine, 2-oxoglutarate 5-dioxygenase 2. long variant.- Rat
AAC52207	RNU09357 NID: - Rattus norvegicus
AAQ02379	AY238343 NID: - Rattus norvegicus



B55915	guanylate cyclase (EC 4.6.1.2) 2F precursor - rat
AAA17831	RNU08258 NID: - Rattus norvegicus
BAD06369	AB113387 NID: - Rattus norvegicus
Q923K1	Sweet taste receptor T1R3.- Rattus norvegicus - (Rat).
Q62819	Aromatic L-amino acid decarboxylase - Rattus norvegicus (Rat).
AAA73342	RATALTSPLB NID: - Rattus norvegicus
AAA85463	RATVDCCA NID: - Rattus norvegicus
Q9WUF7	Hyaluronan receptor RHAMM.- Rattus norvegicus - (Rat).
Q9JJS5	SH3-domain binding protein 4.- Rattus norvegicus - (Rat).
AAQ23131	AY345164 NID: - Rattus norvegicus
BAD08353	AB116149 NID: - Rattus norvegicus
I56577	2',3'-Cyclic-nucleotide 3'-phosphodiesterase (EC 3.1.4.37) - rat
JH0422	voltage-dependent calcium channel complex. alpha-1 chain - rat
Q9ER34	Mitochondrial aconitase precursor.- Rattus norvegicus - (Rat).
AAQ96263	AY383705 NID: - Rattus norvegicus
AAA41080	RATDBP NID: - Rattus norvegicus
CAD48615	Sequence 11 from Patent WO2059612.- Rattus norvegicus - (Rat).
BAD01656	AB096213 NID: - Rattus norvegicus
CAA78936	RNGLURCA NID: - Rattus norvegicus
XORTDH	Xanthine dehydrogenase (EC 1.1.1.204) / Xanthine oxidase (EC 1.1.3.22) - rat
AAS66290	AY539950 NID: - Rattus norvegicus
TAU RAT	Microtubule-associated protein tau (Neurofibrillary tangle protein)
B28821	1-phosphatidylinositol-4.5-bisphosphate phosphodiesterase (EC

	3.1.4.11) delta-1
CAA27067	RNTUBB15 NID: - Rattus norvegicus
Q9Z1X1	GLUT4 vesicle protein.- Rattus norvegicus - (Rat).
CAA49905	RNENACA NID: - Rattus norvegicus
MOES RAT	Moesin (Membrane-organizing extension spike protein).- Rat
AJRTRS	argininosuccinate synthase (EC 6.3.4.5) - rat
I59422	rsec8 - rat (fragment)
A25113	tubulin beta chain 15- rat
AAM75358	AF521008 NID: - Rattus norvegicus
P70625	Zonula occludens 2 protein (Fragment).- Rattus norvegicus - (Rat).
T42842	bile salt transport protein. ATP-dependent - rat
AAG29823	AF304446 NID: - Rattus norvegicus
AAA41280	RATGRT NID: - Rattus norvegicus
D40170	glutamate receptor - rat
CAA07267	RNAJ6855 NID: - Rattus norvegicus
OXRTA1	acyl-CoA oxidase (EC 1.3.3.6) chain A. peroxisomal splice form 1- rat
Q9QXU8	Dynein light intermediate chain 1.- Rattus norvegicus - (Rat).
A30363	glycoprotein GP330. renal - rat (fragments)
AAC36065	AF057026 NID: - Rattus norvegicus
AAA96256	RNU32314 NID: - Rattus norvegicus
S55255	lamina-associated protein 2 - rat
AAN59930	AF548738 NID: - Rattus norvegicus
AAB47753	RNU81035 NID: - Rattus norvegicus

UD18 RAT	UDP-glucuronosyltransferase 1-8 precursor. microsomal
AAG23699	AF311311 NID: - Rattus norvegicus
BAD01114	AB119249 NID: - Rattus norvegicus
AAC33292	AF083331 NID: - Rattus norvegicus
Q9ESH7	Kinesin light Chain KLCt.- Rattus norvegicus - (Rat).
A48758	protein tyrosine-phosphatase (EC 3.1.3.48). receptor-linked form PI precursor
CAA67142	RNMME NID: -Rattus norvegicus
CAC08185	RNO293948 NID: - Rattus norvegicus
Q7TP84	Ab1 -346 - Rattus norvegicus (Rat ).
AAR20710	AY455861 NID:Rattus norvegicus
CAA35050	RNGLUR1 NID: - Rattus norvegicus
AAQ91054	AY387084 NID: - Rattus norvegicus
S15904	alpha-I proteinase inhibitor III. variant 1 precursor - rat
AAB06043	RNU58857 NID: - Rattus norvegicus
AAD10403	RNU57836 NID: - Rattus norvegicus
XNTRO	ornithine-oxo-acid transaminase (EC 2.6.1.13) precursor - rat
Q9QW67	LAR. leukocyte common antigen-related
Q8CIZ0	ERC2.- Rattus norvegicus - (Rat).
S19595	chloride channel protein - rat
A33505	somatotropin receptor precursor - rat
B48758	protein-tyrosine-phosphatase (EC 3.1.3.48). receptor-linked form PS precursor -
AAS66224	AY539884 NID: - Rattus norvegicus

JH0790	lipoprotein lipase (EC 3.1.1.34) precursor - rat
AAF74258	AF227741 NID: - Rattus norvegicus
S08211	dnaK-type molecular chaperone hst70 - rat
Q8VH46	Actin filament associated protein.- Rattus norvegicus - (Rat).
AAL84229	AF446001 NID: - Rattus norvegicus
T10811	channel associated protein of synapse 2 - rat
A39368	sterol carrier protein 2 precursor - rat
S07624	acylaminoacyl-peptidase (EC 3.4.19.1) - rat
BAA83593	AB022699 NID: - Rattus norvegicus
Q8R458	Protein kinase for Splicing component.- Rattus norvegicus - (Rat).
BAB21439	AB046442 NID: - Rattus norvegicus
AAP92621	AY325220 NID: - Rattus norvegicus
AAC33895	AF068202 NID: - Rattus norvegicus
AAA40608	RAT3H3M NID: -Rattus norvegicus
AAL27988	AF350422 NID: - Rattus norvegicus
JH0811	acetylcholinesterase (EC 3.1.1.7) catalytic chain precursor - rat
AAH34645	B034645 NID: - Mus musculus
T46635	phospholipase D (EC 3.1.4.4) 1a - rat
AAA42284	RATTRKCC NID: - Rattus norvegicus
O08721	transmembrane receptor UNC5H1.- Rattus norvegicus - (Rat).
Q9JMG8	Dihydropyrimidinase-related protein.- Rattus norvegicus - (Rat).
BAC97816	AB100356 NID: - Rattus norvegicus
AAS78929	AY533525 NID: - Rattus norvegicus
O88752	Epsilon 1 globin.- Rattus norvegicus - (Rat).

BAA13413	D87515 NID: - Rattus norvegicus
Q9R1L1	NBC-like protein 3.- Rattus norvegicus
AAA41625	RATMLCK NID: -Rattus norvegicus
BAA09091	RATCLC5 NID: - Rattus norvegicus
AAB71745	RNU76206 NID: -Rattus norvegicus
CAE83966	BX883044 NID: - Rattus norvegicus
AAB48046	RNU88294 NID: - Rattus norvegicus
BAB23530	AK004749 NID: - Mus musculus
Q8CG07	Werner syndrome-interacting protein-like protein. - Rattus norvegicus - (Rat).
RIN1 RAT	Ras and Rab interactor 1 (Rat interaction/interference protein 1).- Rat
AAB58256	RNU80076 NID: - Rattus norvegicus
AAS66220	AY539880 NID: - Rattus norvegicus
BAD13422	AB126168 NID: - Rattus norvegicus
BAB19011	AB052294 NID: - Rattus norvegicus
Q80Z07	ATP-binding cassette protein 5.- Rattus norvegicus - (Rat).
AAL73196	AF335505 NID: - Rattus norvegicus
CAC21554	RNO298278 NID: - Rattus norvegicus
SI3064	1D-myo-inositol-trisphosphate 3-kinase (EC 2.7.1.127) A - rat
AAD52710	AF121893 NID: - Rattus norvegicus
AAN64275	AY145899 NID: - Rattus norvegicus
BAA90553	AB032551 NID: - Rattus norvegicus
O70408	Outer dense fiber protein ODF84.- Rattus norvegicus - (Rat).

AAA41392	RATIGFIRT NID: - Rattus norvegicus
AAL84222	AF445994 NID: - Rattus norvegicus
AAB86910	RNU69550 NID: - Rattus norvegicus
AAP82452	AY330292 NID: - Rattus norvegicus
MLRS RAT	Myosin regulatory light chain 2, skeletal muscle isoform
Q811M5	Complement factor 6.- Rattus norvegicus - (Rat).
AAC52849	RNU55836 NID: - Rattus norvegicus
A44839	glutamate receptor 4c - rat
AAH67245	BC067245 NID: - Rattus norvegicus
AAA83235	RNU40652 NID: - Rattus norvegicus
RIP1 RAT	Peripheral-type benzodiazepine receptor-associated protein 1
Q9JLS3	Serine/threonine protein kinase TAO2.- Rattus norvegicus - (Rat).
A35956	thyrotropin receptor - rat
A42497	anion exchanger 3, cardiac splice form - rat
AAP42419	AY208851 NID: - Rattus norvegicus
T08423	Axin homolog Axil - rat
CAE83959	BX883044 NID: - Rattus norvegicus
OXRTA2	acyl-CoA oxidase (EC 1.3.3.6) chain A, peroxisomal Splice form II rat
S02003	neurofilament triplet H protein - rat (fragment)
S40482	serine/threonine-specific protein kinase (EC 2.7.1.-) - rat
AAB03365	RNU08136 NID: - Rattus norvegicus
AAD25916	AF072509 NID: - Rattus norvegicus
AAF05769	AF194371 NID: - Rattus norvegicus

AAA88511	RATP4502A3 NID: -Rattus norvegicus
AAD22522	AF091457 NID: - Rattus norvegicus
AAA41457	RATITK NID: - Rattus norvegicus
AAF70456	AF221952 NID: - Rattus norvegicus
Q811X6	CRY - Rattus norvegicus - (Rat).
A48801	2-hydroxyacylsphingosine 1-beta-galactosyltransferase (EC 2.4.1.45) precursor
O54858	Carboxypeptidase Z.- Rattus norvegicus - (Rat).
BAD11366	AB162856 NID: - Rattus norvegicus
A34307	Ca <sup>2+</sup> transporting ATPase (EC 3.6.3.8) - rat
Q7TMR7	Monocarboxylate transporter 7B splice variant.- Rattus norvegicus - (Rat).
Q91XJ3	IIIG9 long form.- Rattus norvegicus - (Rat).
AAC19367	AF067793 NID: - Rattus norvegicus
CAA39884	RNNG2 NID: - Rattus norvegicus
JC2447	carboxylesterase (EC 3.1.1.1) ES-3 precursor - rat
AAB05930	RNU63971 NID: - Rattus norvegicus
S28857	glutamate receptor delta-1 chain precursor- rat
AAP82451	AY330291 NID: - Rattus norvegicus
P97559	Tap1 protein.- Rattus norvegicus - (Rat).
PN0473	valine-tRNA ligase (EC 6.1.1.9) - rat (fragment)
CAD54073	RNO511273 NID: - Rattus norvegicus
Q8K1M8	BMP/retinoic acid-inducible neurai-specific protein-2 - Rattus norvegicus

Q9Z2J3	S-nexilin.- Rattus norvegicus - (Rat).
Q9Z2J4	F-actin binding protein b-Nexilin.- Rattus norvegicus - (Rat).
BAA25987	D82883 NID: - Rattus norvegicus
AAB24228	S48813 NID: - Rattus sp.
A42764	Ca <sup>2+</sup> transporting ATPase (EC 3.6.3.8) - rat
JH0527	carbonate dehydratase (EC 4.2.1.1) II - rat
CAA15426	RNO236911 NID: - Rattus norvegicus
A26186	pyruvate kinase (EC 2.7.1.40) isozyme M2 - rat
Q9QXF7	CYP2J4 protein.- Rattus norvegicus - (Rat).
Q7TSB4	ADAM28 isoform-1.- Rattus norvegicus - (Rat).
Q8R427	ATP-binding cassette protein Blb.- Rattus norvegicus - (Rat).
O35265	Putative pheromone receptor.- Rattus norvegicus - (Rat).
T13957	period protein PER2 - rat
BAA06170	RATP130CAS NID: - Rattus norvegicus
Q63618	Espin.- Rattus norvegicus - (Rat).
TVRTNU	protein-tyrosine kinase (EC 2.7.1.112) neu precursor - rat
Q7TNA8	Lactate dehydrogenase A-like protein.- Rattus norvegicus - (Rat).
A34164	Cholestrol monooxygenase (side-chain-cleaving)
Q7TT74	Chloride channel-isoform 5 (Fragment).- Rattus norvegicus (Rat)
ABG8 RAT	ATP-binding cassette, sub-family G. member 8 (Sterolin - 2) Rat
O88370	Phosphatidylinositol 5-phosphate 4-kinase gamma.- Rattus norvegicus - (Rat).
AAH60586	BC060586 NID: - Rattus norvegicus
AAB49519	S83279 NID: - Rattus sp.



Q920D5	Capsase-12 - Rattus norvegicus - (Rat).
AAC23707	RNU91561 NID: - Rattus norvegicus
BAA94745	AB041723 NID: - Rattus norvegicus
BAA14107	D90059S5 NID: - Rattus norvegicus
AAQ91044	AY387074 NID: - Rattus norvegicus
AAQ96248	AY383690 NID: - Rattus norvegicus
S27258	activin receptor type II - rat
Q9JKW1	TIM 22 preprotein translocase (Fragment).- Rattus norvegicus - (Rat).
S53531	gamma-aminobutyric acid beta 2 chain - mouse
BAD06375	AB113393 NID: - Rattus norvegicus
AAS78661	AY496961 NID: - Rattus norvegicus
Q91WX9	Voltage-gated calcium channel pore forming subunit CaV1. 3 alpha I - Rat
Q80W87	ROBO4.- Rattus norvegicus - (Rat).
S29509	insulysin (EC 3.4.24.56) precursor [validated] - rat
A27366	AMP deaminase (EC 3.5.4.6), skeletal muscle - rat
AAG37066	AF306546 NID: - Rattus norvegicus
C40170	glutamate receptor C precursor - rat
AAB03281	RNUS2103 NID: - Rattus norvegicus
A61208	chondroitin sulfate proteoglycan NG2 - rat
Q8CFC4	Histo-blood group ABO transferase (B blood group galactosyltransferase)
I56333	apolipoprotein B - rat (fragment)

O55007	Tulip 1.- Rattus norvegicus - (Rat).
BAA23122	AB008422 NID: - Rattus norvegicus
I58159	protein kinase C-regulated chloride channel - black rat
AAB51398	RNU93052 NID: - Rattus norvegicus
A46748	Na <sup>+</sup> /H <sup>+</sup> exchanging protein NHE-2 - rat
OYRTA1	guanylate cyclase (EC 4.6.1.2). soluble, alpha-1 chain - rat
CAA10046	RNO012482 NID: - Rattus norvegicus
Q9EQM9	Angiotensin-converting enzyme.- Rattus norvegicus - (Rat).
Q7TQ85	Ac1 164- Rattus norvegicus - (Rat).
CAA34160	RNALPH03 NID: - Rattus norvegicus
Q8R3Z7	Pincher.- Rattus norvegicus - (Rat).
1BG3A	hexokinase (EC 2.7.1.1), chain A - norway rat (fragments)
1BG3B	hexokinase (EC 2.7.1.1), chain B - norway rat (fragments)
NFAS RAT	Neurofascin precursor.- Rattus norvegicus - (Rat).
AAA41672	RATNALPH2 NID: - Rattus norvegicus
Q9JMA8	Reg receptor.- Rattus norvegicus - (Rat).
I65413	sodium-dependent neurotransmitter transporter - rat (fragment)
CAC08993	Sequence 1 from Patent WO0026348.- Rattus norvegicus
Q925T8	BMP/retinoic acid-inducible neural-specific protein.- Rattus
HCN2 RAT	Potassium/sodium hyperpolarization-activated cyclic nucleotide-gated channel
O35470	cAM P-specific phosphodiesterase.- Rattus norvegicus - (Rat).
Q9Z221	Outer dense fiber ODF3.- Rattus norvegicus - (Rat).
BAC21666	AB073215 NID: - Rattus norvegicus

A42046	surfactant protein D - rat
BAA09922	RATPBMP3 NID: - Rattus norvegicus
Q80XF7	Gap junction channel protein connexin47 (Fragment).- Rattus norvegicus - (Rat).
AAQ96245	AY383687 NID: - Rattus norvegicus
CAD13342	RNO421447 NID: - Rattus norvegicus
Q8CFG7	Calcium channel alpha-2 delta -1 subunit isoform e.- Rattus norvegicus - (Rat).
A44147	calcium channel protein alpha-2 chain precursor - rat
BAA22224	D85509 NID: - Rattus rattus
Q9ER28	Endothelial type gp91-phox.- Rattus norvegicus - (Rat).
A36121	aromatase (EC 1.14.14.-) cytochrome P450 19 - rat
JC6136	kexin-like protein convertase (EC 3.4.-.-) - rat
Q9R1Q3	Glial fibrillary acidic protein alpha.- Rattus norvegicus - (Rat).
AAA41476	RATKEX2A NID: - Rattus norvegicus
BAD06378	ABII3396 NID: - Rattus norvegicus
Q9QYJ5	PDE10A3 (EC 3.1.4.17) Rattus norvegicus - (Rat).
AAA74248	RATC1H4SY NID: - Rattus norvegicus
AAA40674	RATACTRII NID: - Rattus norvegicus
AAL84224	AF445996 NID: - Rattus norvegicus
AAQ96256	AY383698 NID: - Rattus norvegicus
EGRT	epidermal growth factor precursor - rat
TRIF RAT	Troponin I, fast skeletal muscle (Troponin I, fast-twitch isoform) - Rat

Q8VHN2	NMDA ligand-gated receptor 3B subunit.- Rattus norvegicus
Q9Z213	Hypothetical protein.- Rattus norvegicus - (Rat).
O55163	Proton-gated cation channels modulatory subunit MDEG2.- Rattus norvegicus
AAB96560	RNU95748 NID: - Rattus norvegicus
AAA56637	RNSGIII NID: - Rattus norvegicus
AAG23357	Beta ig-h3 (Fragment).- Rattus norvegicus - (Rat).
AAQ96259	AY383701 NID: - Rattus norvegicus
AAH63161	BC063161 NID: - Rattus norvegicus
B34488	calpain (EC 3.4.22.17) large chain 3 - rat
AAA41043	RATCYPA NID: - Rattus norvegicus
CAA62002	RNTSP4 NID: - Rattus norvegicus
Q7TP21	Cb1-727 - Rattus norvegicus - (Rat).
Q06884	Testosterone-6-beta hydroxylase.- Rattus norvegicus - (Rat).
C43274	N-methyl D-aspartate receptor (NMDR)
P70540	Peroxisomal multifunctional enzyme type II.- Rattus norvegicus
Q9JL4	GTP-binding protein tc10.- Rattus norvegicus (Rat ).
S00289	alkaline phosphatase (EC 3.1.3.1), hepatic precursor - rat
Q9JM01	Serine/threonine kinase NKIATRE alpha.- Rattus norvegicus
AAA99237	RATSUR NID: - Rattus norvegicus
AAG28597	AF225961 NID: - Rattus norvegicus
Q80ZE7	CD2AP/CMS.- Rattus norvegicus - (Rat).
A28166	Kupffer cell receptor - rat
CAC13969	RNO250313 NID: - Rattus norvegicus

KHRTH	cathepsin H (EC 3.4.22.16) precursor - rat
CAC13957	RNO250329 NID: - Rattus norvegicus
SYRTDT	aspartate-tRNA ligase (EC 6.1.1.12) - rat
Q9QX10	Na-K-Cl cotransporter.- Rattus norvegicus - (Rat).
JC4239	phospholipase A2-activating protein - rat
Q9EPI1	Xylosyltransferase I (EC 2.4.2.26) (Fragment).- Rattus norvegicus
KCB2 RAT	Potassium voltage-gated channel subfamily B member 2
P70539	Activin receptor-like kinase 7.- Rattus norvegicus - (Rat).
CAB61692	RNO251245 NID: - Rattus norvegicus
AAC39689	AF004563 NID: - Homo sapiens
Q9Z1Z9	LIM-domain protein LMP-1.- Rattus norvegicus - (Rat).
Q810C2	Spergen-2.- Rattus norvegicus - (Rat).
Q9ER23	RP59 protein.- Rattus norvegicus - (Rat).
CAF25053	AJ626743 NID: - Rattus norvegicus
AAF19354	AF185637 NID: - Rattus norvegicus
DIRTR1	protein-arginine deiminase (EC 3.5.3.15) 1 - rat
R5RTL7	ribosomal protein L7. cytosolic [validated] - rat
Q7TN97	Keratin 5.- Rattus norvegicus - (Rat).
AAH62060	BC062060 NID: - Rattus norvegicus
S60588	drebrin A - rat
Q9QYV3	C3G protein (Fragment).- Rattus norvegicus - (Rat).
A28114	alkaline phosphatase (EC 3.1.3.1) precursor - rat
A25516	propionyl-CoA carboxylase (EC 6.4.1.3) beta chain precursor - rat
Q9JMA0	tRNA-guanine transglycosylase (EC 2.4.2.29). - (Rat).

Q63662	Rat 3-methylcholanthrene-inducible truncated UDP glucuronosyltransferase
AAR92226	AY389807 NID: - Rattus norvegicus
AAA41065	RATCYPPB NID: - Rattus norvegicus
CAA00863	BRL-3A BINDING PROTEIN PRECURSOR.- Rattus norvegicus - (Rat).
AAC52855	RNU59241 NID: - Rattus norvegicus
A36443	seminal vesicle secretory protein II precursor - rat
AAD27869	AF133731 NID: - Rattus norvegicus
ENOB RAT	Beta enolase (EC 4.2.1.11) (2-phospho-D-glycerate hydro-lyase)
Q91YB6	Complement inhibitory factor H.- Rattus norvegicus
CAA58233	RNPAlHC3 NID: - Rattus norvegicus
P70603	Activin-like receptor kinase-7 - Rattus norvegicus
CAE84034	BX883048 NID: - Rattus norvegicus
A53455	syntaxin-binding protein n-Secl - rat
O54720	Kinesin-related protein 3A (Fragment).- Rattus norvegicus - (Rat).
AAR20449	AY426740 NID: - Rattus norvegicus
AAA57129	RATAPMK NID: - Rattus norvegicus
Q9R189	Munc13-4 protein. - Rattus norvegicus - (Rat).
A53621	hydroxymethylglutaryl-CoA reductase (NADPH2) kinase (EC 2.7.1.109) - rat
AAQ91026	AY387056 NID: - Rattus norvegicus
AAB95646	RNU23443 NID: - Rattus norvegicus
TVRTK6	ribosomal protein S6 kinase (EC 2.7.1.-), 70K - rat

CATC RAT	Dipeptidyl-peptidase I precursor
S36126	neural cell adhesion molecule L1 - rat
CAA73300	RNLTBP2 NID: - Rattus norvegicus
Q9JM04	Late gestation lung 2 protein.- Rattus norvegicus - (Rat).
Q7TPH4	Dystrophin Dp71a.- Rattus norvegicus - (Rat).
CSRT	catalase (EC 1.11.1.6) - rat
Q62884	Density-enhanced phosphatase-1 precursor
JC2130	protein kinase (EC 2.7.1.37) - rat
BAA95006	AB023896 NID: - Rattus norvegicus
Q8R4B6	Testosterone-regulated prominin-related protein.- Rattus norvegicus - (Rat).
Q91XT9	Ceramidase.- Rattus norvegicus - (Rat).
AAS75313	AY569010 NID: - Rattus norvegicus
TMRTF1	tropomyosin 1,-embryonic fibroblast - rat
O4RTD5	cytochrome P450 2D5 - rat
Q8CFG6	Calcium channel alpha-2 delta-2 subunit.- Rattus norvegicus
Q924N5	Gonadotropin-regulated long chain acyl-CoA synthetase.
Q7TNY7	Myosin VIIA and Rab interacting protein.- Rattus norvegicus
BAD10946	AB038233 NID: - Rattus rattus
Q80WN5	RSB-11-77.- Rattus norvegicus - (Rat).
S07085	cystatin C precursor - rat (fragment)
Q7TP35	Ab2-088 - Rattus norvegicus - (Rat).
O35814	P60 protein.- Rattus norvegicus - (Rat).
CAD29097	Chimeric DNA-directed DNA polymerase bf2-7a (EC 2.7.7.7) - Rat

T46645	sulfonylurea receptor 2B [imported] - rat
BAA75629	AB002563 NID: - Rattus norvegicus
PCK9 RAT	Proprotein convertase subtilisin/kexin type 9 precursor (EC 3.4.21.-) Rattus norvegicus - (Rat).
Q91XW7	Caspase 11.- Rattus norvegicus - (Rat).
A30411	synapsin Ia - rat
Q9QWL9	Dynamin IIIbb isoform. - Rattus norvegicus - (Rat).
CAD97562	Sequence 1 from Patent EP1308514.- Rattus sp.
AAA62508	RNU20796 NID: - Rattus norvegicus
T17187	CL3AB protein - rat
S57953	C4BP protein alpha chain precursor - rat
O70360	Insulin receptor substrate 2 (fragment).- Rattus norvegicus (Rat)
JC7763	neuronal leucine-rich repeat protein-3 - rat
Q9JIH3	Delta kalirin-7.- Rattus norvegicus - (Rat).
BAA08621	RATPK NID: - Rattus norvegicus
AAH61753	BC061753 NID: - Rattus norvegicus
A43344	synaptic vesicle protein SV2 - rat
AAC52355	RNU40819 NID: - Rattus norvegicus
C40204	Na <sup>+</sup> /H <sup>+</sup> exchanging protein 4 - rat
AAB59692	RATIRRB NID: - Rattus norvegicus
S39345	unc-18 protein homolog, 67K - rat
CAA45743	RNCYP3A1R NID: - Rattus norvegicus
JX0205	long-chain-fatty-acid-CoA ligase (EC 6.2.1.3), brain [validated] - rat
AAL59007	AY070268 NID: - Rattus norvegicus



A31373	calpactin I light chain - rat
BAC22515	AB091379 NID: - Rattus norvegicus
JN0336	N-methyl-D-aspartate receptor 1 precursor, splice form B - rat
S59964	procollagen-lysine5-dioxygenase (EC 1.14.11.4) precursor- rat
AAD50905	PAIRED IG-LIKE RECEPTOR-A1- Rattus norvegicus (Rat)
JC6508	brahma related gene associated factor BAF60 b protein - rat
O54772	BAF60b.- Rattus norvegicus - (Rat).
A22952	alpha-1 proteinase inhibitor III precursor - rat
BAA19517	D84434 NID: - Rattus norvegicus
BAA05107	RATCLCK2 NID: - Rattus rattus
Q80Z30	Calmodulin-dependent protein kinase phosphatase N.- Rattus norvegicus - (Rat).
AAB59698	RATGLTPG NID: - Rattus norvegicus
CAA60630	RNRNANE NID: - Rattus norvegicus
ERB2 RAT	Receptor protein-tyrosine kinase erbB-2 precursor
CAC60123	Sequence 28 from Patent WO0153347. - Rattus rattus (Black rat)
Q8VDA0	Ankyrin G107.- Rattus norvegicus - (Rat).
AAA41166	RATFN3M2 NID: - Rattus norvegicus
AAQ96227	AY383669 NID: - Rattus norvegicus
Q9ES75	Proline-rich acidic protein.- Rattus norvegicus - (Rat).
AAH60515	BC060515 NID: - Rattus norvegicus
BAD14292	AB175782 NID: - Rattus norvegicus
AAA41653	RATMYHCA NID: - Rattus norvegicus
AAB31934	S73559 NID: - Rattus sp.

A46206	voltage-gated sodium channel alpha subunit - rat (fragment)
Q7TN78	Olfactory specific medium-chain acyl CoA synthetase. Rattus norvegicus - Rat
AAC63367	AF093139 NID: - Rattus norvegicus
Q62977	KRAB/zinc finger suppressor protein 1.- Rattus norvegicus - (Rat).
AAC52536	RNU34841 NID: - Rattus norvegicus
S62785	cytochrome P450 2C11 - rat
Q8CG40	Putative alpha3-fucosyltransferase.- Rattus norvegicus - (Rat).
AAA41049	RATCYPC NID: - Rattus norvegicus
Q9EQN5	Antifreeze-enhancer binding protein AEP.- Rattus norvegicus - (Rat).
AAA41701	RATNHEPSUL NID: - Rattus norvegicus
A40670	nuclear envelope protein POM 121 - rat
O89049	Thioredoxin reductase.- Rattus norvegicus - (Rat).
Q9Z1S6	Melanocyte-specific protein 1.- Rattus norvegicus - (Rat).
S07390	glucuronosyltransferase (EC 2.4.1.17) 3 precursor - rat
S16788	probable reverse transcriptase - rat
AAG09802	AF264765 NID: - Rattus norvegicus
Q80ZB6	Purkinje cell espin isoform 2+.- Rattus norvegicus - (Rat).
Q9Z182	Stretch-inhibitable nonselective channel (SIC).- Rattus norvegicus - (Rat).
AAQ96229	AY383671 NID: - Rattus norvegicus
AAB632209	AF008201 NID: - Rattus norvegicus
O54821	Chloride channel 2. - Rattus norvegicus - (Rat).

AAB05672	RNU41853 NID: - Rattus norvegicus
T03096	CDO protein - rat
A26294	uncoupling protein - rat
AAC98728	AF023303 NID: - Rattus norvegicus
Q8K1Q4	ProSAPiP1 protein.- Rattus norvegicus - (Rat).
O88867	Kynurenine 3-hydroxylase.- Rattus norvegicus - (Rat).
A46702	methionyl aminopeptidase (EC 3.4.11.18) 2 - rat
S13875	nicotinic acetylcholine receptor delta chain precursor - rat
Q8K3V0	Osteoregulin-like protein.- Rattus norvegicus - (Rat).
Q8HW97	9 days embryo whole body cDNA, RIKEN full-length enriched library
A36330	interferon regulatory factor 1 - rat
AAA18885	RN10188 NID: - Rattus norvegicus
AAC52817	RNU53420 NID: - Rattus norvegicus
A36304	cytochrome P450 4A8 - rat
Q7TQ90	Acl002.- Rattus norvegicus - (Rat).
GLK2 RAT	RAT Glutamate receptor. ionotropic kainate 2 precursor (Glutamate receptor 6)
S13913	hexokinase (EC 2.7.1.1) III [similarity] - rat
O35804	Janus protein tyrosine kinase 2 (Fragment).- Rattus norvegicus - (Rat).
CAB25334	RAT PYRUVATE KINASE M INTRONLESS PROCESSED PSEUDOGENE
AAQ63060	AY294938 NID:- Rattus norvegicus

DCRTO	ornithine decarboxylase (EC 4.1.1.17) - rat
Q8K1Q5	ProSAPiP2 protein.- Rattus norvegicus - (Rat).
BAA10926	RATPI3KB NID: - Rattus norvegicus
ADDG RAT	Gamma adducin (Adducin-like protein 70)
Q7TPH3	Dystrophin Dp71ab.- Rattus norvegicus - (Rat).
AMPN RAT	Aminopeptidase N (EC 3.4.11.2) (rAPN) (Alanyl aminopeptidase)
CAA55887	RNTEST6 NID: - Rattus norvegicus
BAA04958	RATRP NID: - Rattus norvegicus
AAF62175	AF147452 NID: - Rattus norvegicus
O35825	Inositol polyphosphate 4-phosphatase type II-beta.- Rattus norvegicus - (Rat).
Q920L2	Flavoprotein subunit of succinate-ubiquinone reductase.- Rattus norvegicus
AAD24413	AF057308 NID: - Rattus norvegicus
A44315	cartilage oligomeric matrix protein precursor - rat
I58144	corticotropin-releasing factor receptor - rat
A46216	transcription factor Skn-1, splice form a - rat
A49413	perilipin A - rat
AAH62000	BC062000 NID: - Rattus norvegicus
O4RTLO	laurate omega-hydroxylase (EC 1.14.15.3) cytochrome P450 4A1 - rat
JN0710	ubiquitin-like protein - mouse
AAC98727	AF023302 NID: - Rattus norvegicus
I56606	estrogen sulfotransferase isoform 3 - rat

KAPA RAT	cAMP-dependent protein kinase. alpha-catalytic subunit
O70142	Sck (Fragment).- Rattus rattus (Black rat).
AAB48561	RNU53367 NID: - Rattus norvegicus
AAH63164	BC063164 NID: - Rattus norvegicus
Q9JI56	SNAP-29 protein.- Rattus norvegicus - (Rat).
Q91ZM1	Transient receptor potential channel 4 alpha splice variant - Rattus norvegicus
CAD20352	RNO427342 NID: - Rattus norvegicus
AAC19167	AF043106 NID: - Rattus norvegicus
AAH59158	BC059158 NID: - Rattus norvegicus
CAA69358	RN2ARYLCO NID: - Rattus norvegicus
AAD31015	AF130819 NID: - Rattus norvegicus
S38783	integrin alpha chain - rat (fragment)
AAR95653	AY435152 NID: - Rattus norvegicus
AAB06509	RATJAPR NID: - Rattus norvegicus
B32985	somatotropin-binding protein precursor - rat
I57939	taurine transporter - rat
1DJGA2	1-phosphatidylinositol-4,5-bisphosphate phosphodiesterase
AAH61717	BC061717 NID: - Rattus norvegicus
Q924H6	Testis-specific transporter TST1.- Rattus norvegicus - (Rat).
Q9QZP2	Zinc finger protein.- Rattus norvegicus - (Rat).
BAA28746	AB015042 NID: - Rattus norvegicus
S51005	protein-tyrosine-phosphatase (EC 3.1.3.48) 2E - rat
Q9Z2A1	Patched (Fragment).- Rattus norvegicus - (Rat).

JC4534	cytochrome P450 4F6 protein - rat
AAH62402	BC062402 NID: - Rartus norvegicus
Q9ET34	Spliceosomal protein SAP155 (Fragment).- Rattus norvegicus
T17455	translation initiation factor eIF-2 alpha chain kinase (EC 2.7.1.-) rat
S43506	hypothetical protein - rat
Q9Z2I7	SV2 related protein.- Rattus norvegicus (Rat ).
I73679	estrogen sulfotransferase isoform 6 - rat
AAQ08184	AF515735 NID: - Rattus norvegicus
S52097	cytochrome P450III - rat
JH0695	gamma-aminobutyric acid transporter protein 3 - rat
O35102	Dihydroorotase (Fragment).- Rattus rattus (Black rat).
Q9JHE0	Yotiao protein (Fragment).- Rattus norvegicus - (Rat).
JC5669	Ca <sup>2+</sup> /calmodulin-dependent protein kinase kinase (EC 2.7.1.-) beta chain - rat
O54822	Chloride channel 2.- Rattus norvegicus - (Rat).
AAH61840	BC061840 NID: - Rattus norvegicus
I56563	interleukin-3 receptor beta-subunit - rat
O54975	Cytoplasmic aminopeptidase P.- Rattus norvegicus - (Rat).
ANRT	angiotensin precursor - rat
AAA85720	RNU22952 NID: - Rattus norvegicus
Q8QZV1	cGMP phosphodiesterase (Phosphodiesterase type 9).- Rattus norvegicus - (Rat).
Q9JK99	Telomerase catalytic subunit (Fragment).- Rattus norvegicus - (Rat).
AAS66238	AY539898 NID: - Rattus norvegicus

A49681	long-chain-fatty-acid beta-oxidation multienzyme complex alpha chain precursor
Q80Z29	Pre-B-cell colony-enhancing factor.- Rattus norvegicus - (Rat).
Q9WV57	Mpg-1 protein.- Rattus norvegicus - (Rat).
Q9Z2Y9	Klotho.- Rattus norvegicus - (Rat).
S34226	cyclin B - rat
I65309	autoantigen p69 - rat
AAB48545	RNU39943 NID: - Rattus norvegicus
Q7TP16	Ccl-3.- Rattus norvegicus - (Rat).
Q9QZM5	Eps8 binding protein.- Rattus norvegicus - (Rat).
Q8VIA9	Ecotropic retrovirus receptor - Rattus norvegicus - (Rat).
GCRT	glucagon precursor - rat
A53433	ribose-phosphate diphosphokinase (EC 2.7.6.1) 39K regulatory chain - rat
ET1R RAT	Endothelin-1 receptor precursor (ET-A).- Rattus norvegicus - (Rat).
A36275	long-chain-fatty-acid-CoA ligase (EC 6.2.1.3), brain - rat
AAH06581	BC006581 NID: - Mus musculus
AAR83745	AY390379 NID: - Rattus norvegicus
Q923Z2	Tropomyosin alpha isoform.- Rattus norvegicus - (Rat).
AAQ22768	AY338396 NID: - Rattus rattus diardii
Q63636	Natural killer cell protease 4.- Rattus norvegicus - (Rat).
AAH61812	BC061812 NID: - Rattus norvegicus
Q64584	Rat cytochrome P-450b (phenobarbital-inducible) - Rattus norvegicus - (Rat).

CAB35519	Cytochrome P450.- Rattus norvegicus - (Rat).
AAC05303	AF029105 NID: - Rattus norvegicus
ACM4 RAT	Muscarinic acetylcholine receptor M4.- Rattus norvegicus - (Rat).
Q9EPT7	Prothrombinase FGL2.- Rattus norvegicus - (Rat).
Q80WF4	GRP78 binding protein.- Rattus norvegicus - (Rat).
AAA41654	RATMYHCB NID: - Rattus norvegicus
Q8K4V4	PDZ protein Mrt1A.- Rattus norvegicus - (Rat).
B56021	probable cell division control protein p55CDC - rat
I56531	beta-adrenergic-receptor kinase (EC 2.7.1.126) 1 - rat
Q7TP91	Abl-205 - Rattus norvegicus - (Rat).
JH0819	calreticulin precursor - rat
AAK71880	AY039651 NID: - Rattus norvegicus
A42811	nuclear RNA helicase (DEAD family) homolog - rat
A28055	K-kininogen, LMW 1 precursor - rat
Q924K5	Myocilin - Rattus norvegicus - (Rat).
O08963	Protocadherin 4.- Rattus rattus (Black rat).
A26685	cytochrome P450 2C11 - rat
CAC34480	RNO306427 NID: - Rattus norvegicus
AAF15588	AF188333 NID: - Rattus norvegicus
JC1285	protein-tyrosine-phosphatase (EC 3.1.3.48), receptor type alpha precursor - rat
T10772	calpastatin - rat
AAD33896	AF143545 NID: - Rattus norvegicus
Q7TPJ8	Ac2-143.- Rattus norvegicus - (Rat).



AAH61839	BC061839 NID: - Rattus norvegicus
Q80WA5	Sodium myo-inositol transporter 1.- Rattus norvegicus - (Rat).
AAL26912	AF320054 NID: - Rattus norvegicus
S12736	hydroxymethylglutaryl-CoA synthase (EC 4.1.3.5), cytosolic - rat
Q9EPH2	Mac-MARCKS protein.- Rattus norvegicus - (Rat).
JE0344	contraception associated protein 1 - rat
AAC83348	AF085693 NID: - Rattus norvegicus
CAC16598	RNO277748 NID: - Rattus norvegicus
GBP2 RAT	Interferon-induced guanylate-binding protein 2 (GTP-binding protein 2)
Q9Z1J7	Sodium-dependent neutral amino acid transporter, ASCT2. - Rattus norvegicus
B39667	brain-derived neurotrophic factor receptor precursor, splice form T1 - rat
A36205	mitochondrial processing peptidase (EC 3.4.24.64) alpha chain precursor
Q7TQ77	Ac1288.- Rattus norvegicus - (Rat).
T17367	potassium channel protein elk1 - rat
AAA41880	RATPKL NID: - Rattus norvegicus
Q9Z0R8	Putative taste receptor TR1 (Fragment).- Rattus norvegicus - (Rat).
Q810H6	Disrupted-in-schizophrenia-1.- Rattus norvegicus - (Rat).
S11737	resistance protein Mx3, interferon-regulated - rat
Q8K451	GABAB-related G-protein coupled receptor.- Rattus norvegicus
CAC14912	RNO296090 NID: - Rattus norvegicus

MK06 RAT	Mitogen-activated protein kinase 6
O70498	Nuclear RNA helicase.- Rattus norvegicus - (Rat).
A36116	prolactin receptor 2 precursor - rat
A27274	ribophorin I precursor - rat
AXN1 RAT	Axin 1 protein (Axis inhibition protein 1) (rAxin).- Rattus norvegicus - (Rat).
Q8K1Q1	Vesicular glutamate transporter 3.- Rattus norvegicus - (Rat).
AAH61996	BC061996 NID: - Rattus norvegicus
JC5261	salt-tolerant protein - rat
AAS66230	AY539890 NID: - Rattus norvegicus
S49162	ZG-21p protein - rat
FXM1 RAT	Forkhead box protein M1 (Winged helix factor from INS-1 cells)
AAN33055	AF538953 NID: - Rattus norvegicus
JC4841	regeneration associated serpin-1 precursor - rat
MK10 RAT	Mitogen-activated protein kinase 10
Q8SEZ7	NADH dehydrogenase subunit 2 (Fragment).- Rattus norvegicus
AAC63994	AF058795 NID: - Rattus norvegicus
AAC52771	RNU4001 NID: - Rattus norvegicus
NUCL RAT	Nucleolin (Protein C23).- Rattus norvegicus - (Rat).
Q8CHN8	Mannose-binding protein associated serine protease-1- Rattus norvegicus
Q9JJ09	Type IIb sodium-phosphate transporter.- Rattus norvegicus
O08623	PKC-zeta-interacting protein (ZIP).- Rattus norvegicus - (Rat).
Q99N97	H-caldesmon (Fragment).- Rattus norvegicus - (Rat).

Q91ZV2	Endothelial and smooth muscle cell-derived neuropilin-like protein - Rat
Q63614	Tyrosine kinase receptor (Fragment).- Rattus norvegicus - (Rat).
Q63778	Hypothetical protein.- Rattus norvegicus - (Rat).
AAA75166	RNU21683 NID: - Rattus norvegicus - (Rat).
T17156	CL1BB protein - rat
JC5614	RNB6 protein - rat
I59331	thyrotropin-releasing hormone degrading enzyme (EC 3.4.11.-) rat
Q91XR7	Amino acid transporter system N2.- Rattus norvegicus - (Rat).
A55622	cytochrome P450 C11B3 - rat
DYMSD2	dopamine receptor D2 - mouse
Q91XJ1	Bcl-2 -interacting coiled-coil protein beclin.- Rattus norvegicus
CAA72533	RNECTOATP NID: - Rattus norvegicus
SRE1 RAT	Sterol regulatory element binding protein-1 (SREBP-1)
GB12 RAT	Guanine nucleotide-binding protein, alpha-12 subunit (G alpha 12) - Rat
I51883	alpha-2B-adrenergic receptor - rat
JC2054	complement regulatory protein. 5I2 antigen precursor - rat
S36327	clathrin assembly protein API80 long form - rat
A47503	epoxide hydrolase (EC 3.3.2.3), cytosolic - rat
CAD55407	RNO512838 NID: - Rattus norvegicus
Q9JHZ9	Amino acid system N transporter.- Rattus norvegicus - (Rat).
S51605	receptor-like tyrosine kinase Ehk-2 - rat
A46595	tricarboxylate transport protein precursor. mitochondrial - rat

O35260	NAC-1 protein.- Rattus norvegicus - (Rat).
S68200	glucuronosyltransferase (EC 2.4.1.17) precursor - rat
I58099	gene PZX3 protein - rat
JH0672	brain factor 1 protein - rat
AAB38506	RNU80054 NID: - Rattus norvegicus
A39030	androgen-binding protein 1 precursor - rat
Q7TP48	Ab2-305 - Rattus norvegicus - (Rat).
SAHH RAT	Adenosylhomocysteinase (EC 3.3.1.1)
AAQ91067	AY387097 NID: - Rattus norvegicus
Q7TMD5	Nuclear protein UKp83.- Rattus norvegicus - (Rat).
B38656	vacuolar proton pump 116K chain - rat
Q7TMA9	Ac1262 (Aal249) (Ac1-114) (Ac2-069) (Ab2-196) (Ab1-341) (Ba2-693) - Rat
Q9EQ23	C-kit receptor (Fragment).- Rattus norvegicus - (Rat).
XURT	acetyl-CoA C-acyltransferase (EC 2.3.1.16), mitochondrial - rat
Q9ESN0	Niban.- Rattus norvegicus - (Rat).
I59282	diacylglycerol kinase (EC 2.7.1.107) gamma - rat
JC1450	Fibroblast growth factor receptor 4 - rat
O70177	Carboxylesterase precursor (EC 3.1.1.1).- Rattus norvegicus
AAA40950	RATCP450 NID: - Rattus norvegicus
A53047	6-phosphofructokinase, (EC 2.7.1.11) - rat
A30314	protein kinase C (EC 2.7.1.-) zeta - rat
RIP2 RAT	RIM binding protein 2 (RIM-BP2).- Rattus norvegicus - (Rat).
B47417	insulin receptor-related receptor, secreted splice form 2 precursor -

	rat
Q99PW1	Protein tyrosine kinase c-Yes (Fragment).- Rattus norvegicus
A54139	Na <sup>+</sup> /Ca <sup>2+</sup> exchanging protein NCX2 - rat
Q8VHY4	Transcription factor GATA-2.- Rattus norvegicus - (Rat).
B39816	tropomyosin 3. fibroblast - rat
CTRTP	corticotrophin / lipotropin precursor - rat
Q9WUV7	Serine/threonine specific protein phosphatase (EC 3.1.3.16)
Q8VHU3	Hypothetical RNA binding protein RDA288.- Rattus norvegicus
A34695	axonal glycoprotein TAG-1 precursor- rat
XXRTAC	acetyl-CoA C-acetyltransferase (EC 2.3.1.9) precursor, mitochondrial - rat
Q80YG1	Phosphoserine aminotransferase.- Rattus norvegicus - (Rat).
Q9ER33	Cyclic nucleotide-gated channel 2b.- Rattus norvegicus - (Rat).
CHRTD1	potassium channel protein drk1 - rat
O54771	BAF60b (Fragment).- Rattus norvegicus - (Rat).
AAC12270	AF026554 NID: - Rattus norvegicus
Q80W59	Histidine-rich calcium binding protein.- Rattus norvegicus - (Rat).
A39257	cytochrome P450 2C22 - rat
Q9Z311	Nuclear receptor binding factor-1.- Rattus norvegicus - (Rat).
S41627	probable anti-mullerian hormone receptor - rat
RGHYA2	GTP-binding regulatory protein Gs alpha-2 chain
T42260	guanylate cyclase (EC 4.6.1.2) G precursor- rat
A34625	gamma-aminobutyric acid/benzodiazepine receptor type A delta chain precursor

O88292	Protein C inhibitor.- Rattus norvegicus - (Rat).
JC4163	DNA-binding protein 5E5 - rat
Q9WVG4	Gliosarcoma-related antigen MIDAl (Fragment).- Rat.
QYRTGP	phosphoenolpyruvate carboxykinase (GTP) (EC 4.1.1.32) cytosolic - Rat
Q62916	Metabotropic glutamate receptor 4b.- Rattus norvegicus - (Rat).
AAQ93383	AY393999 NID: - Rattus norvegicus
Q8K3F0	Na <sup>+</sup> dependent amino acid transporter ASCT2.- Rattus norvegicus - (Rat).
SMS1 RAT	Phosphatidylcholine:ceramide cholinephosphotransferase 1
Q99PJ8	Zinc finger protein HIT-10.- Rattus norvegicus - (Rat).
JU0133	translation elongation factor eEF-1 alpha chain - Chinese hamster
S34780	gelatinase A (EC 3.4.24.24) precursor - rat
Q9EQH5	Ribeye.- Rattus norvegicus - (Rat).
MUCL RAT	Intestinal mucin-like protein (MLP) (Fragment).- Rattus norvegicus
A27671	spectrin alpha chain. nonerythroid - rat (fragment)
Q99NC1	Nuclear protein UKp68.- Rattus norvegicus - (Rat).
Q9QYU1	PxF protein.- Rattus rattus (Black rat).
Q810W9	CASK-interacting protein CIP98.- Rattus norvegicus - (Rat).
A41028	aldehyde dehydrogenase [NAD] (EC 1.2.1.3) 4 microsomal [similarity] - rat
Q99MZ8	LASP-1 Rattus norvegicus - (Rat).
A56517	nucleoporin Nup98 - rat
A41158	dipeptidyl-peptidase I (EC 3.4.14.1) precursor - rat

I60373	uKATP-1 rat
JC5803	ring finger protein, BFP - rat
Q64718	Elongation factor-1 alpha.- Rattus norvegicus - (Rat).
A35730	H <sup>+</sup> transporting two-sector ATPase (EC 3.6.3.14) alpha 4 chain precursor - rat
I66868	cdc25B - rat
JC5701	ErbB kinase activator alpha1, brain and thymus - rat
A48189	sodium/phosphate cotransport protein. renal cortex - rat
Q63158	Zinc finger protein - Rattus norvegicus - (Rat).
Q9ES02	Osteoregulin.- Rattus norvegicus - (Rat).
A25047	beta-glucuronidase (EC 3.2.1.31) precursor - rat
TMRBB	tropomyosin beta chain, skeletal muscle [validated] - rabbit
T42218	slit-1 protein homolog - rat
I55462	retinol dehydrogenase (EC 1.1.1.105) type II, 29K - rat
Q4RTPB	cytochrome P450 2B1 - rat
A53582	Na <sup>+</sup> /glucose cotransporter SGLT1 - rat
I63224	clathrin-associated adaptor protein - rat
Q8CG04	cAMP-specific phosphodiesterase PDE4D7.- Rattus norvegicus
Q9QZX1	Nucleolin-related protein NRP.-Rattus norvegicus - (Rat).
TDRTLTL	leukocyte common antigen precursor, splice form 4 - rat
Q9EPG9	ABC transporter, white homologue.- Rattus norvegicus - (Rat).
A29514	muscarinic acetylcholine receptor M1 - rat
Q9R1K3	P2X3b receptor (P2X purinoceptor) (ATP receptor) (Purinergic receptor) Rat

S23431	choline transport protein - rat
CAD35208	Sequence 52 from Patent WO0226984.- Rattus sp.
Q9Z1R8	Guanine nucleotide-binding protein.- Rattus norvegicus - (Rat).
A42499	mullerian inhibiting factor precursor - rat



TABLE 4.2. **Proteins in abnormal CSF not present in normal CSF.**

<b>PROTEIN ID</b>	<b>CHEMICAL NAME</b>
S16233	nitric oxide synthase - rat
AAQ96265	AY383707 NID: - Rattus norvegicus
AAR95664	AY480031 NID: - Rattus norvegicus
S37146	myosin 1 heavy chain - rat
UBRTA	tubulin alpha chain - rat
AAS66264	AY539924 NID: - Rattus norvegicus
S57329	tuberous sclerosis 2 homolog - rat
3FYGA	mu class tetradeca - (3-fluorotyrosyl)-glutathione s-transferase of isoenzyme
Q9QXL9	Dynamin IIIbb isoform - (Rat).
Q91ZD8	Synaptojanin 2B2. - Rattus norvegicus - (Rat).
CAF05438	AX95162 NID: - Rattus norvegicus
A53933	myosin I myr 4 - rat
Q7TMC7	Ab2-417 (Cc1-8).- Rattus norvegicus - (Rat).
C41539	kinesin light chain C - rat
T17158	CL2AB protein - rat
O35303	Dynamin-like protein (DLP1 splice variant 3). - (Rat).
Q7TNX0	Liver regeneration-related protein LRRG03. - (Rat).
DNM1 RAT	DNA (cytosine-5)-methyltransferase 1
A32202	prostaglandin-D synthase - rat
T03301	rab3 effector protein Rim - rat

Q9ERD4	Ankyrin repeat-rich membrane-spanning protein. - (Rat).
A45439	myosin I heavy chain - rat
I58166	rabphilin-3A - rat
S52517	myosin I heavy chain - rat
S49163	transferrin precursor - rat
Q8VHT3	L-type calcium channel alpha-1c subunit. - (Rat).
Q7TN17	Kinesin-like protein KIF15. -(Rat).
O35774	75 kDa fibrous sheath protein. - (Rat).
Q9QWG5	Inositol polyphosphate 4-phosphatase type II-alpha.
Q8VD81	cAMP-specific phosphodiesterase isoform PDE4B4. - rat
A40439	UBF transcription factor, long form - rat
T14050	protein kinase beta, myotonic dystrophy-associated - rat
S02180	secretogranin II - rat
Q9Z200	APS protein.- Rattus norvegicus - (Rat).
S68453	sodium channel protein SNS - rat
Q62744	Alpha actinin.- Rattus norvegicus - (Rat).
Q8R4C9	RNA-binding protein staufen splice form B. - (Rat).
Q9QUI9	CENTAURIN beta.- Rattus norvegicus - (Rat)
S70581	dihydropyrimidinase rat
A53300	ribosomal protein S6 kinase (EC 2.7.-.-) II - rat
ACC8 RAT	Sulfonylurea receptor 1. - (Rat).
Q812D9	DRE1.- Rattus norvegicus - (Rat)
Q9JIG0	Kalirin-7c isoform.- (Rat).
T42759	Munc13-3 protein - rat

5FWGA	tetra-(5-fluorotryptophanyl) -glutathione transferase mu class (EC 2.5.1.18) mutant 4 tryptophans M
Q9EPH6	Uncoupling protein UCP-4, isoform b .- (Rat).
A41009	glutaminase (EC 3.5.1.2) precursor, mitochondrial - rat
S06017	neuraxin - rat
Q9R019	Checkpoint kinase Chk2. - (Rat).
Q9JJ32	NBC-like protein. - (Rat).
CAA04248	RNAJ696 NID: - Rattus norvegicus
AAC06273	RNU69278 NID: - Rattus norvegicus
AAA40724	RATALS NID: - Rattus norvegicus
B54091	rab GDP dissociation inhibitor beta - rat
Q9JJ40	PDZ domain containing protein. - (Rat).
Q63560	Stop protein. Rattus norvegicus - (Rat).
Q9EQV7	Nadrin. Rattus norvegicus - (Rat).
Q63939	Myosin heavy chain (Fragment).- Rattus sp.
AAC72251	RNU48247 NID: - Rattus norvegicus
A31982	Ca <sup>2+</sup> transporting ATPase (EC 3.6.3.8) RB2-5, brain
RL10 MOUSE	60S ribosomal protein L10 (QM protein homolog) - (Mouse), and (Rat)
ANX2 RAT	Annexin A2 (Annexin II) (Lipocortin II)
A28807	protein disulfide-isomerase ER60 precursor - rat
I56581	dnaK-type molecular chaperone grp75 precursor - rat
Q9ES53	UFD1.- Rattus norvegicus - (Rat).
Q7TSC6	Jacob - Rattus norvegicus - (Rat).

A53742	calponin, acidic - rat
Q9QVN4	R NR-CaM 22 protein. Rattus sp.
KIRTPL	pyruvate kinase, hepatic splice form L - rat
KLC1 RAT	Kinesin light chain 1 (KLC 1) - (Rat).
LURT3	annexin III - rat
A48157	renal transcription factor Kid-1 - rat
Q810Y4	Alpha 1 type XXIII collagen. - (Rat)
A54766	metastasis-associated protein mta-1 - rat
S15074	calpastatin - rat
Q9EQR2	Alkyl-dihydroxyacetonephosphate synthase - (Rat).
T14327	alpha-latrotoxin receptor 3, calcium-independent
S34656	amine oxidase, precursor - rat
Q7TMB1	AC1147 (Aa1011) (Aa1262) (Ab2-057).- (Rat).
S27267	lamin A - rat
JN0065	ribophorin II precursor - rat
Q920L0	SLP-76 adaptor protein.- Rattus norvegicus - (Rat).
B29231	glutathione transferase (EC 2.5.1.18) Yb4 - rat
O55153	Calpastatin,- Rattus norvegicus - (Rat).
PC7034	Na <sup>+</sup> bicarbonate cotransporter - rat
Q9EPI6	Jacob protein.- Rattus norvegicus - (Rat).
Q8R471	Kinesin-related protein 3B (Fragment) - (Rat).
CAD34650	Sequence 5 from Patent WO0224187. - (Rat) .
Q7TNJ9	stonin.- Rattus norvegicus - (Rat).
A56039	GTPase-activating protein Gap1 (m) - rat

S11508	D100 protein - rat
Q8K4G7	Rho GTPase activating protein 4. - (Rat).
A36001	choline-phosphate cytidyltransferase - rat
JX0334	cytochrome P450 SA RL33 - rat
Q9JHX9	Fibroblast growth factor receptor 3 - (Rat).
Q7TQ08	Scinderin.- Rattus norvegicus (Rat).
Q925V4	Cyclooxygenase-2.- Rattus norvegicus - (Rat).
I67945	3',5'-cyclic-nucleotide phosphodiesterase - rat
JC7186	alpha-actinin-4 - rat
Q8K4M9	Oxysterol-binding protein.- Rattus norvegicus - (Rat).
Q8CFM6	Hyaluronan receptor for endocytosis HARE precursor
S29840	fibroblast growth factor receptor 1 - rat
O89000	Dihydropyrimidine dehydrogenase (EC 1.3.1.2). - (Rat)
AAC24984	AF027571 NID: - Rattus norvegicus
Q923H3	Insulin receptor tyrosine kinase substrate protein p53 - rat
T09222	exocyst complex protein Exo84 - rat
A55913	transcytosis-associated protein p115 - rat
A60560	formyltetrahydrofolate dehydrogenase (EC 1.5.1.6) / aldehyde dehydrogenase (NADP) (EC 1.2.1.4) - Rat
T17365	serine/threonine protein kinase TAO1. - rat
Q8CFG5	Calcium channel alpha-2 delta-3 subunit - (Rat) .
A499128	cell-fate determining gene Notch2 protein - rat
Q7TP30	Ac2-155.- Rattus norvegicus - (Rat) .
A46691	E-box-binding protein beta form - rat

AAB37540	RNU384181 NID: - Rattus norvegicus
I53417	type I serine-threonine kinase receptor - rat
SCP1 RAT	Synaptonemal complex protein 1 (SCP-1 protein) - (Rat).
MPT1 RAT	Protein phosphatase 1 regulatory subunit 12A
A33569	alcohol sulfotransferase (EC 2.8.2.2) - rat
Q8K4C8	Frizzled-9.- Rattus norvegicus - (Rat).
EF2 RAT	Elongation factor 2 (EF-2) .- Rattus norvegicus - (Rat).
WZRTRS	argininosuccinate lyase (EC 4.3.2.1) - rat
KPY2 RAT	Pyruvate kinase, M2 isozyme (EC 2.7.1.40) - (Rat).
S54342	protein-tyrosine-phosphatase, receptor type N precursor - rat
NFM RAT	Neurofilament triplet M protein (160 kDa neurofilament protein) - (neurofilament medium polypeptide)
A38135	ADP-ribosylarginine hydrolase - rat
Q7TP95	Ab1-351.- Rattus norvegicus - (Rat).
S57901	estradiol 17beta-dehydrogenase (EC 1.1.1.62) - rat
Q9ES38	Bile acid CoA ligase.- Rattus norvegicus - (Rat).
GERTX1	matrix glycoprotein SC1 precursor - rat
RGHYO1	GTP-binding regulatory protein Go alpha chain, splice form alpha-1 - golden hamster
AATC RAT	Aspartate aminotransferase, cytoplasmic
Q80YN5	Histone acetyltransferase.- Rattus norvegicus (Rat).
TVRTRF	protein kinase raf-1 (EC 2.7.1.-) - rat
CAA35934	RNA1B NID: - Rattus norvegicus
Q62775	SH3 domain binding protein.- Rattus norvegicus - (Rat).

Q8CJ98	Sodium channel associated protein 1B. - (Rat) .
Q9ESY8	Staufen isoform Stau-I6.- Rattus norvegicus - (Rat).
A30303	interferon-related protein PC4 - rat
S42880	amyloid precursor-like protein - rat
Q9ERD5	Synaptotagmin 13.- Rattus norvegicus - (Rat).
AAC52383	RNU04998 NID: - Rattus norvegicus
A48508	cyclic-nucleotide phosphodiesterase, cGMP-inhibited - rat
S09583	peptidylglycine monooxygenase B precursor - rat
NAC1 RAT	sodium/calcium exchanger 1 precursor - (Rat).
ATB2 RAT	Plasma membrane calcium-transporting ATPase 2
Q9WVJ6	Tissue-type transglutaminase. - (Rat).
PCK5 RAT	Proprotein convertase subtilisin/kexin type 5 precursor
AAC32866	AF083341 NID: - Rattus norvegicus
Q99JE4	Guanine nucleotide release/exchange factor - (Rat) .
JC7265	neprilysin (EC 3.4.24.11) II - rat
Q9QUL6	N-ethylmaleimide sensitive factor.- (Rat)
B49555	enhancer of split homolog R-esp2 - rat
A29952	alpha-1 proteinase inhibitor III precursor - rat
AAD37861	AF142759 NID: - Rattus norvegicus
SUHA RAT	Alcohol sulfotransferase A
T17200	CL3BC protein - rat
I55476	growth potentiating factor - rat
T17188	CL3AC protein - rat
Q9QYJ6	PDE10A2 (EC 3.1.4.17) .- Rattus norvegicus - (Rat) .

Q9WU06	Pervin.- Rattus norvegicus - (Rat).
A54065	sodium transport protein gamma chain - rat
A55620	apical endosomal protein precursor - rat
ATHA RAT	Potassium-transporting ATPase alpha chain 1
Q63477	Protein tyrosine phosphatase epsilon C - (Rat).
Q8K4S6	Centrosomal protein CG-NAP (Fragment) - (Rat).
Q9R120	Heat shock factor 2.- Rattus norvegicus - (Rat).
1B5A	ferrocytochrome b5 as axial ligands - E.Coli
Q99PD9	Down-regulated in adenoma DRA (Fragment) - (Rat) .
I60173	adenine nucleotide translocator - rat
AAH60533	BC060533 NID: - Rattus norvegicus
Q9JKZ4	Thioredoxin reductase 1.- Rattus norvegicus - (Rat).
Q8K4H3	TUC-4b.- Rattus norvegicus - (Rat).
A40452	keratin 21, type I, cytoskeletal - rat
AAF26878	T cell receptor V delta 6 (fragment).- (Rat).
Q925G1	Hepatoma-derived growth factor 3. - (Rat) .
Q9WVT5	Sterol 12alpha-hydroxylase P450. - (Rat).
Q8R5I3	Ras guanine nucleotide releasing protein 4 variant 1- rat
Q9Z1I2	P90 S6 kinase (Fragmant).- Rattus norvegicus - (Rat).
Q924M0	GABA type B receptor 1f- Rattus norvegicus - (Rat) .
Q91YB4	Putative RNA binding protein 1 (Fragment). - (Rat).
T31096	cyclin G-associated kinase GAK - rat
Q35470	cAMP-specific phosphodiesterase. - (Rat).
S21347	hypothetical protein 3 - rat



Q924Y2	Na <sup>+</sup> /Ca <sup>2+</sup> exchanger.- Rattus norvegicus - (Rat).
I84692	nuclear orphan receptor HZF-3 - rat
Q80WX7	Soluble guanylyl cyclase beta 2 subunit. - (Rat).
S38361	calpain (EC 3.4.22.17) II large chain - rat
GDIA RAT	Rab GDP dissociation inhibitor alpha (Rab GDI alpha) - rat
Q8CGZ2	Afadin-and alpha actinin-binding protein ADIP. - (Rat).
BAA03369	RATCLS4A NID: - Rattus norvegicus
AAF08536	AF1E0350 NID: - Rattus norvegicus
A33837	insulin-like growth factor I receptor precursor - rat
Q920F3	Nuclear RNA binding protein SLM-1. - (Rat).
S52913	nuclear receptor Rev-ErbA beta - rat
S16385	macrophage colony-stimulating factor 1 receptor precursor - rat
A27449	T-cell surface glycoprotein CD4 precursor - rat
URRTAP	peptidylglycine monooxygenase precursor - rat
O35788	Cyclic nucleotide-gated channel beta subunit. - (Rat) .
A32140	Steroid 15beta-monooxygenase, cytochrome P450 2C12 - rat
Q9JK64	Multidrug resistance protein 1a. - (Rat).
AAQ91035	AY387065 NID: - Rattus norvegicus
P70591	KRAB-zinc finger protein KZF-2. - (Rat).
ANX1 RAT	Annexin A1 (Annexin I) (Lipocortin I) (Calpactin II)
Q9Z2M4	Putative peroxisomal 2,4-dienoyl-CoA reductase. - (Rat)
S23399	chloride channel protein 2 - rat
Q8K3G2	Hypertrophied skeletal muscle protein GTF3 (Fragment) - rat
AAA41875	RATPKCII NID: - Rattus norvegicus

A36087	histidine ammonia-lyase (EC 4.3.1.3) - rat
Q924Z9	Netrin-1.- Rattus norvegicus - (Rat).
Q9JMB2	Type II brain 4.1 minor isoform. - (Rat).
Q9ERS3	Voltage-gated calcium channel alpha2/delta-1 subunit-rat
Q8R455	Cold/menthol receptor 1.- Rattus norvegicus - (Rat).
Q925V9	Cationic amino acid transporter-2A. - (Rat).
KHRTD	cathepsin D (EC 3.4.23.5) precursor - rat
Q9EQR7	Cyclic AMP phosphodiesterase PDE4A10 (Fragment) - (Rat)
Q99N33	R8f DNA-binding protein.- Rattus norvegicus - (Rat).
AAS21245	AY462093 NID: - Rattus norvegicus
Q99NH5	GATA-3.- Rattus norvegicus - (Rat).
CAC18955	Sequence 1 from Patent WO0068386.- Rattus sp.
P70593	A-kinase anchoring protein AKAP150. - (Rat).
S53457	dominant autoantigen gp 330 - rat (fragment)
I54195	parathyroid hormone/parathyroid hormone related-peptide receptor - rat
T09054	capsaicin receptor - rat
KAP0 RAT	cAMP-dependent protein kinase type 1-alpha regulatory chain - (Rat)
Q7TP36	Ab2-404 - Rattus norvegicus - (Rat).
AAA75407	RATPTPP1 NID: - Rattus norvegicus
S43677	Protein tyrosine kinase JAK3 - rat
Q9R1J8	Leprecan.- Rattus norvegicus - (Rat).
E49164	chromogranin-B - rat (fragment)

CLAT RAT	Choline O-acetyltransferase (CHOACTase) (Rat) .
Q7TPK0	Ac2-125 - Rattus norvegicus - (Rat).
T10799	sucrose alpha-glucosidase / oligo-1,6-glucosidase - rat
O88941	Glycoprotein processing glucosidase I. - (Rat).
Q9QYD5	Putative sodium bicarbonate cotransporter. - (Rat) .
A54756	Isocitrate dehydrogenase (NADP) cytosolic - rat
UCP1 RAT	Mitochondrial brown fat uncoupling protein 1 - (Rat).
Q9JKC1	Butyrylcholinesterase - Rattus norvegicus - (Rat).
S33777	hepsin (EC 3.4.21.-) - rat
Q7TQ86	Ac1158.- Rattus norvegicus - (Rat).
Q9Z327	Synaptopodin.- Rattus norvegicus (Rat).
Q8R560	Ankyrin-repeat protein.- Rattus norvegicus - (Rat).
9QWJ1	Retinoic acid receptor alpha 2 isoform. - (Rat).
S59927	14-3-3 protein, theta subtype - rat
JH0562	metabotropic glutamate receptor 3 precursor - rat
Q9QZP9	Septin-like protein SLP-b.- Rattus norvegicus - (Rat).
JC5399	dual leucine zipper kinase (EC 2.7.-.-) - rat
S41053	1D-myo-inositol-trisphosphate 3-kinase B - rat
C24639	Na <sup>+</sup> /K <sup>+</sup> exchanging ATPase (EC 3.6.3.9) alpha-3 chain - rat
Q8VIH3	Concentrative Na <sup>+</sup> -nucleoside cotransporter protein - rat
AAD08899	AF041838 NID: - Rattus norvegicus
R5HU7A	ribosomal protein L7a, cytosolic - human
O08619	Factor XIIIa.- Rattus norvegicus - (Rat).
A55915	guanylate cyclase (EC 4.6.1.2) 2E precursor - rat

SUHS RAT	Alcohol sulphotransferase - (Rat).
T14154	serine/threonine protein kinase ANPK, nuclear - rat
S34667	inward rectifier potassium channel - rat
UD12 RAT	UDP-glucuronosyltransferase 1-2 precursor, microsomal
PRS7 RAT	26S protease regulatory subunit 7 (MSS1 protein) - (Rat)
A28821	1-phosphatidylinositol-4,5-bisphosphate phosphodiesterase I - rat
A31870	amine oxidase (flavin-containing) (EC 1.4.3.4) B - rat
Q9JMB3	Type II brain 4.1.- Rattus norvegicus (rat).
JC5285	carbonyl reductase (NADPH2) , noninducible - rat
S12061	hexokinase (EC 2.7.1.1) type IV - rat
P97842	5-hydroxytryptamine7 receptor isoform c - (Rat)
AAA41648	RATMYHAB2 NID: - Rattus norvegicus
S47647	Nitric oxide synthase (EC 1.14.13.39) - rat
1B9YC	phosducin, chain C - rat (fragments)
MACS RAT	Myristoylated alanine-rich C-kinase substrate - (Rat)
T17138	CL1AA protein - rat
Q9JJZ7	CTL1 protein.- Rattus norvegicus - (Rat).
S12002	thyroid nuclear factor 1 - rat
A45988	dentin matrix acidic phosphoprotein AG1 - rat
O88882	Brain-enriched guanylate kinase-associated protein 2 - rat
Q99PJ6	Zinc finger protein HIT-40 - Rattus norvegicus - (Rat).
Q7TQ14	Aa1017.- Rattus norvegicus (Rat) .
I52644	neuronal protein - rat
S58279	GTP-binding protein rab4b - rat

ADDB RAT	Beta adducin (Erythrocyte adducin beta subunit) - (Rat)
S03116	gene 33 protein, hepatic - rat
O70596	Kir2.4 protein.- Rattus norvegicus - (Rat).
JC8009	choline dehydrogenase (EC 1.1.99.1) precursor - rat
Q64183	Follicle-stimulating hormone receptor.- Rattus ap.
O88461	VIP-receptor transcriptional repressor protein - (Rat).
Q9WU70	B-tomoyin isoform.- Rattus norvegicus - (Rat).
I69008	MHC class I RT1.E - rat
JQ1484	activin receptor precursor - rat
S00726	protein kinase A-raf-1 (EC 2.7.1.-) - rat
GCR RAT	Glucocorticoid receptor (GR) - (Rat).
I84639	L-lactate dehydrogenase chain X [validated] - rat
HCK RAT	Tyrosine-protein kinase HCK (EC 2.7.1.112) - Rat
I59350	karyopherin beta - rat
Q99MK3	FE65.- Rattus norvegicus - (Rat).
AAH61804	BC061884 NID: - Rattus norvegicus
JH0467	fumarylacetoacetase (EC 3.7.1.2) - rat
CAC29904	Sequence 3 from Patent EP1074627 (Fragment) - (Rat).
Q99P63	SMHS2.- Rattus norvegicus - (Rat).
AAA41239	RATGLUKB NID: - Rattus norvegicus
A54155	natriuretic peptide receptor C precursor - rat
Q9ERC0	Neuropeptide Y/peptide YY-Y2 receptor. - (Rat).
Q9WVK3	Putative short-chain dehydrogenase/reductase mRNA, complete CDS - (Rat)

T10756	Nel-homolog protein - rat
I56579	protein-tyrosine kinase (EC 2.7.1.112) batk - rat
B40204	Na <sup>+</sup> /H <sup>+</sup> exchanging protein 3 - rat
NOS3 RAT	Nitric-oxide synthase, endothelial (EC 1.14.13.39)
JC7668	dipeptidyl-peptidase II (EC 3.4.14.2) - rat
A46631	lactose-binding lectin L-36 - rat
Q99N78	Transient receptor potential ca <sup>2+</sup> channel 6A. - (Rat).
NAB1 RAT	NGFI-A binding protein 1 (EGR-1 binding protein 1) - rat
S15892	pyruvate dehydrogenase (lipoamide) (EC 1.2.4.1) beta chain - rat
Q96J19	Similar to adaptor-related protein complex 2, beta 1 subunit (Human)
A34366	Ca <sup>2+</sup> /calmodulin-dependent protein kinase II delta chain - rat
Q9JHK1	Caspase-9 (Caspase-9 long isoform). - (Rat).
Q8CJC4	Frizzled-3 protein.- Rattus norvegicus - (Rat) .
Q80Z32	Origin recognition complex subunit 1. - Rattus (Rat).
Q923L9	Brain-muscle-ARNT-like protein 2b (Fragment). - (Rat).
T14272	cortactin-binding protein 1 - rat
Q99NG8	T:G mismatch thymine glycosylase. - (Rat) .
JC8027	type 1 angiotensin II receptor associated protein 1 - rat
QRRTLD	LDL receptor precursor - rat
KIRTC	protein kinase C (EC 2.7.1.-) alpha - rat
I56526	interleukin 1 receptor type I - rat
Q7TPJ9	Ac2-141.- Rattus norvegicus - (Rat).
Q99MB4	Dopamine responsive protein. - (Rat).

ATPB RAT	ATP synthase beta chain, mitochondrial precursor - (Rat).
B43404	beta-arrestin1 - rat
T14152	synaptic scaffolding protein S-SCAM - rat
A34845	protein-tyrosine-phosphatase, nonreceptor type 1B - rat
I53273	gastric inhibitory polypeptide receptor - rat
Q8K583	Fibronigen-like protein - Rattus norvegicus - (Rat).
JN0773	calponin H1 - rat
A33270	snRNF protein N - human
Q9Z220	cp431 (Fragment).- Rattus norvegicus (Ratt).
KCRTS2	stromelysin 2 (EC 3.4.24.22) precursor - rat
Q9JI01	Corneal wound healing related protein. - (Rat).
Q7TP45	Ab2-389 - Rattus norvegicus - (Rat).
A42345	3-hydroxybutyrate dehydrogenase precursor - rat
O70253	Muscle carnitine palmitoyltransferase I.- (Rat).
ADDA RAT	Alpha adducin (Erythrocyte adducin alpha subunit) - Rat
AAD50899	Paired Ig-like receptor-B.- Rattus norvegicus - (Rat).
S49015	receptor tyrosine kinase Ehk-1 - rat
A48319	choline O-acetyltransferase (EC 2.3.1.6) - rat
CAD28393	Sequence 10 from Patent WO0212341 - (Rat).
TXN2 RAT	Thioredoxin reductase 2, mitochondrial precursor - (Rat)
S44204	procollagen-proline dioxygenase (EC 1.14.11.2) alpha chain - rat
T00011	ccal protein - rat
Q9QYG9	DLG6 gamma,- Rattus norvegicus - (Rat).
Q8CFC1	Mina53.- Rattus norvegicus - (Rat).

CAE84022	BX883047 NID: - Rattus norvegicus
A55887	caldesmon, non-muscle - rat
S11735	resistance protein Mxl, interferon-regulated - rat
Q63774	Hypothetical protein.- Rattus norvegicus - (Rat).
S00550	Alzheimer's disease amyloid beta protein precursor - rat
T31425	C-terminal domain-binding protein rA4, eplice form 2 - rat
S71321	acyl-CoA dehydrogenase short-branched chain precursor - rat
AMD3 RAT	AMP deaminase 3 (AMP deaminase isoform E) - (Rat).
A42895	H <sup>+</sup> /K <sup>+</sup> exchanging ATPase alpha chain, colon Specific - rat
BAA82517	AB024400 NID: - Rattus norvegicus
S47489	receptor tyrosine kinase - rat
KIRTC2	protein kinase C (EC 2.7.1.-) beta-II - rat
I52646	DNA binding protein - rat
Q91WX0	Complement factor H-related protein. - (Rat).
Q8R421	Kidney-type glutaminase GAC isoform (Fragment). - (Rat).
I58311	HMG-box containing protein 1 - rat
S65756	gamma-aminobutyric acid receptor rho-3 chain precursor
O4RTV3	Vitamin D3 25-monooxygenase cytochrome P450 27 precursor, mitochondrial - rat
DESM RAT	Desmin.- Rattus norvegicus - (Rat).
Q9JII4	Prolactin-like protein L. - Rattus norvegicus - (Rat) .
Q99PJ7	Zinc finger protein HIT-39.- Rattus norvegicus - (Rat).
I56896	gene gfi-2 protein - rat
S35637	high mobility group 1 protein homolog - rat (fragment)



O4RTMC	unspecific monooxygenase cytochrome P450 1A1, hepatic
JW0046	estrogen receptor beta2 - rat
AAB47997	RNUB7983 NID: - Rattus norvegicus
A24639	Na+/K+ exchanging ATPase alpha -1 chain [validated] - rat
AAA421683	RATNCPR6 NID: - Rattus norvegicus
FGRTGA	Fibrinogen gamma-A chain precursor - rat
Q923L8	Brain-muscle-ARNT-like protein 2c (Fragment) - (Rat).
1AR0A	nuclear transport factor 2 mutant E42K, chain A - rat
Q9WV25	RNA-binding protein SiahBP (Fragment). - (Rat).
JH0159	histone H1d - rat
XDH RAT	Xanthine dehydrogenase/oxidase
Q7TMB6	Aa2-174 (Cc1-38) .- Rattus norvegicus - (Rat).
Q7TP68	Ab2-002 - Rattus norvegicus - (Rat).
A53204	ribosomal protein L13a, cytosolic [validated] - rat
AAP37037	AY283175 NID: - Rattus norvegicus
Q7TME5	Ac1-581 (Ab1-181) (Ab1-216).- Rattus norvegicus - (Rat).
AAC40042	AF041246 NID: - Rattus norvegicus
S26299	transcription initiation factor IIB - rat
S31416	pyruvate dehydrogenase (lipoamide) E1-alpha-2 chain - rat
S28901	glutamate transport protein - rat
P70534	Transmembrane protein tMDC I precursor. - (Rat).
Q9ESM0	Inositol hexakisphosphate kinase. - (Rat).
Q9QWT3	Retinoic acid receptor alpha2 (Fragment). - (Rat).
Q99JC8	Neurotrypsin.- Rattus norvegicus - (Rat).

Q9JJ10	Neuronal C-SRC tyrosine-specific protein kinase. - (Rat).
AAC33823	AF018261 NID: - Rattus norvegicus
P70610	Doc2B.- Rattus norvegicus - (Rat).
NR41 RAT	Nerve growth factor induced protein I
AAF26890	T cell receptor V delta 6 (fragment) .- (Rat) .
O70513	Mama.- Rattus norvegicus - (Rat).
CITC RAT	C-1-tetrahydrofolate synthase, cytoplasmic (C1-THF synthase) [includes: methylenetetrahydrofolate dehydrogenase (EC 1.5.1.5) methenyltetrahydrofolate cyclohydrolase (EC 3.5.4.9)]
Q9QVN5	NEUROFASCIN isoform Rattus Sp.
Q8R1R5	MIC2L1.- Rattus norvegicus - (Rat).
S16319	secretin receptor - rat
VYRTD	vitamin D-binding protein precursor - rat
Q91YG2	Carboxylic ester hydrolase (EC 3.1.1.1) - (Rat).
KCB1 RAT	Potassium voltage-gated channel subfamily B member 1 - (Rat).
A49664	activin type I receptor - rat
Q9Z251	Lin-7-Ba.- Rattus norvegicus - (Rat).
I56552	synapse-associated protein 97 - rat
A35484	tryptophan 2,3-dioxygenase (EC 1 13.11.11) - rat
S04328	protein-tyrosine kinase (EC 2.7.1.112) flk - rat
A45445	janusin precursor, long form - rat
HHRTGB	dnak-type molecular chaperone precursor - rat
Q924V4	Peptide histidine transporter 1 homolog rPHT2. - (Rat).
A35816	transcription regulator Pan-2 - rat

O70260	Potassium channel regulatory protein KChAP. - (Rat).
S45116	natriuretic peptide clearance receptor homolog - rat
A31342	fructose-bisphosphatase (EC 3.1.3.11), hepatic - rat
A41785	system b(0,+) amino acid transporter-involved protein - rat
OQRT	hemopexin precursor - rat
Q31256	MHC class I RT1.Au heavy chain precursor. - (Rat).
A46195	cholecystokinin B receptor subtype - rat
Q9ESE8	Inhibitor of apoptosis protein 2. - (Rat).
Q80YN6	Ribonuclease/angiogenin inhibitor (Fragment). - (Rat).
S72266	translation initiation factor eIF2B gamma chain - rat
A35362	glycogen (starch) synthase (EC 2.4.1.11) , hepatic - rat
BAB63256	AB054539 NID: - Rattus norvegicus
Q7TP63	Ab2-064 - Rattus norvegicus - (Rat).
S21091	dodecenoyl-CoA Delta-isomerase (EC 5.3.3.8) - rat
T31100	probable potassium channel 2 - rat
Q7TNL4	Ser/Thr-like protein kinase lyk4. - (Rat).
AAA21252	RNU10097 NID: - Rattus norvegicus
AAQ96230	AY383672 NID: - Rattus norvegicus
AAF26903	T cell receptor J delta 2 (fragment). - (Rat).
A35447	carnitine O-palmitoyltransferase II precursor, mitochondrial - rat
Q35217	Hepatic multiple inositol polyphosphate phosphatase - (Rat).
O88869	PAM COOH-terminal interactor protein 1.- (Rat).
Q99M88	Caspase-9 CDT isoform - Rattus norvegicus - (Rat).
Q91ZL9	Transient receptor potential channel 4 beta-2 splice variant - (Rat).

JC7782	C1- pump- associated 55k protein, CIP55 - rat
JC4386	adenylyl cyclase-associated protein CAP2 - rat
JH0674	L-proline transport protein - rat
Q921A2	Proton myo-inositol transporter. - (Rat).
AMPB RAT	Aminopeptidase B (EC 3.4.11.6) (Ap-B)
CAB70590	Sequence 3 from Patent WO9909054 - Rattus rattus
Q8R5M4	FIP2 like protein.- Rattus norvegicus - (Rat).
Q9Z0N8	ZG29p.- Rattus norvegicus - (Rat).
B53764	beta2-chimerin, cerebellar - rat (fragment)
Q7TSS5	CD2-associated protein. - (Rat).
WHRTW	tryptophan 5-monooxygenase (EC 1.14.16.4) - rat
G42148	GTP-binding protein rab16 - rat
S21126	proteasome endopeptidase complex chain RC1 - rat
Q9JI12	Differentiation-associated Na-dependant inorganic phosphate cotransporter. - (Rat)
S52284	Lumicon, secretory interstitial proteoglycan precursor - rat
1B9XC	phosducin mutant YES, chain C - rat (fragments)
Q920G0	Putative SKAP55.- Rattus norvegicus - (Rat).
Q9JHY1	Junctional adhesion molecule JAM. - (Rat).
KIRTCE	protein kinase C (EC 2.7.1.-) epsilon - rat
JE0155	mitochondrial inner membrane translocating protein, rTIM44 - rat
Q91XV2	Gonadotropin inducible ovarian transcription factor 1- rat
G6PD RAT	Glucose-6-phosphate 1-dehydrogenase (G6PD) - (Rat).
Q8K4H4	FHA-HIT.- Rattus norvegicus - (Rat).

I2C2 RAT	Eukaryotic translation initiation factor 2C 2 (eIF2C 2)
NCT3 RAT	Natural cytotoxicity triggering receptor 3 precursor
Q9TP50	MHC class Ia antigen (Fragment). - (Rat).
O54963	Zinc finger transcription factor REST protein. - (Rat).
CAA40861	RNA2C4 NID: - Rattus norvegicus
Q9ESY1	TEMO.- Rattus norvegicus - (Rat).
CAC33148	Sequence 51 from Patent WO0100826. - Rattus rattus
Q9QVT8	BSPL=NEURAL membrane CD26 peptidase-like protein.- Rattus sp.
S52477	disintegrin (EC 3.4.24.-) precursor - rat (fragment)
AAG59704	TCR delta (Fragment).- (Rat).
Q9QYC2	RRM-type RNA-binding protein BRPTB (PTB-like protein) (Splicing regulator nPTB2) - Mus musculus (mouse) and Rattus rattus
Q9R186	Calcium transporter CaT1.- Rattus norvegicus - (Rat).

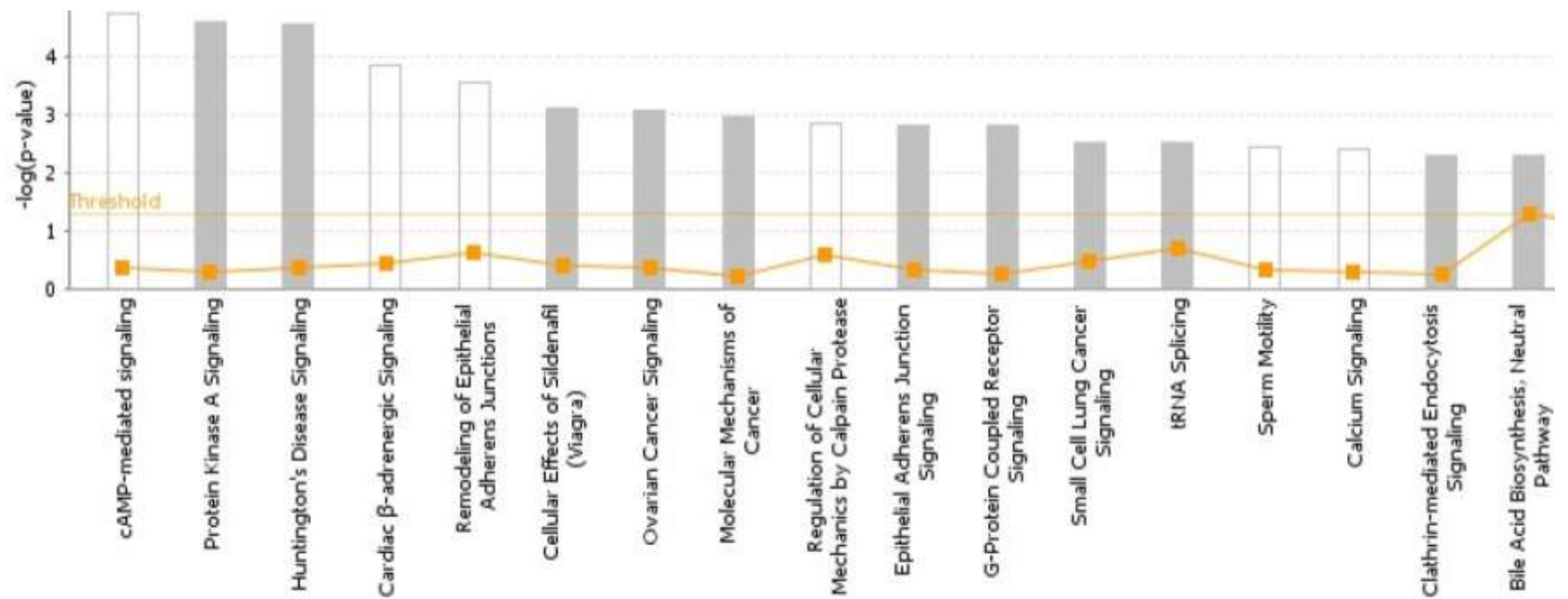
### 4.3.2 IPA results

#### 4.3.2.1 Normal and hydrocephalic CSF do not share the same protein profile and metabolic pathways

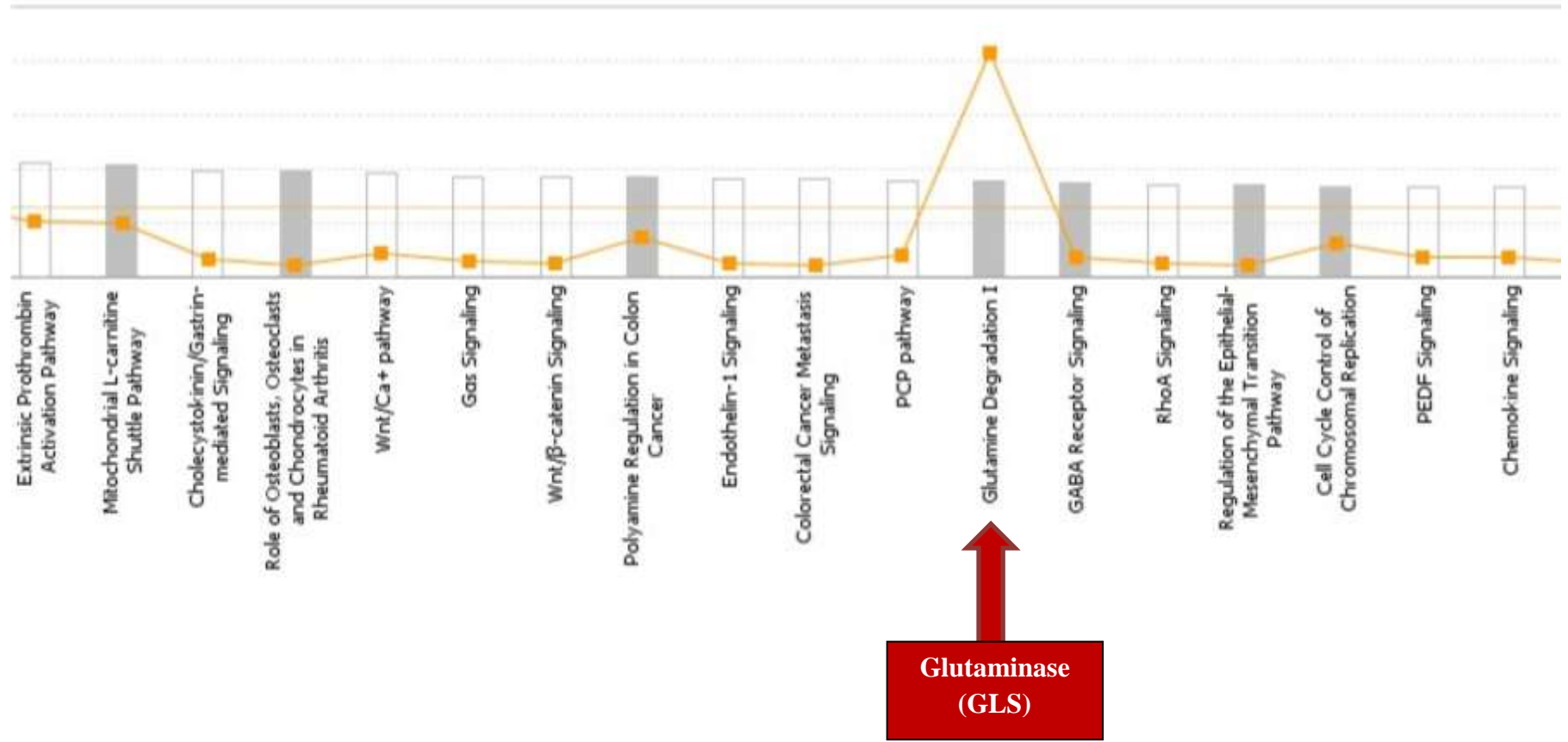
Core IPA analysis produced two large graphs representing normal and abnormal CSF respectively. The left axis on the graphs relates to the  $-\log$  of p-values (significance of results) meaning that the association made by IPA between the selected proteins found in CSF and the chosen canonical pathways did not happen by chance. Therefore, the smaller the p value, the greater the chance the IPA association was not matched randomly. In other words, the smaller the p value the greater the value of the “ $-\log$  (P-value)”. On the other hand, the right axis indicates the ratio. The ratio is the number of proteins found in the experimental dataset that fall in a canonical pathway divided by the total number of proteins in the reference canonical pathway. Ratio values below the threshold ratio should not be considered. “ $-\log$  (P-value)” and ratio should increase together, otherwise the obtained values may represent only false positives ([www.ingenuity.force.com](http://www.ingenuity.force.com)).

In the present study, grey color bars were obtained, indicating that this analysis does not have directionality (i.e. we don't know whether gene expression is upregulated or downregulated), as we did not include data about quantification of gene expression. Moreover, grey bars mean that the set of molecules included in the canonical pathways, although eligible for this pathway, still lack a predictive value. Figures 4.3 and 4.4 shows canonical pathways found for category 1 (proteins only found in normal CSF) and category 2 (proteins only found in abnormal CSF). Canonical pathways with ratios above the threshold are highlighted with red arrows on Figure 4.3, and purple arrows on Figure 4.4 below.

Figure 4.3. Canonical pathways for proteins only found in normal CSF.

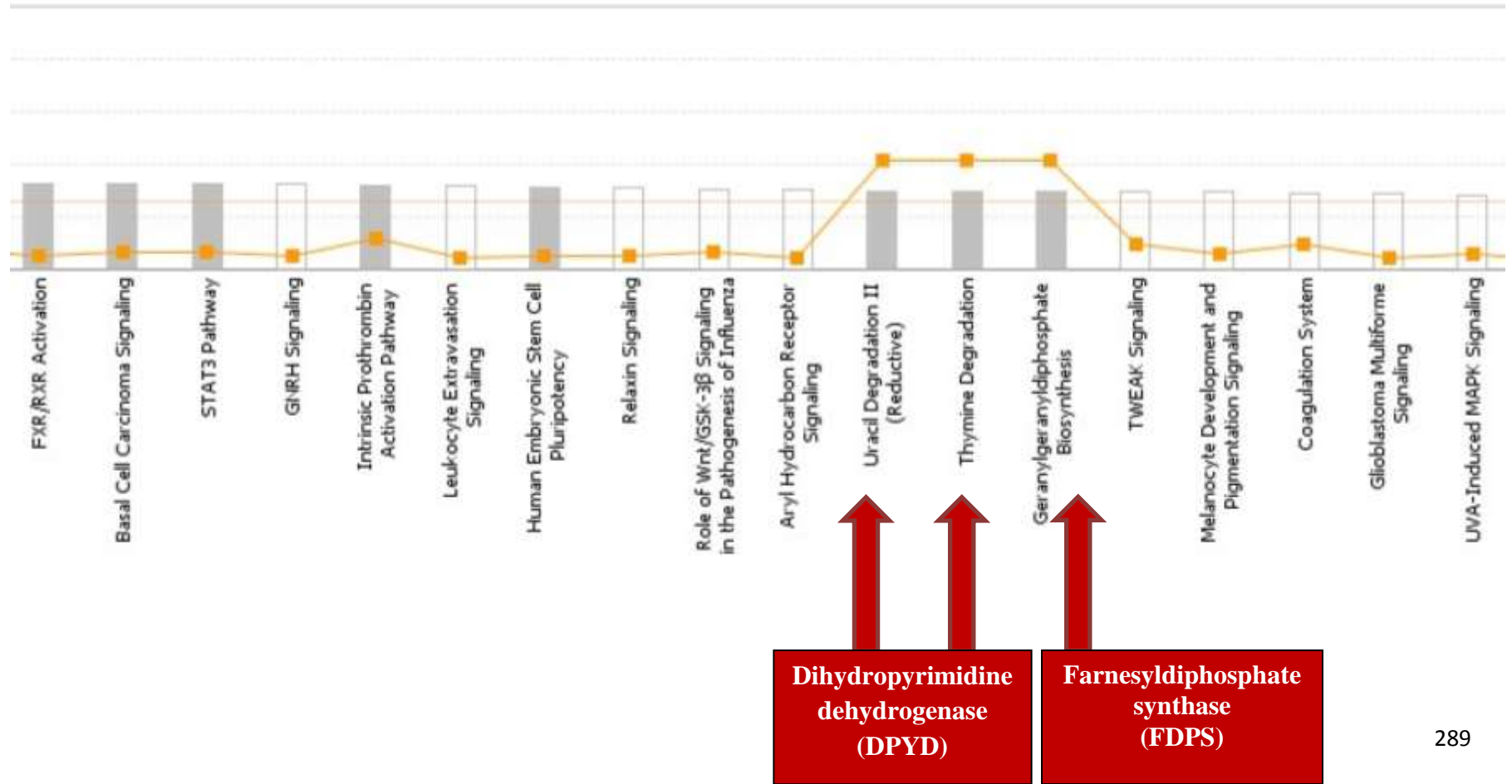


2000-2015 QIAGEN. All rights reserved.



**Glutaminase (GLS)**





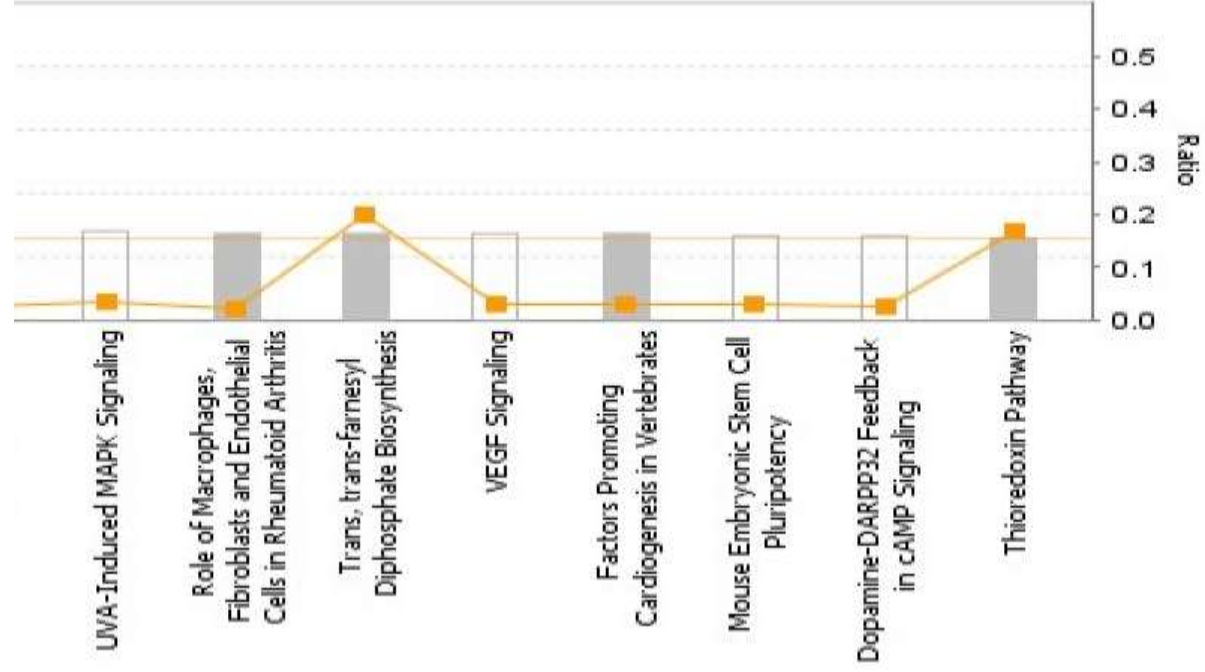
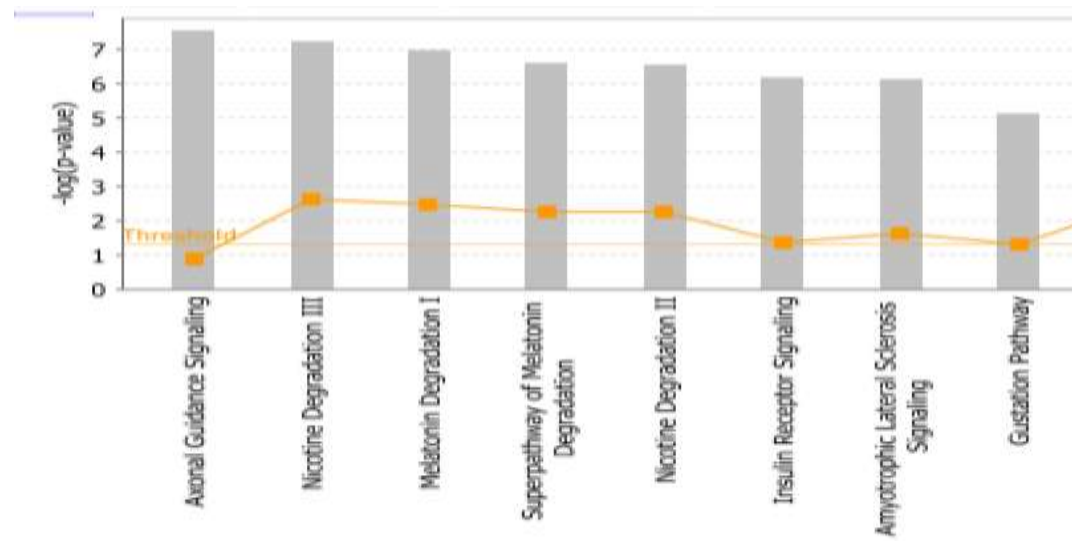
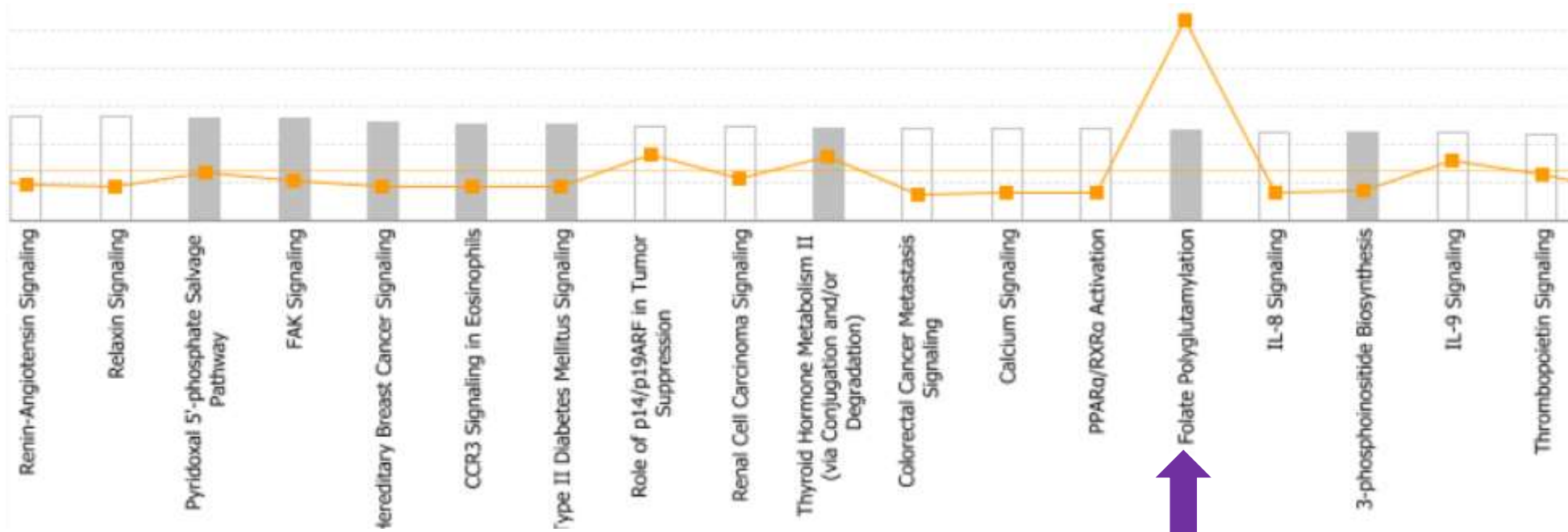


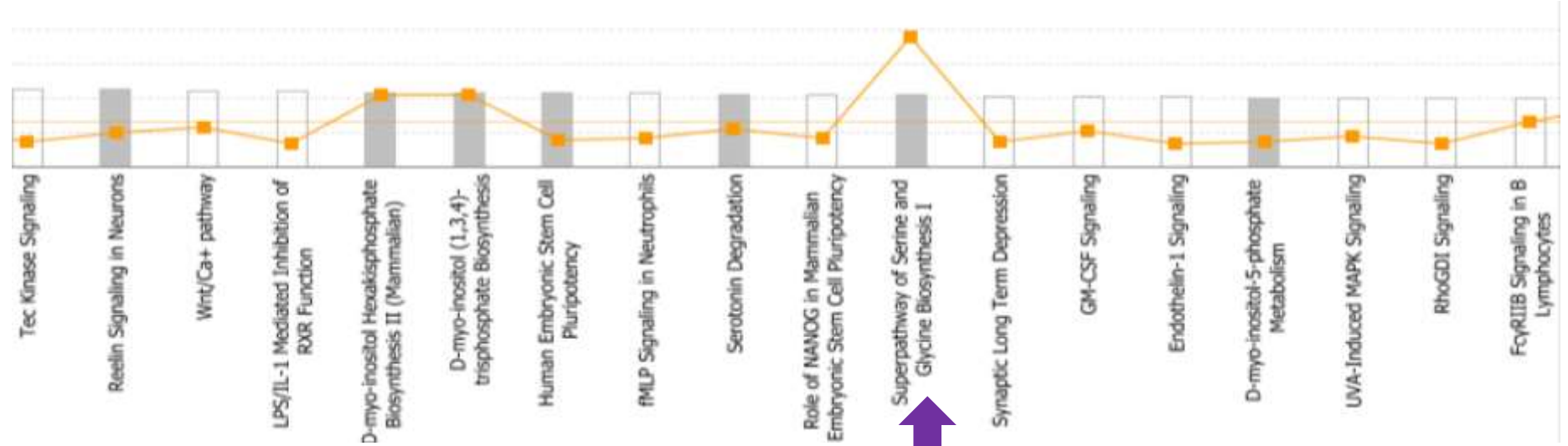
Figure 4. 4. Canonical pathways for proteins only found in abnormal CSF.




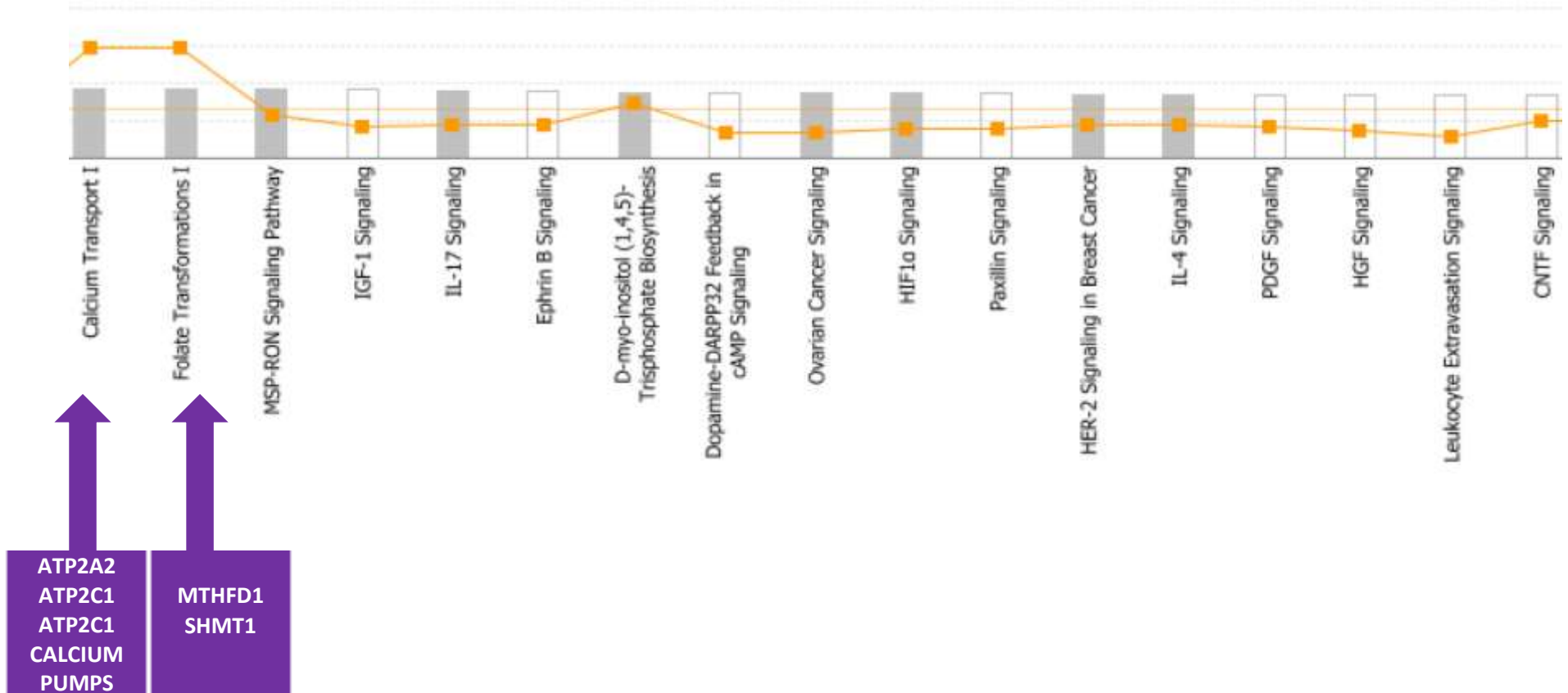
© 2000-2015 QIAGEN. All rights reserved.

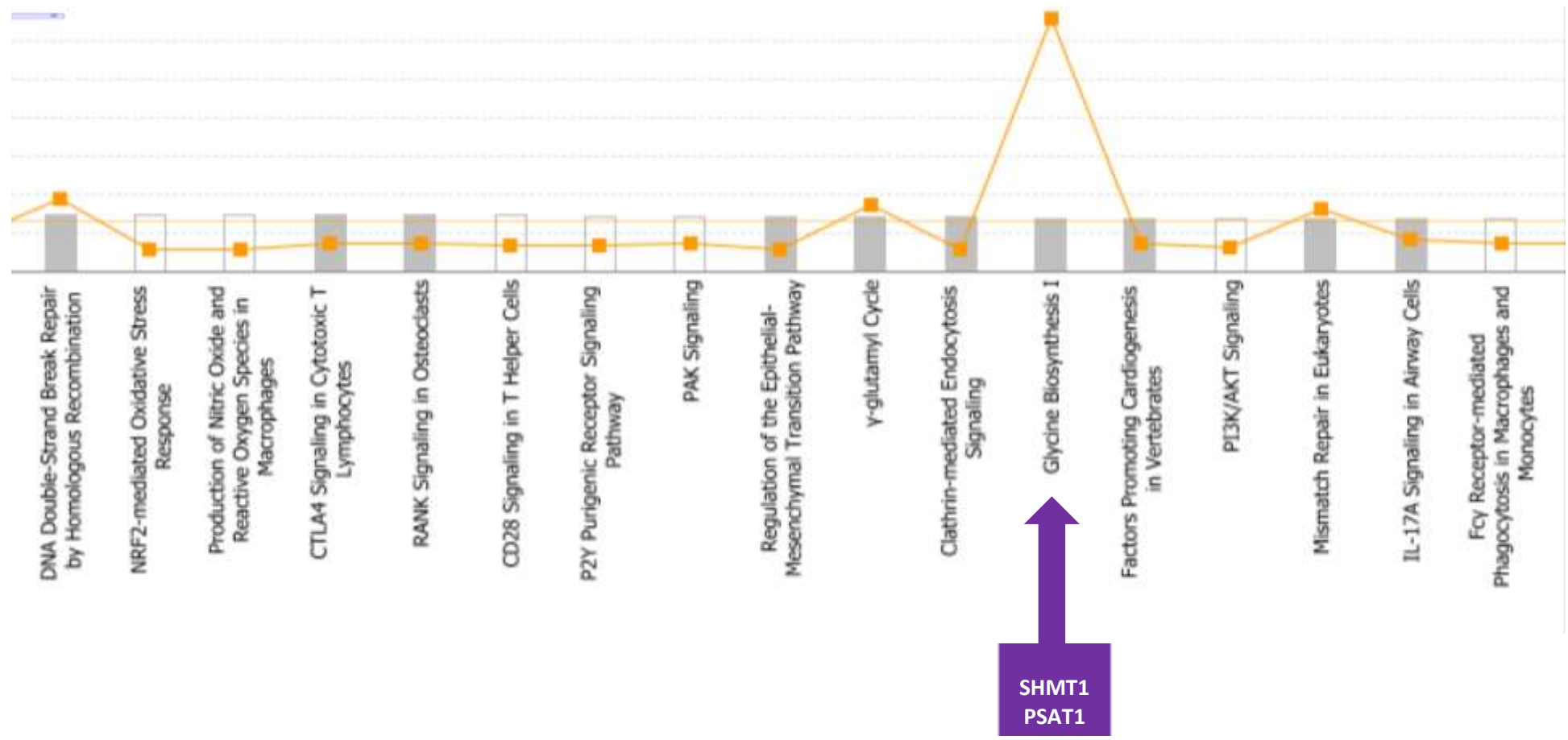


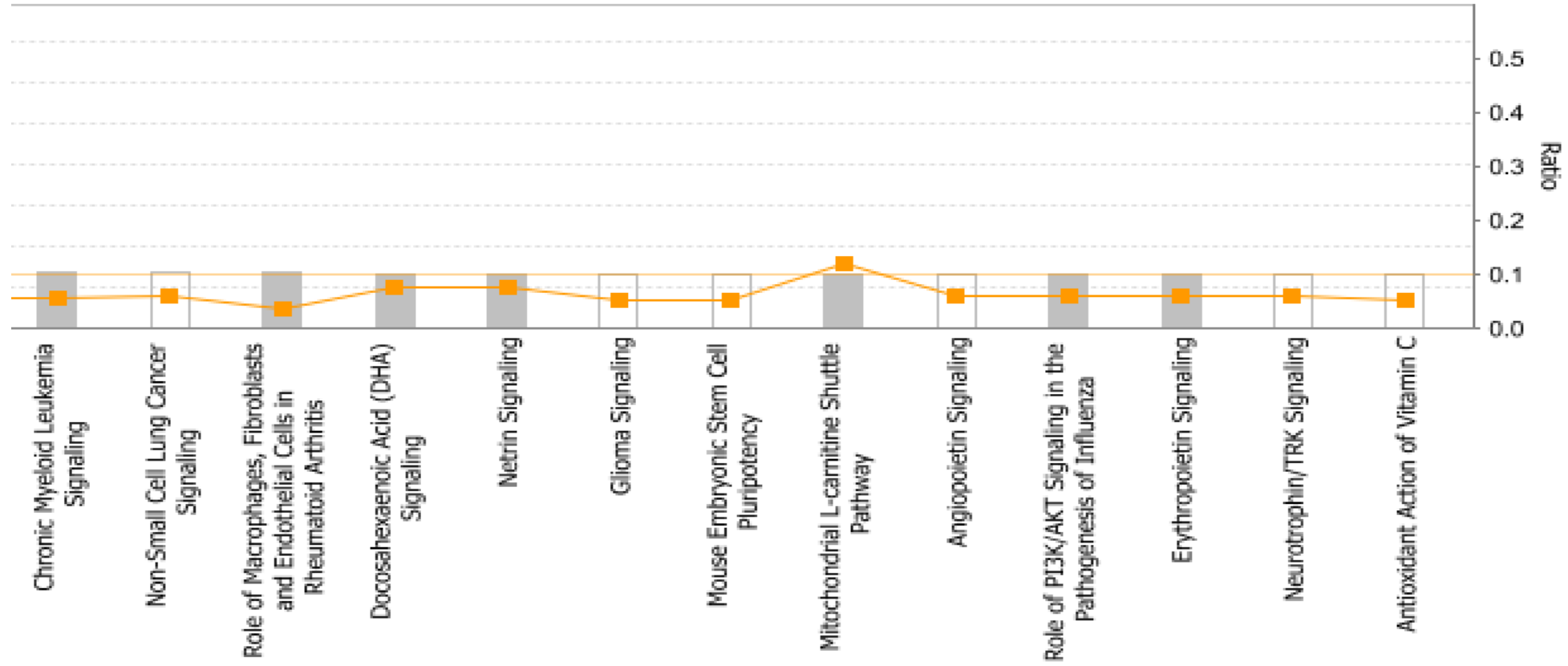
**METHYLtetrahydrofolate  
 DEHYDROGENASE  
 (MTHFD1)**  
**SERINE HYDROXYMETHYL  
 TRANSFERASE  
 (SHMT1)**




  
**SERINE HYDROXYMETHYL  
TRANSFERASE  
(SHMT1)**  
**PHOSPHOHYDROXYTHREONINE  
AMINOTRANSFERASE  
(PSAT1)**









#### 4.3.2.2 Different top canonical pathways were found in normal and hydrocephalic CSF

IPA analysis gave rise to graphs representing all canonical pathways where the molecules found in CSF may fall. Since only data with values higher than the threshold (top canonical pathways) can be considered to have any significance, we have grouped these metabolic pathways according to ratio and  $-\log(p\text{-value})$  as shown in tables 4.3 (Normal CSF) and 4.4 (Abnormal CSF) :

<b>CANONICAL PATHWAY</b>	<b>MOLECULES</b>	<b>RATIO</b>	<b>-LOG(P-VALUE)</b>
<b>Glutamine degradation I</b>	<b>GLS</b>	<b>0.4</b>	<b>&gt;1.5</b>
<b>Uracil degradation II</b>	<b>DPYD</b>	<b>0.2</b>	<b>1.09</b>
<b>Thymine degradation</b>	<b>DPYD</b>	<b>0.2</b>	<b>1.09</b>
<b>Geranylgeranyl diphosphate biosynthesis</b>	<b>FDPS</b>	<b>0.2</b>	<b>1.09</b>

**Table 4.3. Top canonical pathways uniquely identified in normal CSF(ratio>threshold)**

Table 4.3 shows how normal CSF contains molecules that fall mainly in the glutamine degradation I metabolic pathway (glutaminase, GLS). This top pathway presented the highest molecule ratio (0.4) and significance at  $p < 0.05$ ; ( $p = 0.03$ ). Interestingly, uracil and thymine degradation pathways were also selected by IPA, as well as geranylgeranyl diphosphate biosynthesis, but they had half the ratio values of the top pathway (glutamine degradation), showing  $p$  values  $> 0.05$  and therefore indicating no significance. This was due to a low  $-\log(p\text{ value})$ ; ( $>1$ ) as  $p\text{ value} = 0.08$ ;  $-\log(0.08) = 1.09$ . Nevertheless, IPA identified the enzyme, dihydropyrimidine dehydrogenase (DPYD), which falls in both uracil and thymine degradation pathways. Similarly, detection of the enzyme farnesyl diphosphate synthase (FDPS) was also made by IPA and associated with biosynthesis of geranylgeranyl diphosphate. All molecules found in normal CSF by IPA are listed in Appendix 1.

CANONICAL PATHWAY	MOLECULES	RATIO	-LOG(P-VALUE)
Folate polyglutamation	MTHFD1 SHMT1	0.5	>2
Superpathway of serine & glycine biosynthesis I	SHMT1 PSAT1	0.3	>2
Calcium transport I	ATP2A2 ATP2C1 ATP2C2	0.3	>3
Folate transformations I	MTHFD1 SHMT1	0.3	>3

**Table 4.4 Top canonical pathways uniquely identified in abnormal CSF(ratio>threshold).**

With regard to top canonical pathways identified in abnormal CSF, IPA found 50% of molecules pertaining to the folate polyglutamation pathway (Table 4.4). These molecules were methyltetrahydrofolate dehydrogenase 1 (MTHFD1) and serine hydroxymethyltransferase (SHMT1) (ratio=0.5). This value concurred with the association's significance made by IPA, which showed  $-\log(p \text{ value}) > 2$  and, therefore, significant at  $p < 0.01$ .

IPA analysis also revealed other three important metabolic pathways, each with 30% of their related molecules present in abnormal CSF. These molecules belonged to the superpathway of serine and glycine biosynthesis I: SHMT1 and phosphohydroxythreonine aminotransferase 1 (PSAT1), calcium transport I: ATP2A2, ATPC1 and ATPC2 (calcium pumps) and folate transformations I: MTHFD1 and SHMT1, respectively. Ratio values (0.3) for these three pathways were all in agreement with IPA associations' significance values ( $p < 0.01$ ), implying a significant relationship between molecules detected in abnormal CSF and the IPA selected metabolic pathway.

All molecules found in abnormal CSF by IPA are listed in Appendix 2.

#### 4.3.2.3 Different biological functions were associated to normal and hydrocephalic CSF

IPA analysis also allows matching of biological functions/dysfunctions with sets of proteins/genes identified in CSF. Our hypothesis is that the presence of specific metabolically related proteins in CSF is indicative of a given biological process occurring in this fluid. The obtained p values were all <0.05, and therefore the associations between molecules and biological function should be considered significant. A summary of the top biological functions detected in normal and abnormal CSF is described in tables 4.5 and 4.6 below.

<b>BIOLOGICAL FUNCTION</b>	<b>% PROTEINS IN NORMAL CSF LINKED TO SPECIFIC BIOLOGICAL FUNCTION</b>
<b>Cellular growth and proliferation</b>	<b>17.93</b>
<b>Tissue development</b>	<b>16.28</b>
<b>Cell morphology</b>	<b>15.05</b>
<b>Cellular function and maintenance</b>	<b>14.22</b>
<b>Nervous system development and function</b>	<b>13.19</b>
<b>Organismal development</b>	<b>13.19</b>
<b>Molecular transport</b>	<b>12.98</b>
<b>Cellular assembly and organization</b>	<b>11.54</b>
<b>Embryonic development</b>	<b>11.34</b>
<b>Behaviour</b>	<b>6.39</b>

**Table 4.5. IPA summary of biological functions associated with proteins found in normal CSF.**

Percentages were calculated taking into account the overall number of proteins considered in the IPA study for normal and abnormal CSF respectively. Overall, table 7 shows that most of the biological functions identified by IPA in normal CSF related to cell development, growth, and assembly and organization, with proteins within a 10-20% range falling in those biological processes. Nevertheless, proteins linked to molecular transport (12.98%) were also detected, as were behavioural proteins (6.39%). Molecules corresponding to biological functions identified by IPA in normal CSF are listed in Appendix III.

<b>BIOLOGICAL FUNCTION</b>	<b>% PROTEINS IN ABNORMAL CSF LINKED TO SPECIFIC BIOLOGICAL FUNCTION/DYSFUNCTION</b>
<b>Liver hyperplaxia/hyperproliferation</b>	<b>39</b>
<b>Cellular function and maintenance</b>	<b>34.71</b>
<b>Molecular transport</b>	<b>33.88</b>
<b>Cell death and survival</b>	<b>33.67</b>
<b>Organismal development</b>	<b>31.81</b>
<b>Cell morphology</b>	<b>31.40</b>
<b>Cell assembly and organization</b>	<b>26.03</b>
<b>Nervous system development</b>	<b>25.20</b>

**Table 4.6. IPA summary of biological functions associated with proteins found in abnormal CSF.**

With respect to biological functions linked to proteins found uniquely in abnormal CSF, IPA analysis found that more than 30% of molecules present in this CSF were associated with liver hyperproliferation, cellular function and maintenance, and cell death and survival (table 4.6). Abnormal CSF also shared biological functions with normal CSF, and molecular transport, organismal development cell morphology and assembly, as well as nervous system development were common to both types. However, the percentage of proteins related to those biological functions was higher in abnormal CSF >30% than in normal CSF (<18%), (table 4.5 and table 4.6). To understand the high percentage values in table 4.6, it is necessary to also understand that one protein can be shared by more than one canonical pathway. Molecules corresponding to biological functions identified by IPA in abnormal CSF are listed in Appendix IV.

#### 4.4 CONCLUSION-DISCUSSION

CSF is a protein's reservoir which reflects the physiological state of the brain. Thus, changes in normal CSF constituents, and variations in the normal protein profile specifically can be used for disease prediction (Puchades et al. 2003) and clinical diagnoses by means of clinical tests based on disease biomarker identification (Anderson, 2002).

Since LCMS and IPA aims to identify and quantify molecules that are present in the same chemical class and/or metabolic pathway (Metz et al. 2007), we propose that the specific proteins exclusively present in hydrocephalic CSF should be considered biological markers of congenital hydrocephalus. Even more importantly, we demonstrate that these molecules are related and fall into relevant canonical pathways identified by IPA analysis.

Consequently, we believe our results can be useful as a starting point to develop a clinical tool for diagnosis of congenital hydrocephalus and future adequate choice of treatment.

In past studies, LCMS CSF analysis of normal and hydrocephalic fetal CSF produced two corresponding data sets that were compared with the aim of finding differences in folate enzyme profile. Only one folate enzyme was found not to be present in hydrocephalic CSF i.e.: FDH, and for this reason, most of the latest studies in our lab were related to the study of this folate binding protein mainly.

In the present study, we pay special attention to the identification of metabolic pathways potentially activated and inactivated in normal and abnormal brain, based on the presence and absence of proteins in each specific type of CSF. The strategy consists of grouping each LCMS data-set, representing normal and abnormal CSF respectively into two groups: a first group including proteins which are not common to normal CSF and present only in

abnormal CSF, and a second group containing proteins which are not common to abnormal CSF but present in normal CSF. Excel analysis was used to group the data in this fashion. Once proteins have been appropriately grouped, IPA analysis was carried out for identification of metabolic pathways and biological functions unique to each type of CSF. Interestingly, IPA analysis of normal CSF allowed the detection of proteins (GLS) present in a key metabolic pathway, the glutamine degradation pathway. IPA association between CSF proteins and this canonical pathway was significant ( $p < 0.05$ ), as were the associations also created by IPA between molecules in hydrocephalic CSF and folate polyglutamation (MTHFD1 and SHMT1), the superpathway of serine and glycine biosynthesis I (PSAT1 and SHMT1), calcium transport I (ATP2C2, ATP2C1, ATP2A2) and folate transformations I pathways (MTHFD1 and SHMT1). Interestingly, SHMT1 was an enzyme present in most of the metabolic pathways associated with hydrocephalic CSF, which highlights this protein as a key molecule involved in the outcome of congenital hydrocephalus.

Given our approach in this study, and according to our results, we postulate that glutamine degradation is activated in normal CSF, but inactivated in abnormal CSF. A lack of glutamine degradation by the enzyme GLS implies that glutamine-degradation associated biological processes are impaired in hydrocephalus, with negative consequences for brain development. Furthermore, glutamine degradation is needed for the net production of both purines and pyrimidines for nucleotide biosynthesis and cell division, as well as for synthesis of precursors for N-linked and O-linked glycosylation reactions, for modifications of lipids and proteins involved in signal transduction, protein transport and other processes (DeBerardinis et al. 2007). Moreover, glutamine is converted into

glutamate by GLS in axonal terminals of neurons in the presence of water, producing ammonia (Botman et al. 2014) as below:



Glutamate is the most abundant neurotransmitter in the nervous system that is involved in neural activation and synaptogenesis. It is also crucial for the production of glutamate pools for polyglutamation of intracellular folate and folate storage (Ramaekers et al. 2004). Glutamate pools are also needed for cells to acquire cysteine, and for the production of glutathione, an anti-oxidant needed for cell survival in situations of high cell activity and oxidative stress (Estrela et al. 2006). Finally, glutamine has a role in extracellular signal-regulated protein kinase signalling (ERK), through its conversion to glutamate and the binding of this neurotransmitter to receptors expressed in neuronal tissues. This indicates that glutamate also has a role in signalling and activation of ERK and phosphatidylinositol 3'kinase signalling (Skerry and Genever 2001, Nicoletti et al. 2007). Thus, this study's outcome reveals GLS as an important candidate for future genetic expression analysis to investigate whether or not GLS is downregulated in congenital hydrocephalus as it is not found by IPA in hydrocephalic CSF but in normal CSF.

In conclusion, since glutamine degradation is crucial for supporting cell growth, proliferation and survival, it is not surprising that the glutamine degradation pathway is triggered in the normal brain during development, and that molecules linked to this pathway were found by IPA analysis in normal CSF. Also, because these molecules were not present in abnormal CSF, we suggest that the hydrocephalic brain lacks the ability to produce glutamate from glutamine via the normal route through GLS. Consequently the functions attributed to GLS are bound to be negatively affected.



With regards to our results from hydrocephalic CSF, these are controversial as folate polyglutamation seems to be activated. This result suggests that a source of glutamate other than from the GLS route is available in hydrocephalus. This may be explained by the existence of alternative metabolic routes for glutamate production in the body. Thus, glutamate is produced in the GABA shunt cycle from  $\alpha$ -ketoglutarate or 2-oxoglutarate by glutamate dehydrogenase (GLDH) in parallel with the production of semialdehyde succinic acid (SSA) from  $\gamma$ -aminobutyric acid GABA (synapsis inhibitory neurotransmitter) by GABA transaminase, as shown below:



Interestingly, SSA is toxic to cells if it is not converted to succinic acid by the enzyme succinic semialdehyde dehydrogenase (SSADHD). Deficiencies in this enzyme are linked to increased gaba-hydroxybutirate (GHB), a neurotoxic agent that accumulates in CSF and leads to developmental delay and mental retardation (Robbins E. 2004).

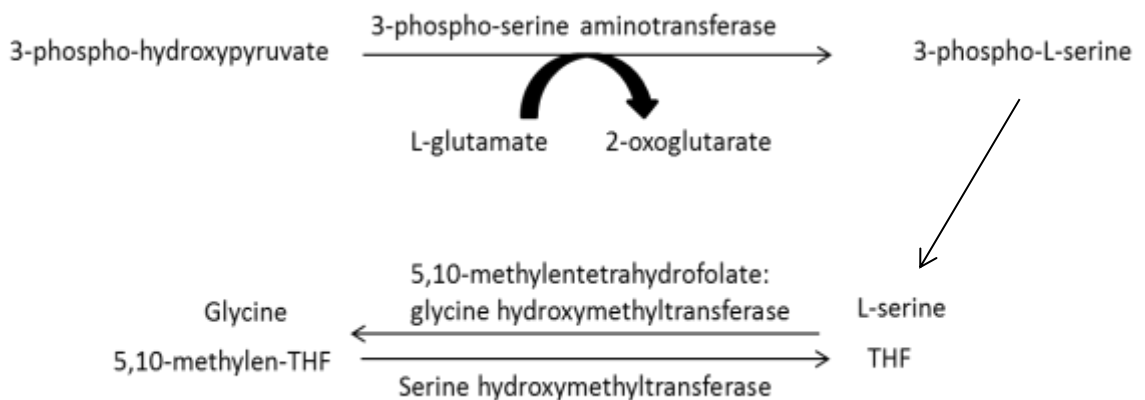
However, GABA receptor GABR2 (appendix 2) rather than GLDH and SSADH was identified by IPA suggesting GABA signalling metabolic pathway is activated. Yet, this pathway was lower than the threshold chosen for IPA analysis (0.1). IPA low ratio and/or underdetection of molecules like GLDH and SSADH is common in LCMS analysis due to undersampling, a drawback of this technology that leads to molecules being undetected (Metz et al. 2007). Therefore, we propose GLDH and SSADH to be part of future gene expression studies to verify if they are involved in congenital hydrocephalus at all.

Moreover, there is an alternate route for production of glutamate from  $\alpha$ -ketoglutarate or 2-oxoglutarate, as source of glutamate which is needed for folate polyglutamation. Folates are bound to just one molecule of glutamate in CSF (monoglutamated state), and gain access to choroidal cells through active transport mediated by folate receptors. Once monoglutamated folates are inside cells, they are converted into folyl-polyglutamated folates by folylpoly-gamma-glutamate synthetase for storage, or they are transformed into dihydrofolate and tetrahydrofolate in the folate metabolic cycle (Ramaekers et al. 2004). In this context, activation of folate polyglutamation in hydrocephalic CSF means an elevated use of glutamate, and we suggest this is provided by tricarboxylic cycle activation in mitochondria. Interestingly, the Krebs cycle is intertwined with the glycine and serine superpathway another metabolic pathway identified by IPA through detection of PSAT1 and SHMT1.  $\alpha$ -ketoglutarate or 2-oxoglutarate is produced in the glycine and serine superpathway, thereby feeding the tricarboxylic cycle with this metabolite. This concurs with our results; as more than 30% of molecules (PSAT1 and SHMT1) in abnormal CSF belonged to the glycine and serine superpathway. Therefore, this finding suggests that the glycine and serine metabolic pathways may be activated in congenital hydrocephalus; they are likely to feed the Krebs cycle for production of  $\alpha$ -ketoglutarate or 2-oxoglutarate, and later of glutamate for folate polyglutamation.

Intracellular calcium is needed for mitochondria (Krebs cycle) and reticulum endoplasmic activity in neurons, and has a key role as a second messenger in glutamate release (Miller 1991). This means that glutamate release depends on activation of calcium flux through internal membranes. On the other hand, membrane calcium transport is dependent on receptor activation by glycine and glutamate (Laube et al. 1997 and Li et al. 2009). These facts are also directly connected to our results regarding stimulation of calcium transport

metabolic pathway and serine and glycine biosynthesis superpathway, linked to the ATPase pumps (ATP2C2, ATP2C1, and ATP2A2) found in hydrocephalic CSF by IPA analysis. In conclusion, IPA identification of the described metabolic pathways in abnormal CSF suggests that calcium transport (calcium flux through membranes) followed by glutamate synthesis activation and glycine production as well as  $\alpha$ -ketoglutarate or 2-oxoglutarate synthesis in the glycine and serine biosynthesis superpathway are all activated and linked in congenital hydrocephalus.

$\alpha$ -ketoglutarate or 2-oxoglutarate produced in the glycine and serine biosynthesis superpathway is converted to glutamate for polyglutamation in the GABA shunt cycle (Rowley 2012). The glycine and serine biosynthesis superpathway and concomitant production of 2-oxoglutarate is briefly described below:



Furthermore, folate transformations I (folate metabolic reactions involved in production of THF) appear to be activated since MTHFD1 and SHMT1 were also identified by IPA in abnormal CSF. This outcome is inconclusive as these folate transformations are needed in normal brain, and should be present in normal CSF too (see diagram below). This result may imply folate transformations I pathway happens at a different time point in development, and for this reason they are not present in normal CSF at the embryonic day

chosen for our investigations, yet, present in hydrocephalic CSF. In any case, this finding agrees with the serine and glycine biosynthesis superpathway too and both pathways point to a production of THF as indicated in the glycine and serine biosynthesis superpathway described above. THF is a folate that seems to be in demand in the hydrocephalic brain, and it has been proven that treatment with this folate, when stable, improves congenital hydrocephalus and encourages growth of cerebral cortex cells. In view of this facts, we hypothesize that the glycine and serine biosynthesis metabolic superpathway and the folate transformations I canonical pathway may be activated to supply THF due to a lack of this folate in the hydrocephalic brain. However, THF transport and delivery to areas like the cerebral cortex may be compromised by the low FDH levels identified in hydrocephalic CSF (Cain et al. 2009), since FDH is thought to act as a THF reservoir and folate transporter. In conclusion, the folate enzymes MTHFD1, SHMT1 and FDH should be considered for future genetic expression analysis to establish if they are overexpressed or under-expressed as well as to explore their potential as biomarkers of this condition.

In respect of biological functions and dysfunctions associated with the CSF protein profile, the most relevant outcome was the presence of nearly 40% of proteins in hydrocephalic CSF falling into the liver hyperplasia and proliferation dysfunction. This finding suggests that there is a degeneration of the fetal liver or the mother's liver, with maternal liver proteins reaching the CSF through the placenta. Furthermore, the liver expresses PCFT and FR $\alpha$  folate transporters, and provides plasma with soluble folate transporters (sFR $\alpha$ ), hence; deterioration of liver in the mother means low levels of sFR $\alpha$  in plasma and folate provision to the brain through the placenta, as well as to CSF at early pregnancy (Wani et al. 2013) .

Interestingly, molecular transport proteins were found in both normal and abnormal CSF, and therefore this finding is inconclusive according to our experimental approach based on protein presence (gene activation) and non-presence (gene inactivation). This finding confirms the need for quantification of gene expression and its inclusion in the IPA analysis, and only comparison between IPA analyses, along with gene expression measurements in each type of CSF, will allow any conclusions about molecular transport. In spite of this result, this finding suggests that our studies are leading in the right direction, as FDH is a folate binding protein that is thought to be involved in vitamin transport in CSF, located together with FR $\alpha$  within exosomes in CSF. Finally, another biological function exclusively related to hydrocephalic CSF was cell death and survival, with more than 30% proteins belonging to this function. This function was not identified by IPA analysis in normal CSF, which is controversial as it is known that apoptosis and DNA degradation are part of normal brain development, and programmed cell death is important for the formation of the nervous system (Vaux et al. 1999). Therefore, questions arise about LCMS identification of small concentrations of proteins in normal CSF lower than 50 femtomols that may pass undetected. This conclusion also applies to the folate transformations I canonical pathway, explained previously, which is not identified in normal CSF either. Another possibility is that may these two processes happen later in development for normal CSF, and that they are activated specifically at embryonic day 18 only in hydrocephalic CSF.

Due to the limited time frame of this investigation, gene expression quantification was not performed. This was a drawback to our study, and the reason for the lack of a final predictive value in terms of gene activation/inactivation. Therefore, this study should be considered as a starting point to more extensive and complementary research in the future.

RTPCR assays should be performed to measure overexpression or underexpression of “focus genes” (GLS, MTHFD1, SHMT1, PSAT1, ATP2C2, ATP2C1, ATP2A2) in the canonical pathways elected by IPA followed by IPA re-analysis with integration of gene expression data. Nevertheless, only significant IPA associations ( $p < 0.05$ ) between CSF proteins and top canonical pathways were studied. Thus, our research provides a useful source of reference data for future production of efficient and reliable diagnostic tests based on the identification of molecules unique to hydrocephalic CSF and/or decreased or increased mRNA quantification in relation to normal expression levels.

#### 4.5 REFERENCES

- Anderson N.L. (2002). The human plasma proteome history, character, and diagnostic prospect. Review. *Molecular and Cellular proteomics*. (1.11): 845-867
- Antony, A.C. (2007). In utero physiology: role of folic acid in nutrient delivery and fetal development. *Am. J. Clin. Nutr.* 85: 5985-6035.
- Arpino, P. (1992). Combine liquid chromatography mass spectrometry. *Mass Spectrometry book. Reviews. PartIII. Applications of thermospray.* 11: (1); 3-40. Ed. John Willey & Sons.
- Baek J.Y. et al. (2000). Assignment of human 3-phosphoglycerate dehydrogenase (PHGDH) to human chromosome band 1p12 by fluorescence in situ hybridization. *Cytogenet. Cell Genet.* 89 (1-2): 6-7.
- Baek JY et al. (2003). Characterization of human phosphoserine aminotransferase involved in the phosphorylated pathway of L-serine biosynthesis. *Biochem J.* 373 (Pt. 1);191-200.
- Botman D. et al. (2014). Determination of phosphate activated glutaminase activity and its kinetics in mouse tissues using metabolic mapping (Quantitative Enzyme Histochemistry). *J. Histochem. Cytochem.* 62 (11): 813-826.
- Calvano S.E. et al. (2005). A network-based analysis of systemic inflammation in humans. *Nature.* 437: 1032-1037.
- Dai, L et al. (2009). Comparative proteomic study of two closely related ovarian endometrial Adenocarcinoma cell lines using CIEF fractionation and Pathway analysis. *Electrophoresis.* 30 (7): 1119-1131.
- DeBerardinis R.J. et al. (2007). Beyond aerobic glycolysis: transformed cells can engage in glutamine metabolism that exceeds the requirement for protein and nucleotide synthesis. *Proc. Natl. Acad. Sci. Vol. (104):* 19345–19350.
- DeBerardinis R.J. & Cheng T. (2010). Q's next: the diverse functions of glutamine in metabolism, cell biology and cancer. *Oncogene. Vol. (29):* 313–324
- Glish, GL & Vacher, RW. (2003). The basics of mass spectrometry in the twenty-first century. *Nat. Rev. Drug. Discov.* 2: 140-150.
- Grapp, M. et al. (2013) Choroid Plexus transcytosis and exosome shuttling deliver folate into brain parenchyma. *Nature.* 2123: 589-93.
- Estrela J.M, Ortega A., Obrador E. (2006). Glutathione in cancer biology and therapy. *Crit. Rev. Clin. Lab. Sci. Vol. ( 43):* 143–181.
- Johnson et al. 2005. Contemporary clinical usage of LC/MS: analysis of biologically important carboxylic acids. *Clin. Biochem. Vol (38); (4):*351-61.
- Laube B et al. (1997). Molecular determinants of agonist discriminator by NMDA receptor subunits: analysis of the glutamate bind to site on the NR2B subunit. *Neuron Vol. (18); (3):*493-503.

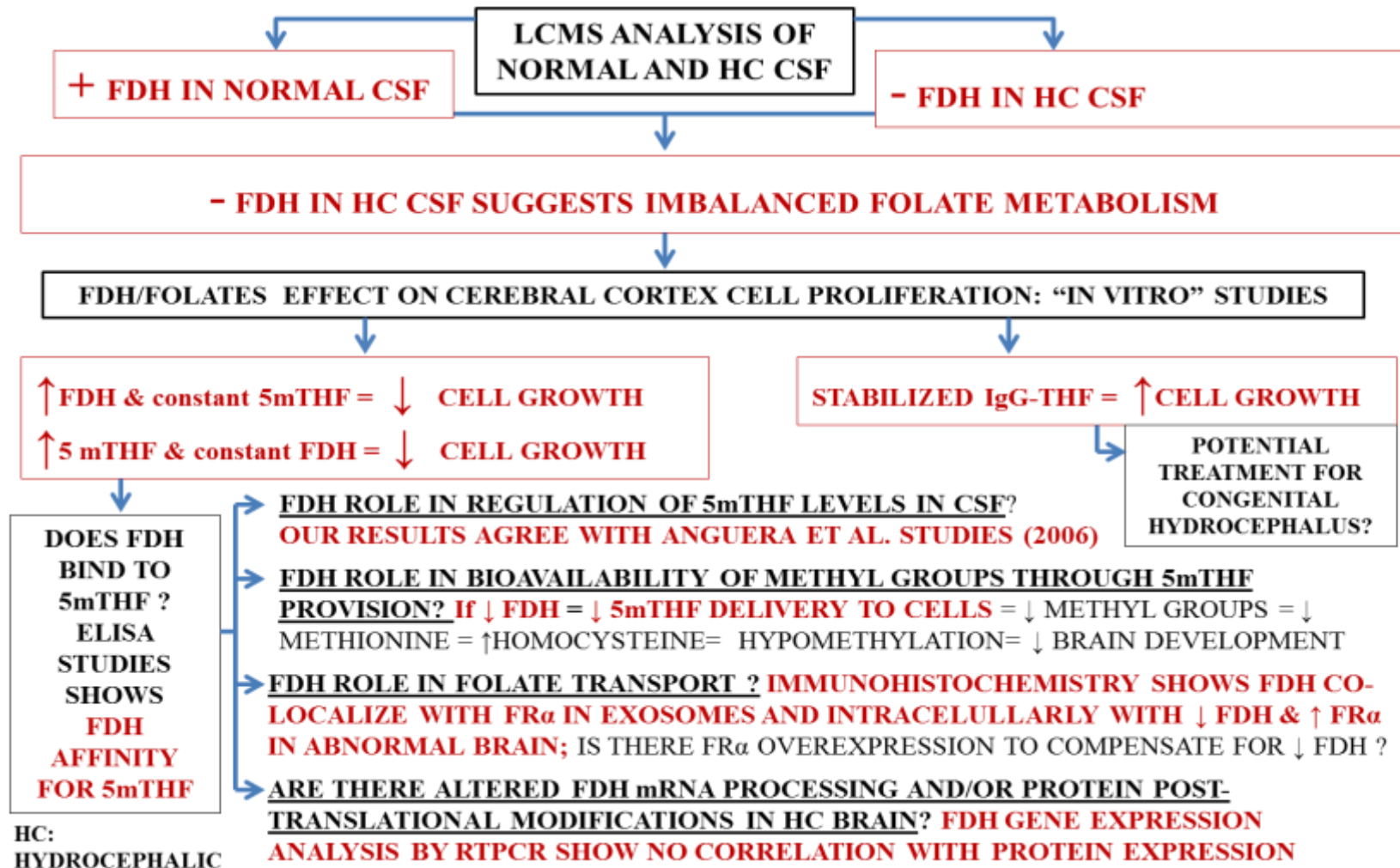
- Li F. et al. (2009). Memory and the NMDA receptors. *N. Engl. J. Med.* Vol. (361); (3):302-3.
- Metz, T.O. et al. (2007) The future of liquid chromatography-mass spectrometry (LC-MS) in metabolic profiling and metabolomic studies for biomarker discovery. *Biomark. Med.* 1 (1): 159-185.
- Miller R.J. (1991). The control of neuronal Ca<sup>2+</sup> homeostasis. *Prog. in Neurobiol.* Vol (37).
- Mischoulon, D & Maurizio, F (2002). Role of S-adenosyl-L-methionine in the treatment of depression: a review of the evidence. *Am. J. Nutr.* 76 (suppl.): 1158S-61S.
- Nabiuni M. Analysis of protein content of cerebrospinal fluid in developing hydrocephalic texas rat. Faculty of Life Sciences. Manchester,UK: The University of Manchester, 2006
- Puchades, M et al. 2003. Proteomics studies of potential cerebrospinal fluid protein markers for Alzheimer's disease. *Mol. Brain Res.* Vol (118): 140-146.
- Nicoletti F. et al. (2007). Metabotropic glutamate receptors: new targets for the control of tumor growth? *Trends Pharmacol. Sci.* (28):206–213.
- Ramaekers, V.R. et al. (2004). Cerebral folate deficiency. *Dev. Med Child Neurol* 46: 843-51.
- Robbins E. 2004. Succinic Semialdehyde Dehydrogenase Deficiency. *Georgetown University Journal of Health. GUJHS.* Vol (1): 3.
- Rowley N.M. (2012). Glutamate and GABA synthesis release, transport and metabolism as targets for seizure control. *Neurochem. Int.* Vol (61): (4): 546-558.
- Salway, J.G. 2004. Metabolism at a glance. *Biochemistry.* 3<sup>rd</sup> Edition. John Wiley & Sons. Inc. Blackwell publishing. Malden Ma USA.
- Skerry T.M., & Genever PG. (2001). Glutamate signalling in non-neuronal tissues. *Trends Pharmacol. Sci.* Vol. (22): 174–181.
- Solanky N. et al. (2010). Expression of folate transporters in human placenta and implications for homocystein metabolism. *Placenta.* Vol. (31): 134-143.
- Steinfeld, R. et al. (2009). Folate receptor alpha defect causes cerebral folate transport deficiency: A treatable neurodegenerative disorder associated with disturbed myelin metabolism. *The Amer. J. of Hum. Gen.* Vol. (85): 354-363.
- Uriarte, S.M. (2008). Comparison of proteins expressed on secretory vesicles membranes and plasma membranes of human neutrophils. *J.Immunol.* 180: 5575-5581.
- Wang J.H. (1999). Proteomics in drug discovery. *Drug discovery today.* Vol 4 (3): 129-133.



Wani, N.A. (2013). Decreased activity of folate transporters in lipids rafts resulted in reduced hepatic folate uptake in chronic alcoholism in rats. *Genes Nutr.* Vol (8): (2): 209-219.

## CHAPTER 5. CONCLUDING REMARKS, DISCUSSION, AND FUTURE AIMS

### 5.1.1. Chapter 2 concluding remarks flow chart. Figure 5.1:



### **5.1.2. Chapter 2 concluding remarks and discussion**

#### **□ POTENTIAL ROLE OF FDH IN REGULATION OF 5mTHF LEVELS IN CSF**

“In vitro” work and “in house” immunoassay studies demonstrated that FDH has affinity for 5mTHF, suggesting a role of FDH in regulation of 5mTHF levels in CSF when FDH is present at high concentration  $p < 0.001$ . Therefore, we propose that FDH binds to folates acting as a 5mTHF reservoir in CSF when FDH is abundant. On the other hand, at low concentration, FDH detaches from 5mTHF and both molecules enter the cells, activating the folate metabolic cycle and encouraging cell growth. Thus, a total lack of FDH in CSF, i.e.: hydrocephalic CSF can be detrimental for regulation of extracellular and intracellular 5mTHF, which may have a negative knock-on effect on areas of the brain such as the cerebral cortex and the arachnoid.

#### **□ POSSIBLE ROLE OF FDH IN 5mTHF HANDLING AND TRANSPORT ALONG WITH FR $\alpha$ .**

FDH affinity studies using commercial and “in house” ELISAs, as well as tissue immunolocalization analysis, reveal FDH as a protein involved in 5mTHF handling. FDH may work in a similar fashion to FR $\alpha$ , a soluble membrane receptor with high affinity for 5mTHF. In the present work, FDH, FR $\alpha$  and 5mTHF share the same location within the choroid plexus, CSF exosomes and the cerebral cortex, which is evidence that the two proteins work together to provide the brain with folate.

□ LOCATION OF FDH ALONG WITH FR $\alpha$  WITHIN EXOSOMES.

5mTHF is located with FDH and FR $\alpha$  within vesicles in CSF. 5mTHF transport within vesicles forming folate-protein conjugates suggests that this is a protective mechanism against the physicochemical changes between the extracellular media or CSF and within the cell's different compartments as folates are sensitive to oxygen and changes in pH.

□ STABILIZED THF AS A SUITABLE FOLATE CANDIDATE FOR TREATMENT OF CONGENITAL HYDROCEPHALUS.

FDH's product of reaction (THF) encourages cell growth only if linked to complementary molecules such as THF antibodies (IgG), proving that folates may only be active if they are transported when linked to molecules that promote stabilization. The present study demonstrates the suitability of stabilized THF as a potential candidate for treatment of hydrocephalus.

□ FDH PROTEIN IS UNDEREXPRESSED IN HYDROCEPHALIC CEREBRAL CORTEX.

Protein expression at tissue levels is decreased in the hydrocephalic cerebral cortex, whereas FR $\alpha$  and 5mTHF are increased, implying that there is a compensatory mechanism to provide the cerebral cortex with 5mTHF through an elevated production of FR $\alpha$  as FDH is low. However, since FR $\alpha$  is not synthesized in the brain, we suggest that the FR $\alpha$ -5mTHF folate delivery system is controlled by the placenta, indicating that this auxiliary fetal organ is impaired in hydrocephalus. Our FDH protein expression in brain tissue agrees with past results from CSF analysis in our lab where FDH appears to be decreased in hydrocephalic CSF.

- FDH PROTEIN EXPRESSION DOES NOT CORRELATE WITH mRNA EXPRESSION LEVELS IN THE HYDROCEPHALIC BRAIN.

FDH mRNA/cDNA expression quantification did not correlate with the high levels of protein found, which indicates that mRNA transcription and/or translation processes may be altered in congenital hydrocephalus, resulting in low FDH protein biosynthesis at tissue level and later secretion into CSF. On the other hand, FDH high mRNA expression in hydrocephalic cerebral cortex suggests a negative feedback loop to compensate for a decreased FDH protein biosynthesis.

- PROSPECTIVE ROLE OF FDH IN CELL METHYLATION STATUS

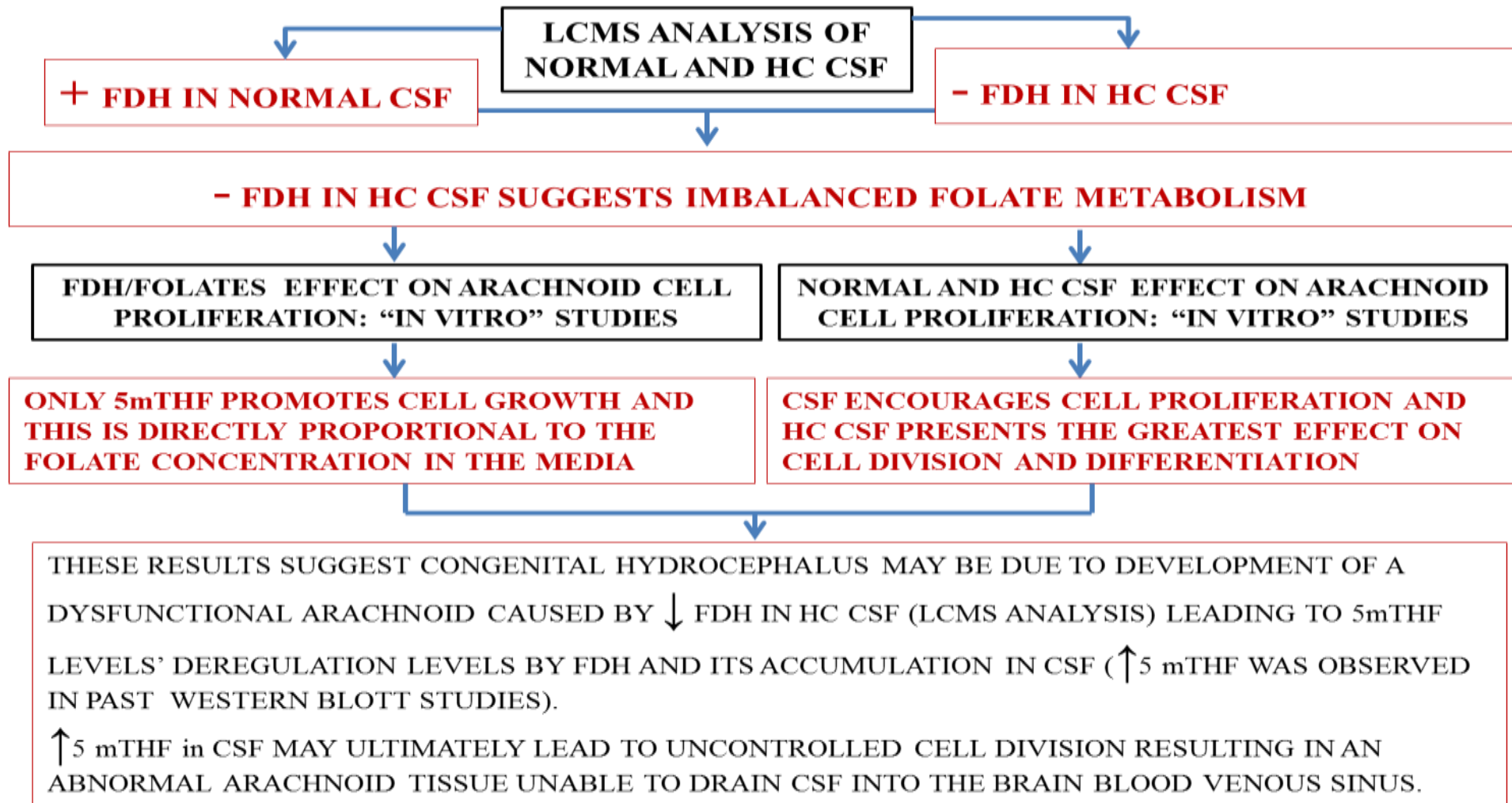
The ability of FDH to bind to 5mTHF also implies a role in the provision of methyl groups for diverse metabolic reactions, such as DNA methylation, production of the universal methyl group donor SAM, as well as the production of methionine. Because balanced levels of methionine and homocysteine are crucial for development, a low methyl group bioavailability due to low 5mTHF provision by FDH means homocysteine is in excess. High levels of homocysteine is associated with hypomethylation and cell cycle arrest, as well as damage to the interior lining of the blood vessels walls like the carotid arteries in the brain. Furthermore, increased homocysteine can have a negative impact in placenta formation, and may lead to abruption as well as pre-eclampsia during pregnancy.

### 5.1.3. Future aims

- Further FDH protein and gene expression quantification in relation to FR $\alpha$  and 5mTHF in cerebral cortex, choroid plexus and placenta could help to confirm the extent to which FDH and FR $\alpha$  gene expression is upregulated in congenital hydrocephalus. Whereas in this study RTPCR allowed gene expression quantification in normal and abnormal cerebral cortex, this technique was not used with choroid plexus tissue due to technical problems related to the concentration of this tissue. Since fluorescence “in situ” RTPCR allows location as well as quantification of mRNA expression in both choroid plexus and cerebral cortex, this technique is proposed as more convenient for our purposes to quantify FDH and FR $\alpha$  mRNA in normal and abnormal brain. In relation to localization, fluorescence immunostaining allowed location and quantification of FDH and FR $\alpha$  proteins; however, further studies using Western Blotting are also suggested for double confirmation of this result.
  
- Past studies revealed a combination of two folates (THF and Folinic acid) as a potential suitable treatment for congenital hydrocephalus. Whilst Folinic acid on its own does not reduce the incidence of this condition in Texas rats animal models, THF did encourage cell growth “in vitro”, highlighting the importance of this folate as a suitable candidate for treatment. Further “in vivo” experiments using stabilized THF, either with specific anti-THF IgG or FDH to Texas rats, should be carried out to ascertain whether there is any reduction in the incidence of congenital hydrocephalus with this folate.

- High homocysteine levels are thought to be occurring in hydrocephalic CSF due to low bioavailability of methyl groups caused by low FDH and therefore 5mTHF provision, leading to low methionine production. High homocysteine and low methionine levels in plasma are linked to high blood pressure, hypomethylation and placental and brain developmental problems. Thus, a future aim in this research should be the measurement of homocysteine concentration in hydrocephalic CSF to determine whether this is raised compared to normal CSF.

5.2.1. Chapter 3 concluding remarks flow chart. Figure 5.2:



HC: HYDROCEPHALIC



### **5.2.2. Chapter 3 concluding remarks and discussion**

- FOLATES' EFFECT ON CELL DIVISION ON ARACHNOID PRIMARY CELL CULTURES REVEALED 5MTHF AS THE ONLY FOLATE ABLE TO ENCOURAGE CELL ARACHNOID PROLIFERATION AND DIFFERENTIATION.

5mTHF potentiated cell to cell connections, which suggests that this folate is needed for flow regulation through cell junctions and is vital for the correct development of a functional arachnoid in early pregnancy.

- 5MTHF AT HIGH CONCENTRATION WAS COUNTERPRODUCTIVE FOR CELL GROWTH IN THE PRESENCE OF CONSTANT 5mTHF AND ACTIVE FDH AND VICE VERSA.

These outcomes provide support for previous "in vitro" work about the effects of folates on cerebral cortex cells. In conclusion, these results reaffirm FDH's affinity for 5mTHF, pooling this folate when in excess, and acting as a regulatory enzyme to store it in situations of low demand. Therefore, a lack of FDH leads to increased 5mTHF levels in hydrocephalic CSF.

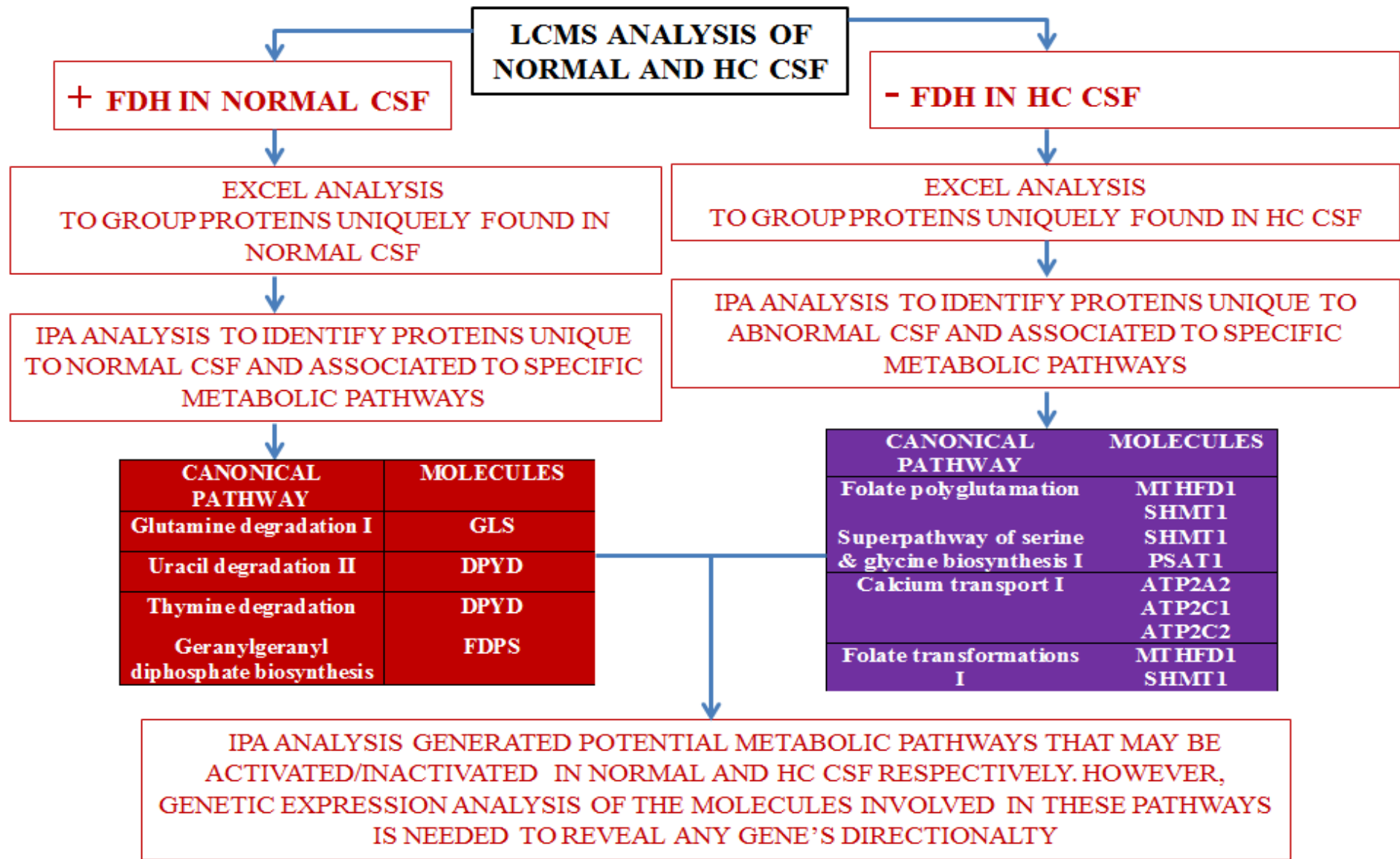
- PRIMARY ARACHNOID CELL CULTURE IS HIGHLY PROMOTED BY HYDROCEPHALIC CSF.

This outcome corroborates the impact of high levels of 5mTHF on arachnoid cell proliferation in the absence of FDH (HC CSF composition), providing further evidence about the role of FDH in 5mTHF regulation levels in CSF.

### **5.2.3. Chapter 3 future aims**

- In the present study, all “in vitro” work was performed on arachnoid tissue from normal brain. Future experiments to study the effect of folates as well as normal CSF on arachnoid primary cell cultures from hydrocephalic fetal brain may confirm further whether 5mTHF is beneficial for primary hydrocephalic arachnoid cell culture.
  
- Further FDH and FR $\alpha$  protein and gene expression analysis on arachnoid tissue may also contribute to a better understanding of the role of folate transport and folate metabolism in the development of the fetal arachnoid during early pregnancy in normal and abnormal brain.

5.3.1 Chapter 4 concluding remarks flow chart. Figure 5.3:



### **5.3.2. Chapter 4 concluding remarks and discussion**

- IPA ANALYSIS OF NORMAL CSF ALLOWED THE DETECTION OF THE ENZYME FDH WHICH FALLS WITHIN THE FOLATE TRANSFORMATION I PATHWAY AND WHICH WAS ABSENT IN ABNORMAL CSF.

FDH is part of the Folate transformations I pathway where FDH transforms 10-formylTHF into THF. This outcome is in agreement with past Western blotting results that showed a lack of FDH in hydrocephalic CSF suggesting this pathway may be missing in the folate metabolic cycle leading to accumulation of 10-formylTHF and a lack of THF synthesis, which is crucial for the production of DNA. On the other hand, it is thought that FDH may also have a role in regulation of 5mTHF levels through its binding to 5mTHF for storage in situations of high 5mTHF concentration in CSF. Thus, depletion of FDH may also lead to increased levels of free 5mTHF in CSF and abnormalities in cell division rate. This conclusion is supported first by past Western Blotting studies that revealed abnormal high levels of 5mTHF in hydrocephalic CSF and second, by our “in vitro” studies that showed how cell division is directly proportional to the 5mTHF concentration in the media.

- IPA ANALYSIS OF NORMAL CSF ALLOWED THE DETECTION OF THE ENZYME FDH WHICH FALLS WITHIN THE FOLATE TRANSFORMATION I PATHWAY AND WHICH WAS ABSENT IN ABNORMAL CSF. GLS IN THE GLUTAMINE DEGRADATION PATHWAY

GLS is involved in the glutamine degradation pathway and was exclusively found in normal CSF. IPA associations between molecules uniquely found in normal CSF and the glutamine degradation pathway were significant at  $p < 0.05$ . According to

this outcome, we postulate that glutamine degradation is activated in normal CSF, but inactivated in abnormal CSF, implying that this metabolic pathway and associated biological processes are impaired in hydrocephalus, with negative consequences for brain development as a lack of glutamine degradation means no production of the key neurotransmitter glutamate.

- IPA ANALYSIS CREATED ASSOCIATIONS BETWEEN MOLECULES ONLY PRESENT IN HYDROCEPHALIC CSF AND FOLATE POLYGLUTAMATION (MTHFD1 AND SHMT1), THE SUPERPATHWAY OF SERINE AND GLYCINE BIOSYNTHESIS I (PSAT1 AND SHMT1) AND CALCIUM TRANSPORT I (ATP2C2, ATP2C1, ATP2A2) AS WELL AS FOLATE TRANSFORMATIONS I PATHWAYS (MTHFD1 AND SHMT1)

In relation to these results we hypothesize that these metabolic pathways are activated exclusively during congenital hydrocephalus at gestational age 18. Interestingly, SHMT1 was an enzyme present in most of the metabolic pathways associated with hydrocephalic CSF, which highlights this protein as a key molecule involved in the onset of congenital hydrocephalus.

### **5.3.3. Chapter 4 future aims**

Drawbacks like undersampling are known features of LCMS technology, which means that there was possible underdetection of small molecules or molecules present at low concentration in the CSF samples used in our experiments. Therefore, we propose further experiments involving CSF fractionation and new mass spectrophotometry analysis using cutting-edge technologies like 6600 Triple ToF mass spectrophotometry, followed by IPA re-analysis in parallel to quantification of gene expression of all molecules associated with

metabolic pathways identified by IPA analysis. This approach will result in a more detailed and exhaustive study of normal and abnormal to establish CSF differences and to determine which genes are activated and inactivated in congenital hydrocephalus.